ANALYSIS OF CELL PROLIFERATION

DURING *C. ELEGANS* INTESTINE DEVELOPMENT

Alexandra Segref
Division of Molecular Genetics
Institute of Biomedical and Life Sciences
University of Glasgow
Glasgow G12 8QQ
UK

This thesis is presented in submission for the degree of Doctor of Philosophy
to the Faculty of Biomedical and Life Sciences

May 2007

Abstract

The precise co-ordination of cell proliferation and developmental pathways is essential for the development of multicellular organisms and the maintenance of tissue homeostasis. The intestine (endoderm) of the nematode *Caenorhabditis elegans* is used as a model system to study the control of cell proliferation during development, because it consists of only 20 cells. These cells are generated in the embryo by a precise division-pattern that is largely invariant between different animals. Previously, a *cdc-25.1(ij48)* gain-of-function allele has been identified that produces increased numbers of intestinal cells. CDC-25.1 belongs to the eukaryotic CDC25 family of positive-acting cell cycle regulators. Intriguingly, in *cdc-25.1(ij48)* mutants, proliferation of other tissues is unaffected, but knockdown of CDC-25.1 by RNAi produces reduced cell divisions in most lineages. Thus, there is a general requirement for *cdc-25.1* function in all embryonic blastomeres, but the *cdc-25.1(ij48)* mutant primarily affects proliferation of the intestine. It is therefore interesting to elucidate the mechanism underlying this tissue-specific phenotype.

The *ij48* lesion in CDC-25.1 constitutes a serine to phenylalanine mutation (CDC-25.1(S46F)) in a highly conserved putative DSG consensus site, which may act as a site of negative regulation of CDC-25.1. In mammalian cells, the DSG motif of CDC25A acts as a recruitment site for the ubiquitin ligase component β-TrCP, mediating ubiquitin-dependent degradation of CDC25A. However, to date no difference in the abundance or localisation of CDC-25.1(S46F) was identified.

In this thesis, I set out to identify negative regulators of CDC-25.1 that control CDC-25.1 through S46, possibly in the intestine. Compelling evidence is provided demonstrating that LIN-23, the *C. elegans* orthologue of human β-TrCP, negatively regulates the abundance of CDC-25.1 through S46 in *C. elegans*, specifically in early embryos. Surprisingly, the control of CDC-25.1 abundance is not restricted to intestinal cells, suggesting that the intestinal cell proliferation is more sensitive to elevated CDC-25.1 protein levels than other cell types. In a search for other molecules that may regulate the DSG site, GSK-3, APR-1 and WRM-1 were found to also cause excess intestinal cells. Intriguingly, their function is independent of S46 in CDC-25.1, because *gsk-3*, *apr-1* or *wrm-1* RNAi produce a synergistic increase in intestinal cells when combined with the *cdc-25.1(ij48)* allele. Thus, this thesis provides new insights to further our understanding of how the multicellular organism *C. elegans* controls proliferation of an entire tissue, the intestine.

Table of contents

Table of contents 2
List of Tables 8
List of Figures 9
Acknowledgements 11
Author's declaration 12
Definitions 13
Chapter 1 17
1 Introduction 18
1.1 Why study *C. elegans*? 18
1.1.1 The phylogenetic features of *C. elegans* 19
1.1.2 The biology of *C. elegans* 19
1.1.3 The *C. elegans* genome 20
1.1.4 *C. elegans* anatomy 20
1.1.5 *C. elegans* embryogenesis 24
1.2 Development of the *C. elegans* intestine 26
1.2.1 Cell autonomous endoderm specification in *C. elegans* 29
1.2.1.1 EMS specification through SKN-1 29
1.2.1.2 SKN-1 transcriptional targets vital for endoderm specification 31
1.2.2 External signals vital for endoderm specification 32
1.2.2.1 Wnt pathway components specify endoderm 33
1.2.2.2 The role of POP-1 in the Wnt pathway 34
1.3 Intestinal cell proliferation is controlled by CDC-25.1 37
1.3.1 CDC25 function in eukaryotes 37
1.3.2 The *C. elegans cdc-25* family 38
1.3.3 CDC-25.1 functions during post-embryonic development 39
1.3.4 CDC-25.1 functions during embryonic development 39
1.3.5 *cdc-25.1* mutants cause hyperplasia 40
1.3.5.1 *cdc-25.1(ij48)* is a gain-of-function allele 40
1.3.5.2 *cdc-25.1(ij48)* promotes tissue-specific hyperproliferation 41
1.3.5.3 The *cdc-25.1(ij48)* mutation and comparison to *cdc-25.1(rr31)* 41
1.4 Research aims and objectives 42
Chapter 2 44
2 Materials and Methods 45
2.1 Materials 45
2.1.1 Chemical Abbreviations 45
2.1.2 Stock solutions and media 46
2.1.3 Molecular weight markers 50
2.1.3.1 DNA markers 50
2.1.3.2 Protein markers 50
2.1.4 Vectors and plasmids 50
2.1.5 Oligonucleotides 51
2.1.5.1 Vector oligonucleotides 51
2.1.5.2 Oligonucleotides for *cdc-25.1* 51
2.1.5.3 Oligonucleotides for *lin-23* 52
2.1.5.4 Oligonucleotides for RNAi clones 52
2.1.6 Strains 53
2.1.6.1 *E. coli* strains 53
2.1.6.2 *C. elegans* strains 54
2.1.6.3 *C. elegans* strains generated in this study 55
2.1.7 Antibodies 56
2.1.7.1 Primary antibodies 56

2.1.7.2 Secondary antibodies 56
2.2 Methods 57
2.2.1 Standard molecular biology techniques 57
2.2.1.1 DNA preparation 57
2.2.1.2 DNA/ RNA electrophoreses 57
2.2.1.3 PCR 58
2.2.1.4 RT-PCR 58
2.2.1.5 Digest and purification of DNA fragments 58
2.2.1.6 Nucleic acid quantification 59
2.2.1.7 DNA ligation 59
2.2.1.8 DNA transformation into *E. coli* 60
2.2.1.9 *E. coli* cultures 60
2.2.1.10 Colony screening for positive transformants 60
2.2.1.11 Sequencing 61
2.2.1.12 Plasmid construction 61
2.2.2 Protein biochemistry 63
2.2.2.1 SDS-PAGE 63
2.2.2.2 Western blotting 64
2.2.2.3 Coomassie staining 64
2.2.2.4 Recombinant expression of proteins in *E. coli* 64
2.2.2.5 Purification of soluble fusion proteins from *E. coli* 65
2.2.2.6 Purification of insoluble fusion proteins from *E. coli* 66
2.2.2.7 Protein dialysis 67
2.2.2.8 Peptide antibody production 67
2.2.2.9 Antibody production against recombinant CDC-25.1 and LIN-23 68
2.2.2.10 Crosslinking of recombinant CDC-25.1 and LIN-23 proteins to CNBr-Sepharose 68
2.2.2.11 Affinity purification of CDC-25.1 and LIN-23 antisera against peptides 69
2.2.2.12 Affinity purification of CDC-25.1 and LIN-23 antisera against recombinant proteins 70
2.2.2.13 Crosslinking of anti-CDC-25.1 and anti-LIN-23 peptide antibodies to Protein A-Sepharose 71
2.2.2.14 Crosslinking of anti-CDC-25.1 and anti-LIN-23 antibodies to Protein A-Agarose 71
2.2.3 *C. elegans* culturing and handling 72
2.2.3.1 Genetic crosses 72
2.2.3.2 Generation of males by heat shock 72
2.2.3.3 Growth of *C. elegans* in liquid culture 72
2.2.3.4 Harvesting embryos from large-scale liquid cultures 73
2.2.4 *C. elegans* transgenesis 74
2.2.4.1 Generation of *C. elegans* strains carrying extrachromosomal arrays 74
2.2.4.2 Chromosomal integration of LAP-tagged *cdc-25.1* 75
2.2.4.3 Microparticle bombardment to integrate *lin-23::FLAG-TY* 75
2.2.5 *C. elegans* RNAi 77
2.2.5.1 Feeding RNAi on NGM plates 77
2.2.5.2 Feeding RNAi in liquid culture 78
2.2.5.3 Double RNAi by feeding 79
2.2.5.4 RNAi by microinjection 79
2.2.6 *C. elegans* molecular biology 80
2.2.6.1 Isolation of *C. elegans* genomic DNA 80
2.2.6.2 RNA isolation from *C. elegans* 80
2.2.6.3 Single worm PCR from embryos and adults 81
2.2.6.4 *cdc-25.1(ij48)* restriction site polymorphism 81

2.2.6.5 *lin-23(e1883)* restriction site polymorphism....82
2.2.7 *C. elegans* biochemistry....82
2.2.7.1 Preparation of embryo extracts....82
2.2.7.2 Preparation of L4-staged extracts....83
2.2.7.3 Preparation of adult worm extracts....83
2.2.7.4 Phosphatase treatment of adult and embryo extracts....83
2.2.7.5 Immunoprecipitation from embryo and L4 extracts....84
2.2.7.6 Purification of LAP::CDC-25.1 on S-Protein Agarose....84
2.2.8 Microscopy....85
2.2.8.1 Preparation of living specimen....85
2.2.8.2 Preparation for fixed specimen....85
2.2.8.3 Indirect immunofluorescence....85
2.2.8.4 Conventional microscopy for fluorescence and Nomarski imaging of fixed and living samples....86
2.2.8.5 Confocal microscopy of immunostained samples....86
2.2.9 Statistics....87
2.2.9.1 Statistics for CDC-25.1 indirect immunofluorescence....87
2.2.10 Bioinformatics....90
Chapter 3....91
3 Identification of CDC-25.1 regulators....92
3.1 Introduction....92
3.1.1 Conservation of the DSG consensus in CDC-25.1....92
3.1.2 Mechanisms of DSG-mediated regulation in higher eukaryotes....93
3.1.2.1 β-TrCP recognition of β–catenin and other substrates....94
3.1.2.2 Diverse kinases implicated in DSG phosphorylation....95
3.1.2.3 β-TrCP recognition of CDC25....95
3.1.2.4 β-TrCP also recognises DSG-like motifs....97
3.1.3 Conservation of mammalian DSG regulators in *C. elegans*....97
3.1.3.1 LIN-23 and CUL-1 function during cell proliferation in *C. elegans*....100
3.1.3.2 SKR-1 functions during cell proliferation in *C. elegans*....101
3.1.4 Hypothesis and aims....101
3.1.4.1 Introduction to RNAi in *C. elegans*....102
3.2 Results....104
3.2.1 RNAi to identify negative regulators of CDC-25.1....104
3.2.2 *lin-23* RNAi mimics the tissue-specific phenotype of *cdc-25.1(ij48)*....108
3.2.3 SCF members control proliferation of intestinal cells through S46 in CDC-25.1....111
3.2.3.1 Strain generation to visualize intestinal cells....111
3.2.3.2 Analysis of intestinal cell numbers....111
3.2.4 *gsk-3* and *apr-1* act independently of *cdc-25.1(ij48)*....113
3.2.5 Cell lineage analysis (by Dr. J. Cabello)....113
3.2.5.1 Cell lineage after *lin-23* RNAi....113
3.2.5.2 Cell lineage after *gsk-3* RNAi....114
3.2.5.3 Cell lineage summary....115
3.2.6 *gsk-3*-mediated extra intestinal cells requires *wrm-1*....117
3.2.7 CDC-25.1 protein levels in the embryo are dependent on S46....118
3.2.8 CDC-25.1(S46F) protein levels are increased in all early embryonic blast cells....120
3.2.9 LIN-23 and CUL-1 regulate CDC-25.1 abundance in all blast cells through S46....125
3.2.10 GSK-3 does not stabilise CDC-25.1 through S46....125
3.3 Discussion....126
3.3.1 *lin-23* and *cul-1* act through the *cdc-25.1(ij48)* allele....126
3.3.1.1 *skr-1* RNAi is synergistic to the *cdc-25.1(ij48)* allele....127

3.3.2 *lin-23* RNAi mimics the *cdc-25.1(ij48)* allele 129
3.3.2.1 Mild *lin-23* RNAi affects primarily intestinal cell proliferation 130
3.3.2.2 LIN-23 regulates CDC-25.1 protein levels through S46 130
3.3.3 CDC-25.1(S46F) is elevated in all embryonic blast cells 131
3.3.4 CDC-25.1 S46 regulation is not tissue-specific 132
3.3.4.1 Is a downstream molecule limiting in non-intestinal tissues? 132
3.3.4.2 Identification of CDC-25.1 downstream partners 133
3.3.4.3 Are additional negative regulators present in non-intestinal tissues? 134
3.3.5 GSK-3 is not the kinase acting on S46 in CDC-25.1 135
3.3.5.1 *gsk-3* RNAi phenotype is novel 135
3.3.5.2 *apr-1* and *wrm-1* RNAi induce extra intestinal cells similar to *gsk-3* RNAi 136
3.3.6 Conclusion 137
Chapter 4 138
4 CDC-25.1 S46 may be crucial for LIN-23 binding 139
4.1 Introduction 139
4.1.1 *C. elegans* SCF components 139
4.1.2 Hypothesis and aims 142
4.2 Results 144
4.2.1 Characterisation of CDC-25.1A and B antibodies 144
4.2.1.1 Setting up healthy embryo preparations 144
4.2.1.2 CDC-25.1 is phosphorylated in embryos 145
4.2.1.3 Characterisation of anti-CDC-25.1 antibodies for immunoprecipitation 147
4.2.2 Generation of a new anti-CDC-25.1 antibody 148
4.2.3 Generation of anti-LIN-23 antibodies 149
4.2.4 Generation of tagged CDC-25.1 in intestinal cells 150
4.2.4.1 Zygotic expression of untagged *cdc-25.1* causes extra intestinal nuclei 153
4.2.4.2 LAP-tagged CDC-25.1 interacts with LIN-23 in the embryo 155
4.2.5 CDC-25.1 physically interacts with LIN-23 in embryos 157
4.2.5.1 The *lin-23::FLAG-TY* allele causes elevated CDC-25.1 levels and hyperplasia 158
4.2.6 CDC-25.1 S46 is crucial for LIN-23 binding in embryos 159
4.3 Discussion 160
4.3.1 Setting up the biochemical assay to study CDC-25.1 interaction to LIN-23 160
4.3.1.1 Testing of anti-CDC-25.1 peptide antibodies 160
4.3.1.2 Purifications of LAP-tagged CDC-25.1 161
4.3.1.3 Purification strategies to pull down LIN-23 161
4.3.2 CDC-25.1 interacts with endogenous LIN-23 in *C. elegans* embryos 162
4.3.3 CDC-25.1 S46 is crucial for LIN-23 binding 163
4.3.3.1 CDC-25.1 is phosphorylated in embryos 165
4.3.4 Overexpression of CDC-25.1 causes hyperplasia 166
4.3.4.1 Zygotic expression of CDC-25.1 166
4.3.4.2 Developmental timing and severity of CDC-25.1 effects 167
4.3.4.3 A chromosomally integrated *lin-23* transgene causes hyperplasia of the intestine 168
4.3.5 Conclusion 169
Chapter 5 170
5 CDC-25.1 tissue specificity 171
5.1 Introduction 171
5.1.1 *cdc-25.1* and *lin-23* function during germline development 172
5.1.2 Hypothesis and aims 173
5.2 Results 175
5.2.1 LIN-23 maternal function during intestinal cell proliferation 175

5.2.2 LIN-23 post-embryonic localisation 178
5.2.3 A *lin-23::FLAG-TY* allele rescues *lin-23* germline defects 178
5.2.4 LIN-23 does not regulate CDC-25.1 in the germline 182
5.3 Discussion 184
5.3.1 Zygotic versus maternal *lin-23* function 184
5.3.2 LIN-23 localisation 186
5.3.3 LIN-23 does not regulate CDC-25.1 in the germline 186
5.3.4 Conclusion 187
Chapter 6 189
6 LIN-23 localisation in the early embryo 190
6.1 Introduction 190
6.1.1 Hypothesis and aims 190
6.2 Results 190
6.2.1 LIN-23 is ubiquitously expressed in embryos 190
6.2.2 LIN-23 embryonic localisation is dynamic 191
6.2.3 LIN-23 influences the CDC-25.1 localisation 195
6.3 Discussion 197
6.3.1 LIN-23 expression in embryos 197
6.3.1.1 LIN-23 influences zygotically expressed CDC-25.1 localisation 198
6.3.1.2 How to set up a system to analyse the localisation of a LIN-23/CDC-25.1 complex 199
6.3.2 LIN-23 localisation is dynamic during the cell cycle 200
6.3.2.1 Further LIN-23 functions in the embryo? 201
6.3.2.2 Does LIN-23 function during centrosome duplication? 201
6.3.2.3 Does LIN-23 function during metaphase-to-anaphase transition? 202
6.3.3 Conclusion 203
Chapter 7 204
7 LIN-62 and CDC-25.1 interaction 205
7.1 Introduction 205
7.1.1 Hypothesis and aims 208
7.2 Results 209
7.2.1 *lin-62(ij52)* and *cdc-25.1(ij48)* genetic interaction 209
7.2.2 *lin-62(ij52)* does not affect the stability of CDC-25.1 in embryos 212
7.2.3 *lin-62(ij52)* mapping 215
7.3 Discussion 216
7.3.1 *lin-62* mapping 216
7.3.2 *lin-62(ij52)* is synergistic to *cdc-25.1(ij48)* 216
7.3.3 LIN-62 does not stabilise CDC-25.1 217
7.3.3.1 Possible functions of LIN-62 217
7.3.4 Conclusion 219
Chapter 8 220
8 Final discussion 221
8.1 Summary of Results 221
8.1.1 LIN-23 controls intestinal cell proliferation through S46 in CDC-25.1 in the embryo 221
8.1.2 *gsk-3*, *apr-1* and *wrm-1* RNAi cause extra intestinal cells independently of the *cdc-25.1(ij48)* allele 222
8.1.3 *lin-62(ij52)* does not act through the *ij48* site in *cdc-25.1* 223
8.2 Discussion 223
8.2.1 CDC-25.1 overexpression causes hyperplasia 223
8.2.2 S46 is vital for CDC-25.1 regulation 224
8.2.2.1 *gsk-3* and *lin-62(ij52)* do not act through *cdc-25.1(ij48)* 225
8.2.3 Tissue specificity 226
8.2.3.1 Are negative regulators of the cell cycle limiting in the intestine? 226

8.2.4 Function of *cdc-25.1*, *gsk-3* and *lin-23* in the endoderm 227
8.2.5 Is cyclin D involved in cell cycle exit? 228
8.2.6 Role of CDC25 in human malignancies 229
8.2.6.1 Overexpression of CDC25 in human malignancies 229
8.2.6.2 β-TrCP/CDC25 in human malignancies 230
8.3 Future Perspectives 232
8.3.1 Does the intestinal cell cycle exit depend on cyclin D? 232
8.3.2 Identification of negative regulators of non-intestinal tissues 232
8.3.3 Identification of the kinase that regulates S46 in CDC-25.1 233
8.3.4 Discovery of novel LIN-23 targets 233
Appendices 234
References 236

List of Tables

Table 2.1 Common vectors and plasmid clones. 50
Table 2.2 Vector oligonucleotides. 51
Table 2.3 *cdc-25.1* oligonucleotides. 51
Table 2.4 *lin-23* oligonucleotides. 52
Table 2.5 RNAi oligonucleotides. 52
Table 2.6 *E. coli* strains. 53
Table 2.7 Common *C. elegans* strains. 54
Table 2.8 *C. elegans* strains created in this study. 55
Table 2.9 Primary antibodies. 56
Table 2.10 Secondary antibodies. 56
Table 2.11 Cycling parameters for PCR amplification. 58
Table 2.12 Concentration of antibiotics for selective *E. coli* growth. 60
Table 2.13 SDS polyacrylamide gel composition. 63
Table 2.14 Growth conditions for protein expression in *E. coli*. 65
Table 2.15 Buffers for HIS_6 and GST fusion proteins. 66
Table 2.16 Lysis conditions for insoluble proteins. 67
Table 2.17 *E. coli* RNAi clones. 78
Table 2.18 Example of CDC-25.1 fluorescence intensity quantification. 88
Table 2.19 Spreadsheet for analysis of CDC-25.1 fluorescence intensities. 90
Table 3.1 *lin-23* RNAi affects different *C. elegans* strain backgrounds equally. 109
Table 3.2 Quantification of intestinal nuclei in *cdc-25.1(+)* (JR1838) and *cdc-25.1(ij48)* (IA530) strains with or without gene-specific RNAi. 112
Table 3.3 *gsk-3* double RNAi with *apr-1* and *wrm-1* in a *cdc-25.1(+)* (JR1838) strain. .117
Table 3.4 *gsk-3* double RNAi with *bar-1* and *hmp-2* in a *cdc-25.1(+)* (JR1838) strain. ..118
Table 3.5 Comparative analysis of CDC-25.1 protein levels in the early embryo by immunostaining. 123
Table 3.6 CDC-25.1 protein levels by immunostaining after gene-specific RNAi compared to control RNAi. 126
Table 4.1 Various experimental conditions to precipitate endogenous CDC-25.1 from embryonic extracts using anti-CDC-25.1A or B antibody. 148
Table 4.2 Intestinal cell number of *C. elegans* strains zygotically expressing *cdc-25.1*. .151
Table 4.3 Hyperplasia of the intestine caused by the *lin-23::FLAG-TY* allele. 158
Table 5.1 Comparison of genotype with phenotype of IA568 embryos. 176
Table 7.1 Embryonic lethality of IA577 and IA575. 210
Table 7.2 A genetic cross between *lin-62(ij52)* and *cdc-25.1(ij48)*. 211
Table 7.3 Comparison of intestinal nuclei of *lin-62(ij52)* and *cdc-25.1(ij48)* single and double mutants. 212
Table 7.4 Three-factor mapping of *lin-62(ij52)* with *unc-8(e49) dpy-20(e1282)*. 215
Table 8.1 Detailed quantification of CDC-25.1 and CDC-25.1(S46F) protein levels after immunostaining. 234

List of Figures

Figure 1.1 *C. elegans* anatomy and development. 23
Figure 1.2 Timeline of *C. elegans* embryogenesis....25
Figure 1.3 *C. elegans* endoderm development....28
Figure 1.4 Schematic representation of *C. elegans* endoderm specification. 30
Figure 3.1 CDC-25.1 and GSK-3 protein alignments....99
Figure 3.2 *C. elegans* excess endoderm phenotypes....106
Figure 3.3 *lin-23* RNAi mimics the *cdc-25.1(ij48)* intestine-specific hyperproliferation phenotype. 110
Figure 3.4 Cell lineage analysis 116
Figure 3.5 *lin-23* but not *gsk-3* RNAi enhances CDC-25.1 stability in *C. elegans* embryos. 121
Figure 3.6 Elevated CDC-25.1 protein levels in the early embryo. 122
Figure 3.7 Quantification of CDC-25.1 fluorescence in embryos after indirect immunostaining against CDC-25.1. 124
Figure 3.8 The 'limiting pool' model....134
Figure 4.1 Schematic representation of the SCF complex. 141
Figure 4.2 Characterisation of CDC-25.1 and LIN-23 antibodies. 146
Figure 4.3 Expression of *elt-2::LAP::cdc-25.1* in *C. elegans* adults and embryos. 152
Figure 4.4 Expression of untagged *cdc-25.1(+)* or a *lin-23::FLAG-TY* allele cause hyperplasia of the intestine....154
Figure 4.5 CDC-25.1(S46F) is crucial for LIN-23 interaction in *C. elegans* embryos....156
Figure 5.1 *lin-23* null mutant adults exhibit extra intestinal nuclei during postembryogenesis. 177
Figure 5.2 Localisation of LIN-23 in the adult hermaphrodite. 180
Figure 5.3 A *lin-23::FLAG-TY* allele rescues *lin-23* null sterility and causes embryonic death. 181
Figure 5.4 LIN-23 does not control CDC-25.1 protein levels in the *C. elegans* germline. 183
Figure 6.1 LIN-23 localisation during *C. elegans* embryogenesis....193
Figure 6.2 LIN-23 localisation changes during the cell cycle in early embryos....194
Figure 6.3 LAP::CDC-25.1 localisation is dependent on S46 and LIN-23. 196
Figure 7.1 Model for tissue-specific cell cycle regulation. 206
Figure 7.2 Analysis of *lin-62(ij52) cdc-25.1(ij48)* mutants. 214

This thesis is dedicated to F.S. (1973 - 2000)

Patientia tua fortitudinem meam est

Acknowledgements

The work presented here was conducted in the laboratory of Dr. I.L. Johnstone, who is acknowledged for corrections on this thesis. I am particularly indebted to the Wellcome Trust for providing me the funding for this project. A big thanks to Bill Cushley for his encouragement and the open door for conversations on various aspects of my PhD and my assessors Marshall Stark and Stephen Goodwin for listening to my outbursts on the *C. elegans* cell cycle. In addition, I'd like to thank Marshall Stark, Luke Chamberlain, Darren Monckton, Bill Cushley, Adrienne Edkins, Liz Rideout and Megan Neville for corrections on various parts of this thesis. Richard Wilson is acknowledged for his fundamental help on statistics and various members of the scientific community (including the Goodwin, Bryant, Stark, Gray and Cushley laboratories) for providing me with reagents, strains or allowing me to use their equipment. I am incredibly grateful for the technical advice from Iain Cheeseman (USA) for setting up *C. elegans* biochemistry in the lab. Thanks to Peter Askjaer (Seville) and Scott Kuersten (Houston) for discussing technical issues, Jane Shingles (Leeds) for her kind help with bombardments and Graham Hamilton (Glasgow) for computing advice. The hospitality of the Goodwin and McInerny labs is acknowledged. My great appreciation goes to the 4-Year Wellcome Students in Glasgow for providing a friendly community atmosphere. I am delighted to have been part of the '2003-cohort', who exemplified that scientific ambition, respect and support for each other are not mutually exclusive. A special thanks to Liz and Jana for their friendship, their interest in my research, the chats about life and lots of laughs together, Mridu for sharing the same taste, Adrienne, Colm, Stephen and Sam for the hikes and common interests in pub-crawls and Stephen for sharing a flat and introducing me to Hollywood. I am also very appreciative to my flatmate Amber for keeping me in the gossip line and teaching me how to cook Chinese food. This page would not be complete without me giving attribution to the magnificent support from my 'Scottish family' Margaret, Dominique and Phil who have made me feel very welcome during all these years of my PhD. The Wednesday dinners, the BBQ's (when the sky permitted), the parties, and the Texas Hold'em poker nights will certainly be missed. A big hug goes to Henk for the relentless encouragement and keeping my spirits up. Ein weiteres Dankeschön geht an meine Freunde in Deutschland und besonders meine Familie für ihre Unterstützung.

Author's declaration

The research presented in this thesis is my own work except where otherwise stated. The thesis contains unique work and has not, in whole or in part, been submitted for any other degree.

Alexandra Segref

May, 2007

Definitions

aa	amino acid
APC	adenomatous polyposis coli
APC/C	anaphase-promoting complex/cyclosome
APR	APC-related
C	mesectoderm precursor
CDC	cell-division cycle
CDK	cyclin-dependent kinase
CKI	cyclin-dependent kinase inhibitor
CK1	casein kinase 1
DNA	deoxyribonucleic acid
E	endoderm precursor
EMS	mesendoderm precursor
cDNA	complementary deoxyribonucleic acid
F1, 2 or 3	first, second or third filial generation
GFP	green fluorescent protein
GSK	gycogen synthase kinase
L1, 2, 3 or 4	first, second, third or fourth larval stage
LIN	abnormal cell lineage

mRNA	messenger RNA
MOM	more mesoderm
MS	mesoderm precursor
n.s.	not significant
OD	optical density
PCR	polymerase chain reaction
POP	posterior pharynx defective
RT-PCR	reverse transcriptase-PCR
RNA	ribonucleic acid
RNAi	ribonucleic acid-mediated interference
β-TrCP	beta-transducin repeat-containing protein
SCF	SKIP1/CULLIN1/F-Box
s.d.	standard deviation
SKN	skin excess
SKR	SKP1 related
WRM	worm armadillo
WB	Western blot
WT	wild-type

C. elegans mutant phenotypes:

dumpy (Dpy), uncoordinated (Unc), abnormal cell lineage (Lin)

Measurements

Amp	ampere
bp	base pair
cm	centimetre
g	value of acceleration due to gravity
hr	hour
kb	kilobase
kDa	kilodalton
L	litre
M	molar
Mb	megabase
mg	milligram
min	minute
ml	millilitre
mm	millimetre
mM	millimolar
ng	nanogram
nm	nanometre
nM	nanomolar
rpm	revolutions per minute

sec	second
V	volt
µg	microgram
µl	microlitre
µm	micrometre
°C	degree Centigrade
%	per cent

Chapter 1

INTRODUCTION

1 Introduction

1.1 Why study *C. elegans*?

The correct integration of cell proliferation with developmental pathways is vital for the generation of multicellular organisms including humans. Though studies on cell proliferation in single cell organisms, such as yeast or mammalian tissue culture cells, have provided fundamental insights into the nature of cell division, clearly they cannot answer how cell division is integrated into the development of a whole multicellular organism. Questions that arise are: how is cell growth, cell division and differentiation co-ordinated to create an organism and to maintain tissue homeostasis? How are endogenous cell proliferation pathways integrated with external signals? Clearly, these are big questions and cannot be answered in a single set of experiments. However, detailed questions as to how proliferation of a single cell lineage of any multicellular organism is controlled will provide a significant piece of information to disentangle the puzzle.

The nematode *C. elegans* is used as a genetic model organism to elucidate the integration of cell proliferation with development in a whole model organism, because it has multiple features, which make it a powerful tool for investigative research (Riddle et al., 1997). It is easy to culture and can be raised in the laboratory on a diet of *Escherichia coli*. Furthermore, it has a rapid life cycle and its profuse growth permits the large-scale production of several million animals. The development of a single animal into a ~1 mm worm is completed within three days and one adult hermaphrodite produces about 300 progeny through self-fertilisation. Its small size allows most assays to be carried out in Petri dishes or in liquid culture, and large-scale screening can even be performed in Microtiter plates. Importantly, the worm is transparent and the use of *in vivo* fluorescence markers allows the analysis of cellular processes, such as cell proliferation during embryogenesis, in the living animal. Additionally, *C. elegans* is the first multicellular organism for which the complete genomic sequence has been unravelled in 1998 (The *C. elegans* Sequencing Consortium, 1998) and this organism is becoming increasingly popular as a biological model system to study numerous aspects of cellular proliferation and development. This in part evolves from the fact that many *C. elegans* genes have considerable homology to mammalian counterparts, some of which have been associated with human disease states (Kamath et al., 2003; Rubin et al., 2000; The *C. elegans* Sequencing Consortium, 1998; Tu et al., 2006). The significance of *C. elegans* research was also recognised by the Nobel Prize awards to *C. elegans* researchers: S. Brenner, J.

Sulston and H.R. Horvitz in 2002 for their findings on the genetic regulation of organ development and programmed cell death and furthermore in 2006 to C.C. Mello and A.Z. Fire for their discovery of gene silencing by double-stranded RNA (RNAi). Their contributions have been widely acknowledged as a major break-through in medical research with the discovery of genes involved in apoptosis and the ability to knock down genes using double-stranded RNA interference (Nobelprize.org, 2007).

Intriguingly, the entire cell lineage of the worm, which comprises the timing, location and ancestral relationship of all cell divisions during embryonic and post-embryonic development, is traced and largely invariant from one animal to the next (Sulston and Horvitz, 1977; Sulston et al., 1983). Thus, it is possible to observe the origin and behaviour of a single cell throughout the development of the worm. Therefore, *C. elegans* provides an excellent model system to study cell proliferation during development.

1.1.1 The phylogenetic features of C. elegans

C. elegans is a free-living organism of the phylum Nematoda and is classified to the terrestrial form of Secernentea belonging to the order Rhabditida and family of Rhabditidae. Members of the phylum Nematoda are diverse and have adapted to inhabit many types of marine and terrestrial environments, however despite their different life styles they have maintained a common body shape. Like all nematodes, the basic body plan of *C. elegans* consists of two concentric tubes separated by a pseudocoelomic space, the gonad. The inner tube consists of the intestine, whereas the outer tube comprises the collagenous cuticle, the hypodermis, musculature and nerve cells (Wood, 1988b).

1.1.2 *The biology of C. elegans*

C. elegans is a simple organism that feeds primarily on bacteria and reproduces with a life cycle of only three days at optimal temperatures. The predominant sex is hermaphrodite, which can produce both oocytes and sperm. Hermaphrodites are able to self-fertilise or cross-fertilise with infrequently occurring males. Both, hermaphrodites and males are approximately 1 mm in length and 70 μm in diameter and can be easily distinguished under the light microscope (Riddle et al., 1997). The body wall and egg shell of *C. elegans* are transparent, which allows the precise observation of developmental processes and has contributed to the identification of exact developmental patterns (Sulston and Horvitz, 1977; Sulston et al., 1983). The time from embryogenesis to hatching comprises about 14 hours post-fertilisation. During this time about 550 cells are generated, such that the newly

hatching larva consists of 558 cells, which increase to 959 in the adult hermaphrodite and 1031 in the adult male and are invariant from one animal to the next (Sulston and Horvitz, 1977; Sulston et al., 1983). All juvenile worms proceed through four larval stages (L1 to L4) and transition between the stages, termed moult, is characterised by the shedding of the old cuticle and production of a new one. A fifth form of larval stage, the dauer larva, has evolved as a means of long-term survival under suboptimal environmental conditions, such as lack of food or too high population density. When optimal growth conditions resume, the dauer larva moults to L4 and continues normal development through adulthood (Riddle, 1988).

1.1.3 The C. elegans genome

The genome of *C. elegans* comprises an approximately 100-megabase sequence, which encodes 19735 predicted protein-coding genes and more than 1300 non-coding RNA genes (Hillier et al., 2005; The *C. elegans* Sequencing Consortium, 1998). These are placed on five autosomes and one sex chromosome. The genome of wild-type N2 Bristol hermaphrodites consists of a diploid set of autosomes and two sex chromosomes, whereas males possess 11 chromosomes comprising five pairs of autosomes and one sex chromosome. The hermaphrodite is the predominant form and males arise spontaneously through chromosomal non-disjunction of the X chromosome during meiosis (Wood, 1988b). More than 40% of *C. elegans* genes show homology to other eukaryotes (Kamath et al., 2003) and many have been implicated in human diseases, such as cancer, cardiovascular or neurological disorders (Kamath et al., 2003; Rubin et al., 2000). 22% of *C. elegans* genes with homology to human disease genes are essential for *C. elegans* viability (Tu et al., 2006).

1.1.4 C. elegans anatomy

The complete *C. elegans* anatomy is known, mainly as the result of electron micrographs of serial sections. Furthermore, the acquired knowledge of the cell division timing within each tissue contributed to the complete assignment of the *C. elegans* anatomy (Sulston et al., 1983). An introduction to the *C. elegans* anatomy is summarised below (mainly according to (White, 1988), see Figure 1.1, A). The cuticle forms the outermost surface of *C. elegans* and functions to maintain the body shape of the worm. It is mainly composed of collagen that is synthesised and secreted by the underlying hypodermis. A series of circumferential ridges (annuli) run along the length of the cuticle and two longitudinal ridges (alae) run along the lateral surface of the L1 larva and the adult worm. These alae

are synthesised by a specialised set of hypodermal cells, the seam cells. The hypodermis that is underlying the cuticle is syncytial, arising by cell fusion during development, and is generally divided into four groups, the main body syncytium (hyp-7), the seam cells, the hypodermal cells of the head and tail, and the interfacial hypodermal cells. The main function of the hypodermis is the secretion of the cuticle and elimination of cells that undergo programmed cell death. A basement membrane separates the hypodermis from the underlying body wall muscles, which are arranged into four stripes running the length of the animal.

The nervous system consists of 302 neurons in the adult hermaphrodite. It has a simple mainly unbranched morphology where processes are organised as bundles that run longitudinally along the ventral and dorsal midline of the animal. A nerve ring of circumferential bundles of processes surrounding the pharynx connects to the preanal ganglion in the posterior of the animal through a ventral cord that extends the length of the animal. The inner surface of the nerve ring comprises axons of motor neurons whereas the outside connects to muscle cells. Hence, the nerve ring functions to integrate sensory information from the head region to the body wall muscle cells.

C. elegans feeds through a pharynx in the anterior, which functions to ingest, concentrate and process food into the intestine. The pharynx is contained as a system of muscle-, epithelial- and nerve cells that are bounded by a basement membrane. The pharynx is connected to the intestine through a pharyngeal-intestinal valve. The intestinal cells are all generated during embryonic development. They form a tube of 20 cells that are arranged as an anterior quartet of cells (int-1) followed by eight posterior pairs of cells (int-2 to int-9) (for details see (1.2)). The major function of the intestine is to digest ingested material through secretion of digestive enzymes into the lumen and absorption of digested material. Additionally, the intestine functions to nurture the germ cells by production of yolk proteins. The intestine is connected to the rectum via an intestinal-rectal valve. The rectum is contained of a set of three muscles that are controlling excretion.

During post-embryonic development, several sex-specific structures are formed leading to the structurally distinct development of the hermaphrodite and male gonad. The *C. elegans* adult hermaphrodite germline is a bilobed organ that expands anteriorly and posteriorly from the centre of the animal. Each gonad arm forms a U shaped structure that originates from a distal ovary into a loop that is connected to the oviduct followed by the spermatheca, the spermathecal valve and the uterus. The ovary consists of a germline syncytium where individual germline nuclei are generated that are each surrounded by a

nuclear membrane but share a common cytoplasm (Hirsh et al., 1976). The germ cell nuclei are kept in a mitotic stage, due to the mitogenic influence of the distal tip cell present at the distal end of each ovary (Kimble, 1981). As the mitotic germ cells progress towards the oviduct they enter the meiotic cycle and complete cellularisation. The first 40 germ cells, generated during the fourth larval stage, differentiate into 150 sperm whereas the remainder develop into oocytes (Hirsh et al., 1976; Ward and Carrel, 1979). The germ cell nuclei present in the loop are found in the pachytene stage and are kept in the diakinesis stage of meiosis I in the oviduct (Hirsh et al., 1976). As the oocytes mature and ovulate they enter the spermatheca where fertilisation occurs (McCarter et al., 1997; Ward and Carrel, 1979). The meiotic divisions complete before entry into the uterus (McCarter et al., 1999) where embryogenesis initiates.

C. elegans males contain a specialised tail, the copulatory bursa, that contains specialised muscles, neurons and hypodermal structures required for mating (Sulston et al., 1980). Males do not contain a rectum, but instead have a cloaca in the posterior ventral region of the animal. The male gonad is a single lobed U-shaped structure that consists of the testis, the seminal vesicle and the vas deference. The testis contains two distal tip cells, which maintain the germ cells in mitosis. All germ cells are connected through a rachis and as they enter into the seminal vesicle proceed through two meiotic divisions to form spermatids, which are stored in the seminal vesicle and are released via the vas deference and cloaca upon copulation (Hirsh et al., 1976).

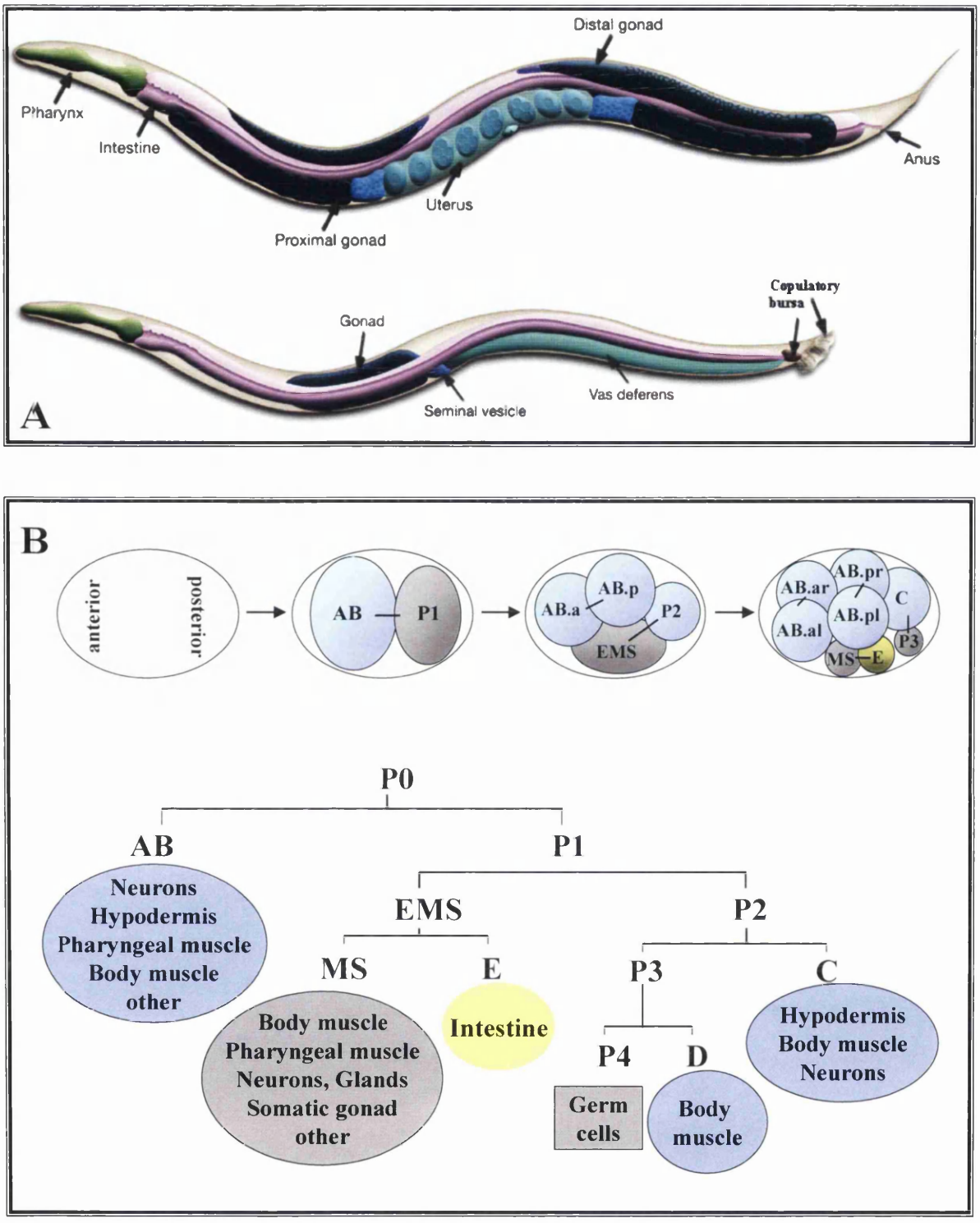

Figure 1.1 *C. elegans* anatomy and development. A) Anatomy of the *C. elegans* hermaphrodite (top) and male (bottom). Adapted from (Altun, 2005). **B)** Formation of founder cells during *C. elegans* early embryogenesis. Top: Formation of anterior-posterior polarity through the first mitotic cleavage of the zygote into AB and P1. Subsequent cleavages of P1 into EMS and P2 provide the progenitor for endoderm (E). Adapted from (Gilbert, 2003), bottom: lineage tree of the five somatic founder cells AB, MS, E, D, C and the germ line precursor P4 and their corresponding cell fates. Adapted from (Sulston et al., 1983).

1.1.5 C. elegans embryogenesis

Embryogenesis, from fertilisation to hatching, takes about 14 hours at 20°C and is commonly divided into three stages: 1) zygote formation and determination of founder cells, 2) gastrulation and 3) morphogenesis. One important feature during early embryogenesis is the formation of five somatic founder cells and a germ line precursor through asymmetric cleavages (Figure 1.1, B). The somatic founder cells, termed AB, MS, E, C and D produce ectoderm (nervous tissue and hypodermis), pharynx (AB), mesoderm (MS), endoderm (E), mesectoderm (C) and body-wall muscles (D), respectively. The germline precursor is termed P4 and a sister blastomere of D.

After fertilisation in the spermatheca, the maternal pronucleus proceeds through the final stages of meiosis I and II and extrudes two polar bodies in the anterior. At this point the eggshell becomes insoluble to most solutes through the synthesis of a vitelline membrane. Turbulent cytoplasmic movements together with contractions of the anterior cell membrane are followed by the initiation of a pseudo-cleavage furrow, which subsequently retracts. The egg pronucleus then moves towards the posterior end of the zygote to meet the sperm pronucleus. Upon meeting, a 90° rotation occurs and the nuclear envelopes break down. The formation of a mitotic spindle initiates the first asymmetric mitotic cleavage along the anterior-posterior axis into the two founder cells AB and P1. During the second division, AB divides equatorially and P1 transversely to produce EMS and P2. Further cleavages result in the formation of E and MS from EMS and P3 and C from P2. P3 further divides to give rise to P4 and D (Figure 1.1, B). Gastrulation is initiated around 130 minutes after fertilisation when the first two E cells move from the ventral side to the centre of the embryo. This time roughly coincides with the delivery of the egg to the exterior environment of the hermaphrodite. The inward movement of the two E cells creates a ring blastopore and movement of the P4 blastomere to the blastopore follows. Mesodermal cells subsequently move inward from the anterior side and are followed by the D, C and AB cells. Further cell divisions and movements occur until around 350 minutes post-fertilisation, where cell proliferation ceases and morphogenesis begins. During this time the round egg develops into an elongated cylindrical worm that hatches at about 800 minutes post-fertilisation (see Figure 1.2; for a detailed description of embryogenesis see (Gilbert, 2003; Wood, 1988a)

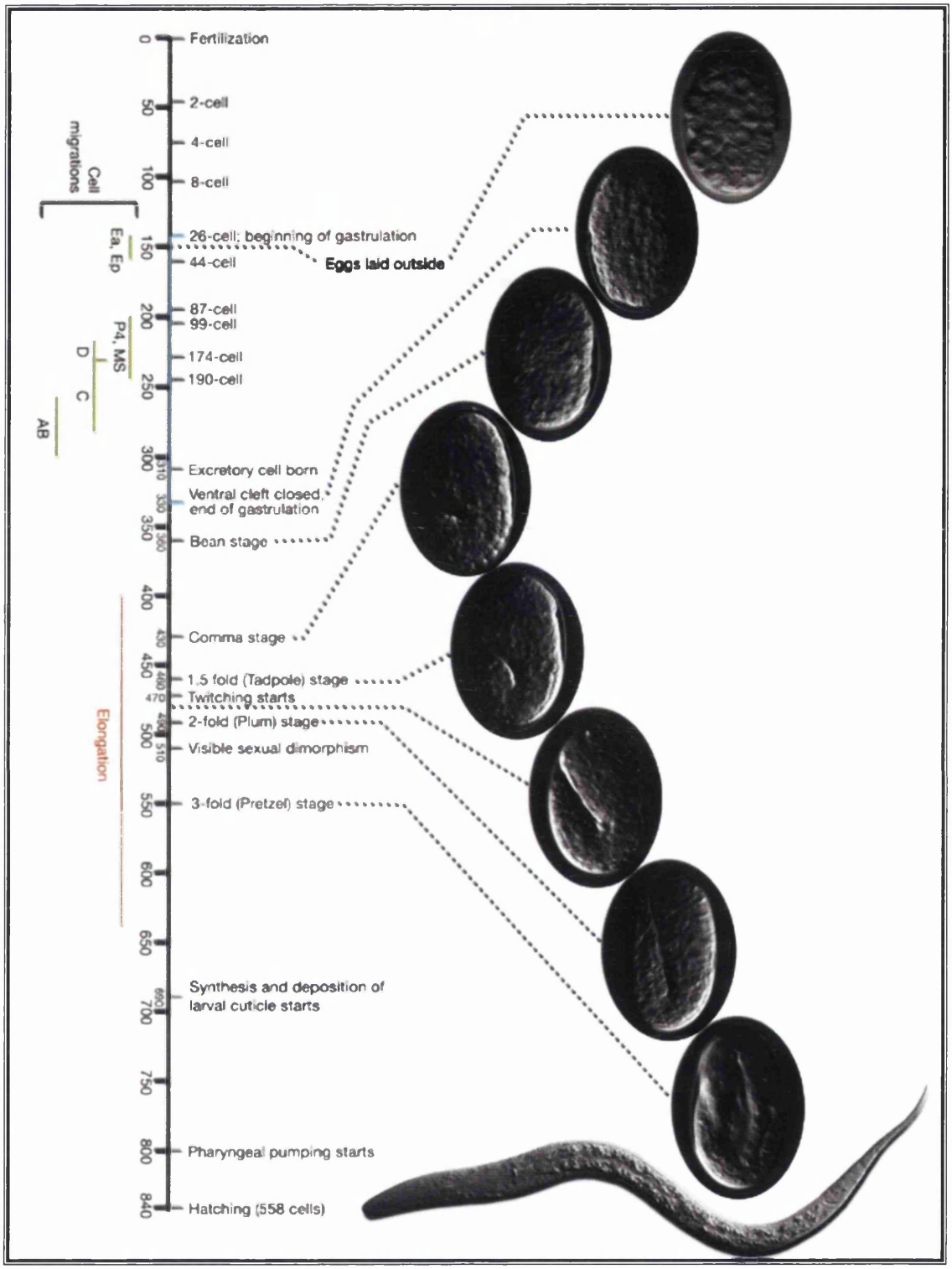

Figure 1.2 Timeline of *C. elegans* embryogenesis. Time-scale (left) of embryogenesis at 20°C from fertilisation to hatching. Developmental stages, according to the cell number, are depicted close to the right of the scale bar. To the right: Nomarski images of main developmental stages. Image from (Altun, 2005).

1.2 Development of the *C. elegans* intestine

The *C. elegans* intestine offers an excellent model system to study cell proliferation, because it only consist of 20 cells that are clonally derived from the single progenitor cell E present in the eight-cell stage embryo (Sulston et al., 1983). In the four-cell stage embryo, the asymmetric cleavage of the endomesodermal precursor EMS into MS (mesodermal precursor) and E (endoderm precursor) is one of the defining features of endoderm development and the result of an external signal of the EMS neighbouring cell P2 (for details see (1.2.2)). Once endoderm is specified, through formation of E from EMS, endoderm can develop independently of any surrounding tissues, as isolation of the E blastomere results in the formation of a complete intestine (Hermann et al., 2000; Laufer et al., 1980; Leung et al., 1999). The specification of endoderm requires also an intrinsic signal of transcriptional activation through endoderm-specific genes (for details see (1.2.1).

Intriguingly, the divisions of the endodermal cells follow a precise timing and pattern that is invariant from one animal to the next and requires both symmetric and asymmetric cleavages, as examined by (Leung et al., 1999; Sulston et al., 1983). The lineage timing of intestinal cells is depicted in Figure 1.3. The first division of E occurs at the ventral surface of the embryo, in an anterior-to-posterior direction, to generate the Ea and Ep descendants. At the 26-cell stage of embryonic development, gastrulation is initiated and the two E descendants migrate into the interior of the embryo. This migration of Ea and Ep generates a ventral cleft. Subsequently, the two E descendants divide in a left-to-right direction to create four intestinal cells. This is followed by further anterior-to-posterior divisions and cell intercalation to generate 16 intestinal cells that are evident as two rows of eight cells at around 300 minutes post-fertilisation. At this time, three anterior cells (int-2 to int-4) generate a 90° twist with respect to the remaining intestinal cells. The three anterior cells in the right row move counter-clockwise to the left, whereas the three cells on the left row move clockwise to the right. This rotation requires the LIN-12 signalling pathway (Hermann et al., 2000) and increases to a further 180° in the hatching larva (Sulston and Horvitz, 1977). Thus, in the embryo, at around 300 min post-fertilisation, the developing intestine consists of 16 cells, 12 of which undergo no further cell division. Only four cells divide further, the anterior cells in a dorsal/ventral direction to generate an anterior quartet of cells and the posterior cells in the anterior/posterior direction.

At hatching, the intestine consists of a tube of 20 cells that is arranged as an anterior quartet of cells followed by eight posterior pairs of cells (Figure 1.3). During post-

embryonic development only the 14 most posterior cells undergo one round of nuclear division early in the L1 lethargus (Sulston and Horvitz, 1977) resulting in binucleate cells. All intestinal cells undergo one round of endoreduplication at each larval moult leading to a polyploidy of 32 N in the adult worm (Hedgecock and White, 1985).

In summary, development of the *C. elegans* intestine is the result of a careful interplay of cell extrinsic and intrinsic signals. At around 300 minutes post-fertilisation, the developing intestine consists of 16 cells, of which only four undergo one further division ultimately producing 20 cells. Hence, there is asymmetry in the cell division pattern of some sister cells. To date, a vast amount of information is available that identified the external and internal signals required for endoderm formation. However, it is equally as fascinating to unscramble the mechanism controlling the regulated cell division pattern during intestinal development on a molecular level.

The Johnstone laboratory has recently identified genes regulating the highly synchronized cell divisions of the E lineage, using a standard genetic approach of performing a mutant screen to detect animals with altered numbers of intestinal nuclei, facilitated by an intestinal-specific GFP marker. This revealed the identification of two alleles, *cdc-25.1(ij48)* and *lin-62(ij52)*, both of which cause extra intestinal cells that are born during embryogenesis (Clucas, 2003; Clucas et al., 2002). CDC-25.1 acts as a general cell cycle regulator, whereas LIN-62 has not been identified to date. This study will mainly focus on the molecular characterisation of CDC-25.1 and information about CDC-25.1 will follow in this introduction. However, to facilitate an understanding of the subject, the extrinsic and intrinsic signals that specify endoderm is firstly summarised below.

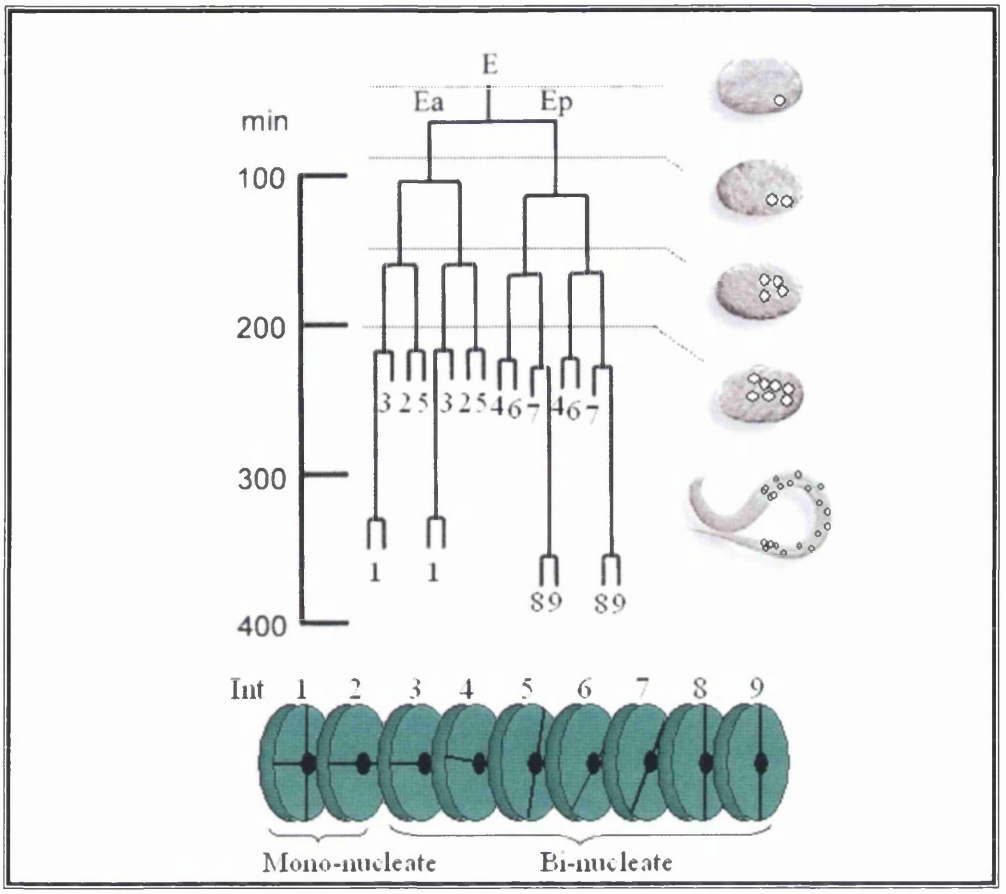

Figure 1.3 *C. elegans* endoderm development. Top: Lineage analysis of embryonic endoderm development. Vertical lines represent cleavages. Left: time after fertilisation. Between 200 and 300 minutes 16 cells are born (numbers represent the intestinal position of each cell in the fully developed intestine). Only four cells undergo one further cleavage generating four int-1, two int-8 and two int-9 cells. To the right: embryo and larva to illustrate the position of endoderm cells. White circles represent positions of intestinal nuclei in the zygote (top) and larva (bottom), 300 min does not represent the larval stage, because the time of hatching is beyond this time-scale. Bottom: schematic representation of the adult intestine. Intestinal numbers correlate with the numbers from the top lineage analysis, adapted from (Maduro and Rothman, 2002, Sulston et al., 1983, White, 1988).

1.2.1 Cell autonomous endoderm specification in C. elegans

1.2.1.1 EMS specification through SKN-1

As mentioned above, *C. elegans* intestinal development is in part specified through cell autonomous signals. Several gene products have been identified that act intrinsically to determine P1-derived somatic founder cells (for a schematic outline see Figure 1.4, A). These proteins are maternally provided and termed SKN-1, PIE-1 and PAL-1. SKN-1 (skin excess), a bZIP/homeodomain transcription factor (Blackwell et al., 1994), is essential for EMS specification as *skn-1(-)* mutants result in loss of pharyngeal and intestinal cells that are normally produced from EMS daughter cells MS and E, respectively (Bowerman et al., 1992). Instead, homozygous *skn-1(-)* mutants produce excess hypodermal cells from EMS, a fate that is normally produced from the EMS sister cell P2 (Bowerman et al., 1993; Bowerman et al., 1992). The function of SKN-1 is restricted to EMS only, though the protein is present in both EMS and P2 (Bowerman et al., 1993). This is achieved through the action of maternal PIE-1, a general transcriptional inhibitor (Batchelder et al., 1999; Seydoux et al., 1996; Tenenhaus et al., 1998), that is segregated to higher levels present in P2 (Mello et al., 1996; Seydoux et al., 1996; Tenenhaus et al., 1998) and shown to prevent SKN-1 activity in P2 (Mello et al., 1992). The C-like fate produced in EMS cells lacking *skn-1* activity is due to the presence of PAL-1, a CAUDAL-like transcription factor (Hunter and Kenyon, 1996). PAL-1 is found in all P1-derived blastomeres and necessary for the specification of C fate. In wild-type EMS cells, PAL-1 activity is masked through SKN-1 activity, thus *skn-1(-)* mutants produce a C-like fate due to the presence of PAL-1. Similarly, *skn-1/pal-1* double mutants produce no muscle cells, indicating that PAL-1 is required for C fate (Hunter and Kenyon, 1996).

However, SKN-1 protein is also present in C cells, but its activity is repressed through the action of the kinase GSK-3 (for glycogen synthase kinase, previously named *sgg-1)* present in the C blastomere (Maduro et al., 2001). Removal of both, *gsk-3* and *pal-1*, by RNAi causes C to acquire an EMS-like fate (in which Ca and Cp adopt an MS and E fate, respectively) that depends on *skn-1* activity (Maduro et al., 2001). This demonstrates that in the absence of *gsk-3* and *pal-1*, SKN-1 can activate mesendodermal targets to induce EMS fate in C. Interestingly, removal of *gsk-3* alone can give rise to E cells from an isolated P2 (Maduro et al., 2001) or C blastomere (Schlesinger et al., 1999), indicating that even in the presence of *pal-1*, but the absence of *gsk-3*, the blastomere C is able to induce endoderm probably from Cp as suggested in one study (Maduro et al., 2001).

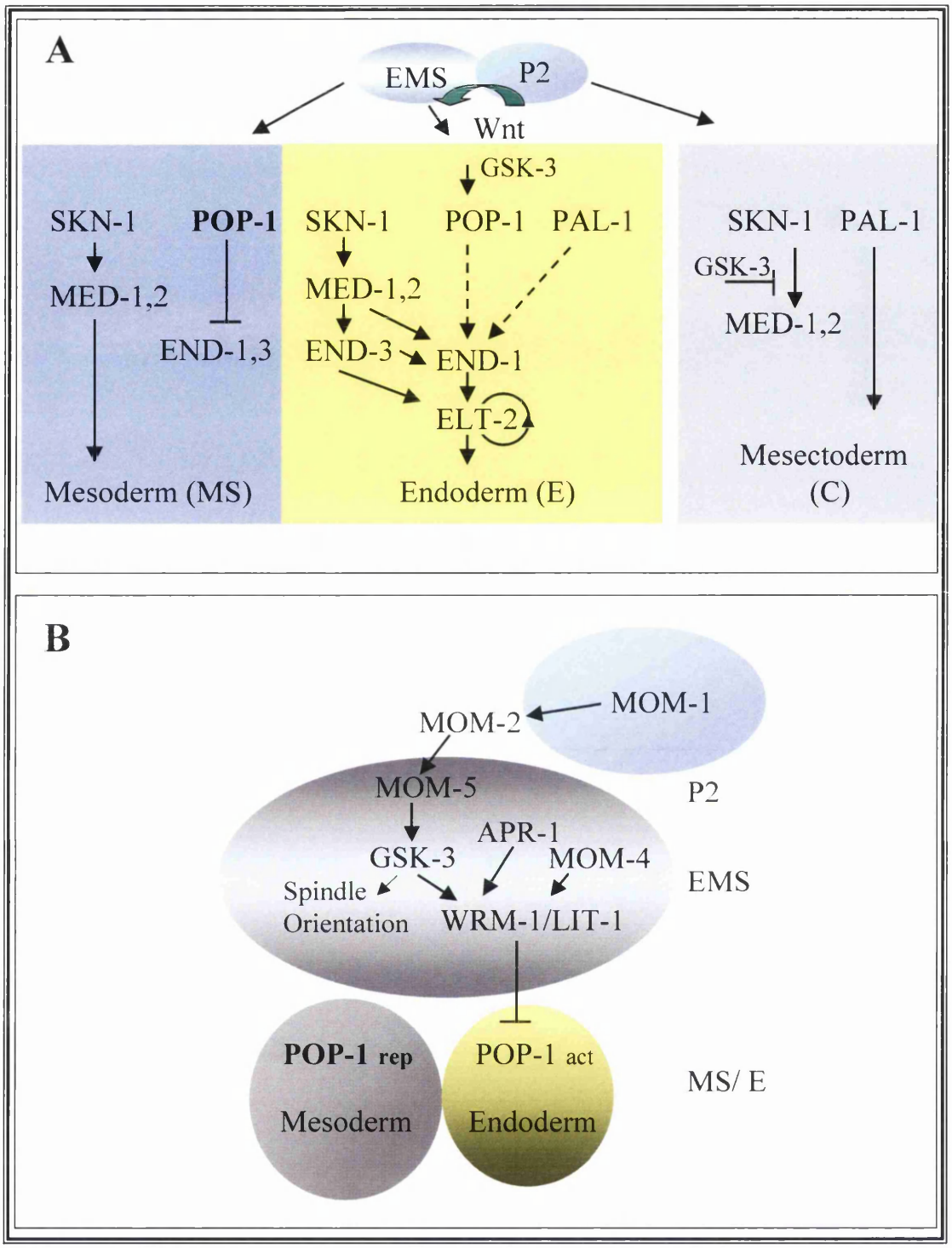

Figure 1.4 Schematic representation of *C. elegans* endoderm specification. A) Transcriptional cascade to specify endoderm. Arrow: activation, blocked arrow: inhibition. Maternal factors SKN-1, POP-1 and PAL-1 are present in EMS and P2 descendants as indicated. The anterior of EMS activates SKN-1 dependent mesodermal genes, high levels of unsignalled POP-1 represses endoderm genes resulting in MS formation. In the posterior of EMS, SKN-1 activates the *med* genes that activate the *end* genes. Wnt-signalled POP-1 can also activate *end-1* and some PAL-1 can activate the *end-1* genes (weak contribution indicated by dashed lines) producing endoderm. In the C lineage (derived from P2), SKN-1 activity is masked through the action of GSK-3, PAL-1 induces C-specific genes. **B)** The Wnt signalling pathway. MOM-1, -2 and -5 activate GSK-3 and orient the EMS mitotic spindle. GSK-3 and APR-1 induce WRM-1 nuclear localisation, whereas MOM-4 activates LIT-1. A WRM-1/LIT-1 complex phosphorylates POP-1 in E and reduces nuclear POP-1 levels. Un-signalled POP-1 in MS represses E formation and induces mesoderm. Low nuclear levels of signalled POP-1 in E activates endoderm. Details are given in the text. Adapted from (Maduro et al., 2007, Maduro et al., 2005b, Maduro and Rothman, 2002, Nakamura et al., 2005, Thorpe et al., 2000).

1.2.1.2 SKN-1 transcriptional targets vital for endoderm specification

Production of intestinal cells from EMS is in part the result of transcriptional activation of endoderm-specific genes. Each transcriptional tier is tightly integrated into a cellular division. On top of this transcriptional cascade acts the SKN-1 protein. Direct targets of SKN-1 in EMS have been identified as *med-1* and *med-2* (mesendoderm determining), two nearly identical genes. The promoters of these genes contain several SKN-1 binding sites (RTCAT) and direct binding of SKN-1 to these sites *in vitro* has been demonstrated (Blackwell et al., 1994; Maduro et al., 2001). Furthermore, removal of *med-1/2* by RNAi mimics the *skn-1(-)* mutant phenotype. Expression of the *med-1,2* mRNA is first detected in the EMS cell (Maduro et al., 2007) and a *med-1::GFP* transgenic reporter is present in the nucleus of the EMS, MS and E cells (Maduro et al., 2001). Ectopic expression of SKN-1 from a heat shock promoter causes widespread expression of MED-1::GFP (Maduro and Rothman, 2002). The *med-1/2* genes encode GATA transcription factors that recognise specific sequence elements ((A/T)GATA(A/G)) present in the 5' promoter sequence of their target substrates.

Downstream targets of the *med* genes are the *end-1* and *end-3* (endoderm determining) genes. MED-1 interacts with both *end* promoters *in vivo* and *in vitro* (Broitman-Maduro et al., 2005; Maduro et al., 2002) and ectopic MED-1 expression results in widespread expression of an END-1::GFP reporter (Maduro and Rothman, 2002). Furthermore, removal of *skn-1*, the upstream activator of the *med* genes by RNAi depletes *end-3* mRNA from the embryo (Maduro et al., 2007). Ectopic expression of *end-1* (Zhu et al., 1998) or *end-3* (Maduro et al., 2005a) can induce endoderm expression and only simultaneous removal of both *end-1* and *end-3* by RNAi results in reduction of endoderm and a conversion of E into mesectodermal C fate (Maduro et al., 2005a). The *end* transcripts are first apparent in the E blastomere and persist up to the stage when two (*end-3*) (Maduro et al., 2007) or four (*end-1*) E cells are born (Maduro et al., 2007; Zhu et al., 1997). Interestingly, at the 2E-cell stage the *end-1,3* mRNA levels are higher in the posterior Ep descendant (Maduro et al., 2007).

Intriguingly, lack of *skn-1* or *med-1,2* result only in a semi-penetrant loss-of-endoderm defect, indicating that another pathway may contribute to the specification of endoderm. Indeed, concomitant loss of *skn-1* by RNAi with *pal-1* or the TCF transcription factor *pop-1* cause a synergistic loss-of-endoderm defect. And concomitant removal of all *skn-1*, *pop-1* and *pal-1* by RNAi results in the complete loss of endoderm (Maduro et al., 2005b). Thus, POP-1 and PAL-1 can contribute to E specification. Binding of GFP::POP-1 to

transgenic *end-3* and *end-1* promoter sequences has been demonstrated *in vivo* (Maduro et al., 2002). Intriguingly, it has become evident that removal of *end-3* and *pop-1* cause the complete absence of *end-1* mRNA transcripts in the 2E-cell stage embryo and a synergistic loss of endoderm (Maduro et al., 2007). This contrasts the finding that removal of *pop-1* alone causes elevated expression of *end-1* mRNA is MS (Maduro et al., 2007) and misspecification of endoderm from the MS lineage (Lin et al., 1995). The explanation for this result is given by the fact that the EMS progenitor of the E cell receives a Wnt signal from its posterior neighbour P2 in the four-cell stage embryo. This causes E to express low levels of Wnt-signalled POP-1, whereas MS possesses high levels of un-signalled POP-1 that acts as a repressor of E fate (the Wnt signalling pathway is explained in (1.2.2.1)). Thus, END-3 and maybe PAL-1 and Wnt-signalled POP-1 can activate *end-1* transcription in E.

The transient expression of the *end* transcripts suggested the presence of other endoderm determining genes in the *C. elegans* E lineage. Indeed, with *elt-2* another GATA factor has been identified that is expressed in the intestine (Fukushige et al., 1998). ELT-2 was initially discovered through its ability to bind to the *ges-1* promoter (Hawkins and McGhee, 1995), a gut-specific esterase that is present in all terminally differentiated intestinal cells (Edgar and McGhee, 1986; Kennedy et al., 1993). The *elt-2* promoter contains several GATA binding sites (Fukushige et al., 1998) and ectopic expression of the *end-1* (Zhu et al., 1998) or *end-3* (Maduro et al., 2005a) genes result in widespread expression of ELT-2. Additionally, ectopic expression of ELT-2 results in the activation of its own promoter. ELT-2 protein is detected in the first two E descendants and persists until adulthood, thus auto-regulation can ensure constitutive expression in terminally differentiated intestinal cells (Fukushige et al., 1998). Global transcriptome analysis of intestine-specific genes revealed that GATA motifs are present in all promoters of intestine-specific genes, including digestive enzymes, stress response genes or proteases (McGhee et al., 2007).

1.2.2 External signals vital for endoderm specification

Apart from cell intrinsic regulations, cell-cell interactions have been described as essential for endoderm specification. (Goldstein, 1992) demonstrated that the EMS blastomere, isolated from an early four-cell stage embryo, gives rise to endodermal cells when it is recombined with its posterior sister cell P2, but not with the anterior sisters of EMS, termed ABa or ABp. This correlates with the finding that P1 but not AB in isolation can induce E cell fate (Priess and Thomson, 1987). Interestingly, the entire EMS blastomere

has the capability to respond to P2. When EMS is isolated from a four-cell stage embryo and its anterior half brought in contact with an isolated P2, the anterior half that would normally produce MS induces E formation (Goldstein et al., 1993). Thus, in the absence of P2 signalling the E lineage takes on the timing of cell divisions similar to the MS lineage (Goldstein, 1992; Goldstein et al., 1993). Signalling of P2 to EMS has to occur at a distinct timeframe of around nine to three minutes prior to cytokinesis in EMS in order to produce endoderm (Goldstein, 1995). Intriguingly, P2 has an intrinsic capability to induce endoderm formation. When SKN-1 activity is not repressed in the P2 blastomere, through an inactivating mutation in the transcriptional repressor *pie-1(-)*, the isolated P2 blastomere has the capability to divide into MS and E (Goldstein, 1995). Furthermore, the P2-derived signal induces a spindle rotation in the EMS blastomere resulting in anterior-posterior polarity through asymmetric cleavage of EMS in the larger MS and a smaller E blastomere that is vital for specification of the endoderm fate (Schlesinger et al., 1999).

1.2.2.1 Wnt pathway components specify endoderm

The components of this P2-EMS signal have been identified and comprise a Wnt, a MAP kinase and Src signalling pathway that converge to induce endoderm formation in EMS (for schematic outline see Figure 1.4, B). First evidence evolved from mutant screens for production of more mesoderm, which identified several maternal factors, the *mom* genes (for more mesoderm), whose loss of activity promote lack of endoderm (Rocheleau et al., 1997; Thorpe et al., 1997). In these mutants EMS produces only mesoderm instead of mesoderm and endoderm. The *mom* genes have been cloned and three genes show significant homology to members of the Wnt signalling pathway in other systems (Rocheleau et al., 1997). *mom-4* has subsequently been identified as a member of the mitogen-activated kinase (MAPK) family (Meneghini et al., 1999). Additionally, reverse genetics led to the discovery of *C. elegans wrm-1* (worm armadillo) and *apr-1* (APC-related). RNAi against *wrm-1* and *apr-1* result in loss of intestinal cells from E, instead E produces pharyngeal tissue (Rocheleau et al., 1997). *wrm-1* shows significant homology to human β-catenin (23% in the arm repeats), and *apr-1* to the human tumour suppressor gene APC (adenomatous polyposis coli, 31% in the arm repeats), respectively (Rocheleau et al., 1997). Furthermore, RNAi against a glycogen synthase kinase homologue, *gsk-3* (formally *sgg-1*), also revealed a positive function in endoderm specification from EMS (Schlesinger et al., 1999). EMS spindle orientation, that is vital for correct partitioning of the MS and E potential, is abrogated in several mutant *mom* genes and after *gsk-3* RNAi, probably accounting for some of the loss-of-endoderm potential. However, no obvious spindle defect was observed by RNAi against *mom-2*, *mom-4*, *apr-1* and *wrm-1*, indicating that

these genes are not involved in EMS spindle orientation (Schlesinger et al., 1999) and act to specify endoderm by other means.

Wnt signalling is a conserved pathway that has been described to contribute in multiple developmental processes, including cell proliferation, tissue polarisation and morphology or synaptic differentiation (Logan and Nusse, 2004). The canonical Wnt-signalling pathway results in the conversion of a transcriptional repressor TCF (T-cell factor) into an activator for expression of Wnt-specific target genes. Secretion of Wnt, a cysteine-rich glycoprotein ligand, causes cytoplasmic stabilisation of β-catenin. In the absence of Wnt, β-catenin is rapidly degraded through the action of the glycogen synthase kinase GSK3β and CK1α in complex with APC and Axin. Stabilised β-catenin then shuttles to the nucleus where it forms a complex with the transcriptional repressor TCF converting it into an activator for the transcription of Wnt-specific target genes (Han, 1997; Kikuchi et al., 2006; Logan and Nusse, 2004; Thorpe et al., 2000). Wnt target genes are very diverse and thus Wnt effects are likely to cause differential effects on target gene transcription.

In *C. elegans*, specification of endoderm fate follows a non-canonical Wnt signalling pathway. In this pathway, Wnt signalling from P2 requires the positive action of the putative destruction components GSK-3 and APR-1. RNAi against the *C. elegans gsk-3* (Schlesinger et al., 1999) and *apr-1* (Rocheleau et al., 1997) result in loss of intestinal cells from EMS. Thus, in *C. elegans* the putative β–catenin destruction components *gsk-3* and *apr-1* are positively required for endoderm induction, which contrasts the canonical Wnt pathway where the presence of the Wnt signal inactivates the GSK-3/APC destruction complex. In *C. elegans*, *wrm-1* (β-catenin) is positively required to induce endoderm, suggesting that GSK-3 and APR-1 do not act to degrade WRM-1 (Rocheleau et al., 1997). The precise mechanism by which GSK-3 and APR-1 act on WRM-1 is not known, but a recent study suggests that GSK-3 and APR-1 function are important to localise WRM-1 to the nuclear compartment in E but not MS (Nakamura et al., 2005).

1.2.2.2 The role of POP-1 in the Wnt pathway

Interestingly, a loss-of-function mutation in the TCF homolog *pop-1* results in opposing phenotypes compared to *gsk-3*, *wrm-1* or *apr-1* RNAi. In *pop-1* mutant embryos, both daughters of EMS adopt an E-like fate (Lin et al., 1995; Thorpe et al., 1997). Wnt signalling from P2 is required to induce asymmetric POP-1 localisation in MS and E. High nuclear POP-1 levels are evident in MS and low levels in E (Calvo et al., 2001; Lin et al., 1998; Lin et al., 1995; Meneghini et al., 1999; Rocheleau et al., 1997; Rocheleau et al.,

1999; Thorpe et al., 1997). A repressive function of POP-1 on endoderm fate has been illustrated. Inhibition of POP-1 activity in MS results in ectopic expression of *end-1::GFP* in MS (Calvo et al., 2001; Shetty et al., 2005). POP-1 can repress the expression of an *end-1* promoter construct in tissue culture cells, probably through the binding of the histone deacetylase HDA-1 and UNC-37. RNAi against HDA-1 results in up-regulated expression of an *end-1*::GFP reporter in MS that is increased after concomitant *unc-37* RNAi (Calvo et al., 2001).

Thus, high POP-1 levels in MS repress endoderm, whereas low POP-1 levels in E are required to release the repressive action of endoderm-specific genes in E and promote endoderm fate. POP-1 nuclear asymmetry requires the action of Wnt pathway components (Rocheleau et al., 1997; Thorpe et al., 1997). Similarly, inactivation of *pop-1* is epistatic to inactivation of other Wnt components for endoderm production (Lin et al., 1998; Rocheleau et al., 1997; Rocheleau et al., 1999). Thus, POP-1 acts as the downstream molecule for P2-derived Wnt signalling to EMS and represses E fate in MS. However, further work revealed a positive function for POP-1 in transcriptional activation of endoderm genes in E as introduced below.

LIT-1 (loss of intestine) is another member of the MAPK pathway and involved in endoderm specification. A *lit-1* mutant causes loss of intestinal cells and up-regulation of POP-1 in E cells (Rocheleau et al., 1999). Furthermore, WRM-1 (β-catenin) and LIT-1 co-expression results in WRM-1/LIT-1 complex formation that phosphorylates POP-1 in mammalian tissue culture cells (Lo et al., 2004; Rocheleau et al., 1999). Phosphorylated POP-1 redistributes into the cytoplasm when co-expressed with WRM-1 and LIT-1 in mammalian cells (Lo et al., 2004; Rocheleau et al., 1999). Furthermore, in *C. elegans* embryos phosphorylated POP-1 is exported from the nucleus likely due to the action of WRM-1 and LIT-1 that are required for the phosphorylation of POP-1 (Lo et al., 2004). However, low POP-1 protein in E alone is not responsible for the activating function of POP-1 in E compared to MS. It has become apparent that POP-1 can activate endoderm-specific genes in E. As introduced in (1.2.1.2), one downstream target of POP-1 is the *end-1* gene. When *pop-1* RNAi is performed under conditions where the upstream transcriptional regulators of *end-1* are depleted by RNAi, a complete loss of the *end-1* transcript and endoderm fate is visible, indicating that POP-1 can activate *end-1* transcription in E. Consistently, expression of an *end-1::GFP* promoter construct in endoderm cells requires the presence of POP-1, and furthermore, relies on an active Wnt signalling pathway (Shetty et al., 2005).

In addition to the Wnt and MAPK pathways, mutations of the *C. elegans* Src pathway enhance endoderm defects of Wnt pathway components that act upstream of GSK-3, WRM-1 and POP-1 (Bei et al., 2002), probably in part through its function to orient the EMS spindle (Walston and Hardin, 2006).

Thus, the Wnt, MAPK and Src pathways co-operate in *C. elegans* endoderm specification to induce anterior-posterior polarity of the endoderm progenitor EMS blastomere. This is accomplished through asymmetric cleavage of the progenitor cell EMS into a larger cell MS and a smaller cell E that differ in their distribution of nuclear POP-1 proteins levels. High nuclear POP-1 levels repress endoderm fate in MS. Wnt signalling causes WRM-1/LIT-1 to phosphorylate POP-1, resulting in POP-1 nuclear export from E. However, a fraction of Wnt-modified nuclear POP-1 in E can activate endoderm fate (see Figure 1.4 B).

To sum up, endoderm formation in *C. elegans* is a highly regulated process that requires the integration of at least two inputs, an internal transcriptional cascade that is coordinated with an external Wnt signalling pathway. Each transcriptional tier is integrated to another round of cell division. However, little data are currently available as to how cell division itself is controlled in this tissue. Gaining mechanistical insight into the proliferation of this tissue is therefore an important task.

Intriguingly, two separate *cdc-25.1* gain-of-function alleles have previously been identified by two independent laboratories that trigger a tissue-specific hyperproliferation of intestinal cells (Clucas, 2003; Clucas et al., 2002; Kostic and Roy, 2002), highlighting the importance of CDC-25.1 for controlling the regulated cell division of the intestine in the embryo. However, a precise mechanism that unravels the control of CDC-25.1 in this tissue has been lacking in these studies. The *cdc-25.1(ij48)* hypermorphic allele has been identified in the Johnstone laboratory in a genetic search for genes that control the regulated pattern of intestinal cell divisions with the aid of an intestinal-specific GFP marker (Clucas, 2003; Clucas et al., 2002). Deciphering the molecular mechanism underlying the dysregulation of *cdc-25.1(ij48)* is vital to further the understanding of CDC-25.1 control during embryogenesis and the focus of this study. Details on the known functions of CDC-25.1 will be introduced below.

1.3 Intestinal cell proliferation is controlled by CDC-25.1

1.3.1 CDC25 function in eukaryotes

CDC-25.1 belongs to the family of CDC25 dual-specific phosphatases that act as positive regulators of the cell cycle (Ashcroft et al., 1998). The founding member of this family was identified in the fission yeast *S. pombe* as a temperature sensitive mutant that resulted in cell division defects (Fantes, 1979; Russell and Nurse, 1986). Subsequently, research on CDC25 in different model systems has expanded rapidly and broadened our understanding as to how the tight regulation of CDC25 maintains a functional division cycle. The eukaryotic cell-division cycle is a conserved highly regulated multi-step process that involves the careful interplay of numerous proteins that guide the cell cycle through a precise sequence of events, terminating with the production of two separate daughter cells (reviewed in (Schafer, 1998; van den Heuvel, 2005)). Vital to this process is the specific temporal activation of cyclin-dependent kinases (CDKs) and their regulatory subunits, the cyclins, that direct the somatic cell through specific morphological stages termed G_1 (gap_1), S (DNA synthesis), G_2 (gap_2) and M (mitosis) phase. However, gap phases are typically omitted during the rapid early embryonic cell cycles in *C. elegans* (van den Heuvel, 2005).

One of the hallmarks of cell cycle control is the specific activation of CDKs at distinct cell cycle stages. CDK activity is controlled by the action of several auxiliary proteins that phosphorylate CDKs on specific tyrosine and threonine residues, resulting in either activation or inhibition of the kinase. Furthermore, binding of cyclin to the kinase is a prerequisite for kinase activation such that degradation of cyclins at specific cell cycle boundaries, through the ubiquitination pathway, further enhances the directionality of cell cycle progression (Schafer, 1998; van den Heuvel, 2005). In metazoans phosphorylation on T14 and Y15 in CDK1 results in inactivation of CDK1 (Atherton-Fessler et al., 1994; Gautier et al., 1991; Norbury et al., 1991). This is achieved by the action of WEE1 (Y15, (Mueller et al., 1995)) or MYT-1 kinase (T14, Y15, (Kornbluth et al., 1994)). The dual-specific phosphatase CDC25 acts as a positive regulator of the cell cycle by dephosphorylating the inhibitory phosphates on T14 or Y15 in CDKs (Gautier et al., 1991; Honda et al., 1993; Sebastian et al., 1993). Additionally, CDKs can regulate CDC25 function through phosphorylation creating a positive feedback loop (Hoffmann et al., 1993; Hoffmann et al., 1994; Izumi and Maller, 1993). Mammalian cells have three different CDC25 counterparts (Galaktionov and Beach, 1991; Sadhu et al., 1990) that cooperate at

different cell cycle stages (Boutros et al., 2006). Common to the CDC25 family members is a catalytic phosphatase domain present in their C-terminus. This region of the protein shares the highest homology between different family members, whereas the N-terminal part is far less conserved, suggesting it might act as a regulatory element (Sadhu et al., 1990).

1.3.2 The C. elegans cdc-25 family

The *C. elegans cdc-25* family consists of four genes, *cdc-25.1* to *cdc-25.4* that were identified by (Ashcroft et al., 1998) and are encoded on different chromosomes. *cdc-25.1*, *2, 3* and *4* are positioned on linkage group I, V, III and II, respectively and thus appear not to have arisen from gene duplication. The exon/intron structures vary greatly and the encoded proteins differ in their length. *cdc-25.1* is the largest protein comprising of 604 amino acids, whereas *cdc-25.2*, *cdc-25.3* and *cdc-25.4* encode for 480, 316 and 372 amino acids, respectively. The overall sequence homology within this gene family is quite low and mainly comprises the phosphatase domain present in the C-terminus (in case of CDC-25.1 between aa 286 - 406), where the overall identity is 31% (Ashcroft et al., 1998).

Northern blot analysis revealed low mRNA expression levels of *cdc-25.1* during the larval stages, but enhanced expression in young adult animals with proliferating germlines (Ashcroft et al., 1999). Furthermore, indirect immunofluorescence, using antibodies against CDC-25.1, revealed expression of CDC-25.1 in the two germline precursors during larval development (Ashcroft and Golden, 2002), the proliferating germline (Ashcroft et al., 1999; Clucas, 2003; Clucas et al., 2002) and in all early embryonic blast cells (Ashcroft et al., 1999; Clucas, 2003; Clucas et al., 2002; Kostic and Roy, 2002) (details on the staining are described in Chapter 5, (5.1.1)). However, the *cdc-25.4* mRNA has not been amplified and the authors suggested that it could be possible that the protein is only transiently expressed during development (Ashcroft et al., 1998). The precise expression patterns for CDC-25.2 and CDC-25.3 in the embryo remain unknown. RNAi suggests a function of CDC-25.2 during embryo (Kamath et al., 2003; Simmer et al., 2003; Sonnichsen et al., 2005) and larval development (Ashcroft et al., 1999; Kamath et al., 2003; Simmer et al., 2003). A *cdc-25.3::GFP* transgene was expressed in all embryonic nuclei beginning at the 24-cell stage (Ashcroft et al., 1999). However, RNAi against *cdc-25.3* suggests that this protein may not be essential for *C. elegans* development (Ashcroft et al., 1999). Thus, it appears that in *C. elegans* multiple *cdc-25* genes are expressed at different developmental stages and might control different aspects of *C. elegans* development.

1.3.3 CDC-25.1 functions during post-embryonic development

RNAi against *cdc-25.1* results in sterility of F1 survivors that are derived from RNAi-treated mothers (Ashcroft and Golden, 2002; Ashcroft et al., 1999; Clucas, 2003; Clucas et al., 2002). Moreover, a deletion mutant of CDC-25.1 demonstrates the importance for zygotic expression of CDC-25.1 (Ashcroft and Golden, 2002). In homozygous *cdc-25.1(nr2026)* deletion mutants, proliferation of germ cells is inhibited resulting in sterile adults. However, unlike *cdc-25.1* RNAi that results in embryonic defects (1.3.4), homozygous progeny that are derived from heterozygous mothers progress normally through embryogenesis and hatch, presumably due to the presence of maternally provided CDC-25.1 coming from heterozygous mothers (Ashcroft and Golden, 2002). Thus, zygotic expression of *cdc-25.1* is important for germline proliferation. Consistent with this, CDC-25.1 protein is detected in germline precursor cells during larval development (Ashcroft and Golden, 2002) and in the proliferating germline (Ashcroft et al., 1999; Clucas, 2003; Clucas et al., 2002).

1.3.4 CDC-25.1 functions during embryonic development

Pioneering work by (Ashcroft et al., 1999) first described an essential function for CDC-25.1 during embryonic development of *C. elegans*. The authors demonstrated that *cdc-25.1* RNAi causes embryonic lethality with embryos arresting at around the 100-cell stage. Subsequent RNAi experiments against *cdc-25.1* confirmed this result (Clucas, 2003; Clucas et al., 2002; Kostic and Roy, 2002), indicating that CDC-25.1 function is required in the early embryo. The detailed analysis by (Ashcroft et al., 1999) reported that *cdc-25.1* RNAi causes defects in the completion of meiosis in fertilised embryos, through aberrant meiotic spindle positioning and chromatin segregation defects, resulting in aneuploidy of the dying embryo. During the first mitotic division of the zygote, *cdc-25.1* RNAi causes a mis-positioning of the mitotic spindle and a delay of the cell division timing compared to the wild-type. Furthermore, failures to execute the physical separation of cells (cytokinesis) in subsequent divisions became apparent. Besides the mainly nuclear localisation of CDC-25.1 in interphase cells of all embryonic blast cells, the authors detected a specific cortical staining of CDC-25.1 in embryos and suggested a possible role for this protein in connecting the microtubule apparatus with the cell cortex during cell divisions. The nuclear and cortical staining was also later observed by the Johnstone laboratory (Clucas, 2003; Clucas et al., 2002). Immunocytochemistry demonstrated that wild-type CDC-25.1 is present in all embryonic blast cells up to the 28-cell stage (Ashcroft

et al., 1999; Kostic and Roy, 2002) or the 100-cell stage (Clucas, 2003; Clucas et al., 2002), indicating that the protein might be functionally required in several early embryonic blastomeres. Indeed, *cdc-25.1* RNAi, using tissue-specific GFP markers for intestinal and hypodermal cells, displayed decreased numbers of both intestinal and hypodermal cells (Clucas, 2003; Clucas et al., 2002), indicating that the proliferation of at least two tissue types requires CDC-25.1 function.

1.3.5 cdc-25.1 mutants cause hyperplasia

The *cdc-25.1(ij48)* allele has been recently identified in the Johnstone laboratory in a mutant screen that was set out to identify genes acting downstream of E specification and controlling the regulated cell division pattern of intestinal cells during embryogenesis (Clucas, 2003; Clucas et al., 2002). The *cdc-25.1(ij48)* mutant phenotype is introduced below.

1.3.5.1 *cdc-25.1(ij48)* is a gain-of-function allele

cdc-25.1(ij48) mutants cause an increase in the number of intestinal cells that are born in the embryo, as evident by the use of an intestinal-specific GFP marker (*elt-2*::GFP), but also by examination of the intestinal cell lineage in the embryo. *cdc-25.1(ij48)* encodes a gain-of-function allele that acts in a strictly maternal pattern. Homozygous *cdc-25.1(ij48)* mothers produce offspring with 100% hyperplasia phenotype. However, heterozygous *cdc-25.1(ij48)* mothers produce offspring with a hyperplasia phenotype that does not follow the Mendelian segregation where genetically wild-type animals display the hyperplasia phenotype. The spectrum of the hyperplasia phenotype in F1 animals from heterozygous mothers ranged from 22 to 96% with an average of 76%. Furthermore, when the *ij48* allele is crossed into wild-type hermaphrodites 100% of the F1 offspring show the wild-type phenotype, consistent with the maternal behaviour of this allele. This indicates that zygotic *cdc-25.1* function in the embryo does not influence the embryonic hyperplasia phenotype. However, when the *cdc-25.1(ij48)* allele is placed over a deficiency, such that mothers carry only one copy of *cdc-25.1(ij48)*, only 2.5% of the F1 offspring display hyperplasia, indicating that lowering the gene-dose can suppress the phenotype. It was thus concluded that the *cdc-25.1(ij48)* allele acts as a hypermorphic maternal effect mutation.

1.3.5.2 *cdc-25.1(ij48)* promotes tissue-specific hyperproliferation

Knockdown of CDC-25.1 by RNAi in a wild-type strain results in decreased numbers of intestinal cells. When *cdc-25.1(ij48)* mothers are treated with *cdc-25.1* RNAi the resulting progeny show some suppression of intestinal hyperplasia. The *ij48* allele causes a true hyperplasia as, unlike the wild-type invariant pattern, in *cdc-25.1(ij48)* animals the pattern of intestinal cell divisions is very variable. There is a general shortening of the intestinal cell cycle, such that the fourth and fifth division occur considerably earlier than in the wild-type, and frequently a fifth and sixth division occur that are not evident in some of the wild-type cells. Other aspects of intestinal cell function are retained and the mutants are viable. The excessive proliferation caused through the *ij48* mutation is specific to the intestinal cell divisions, as cell lineage analysis from a neighbouring blastomere D does not show any proliferation defects. Additionally, there appears to be no defect in germline proliferation or in the number of seam cells, as determined by Nomarski optics or a GFP marker that is specifically expressed in seam cells. Thus, wild-type *cdc-25.1* is required for normal patterns of proliferation in several cell types and the *ij48* mutant of *cdc-25.1* is capable of directing normal proliferation in all those cell types where it is required, however with exception of the intestine where it triggers a hyperplasia.

1.3.5.3 The *cdc-25.1(ij48)* mutation and comparison to *cdc-25.1(rr31)*

The *ij48* lesion is located within the amino-terminal, putative regulatory, region of CDC-25.1 and causes a serine to phenylalanine substitution at residue 46 in the encoded CDC-25.1 protein, CDC-25.1(S46F). This residue falls within a motif that is conserved between CDC-25.1 and CDC-25.2 of *C. elegans*, but is not present in CDC-25.3 or CDC-25.4 and conserved between *C. briggsae* and *C. elegans* CDC-25.1, thus indicating the importance of this region for accurate CDC-25.1 function (Clucas, 2003; Clucas et al., 2002). Confirming the significance of this region for CDC-25.1 function, a *cdc-25.1(rr31)* allele has been independently identified in the Roy laboratory. *cdc-25.1(rr31)* causes a possibly identical intestinal hyperplasia phenotype and encodes a glycine to aspartic acid substitution (G47D) (Kostic and Roy, 2002). This allele is also a gain-of-function mutation (Kostic and Roy, 2002), but unlike the dysregulated pattern described for *cdc-25.1(ij48)* (Clucas, 2003; Clucas et al., 2002), *cdc-25.1(rr31)* causes a synchronized pattern of cell divisions with one additional cell division occurring after the 8E-cell stage giving rise to 32 intestinal cells (Kostic and Roy, 2002). The reason for the differential cell division defects caused through two very similar mutations in *cdc-25.1* is presently unclear and requires further investigation to determine whether both phenotypes are different or not.

The *cdc-25.1(rr31)* allele has been proposed to function at the G_1/S transition during *C. elegans* intestinal development. This has been demonstrated through expression of GFP reporter constructs that are strongly expressed in cells entering S phase (Hong et al., 1998) and transient overexpression of wild-type and mutant CDC-25.1 in the adult hermaphrodite (Kostic and Roy, 2002). However, overexpression of *cdc-25(rr31)* failed to induce extra intestinal divisions under these experimental conditions and given the fact that CDC-25.1 is not normally detected at this late stage, it remains to be identified whether this result truly reflects CDC-25.1 function in the embryo. RNAi experiments against the G_1 type cyclin (*cye-1*) could repress intestinal hyperplasia of *cdc-25.1(rr31)* in the embryo. Such repression was not observed with another G_1 type cyclin (*cyd-1*), indicating that the *cdc-25.1(rr31)* effect might act at the G_1/S transition (Kostic and Roy, 2002). Intriguingly, these authors showed that Wnt signalling is required for the *cdc-25.1(rr31)* mutant phenotype.

Analysis of the *cdc-25.1(ij48)* mutation site revealed that it is part of a conserved DSG phosphodegron motif present in multiple eukaryotic proteins, including human CDC25A, whose abundance are regulated through this site by the ubiquitin ligase β-TrCP (for details see Chapter 3, (3.1.2.3)). It is therefore possible that the conserved region surrounding the site of the *ij48* lesion may be a site of interaction with molecules that negatively regulate the activity of CDC-25.1, possibly specifically in the intestine. LIN-23, the *C. elegans* orthologue of mammalian ß-TrCP, was an interesting candidate, as *lin-23* mutations caused increased nuclei during embryogenesis, but no intestinal-specific hyperproliferation phenotype has been published to date (Kipreos et al., 2000). However, preliminary experiments in the Johnstone lab (Dr. I.L. Johnstone pers. comm.) had detected increased numbers of intestinal nuclei in *lin-23* RNAi-treated embryos, suggesting a possible role for LIN-23 in negatively regulating CDC-25.1. However, in their previous published study no difference in CDC-25.1(S46F) protein stability had been detected when compared to wild-type (Clucas et al., 2002), which contrasts the findings by the Roy laboratory, who reported that the CDC-25.1(G47D) mutant persists longer in embryos than the wild-type protein (Kostic and Roy, 2002).

1.4 Research aims and objectives

Here, the function of the *cdc-25.1(ij48)* allele, generated in the Johnstone laboratory, is further explored in order to decipher the molecular mechanism underlying the tissue-specific regulation of cell divisions in the multicellular organism *C. elegans*. It was

predicted that the *cdc-25.1(ij48)* allele escapes the negative regulation of at least one other factor, possibly in a tissue-specific fashion. Thus, a mixture of reverse genetics and biochemical approaches was utilised in order to identify negative regulators of CDC-25.1 acting through S46.

Chapter 2

Materials and Methods

2 Materials and Methods

2.1 Materials

All chemicals and other materials were purchased from the following commercial sources, unless otherwise indicated:

Abcam (http://www.abcam.com/), Abgene (http://www.abgene.com/), Amersham Biosciences (http://www.amersham.co.uk), Bio-Rad (http://www.bio-rad.com), Covalab (http://www.covalab.com), Difco (http://www.bd.com/industrial), Fisher Scientific (http://www.fisher.co.uk), Fluka (http://www.sigmaaldrich.com/), GibcoBRL Life Technologies (http://www.lifetechnologies.com), Invitrogen (http://www.invitrogen.com/), Menzel GmbH (http://www.menzel.de/), Mobitec (http://www.mobitec.de), Molecular Probes (http://www.probes.com), New England Biolabs (http://www.neb.com), Novagen (http://www.merckbiosciences.co.uk/), Pierce (http://www.piercenet.com), Promega (http://www.promega.com), Qiagen (http://www.qiagen.com), Roche (http://www.roche.com), Santa Cruz Biotechnology (http://www.scbt.com/), Schleicher and Schuell (http://www.schleicher-schuell.de), Sigma (http://www.sigmaaldrich.com), SNBTS (http://www.snbts.org.uk/), Stratagene (http://www.stratagene.com), Vector Laboratories (http://www.vectorlabs.com/).

2.1.1 Chemical Abbreviations

BSA	bovine serum albumin
DAPI	4, 6-diamidino-2-phenylindole
DTT	1,4-dithiothreitol
DMSO	dimethyl sulfoxide
DOC	sodium deoxycholate
dH_20	deionised water
EDTA	ethylenediaminetetraacetic acid
EMS	ethyl methanesulfonate
IPTG	isopropyl β-D-1-thiogalactopyranoside
LB	Luria Bertani broth
NGM	nematode growth medium
PBS	phosphate-buffered saline
PBS-G	phosphate-buffered saline-glycerol

PBS-T	phosphate-buffered saline-Tween 20
PIC	protease inhibitor cocktail
SDS	sodium dodecyl sulfate
SDS-PAGE	sodium dodecyl sulfate-polyacrylamide gel electrophoresis
SWLB	single worm lysis buffer
TBE	tris borate EDTA
Tris-HCl	2-amino-2-hydroxymethyl-1,3-propanediol-hydrochloride
Tween 20	polyoxyethylenesorbitan monolaurate
WLB	worm lysis buffer

2.1.2 Stock solutions and media

Blocking solution (1x): 5% dried milk powder in 1x PBS-T. Made fresh before use.

Tris-Glycine (20x): 250 mM Tris base (30.28 g/L), 1.9 M Glycine (142.6 g/L) filled up to 1 L with dH_2O. Stored at room temperature.

Blotting buffer (1x): 50 ml Tris-Glycine (20x), 20% (v/v) methanol, 0.01% (w/v) SDS, filled up to 1 L with dH_2O. Made fresh prior to use. Pre-cooled at 4°C.

Bleach solution (1x): 2.5 ml 5 M KOH, 6 ml NaOCL (10-20%, Fluka) adjusted to 50 ml with dH_2O. Made fresh prior to use.

Coomassie blue staining solution (1x): 1 g/L Coomassie brilliant blue R-250 (first solubilised in methanol), 45% (v/v) methanol, 10% (v/v) glacial acetic acid in dH_2O. Filtered through Whatman no.1 filter to remove non-solubilised particles. Stored in closed container at room temperature.

Destaining solution (1x): 20% (v/v) ethanol, 10% (v/v) glacial acetic acid in dH_2O. Stored in closed container at room temperature.

DNA sample loading buffer (6x): 40% (w/v) sucrose, 0.02% (w/v) Xylene Cyanol, sterile filtered with 0.2 μm filter, aliquoted and stored at –20°C.

Ethidium bromide: 10 mg/ml stock in dH_2O, final concentration 1 μg/ml in agarose gels. Stored at room temperature, protected from light.

IPTG: 1 M stock in sterile dH_20. Sterile filtered with 0.2 μm filter, aliquoted and stored at -20°C.

L-Broth: 1% (w/v) Bacto tryptone (Difco, Michigan, USA), 0.5% (w/v) yeast extract (Difco), 0.5% (w/v) NaCl in dH_20. Autoclaved at 121°C and stored at room temperature.

L-Broth agar: as for L-Broth + 1.5 g/100 ml Bacto-agar (Difco). Autoclaved and subsequently cooled to around 60°C prior to addition of desired antibiotics (when required), poured with sterile technique onto plastic dishes, allowed to solidify and stored for short periods at 4°C.

M9 Buffer (1x): 20 mM KH_2PO_4, 40 mM Na_2HPO_4, 80 mM NaCl, 1 mM MgSO4. Autoclaved and stored at room temperature.

Na_2EDTA: 0.5 M stock in dH_20, adjusted to pH 8.0 with NaOH. Autoclaved and stored at room temperature.

NGM agar: 0.3% (w/v) NaCl, 2% agar (w/v) (Difco), 0.25% (w/v) peptone (Difco), 0.0005% (w/v) cholesterol (1 ml/L of 5 mg/ml stock in ethanol) in dH_2O. Autoclaved, then $CaCl_2$ and $MgSO_4$ added to 1 mM final concentration (1 ml/L of 1 M stock solution) and potassium phosphate buffer pH 6.0 to 25 mM final concentration (25 ml/L 1 M stock) just prior to pouring plates. Solidified plates stored at room temperature.

NGM agarose: as NGM agar, but agar was substituted with agarose.

Phenol: for DNA manipulations, purchased liquefied (Sigma) and equilibrated with 10 mM Tris HCl pH 8.0,1 mM EDTA. For RNA manipulations, Phenol was purchased liquefied and saturated with 0.1 M citrate buffer, pH 4.3. Stored at 4°C.

Phenol/Chloroform: equal volumes of phenol (above) and chloroform:isoamyl alcohol 24:1 were mixed. Stored at 4°C.

Phosphate buffered saline (1x PBS): 1/10 dilution in dH_2O of purchased aqueous 10x PBS (Gibco) to obtain a 137 mM NaCl, 2.7 mM KCl and 10 mM phosphate buffer solution (pH 7.4 at 25°C).

PBS-G: as PBS with addition of 8.7% (v/v) glycerol. Stored at room temperature.

PBS-T: as PBS with the addition of Tween 20 to a final concentration of 0.1% (v/v). Stored at room temperature.

Potassium citrate (1 M): 210.1 g citric acid monohydrate in 900 ml dH_2O, adjusted to pH 6.0, by addition of KOH pellets, and filled up to 1 L with dH_2O. Autoclaved and stored at room temperature.

Potassium phosphate buffer (1 M): prepared from 1 M KH_2PO_4 and 1 M K_2HPO_4, mixed in appropriate ratio for desired pH. Autoclaved and stored at room temperature.

Proteinase K: 20 mg/ml stock in sterile dH_2O. Stored at –20°C.

S-Basal: 100 mM NaCl (5.9 g/L), 50 mM potassium phosphate pH 6.0 (50 ml/L of 1 M stock solution), 0.0005% (w/v) cholesterol (1 ml/L of 5 mg/ml stock in ethanol). Autoclaved and stored at room temperature.

Protease inhibitor cocktail PIC (50x): complete, EDTA-free protease inhibitor tablets for inhibition of serine and cysteine proteases (Roche) dissolved in dH_2O (1 tablet/1 ml dH_2O) and stored at -20°C for a maximum of four weeks.

RNA lysis buffer (1x): 0.5% (w/v) SDS, 5% (v/v) beta-mercaptoethanol, 10 mM EDTA, 10 mM Tris pH 7.5, 0.5 mg/ml Proteinase K, stored at -20°C.

S-Medium: 10 mM Potassium citrate pH 6.0 (10 ml/L of a 1 M stock solution), 10 ml/L Trace metals, 3 mM $MgSO_4$ (3 ml/L of a 1 M stock solution), 3 mM $CaCl_2$ (3 ml/L of a 1 M stock solution) diluted in 1 L S-basal, using sterile technique, just prior to use.

Sodium dodecyl sulfate (SDS): 20% (w/v) stock solution in sterile dH_2O. Stored at room temperature.

SDS sample loading buffer (2x): 125 mM Tris pH 6.8, 4% (w/v) SDS, 20% (v/v) glycerol, 0.03% (w/v) Bromophenol blue. Sterile filtered with 0.2 µm filter. 250 µl of beta-mercaptoethanol (14.3 M stock) added to 5 ml, stored at –20°C.

SDS running buffer (10x): purchased from Bio-Rad. 250 mM Tris, 1.92 M Glycine, 1% (w/v) SDS. Stored at room temperature.

Single worm lysis buffer (SWLB, 1x): 50 mM KCl, 10 mM Tris (pH 8.3), 2.5 mM $MgCl_2$, 0.45% (v/v) Tween 20, 0.01% (w/v) gelatine. Autoclaved and stored in aliquots at –20°C. Proteinase K (Roche) added to 50 µg/µl prior to use.

Single worm PCR Taq buffer (10x): 100 mM Tris (pH 8.3), 500 mM KCl, 15 mM $MgCl_2$, 0.01% (w/v) gelatine. Autoclaved and stored in aliquots at –20°C.

SOB medium (1L): 20 g Bacto-tryptone, 5 g Bacto-yeast extract, 0.5 g NaCl and 10 ml 250 mM KCl added to 960 ml dH_2O, the pH was adjusted to pH 7.0 with NaOH and the medium autoclaved. 10 ml of 1 M $MgCl_2$ were added prior to use.

Sodium acetate (pH 5.2): 3 M Sodium acetate in dH_2O. Adjusted to pH 5.2 with glacial acetic acid. Autoclaved and stored at room temperature.

SOC medium: 2 ml sterile 1 M glucose added freshly to 100 ml SOB before use. Stored in aliquots at –20°C.

TBE (10x): 0.9 M Tris-HCl, 0.9 M Boric acid, 25 mM Na_2EDTA pH 8.0 in dH_2O. Stored at room temperature.

TE (1x): 1 mM EDTA, 10 mM Tris-HCl (pH as required) in dH_2O. Autoclaved and stored at room temperature. TE at pH 8.0 was used for all DNA manipulations, unless otherwise stated.

Trace metals (100x): 5 mM Na_2EDTA, 2.5 mM $FeSO_4\ 7H_2O$, 1 mM $MnCl_2\ 4H_2O$, 1 mM $ZnSO_4\ 7H_2O$, 0.1 mM $CuSO_4\ 5H_2O$ in 1 L dH_2O. Sterile filtered with 0.2 µm filter, aliquoted in 50 ml conicals and stored at room temperature in the dark.

Tris-HCl: molarity and pH as required (pH adjusted with HCl). Autoclaved and stored at room temperature.

Worm lysis buffer (WLB, 1x): 10 mM Tris pH 8.0, 100 mM NaCl, 10 mM EDTA, 1% (w/v) SDS, 1% (v/v) beta-mercaptoethanol, 100 µg/ml Proteinase K.

2.1.3 Molecular weight markers

2.1.3.1 DNA markers

1 kb plus DNA ladder: 100, 200, 300, 400, 500, 650, 850, 1000, 1650, 2000, 3000, 4000, 5000, 6000, 7000, 8000, 9000, 10000, 11000, 12000 bp (Invitrogen).

2.1.3.2 Protein markers

Prestained Broad Range (6-175 kDa): 6.5, 16.5, 25, 32.5, 47.5, 62, 83, 175 kDa (New England Biolabs).

Prestained Broad Range: 6.9, 20.4, 29.4, 37.2, 53.5, 97.3, 115.6 kDa (Bio-Rad).

2.1.4 Vectors and plasmids

Name	Description	Use	Source
pBluescript II SK(+/-) (pBS)	2961 bp, Amp^r, T7, T3 and *lac* promoter	standard cloning, *C. elegans* DNA transformation	Stratagene
L4440	2790 bp, Amp^r, two T7 promoters in opposite directions	RNAi by feeding	gift from A. Fire
pQE-30	3481 bp, Amp^r, T5 promoter, *lac* operator, N-terminal 6xHis tag	recombinant protein expression in bacteria	Qiagen
pQE-80L	4700 bp, Amp^r, T5 promoter, *lac* operator, N-terminal 6xHis tag, $lacI^q$ gene	recombinant protein expression in bacteria	Qiagen
pREP4	3740 bp, Kan^r, *lacI* gene	recombinant protein expression in bacteria	Qiagen
pGEX-6P-1	4984 bp, Amp^r, *tac* promoter, N terminal GST tag, $lacI^q$ gene	recombinant protein expression in bacteria	Amersham Biosciences
pIC26	16397 bp, Amp^r, *pie-1::GFP-TEV-S*, *unc-119(+)*	LAP tag cloning	gift from I. Cheeseman
p76-16B	Amp^r, 10.7kb, *unc-76(+)*	marker for *C. elegans* DNA transformation	gift from L. Bloom

Table 2.1 Common vectors and plasmid clones.

A. Fire (Stanford University School of Medicine, Stanford, USA), I. Cheeseman (Ludwig Institute for Cancer Research, La Jolla, USA) and L. Bloom (Phylos Inc., Lexington, USA).

2.1.5 Oligonucleotides

2.1.5.1 Vector oligonucleotides

Name	Sequence (5'->3')	Use
M13 reverse	CAGGAAACAGCTATGACC	sequencing, colony screening
T3	AATTAACCCTCACTAAAGGG	sequencing, colony screening
T7	GTAATACGACTCACTATAGGG	sequencing, colony screening
pQE for	GTATCACGAGGCCCTTTCGTCT	sequencing, colony screening
pQE rev	CATTACTGGATCTATCAACAGGAG	sequencing, colony screening
pGex for	ATAGCATGGCCTTTGCAGG	sequencing, colony screening
pGex rev	GAGCTGCATGTGTCAGAGG	sequencing, colony screening
pL4-3'	GTGCTGCAAGGCGATTAAGTTG	sequencing

Table 2.2 Vector oligonucleotides.

2.1.5.2 Oligonucleotides for *cdc-25.1*

Name	Sequence (5'->3')	Use
25seq600	CACAGAGTGACAAATCTTGTC	sequencing
25Seq1100	AGAAAACGGCGAAGCCAGTT	sequencing
25Seq1400	GTGCTTTAACCTCTACTGGAAG	sequencing
LapSeq	TGTAACAGCTGCTGGGATTAC	sequencing
25-343seq	GAGCTGCGTGATGAGCTGACAGAC	sequencing
Elt2xho2	TTTTCTCGAGCGAGCTGAATACACGTGCT	pBS-*elt-2::LAP::cdc-25.1* cloning
Elt-2Bam	TTTTGGATCCTCTATAATCTATTTTCTAGTTTC	pBS-*elt-2::LAP::cdc-25.1* cloning
25gBam	TTTTGGATCCGCTACCACCGGGGAAAAAGC	pBS-*elt-2::LAP::cdc-25.1*, pQE-30-*cdc-25.1* cloning
25gXba	TTTTTCTAGAGCTGAGATTAATGTGAACGC	pBS-*elt-2::LAP::cdc-25.1* cloning
25cSac	TTTTGAGCTCTTATTCGGCGTCGTCAGAAAT	pQE-30-*cdc-25.1* cloning
25.1-Ty-sens	GATCATGGAGGTCCATACTAACCAGGATCCACTTG ACC	pBS-*elt-2::TY::cdc-25.1* cloning
25.1-Ty-as	GATCGGTCAAGTGGATCCTGGTTAGTATGGACCTCC AT	pBS-*elt-2::TY::cdc-25.1* cloning
25.1Notagsen	GATCGCTGCAGGATCATGC	pBS-*elt-2::cdc-25.1* cloning
25.1Notagas	GATCGCATGATCCTGCAGC	pBS-*elt-2::cdc-25.1* cloning

Table 2.3 *cdc-25.1* oligonucleotides.

2.1.5.3 Oligonucleotides for *lin-23*

Name	Sequence (5'->3')	Use
lin-23-473	CAGTGCGACGAATCTGTGAA	sequencing
lin-23-874	GGAGAGTGCATTAAAACGTTAA	sequencing
lin-23-1281	CGTGCGATGCATTCGATTTG	sequencing
lin-23-1683	CTGCTCGTCGACACAATGCC	sequencing
lin-23 prom	CTCACCTGATTATATGAGATC	sequencing
lin-23-Flg	TTTTACTAGTCTTGTCGTCGTCATCCTTGTAGTCTGG GCCACCATCTGGCATCTCTTC	pBS-*lin-23::Flag-TY* cloning
lin-23*tag5*	CGACGAGGAATTGCATGTCTTC	pBS-*lin-23::FLAG-TY* cloning
lin-23-TY	TTTTACTAGTGAGGTCCATACTAACCAGGACCCACT TGACTAAAATCTACACTCCTTCCCATTTT	pBS-*lin-23::FLAG-TY* cloning
lin-23-5'gen	TTTTGGTACCCCAAATTTGCCTCTGATTCCG	pBS-*lin-23* (genomic) cloning
lin-23-3'gen	TTTTGGTACCGTTGCAGAAATGCTCAAATCGG	pBS-*lin-23* (genomic) cloning
lin-23-GSTfl	TTTTCCCGGGTTCTTCACCGCACCGAGCTTCAAC	pGEX-6P1-*lin-23* cloning
lin-23-GSTdf	TTTTCCCGGGTCATGTCTTCTACAGTAAATTATATC CA	pGEX-6P1-*lin-23Δ* F-box cloning
lin-23-GSTSTP	TTTTCCCGGGTTATGGGCCACCATCTGGCATCTC	pGEX-6P1-*lin-23 wt* and *Δ* F-box cloning
lin-23 crssgen	GGAGTGTAGATTTTATGGGC	PCR screening of *lin-23* allele in *C. elegans*

Table 2.4 *lin-23* oligonucleotides.

2.1.5.4 Oligonucleotides for RNAi clones

Name	Sequence (5'->3')	Use
lin-23-RNAi5'	TTTTGAATTCTCATTAGTTCAACATACTGGC	L4440 cloning of *lin-23* RNAi clone 2
lin-23-RNAi3'	TTTTGAATTCGGAAGATTACAGAGGGTTTG	L4440 cloning of *lin-23* RNAi clone 2
cul-2-5	TTTTGAATTCTGCAGATTCCAGACGTCAA	L4440 cloning of *cul-2*
cul-2-3	TTTTGAATTCTCCAAATCCGTCTCCGATA	L4440 cloning of *cul-2*
apr-1-5'	GAATCCTGGAAGTGTTATGAC	L4440 cloning of *apr-1*
apr-1-3'	GATGATTGGCTTGGGATTCTG	L4440 cloning of *apr-1*
wrm-1-5	GGATTGTCAATGCTCTCAGTC	L4440 cloning of *wrm-1*
wrm-1-3	TTTTGAATTCGATCATTCTACACGCTGATAC	L4440 cloning or *wrm-1*
bar-1-5	TTTTGAATTCGCAGGATCTCGGAAAACAAA	L4440 cloning of *bar-1*
bar-1-3	TTTTGAATTCATTCGTTGCACTTTGGGAAC	L4440 cloning of *bar-1*

Table 2.5 RNAi oligonucleotides.

2.1.6 Strains

2.1.6.1 *E. coli* strains

Strains were obtained as indicated. CGC (Caenorhabditis Genetics Centre, University of Minnesota, Minneapolis, USA), M. Stark (University of Glasgow, Glasgow, UK).

Strain name	Use	Antibiotic resistance	Source
AB1157	food source for *C. elegans* (liquid culture)	$Strp^r$	gift from M. Stark
OP50	food source for *C. elegans*, uracil auxotroph	Tet^r	CGC
HB101	food source for *C. elegans* (liquid culture)	Str^r	Promega
HT115 (DE3)	DE3 lysogen: *lacUV5* promoter-T7 RNA polymerase (IPTG-inducible T7 RNA polymerase), RNAse III minus; production of double-stranded RNA for RNAi by feeding	Tet^r	CGC
Epicurian Coli XL10 Gold ultracompetent cells	molecular cloning	Tet^R, Cam^R	Stratagene
BL21 Codonplus IRL competent cells	protein expression from IPTG-inducible non-T7 promoters (containing *lac* operators); contains rare *E. coli* tRNA codons: R (AGA, AGG), I (AUA), L (CUA)	Tet^R, Cam^R	Stratagene

Table 2.6 *E. coli* strains.

2.1.6.2 *C. elegans* strains

Strains were obtained from the CGC, I.L. Johnstone (University of Glasgow, Glasgow, UK), J. Rothman (UC Santa Barbara, Santa Barbara, USA), O. Hobert (Columbia University, New York, USA), P. Askjaer (Seville University, Seville, Spain) and J. White (University of Wisconsin, Madison, USA).

Strain name	Genotype	Source
N2	*C. elegans* wild-type (Bristol variant)	CGC
IA105	*unc-76(e911) V; ijIs12[dpy-7::GFP::LacZ, unc-76(+)]* (ectodermal GFP)	I.L. Johnstone
JR1838	*wIs84[*pJM66 (*elt-2::GFP::LacZ*), pRF4(*rol-6 (su1006dm)]* (intestinal GFP)	J. Rothman
JR1990	*wIs118[*pDPMM016B *unc-119(+)*, pMW025 *(npa-1::GFP::LacZ)]*	J. Rothman
JR1988	*wIs119[pDPMM016B unc-119(+)*, pMW025 *(npa-1::GFP::LacZ)]*	J. Rothman
JR667	*unc-119(e2498::Tc1)III; wIs51[pMF1, pDP#MM106B unc-119(+)]* (seam cell GFP)	CGC
NL2099	*rrf-3(pk1426)II*	CGC
DR439	*unc-8(e49) dpy-20(e1282)IV*	CGC
DR96	*unc-76(e911)V*	CGC
IA268	*cdc-25.1(ij48)I*	I.L. Johnstone
IA123	*cdc-25.1(ij48)I; unc-76(e911) ijIs10[unc-76(+), cpr-5::GFP::LacZ]V* (intestinal GFP)	I.L. Johnstone
IA257	*lin-62(ij52)IV; ijIs10[unc-76(+), cpr-5::GFP::LacZ]V* (intestinal GFP)	I.L. Johnstone
IA399	*cdc-25.1(nr2036)/dpy-5(e61)unc-13(e450)I; ijEx36[cdc-25.1(ij48), wIs84(*pJM66 *elt-2::GFP::LacZ,genomicDNA)]*	I.L. Johnstone
OHT1707	*[lin-23::GFP, rol-6(d)]*	O. Hobert
CB3514	*lin-23(e1883)/dpy-10(e128)II*	CGC
DP38	*unc-119(ed3)III*	CGC
IA331	*lin-62(ij52)IV*	I.L. Johnstone
XA3507	*unc-119(ed3) qaIs3507[pie-1::GFP::lem-2 unc-119(+)]III*	P. Askjaer
WH204	*unc-119(ed3) II; ojIs1[pie-1::GFP::beta-tbb-2, unc-119(+)]*	J. White

Table 2.7 Common *C. elegans* strains.

2.1.6.3 *C. elegans* strains generated in this study

Strain name	Genotype
IA521	*unc-76(e911)V; ijEx30[elt-2::LAP::cdc-25.1(+),* p76-16B *unc-76(+)]*
IA522	*unc-76(e911)V; ijEx31[elt-2::LAP::cdc-25.1(+),* p76-16B *unc-76(+)]*
IA523	*unc-76(e911)V; ijEx32[elt-2::LAP::cdc-25.1(ij48),* p76-16B *unc-76(+)]*
IA524	*unc-76(e911)V; ijEx33[elt-2::LAP::cdc-25.1(ij48),* p76-16B *unc-76(+)]*
IA526	*lin-62(ij52)IV; wIs84[*pJM66 *elt-2::GFP::LacZ,* pRF4 *rol-6 (su1006dm)]*
IA530	*cdc-25.1(ij48)I; wIs84[*pJM66 *elt-2::GFP::LacZ,* pRF4 *rol-6 (su1006dm)]*
IA535	*ijIs16[elt-2::LAP::cdc-25.1(+),* p76-16B *unc-76(+)]*
IA536	*ijIs17[elt-2::LAP::cdc25.1(ij48),* p76-16B *unc-76(+)]*
IA544	*lin-62(ij52)IV; wIS118[*pDPMM016B *unc119(+),* pMW025 *(npa-1::GFP::LacZ)]*
IA545	*lin-62(ij52) dpy20 (e1282)IV; wIs84[*pJM66 *elt2::GFP::LacZ,* pRF4 *rol-6(su1006dm)]*
IA551	*lin-23(e1883)+/+ dpy-10(e128)II; unc-119(ed3)III*
IA559	*unc-76(e911)V ; ijEx34[elt-2::cdc-25.1(+),* p76-16B *unc-76(+)]*
IA560	*unc-76(e911)V ; ijEx35[elt-2::cdc-25.1(+),* p76-16B *unc-76(+)]*
IA565	*lin-23(e1883)/+II; wIs119[*pDPMM016B *unc-119(+),* pMW025 *(npa-1::GFP::LacZ)]*
IA568	*lin-23(e1883)/+I; wIs84[*pJM66 *elt-2::GFP::LacZ,* pRF4 *rol-6(su 1006dm)]*
IA575	*ijEx36[cdc-25.1(ij48), wIs84[*pJM66 *elt-2::GFP::LacZ, genomicDNA]*
IA577	*lin-62(ij52) dpy-20(e1282)IV; wIS118[*pDPMM016B *unc-119(+),* pMW025 *(npa-1::GFP::LacZ)]*
IA582	*unc-119(ed3)III; ijIs18 [lin-23::FLAG-TY, unc-119(+)]*
IA585	*lin-62(ij52)dpy-20 (e1282)IV; ijEx36[cdc-25.1(ij48), wIs84[*pJM66 *elt-2::GFP::LacZ, genomicDNA]*
IA589	*lin-23(e1883)II; unc-119(ed3)III; ijIS18[lin-23::FLAG-TY, unc-119(+)]*
IA592	*lin-23(e1883)II; ijIS18 [lin-23::FLAG-TY, unc-119(+)], wIs84[*pJM66 *elt2::GFP::LacZ,* pRF4 *rol-6(su1006dm)]*
IA593	*cdc-25.1(ij48)I; lin-23(e1883)II; ijIS18 [lin-23::FLAG-TY, unc-119(+)], wIs84[*pJM66 *elt2::GFP::LacZ,* pRF4 *rol-6(su1006dm)]*

Table 2.8 *C. elegans* strains created in this study.

2.1.7 Antibodies

2.1.7.1 Primary antibodies

Name	Species	Antigen	Dilution	Source
CDC-25.1A	rabbit, polyclonal	peptide of aa 495-509 of *C. elegans* CDC-25.1 (CE11778)	1:150 (IIF) 1:400 (WB)	I.L. Johnstone
CDC-25.1B	rabbit, polyclonal	peptide of aa 592-604 of *C. elegans* CDC-25.1 (CE11778)	1:400 (WB)	I.L. Johnstone and this study
CDC-25.1f.l.	rabbit, polyclonal	HIS_6::CDC-25.1 *C. elegans* (CE11778)	1:600 (WB) 40 μg (IP)	this study
LIN-23	rabbit, polyclonal	GST-LIN23 *C. elegans* (CE28600)	1:750 (WB) 1:600 (IIF)	this study
GSK3B (G4414)	mouse, monoclonal	recombinant rabbit GSK3β, recognises *C. elegans* GSK-3 (CE21401)	1:500 (WB)	Sigma
β-ACTIN (AC-15, A1978)	mouse, monoclonal	peptide of N-terminal 15 aa of β-ACTIN, recognises several species including *C. elegans* β–ACTIN	1:2000 (WB)	Sigma
GFP (ab6556)	rabbit, polyclonal	recombinant GFP	4 μg per IP	Abcam
UBIQUITIN (MMS-257P)	mouse, monoclonal	denatured bovine ubiquitin	1:1000 (WB)	Covance
GFP (B-2, sc9996)	mouse, monoclonal	full-length Aequorea victoria	1:300 (WB)	Santa Cruz

Table 2.9 Primary antibodies.

2.1.7.2 Secondary antibodies

Name	Conjugate	Dilution	Source
goat anti-mouse HRP	horseradish peroxidase	1:2000 (WB)	Promega
donkey anti-rabbit HRP	horseradish peroxidase	1:2000 (WB)	Amersham
Alexa Fluor goat anti-rabbit	Alexa Fluor 594	1:200 (IIF)	Invitrogen
Alexa Fluor goat anti-mouse	Alexa Fluor 488	1:200 (IIF)	Invitrogen

Table 2.10 Secondary antibodies.

2.2 Methods

2.2.1 Standard molecular biology techniques

2.2.1.1 DNA preparation

DNA was amplified using the Plasmid Mini, -Midi or -Maxi kits from Qiagen according to the manufacturer's instruction. Briefly, *E. coli* strains carrying the desired plasmid DNA were grown in liquid culture overnight at 37°C (see 2.2.1.9). In case of low-copy plasmids (e.g. pQE-30, pQE-80L) Maxi kits were employed, whereas high-copy plasmids (pBluescript) were purified using the Midi kit. The Mini prep kit was utilized for *E. coli* colony screening after transformation of DNA ligation reactions. The culture volume was 250 ml, 100 ml or 2 ml for Maxi-, Midi- or Mini kit, respectively. To enhance the purity of the DNA, the DNA pellet that was precipitated after elution from the columns provided with the kit, was further purified. To this end, the DNA pellet was resuspended in 200 µl 1x TE and spun for 5 min at 13200 *g* at room temperature in a microcentrifuge. The supernatant was precipitated by addition of 20 µl 3 M sodium acetate pH 5.2 and 600 µl 100% ethanol, mixed by inversion and immediately spun at 13200 *g* for 5 min at room temperature in a microcentrifuge. The resulting pellet was resuspended in 1x TE and kept at –20°C

2.2.1.2 DNA/ RNA electrophoreses

DNA was routinely separated on 0.8 - 1.5% (w/v) agarose gels in 0.5x TBE. Agarose (Invitrogen) was suspended in 0.5x TBE and heated in a microwave until dissolved. The mixture was allowed to cool down to around 60°C and ethidium bromide added to a final concentration of 1 µg/ml. The gel was poured into a 11 cm or 15 cm gel-tank (GIBCO), containing appropriate size combs, and allowed to solidify. The DNA was dissolved in 1x DNA sample buffer and applied to the wells of the gel. The samples were electrophoresed in 0.5x TBE at 10 - 15 V/cm. To obtain highest resolution, large DNA fragments were applied to 0.8 - 1% agarose gels whereas small fragments resolved best at high percentage (1.5 - 1.8%) agarose gels. The DNA was compared to a known DNA Marker and images were taken using a Transilluminator (Bio-Rad) and Quantity One software (Bio-Rad).

2.2.1.3 PCR

PCR reactions for cloning purposes were performed using *PfuTurbo* Polymerase (Stratagene). However, in some cases *TaqPlus* Precision Polymerase (Stratagene) had to be utilised to generate a product. In each case a 50 µl reaction was set up containing 1x reaction buffer, 100 ng of each primer, 100 ng of plasmid DNA or 200 ng of *C. elegans* genomic DNA, 400 µM dNTPs and 2.5 units of *PfuTurbo* Polymerase or 5 units of *TaqPlus* Precision Polymerase. Amplification was performed using a RoboCycler 96 (Stratagene). Cycling parameters were modified according to the annealing temperature of the primer and the length of the fragment to be amplified. A typical starting point is shown in (Table 2.11).

Segment	Temperature (°C)	Time (min)	No. of cycles
1	95	1	1
2	95 50 72	0.5 0.5-1 2/kb (Pfu) 1/kb (Taq)	28
3	72	10	1

Table 2.11 Cycling parameters for PCR amplification.

2.2.1.4 RT-PCR

RNA isolated as in (2.2.6.2) was employed to generate cDNA using the Stratascript FirstStrand synthesis system (Stratagene) according to the manufacturer's instruction. Typically, around 200 - 400 ng of total RNA was annealed with 500 ng of oligo (dT) primer in a total volume of 11 µl and incubated at 65°C for 5 min. The reaction was allowed to cool to room temperature and 1x FirstStrand buffer, 20 units RNAse Inhibitor, 1 mM dNTPs and 50 units Stratascript Reverse Transcriptase were added in a final volume of 20 µl. The mixture was incubated at 25°C for 10 min, followed by 1 hr at 42°C, and the reaction terminated at 70°C for 15 min. Typically, 2 - 4 µl of cDNA were added in a 50 µl PCR reaction using 100 ng of gene-specific primers. PCR reactions were performed according to (2.2.1.3).

2.2.1.5 Digest and purification of DNA fragments

Purified DNA was digested with restriction endonucleases from New England Biolabs (NEB) or Promega. For vector digestion, typically 1.5 µg of vector was digested with 10 units of restriction enzyme in a 50 µl reaction containing 1x restriction buffer and 100

μg/ml BSA. The mixture was incubated for 2 hr at the temperature recommended by the enzyme manufacturer. The cut vector was separated by agarose gel electrophoreses; the band cut out and purified using the Qiaquick gel extraction kit (Qiagen) according to the manufacturer. The cut vector was routinely dephosphorylated using 2 units CIP (NEB) in reaction buffer 2 (NEB) for 45 min at 37°C. The dephosphorylated vector fragment was purified using the Qiaquick PCR purification kit (Qiagen).

Insert fragments were produced by digestion of 8 μg plasmid DNA with 30 - 40 units of restriction enzyme in a 100 μl reaction for 2 hr at enzyme-specific temperature. The fragments were purified from an agarose gel using the Qiaquick gel extraction kit (Qiagen).

PCR fragments were purified after gel electrophoreses using the Qiaquick gel extraction kit. Typically, the entire PCR reaction was cut with 30 - 40 units of enzyme in a 200 μl reaction for 2 hr (temperature enzyme-specific). The digested PCR fragments were further purified using the Qiaquick PCR purification kit.

2.2.1.6 Nucleic acid quantification

Nucleic acids were quantified using a GENOVA spectrophotometer (Jencons, http://www.jencons.co.uk/). DNA/RNA was diluted 100 times in dH_2O and the $OD_{260/280}$ determined. An $OD_{260/280}$ ratio of 1.8 and 2.0 indicates good quality DNA or RNA, respectively. The nucleic acid concentration was determined using the formula:

Abs_{260} x dilution factor x 50 (DNA) or 40 (RNA) = ng/μl

For visual determination of DNA fragments (typically used for ligations), 2 μl DNA was applied on agarose gel together with 500 ng of DNA molecular weight marker. The concentration of fragments was estimated according to the following formula:

DNA size (kb) x 500 ng / 80 (kb) = ng/2μl

2.2.1.7 DNA ligation

Ligation reactions were carried out using 10 - 20 ng of digested and dephosphorylated vector (see 2.2.1.5) and a 5-fold molar excess of insert-to-vector concentration according to the formula:

i) size of vector (kb) / size of insert (kb) = *Y*
ii) ng of vector / *Y* x 5 = ng of insert

Vector and insert were mixed together in 1x T4 DNA ligation buffer (NEB) and 400 units T4 DNA ligase (NEB) in a final volume of 20 µl. The sample was incubated at room temperature for 1 hr (cohesive-end ligation) or at 16°C overnight (blunt-end ligation).

2.2.1.8 DNA transformation into *E. coli*

Routinely, 10 µl of a DNA ligation reaction or 0.5 µg of plasmid DNA were transformed into XL10 Gold ultracompetent cells. For protein expression 0.5 µg of plasmid DNA were transformed into BL21 CodonPlus cells. In all cases cells were transformed according to the manufacturer's recommendation and plated on LB plates containing the appropriate antibiotics (Table 2.12). The plates were incubated overnight at 37°C.

2.2.1.9 *E. coli* cultures

E. coli strains were grown at 37°C on 9 cm LB plates or liquid culture containing the adequate concentration of antibiotics in accordance to the plasmid resistance (Table 2.12).

	Concentration		Storage
	Stock	**Final**	**(stock)**
Ampicillin	100 mg/ml in dH_2O	100 µg/ml	*-20°C*
Chloramphenicol	34 mg/ml in dH_2O	34 µg/ml	*-20°C*
Kanamycin	25 mg/ml in dH_2O	25 µg/ml	*-20°C*
Streptomycin	12.5 mg/ml in dH_2O	12.5 µg/ml	*-20°C*
Tetracycline	12.5 mg/ml in 50% Ethanol	12.5 µg/ml	*-20°C*

Table 2.12 Concentration of antibiotics for selective *E. coli* growth.

2.2.1.10 Colony screening for positive transformants

Typically, colonies that had grown up overnight, after transformation of a ligation reaction into *E. coli* that were plated on LB plates containing the desired antibiotics, were individually picked using a toothpick. 2 ml LB containing the appropriate antibiotics were inoculated with individual colonies and cultures grown overnight at 37°C. The following day the DNA was extracted using the Plasmid Mini kit (Qiagen) according to the

manufactures instruction. DNA was digested using restriction endonucleases and the fragmented DNA pattern examined for bands of the expected size.

In some cases the DNA in the colony was directly amplified by PCR using two known oligonucleotides. Here, the colony was carefully picked, streaked out on another LB plate, to maintain the colony, and the rest resuspended into 40 µl dH_2O. Care was taken to avoid contamination with agar pieces. 4 µl of colony mixture was utilised in a 25 µl standard PCR reaction containing 100 ng gene-specific primer, 1x reaction buffer, 500 µM dNTPs, 2.5 mM $MgCl_2$ and 5 units Taq Polymerase (Abgene) and cycling parameters applied according to (2.2.1.3).

2.2.1.11 Sequencing

Inserts of newly generated plasmids were routinely sequenced. For one sequencing reaction 2 µg of plasmid DNA, as prepared in (2.2.1.1), was precipitated with 1/10 volume of 3 M sodium acetate and 2.5 volume 100% ethanol at -20°C for 30 min, followed by centrifugation for 20 min at 12900 *g* at 4°C. The pellet was washed with 1 ml 70% ethanol, dried at room temperature and sent to MWG-Biotech for sequencing with 10 pmol of the desired primer.

2.2.1.12 Plasmid construction

All oligonucleotide sequences utilised for plasmid construction are depicted in (2.1.5).

pAS1 (pBS-*elt-2::LAP::cdc-25.1(+)*) and pAS2 (pBS-*elt-2::LAP::cdc-25.1(ij48)*): PCR amplification of the 5068 bp *elt-2* promoter was done from the pJM69 vector (gift from J. McGhee, University of Calgary, Canada) using the Elt-2Xho2 and Elt-2Bam oligonucleotides. PCR amplification of a 2569 bp *cdc-25.1* genomic DNA fragment was done using 25gBam and 25gXba oligonucleotides; this fragment starts at the first codon following the *cdc-25.1* ATG and includes 478 bp of 3'UTR. The fragments were cut with *Xho*I/*BamH*I (*elt-2*) and *BamH*I/*Xba*I (*cdc-25.1*) and inserted into pBS-SK that was digested with *Xho*I and *Xba*I. The resulting vector was subsequently digested with *BamH*I and the LAP tag (GFP-S-tag-TEV cleavage site) inserted in frame as a 1086 bp *BamH*I fragment that was derived from *BamH*I digestion of the pIC26 vector. For pAS2 the same procedure was followed, except genomic DNA from the *C. elegans* strain IA123 was utilised to amplify *cdc-25.1(ij48)*.

pAS3 (pBS-*elt-2::cdc-25.1(+)*): 25.1Notagsen and 25.1Notagas oligonucleotides were annealed. The pBS-*elt-2::LAP::cdc-25.1(+)1* (or for pAS4 *cdc-25.1(ij48)*) plasmid was cut with *BamH*I to release the LAP tag cassette and the annealed oligonucleotides ligated into the *BamH*I-cut vector backbone to insert the ATG (performed by A. Coyle). This vector contains two additional amino acids following the ATG compared to the wild-type CDC-25.1 sequence (R and S insertion).

pAS5 (pQE-30-*cdc-25.1(+)*): PCR amplification of a 1815 bp *cdc-25.1* cDNA fragment using the 25gBam and 25cSac oligonucleotides and insertion of the *cdc-25.1 BamH*I/*Sac*I fragment into pQE30 (cut with *BamH*I and *Sac*I). This results in N-terminal tagging of CDC-25.1 with six histidines. (pAS6 [pQE-30-*cdc-25.1(ij48)*] was also generated in this study, similar to pAS5, but using the *cdc-25.1(ij48)* cDNA as a template).

pAS7 (pBS-*lin-23(+)*): genomic *lin-23* was PCR-amplified using oligonucleotides *lin-23*-5'gen and *lin-23*-3'gen to clone 2138 bp of upstream promoter, the complete *lin-23* gene and 766 bp of 3' UTR. The 5.5 kb fragment was digested with *Kpn*I and inserted into the *Kpn*I site of pBS-SK.

pAS8 (pBS-*lin-23::FLAG-TY*): a 1068 bp fragment was generated using the *lin-23*tag5 oligonucleotide with the *lin-23*-Flg and a 832 bp fragment using oligonucleotide *lin-23*TY and M13rev by PCR amplification using the pBS-*lin-23* plasmid as a template. The fragments were digested with *BamH*I and *Spe*I. pBS-*lin-23* was digested with *BamH*I and the 1828 bp *BamH*I fragment removed. The two PCR fragments were inserted in the correct orientation into the *BamH*I-digested vector-backbone to generate pBS-*lin-23::FLAG-TY*. The sequence comprising the tag site generated is: *lin-23* (last codon) - *FLAG* tag - *Spe*I restriction site - *TY* tag - Stop codon.

pAS9 (pBS-*unc-119(+)*): a 5.7 kb *Hind*III/*Xba*I fragment, containing the full *unc-119* genomic sequence, was excised from pIC26 and cloned into the *Hind*III and *Xba*I site of pBS-SK.

pAS10 (pBS-*unc-119(+)-lin-23::FLAG::TY*): the *lin-23::FLAG-TY* sequence of pBS-*lin-23::FLAG-TY* was excised as a 5.6 kb *Kpn*I fragment and inserted into the *Kpn*I site of pBS-*unc-119*. The resulting orientation 5'-> 3' is: *Kpn*I - *lin-23::FLAG* - *Spe*I - *TY* - *Kpn*I - *Hind*III - *unc-119* - *Xba*I.

pAS11 (pGEX-6P-*lin-23(+)*): the 1995 bp *lin-23* cDNA (lacking the endogenous ATG) was PCR-amplified using *lin-23*-GSTfl and *lin-23*-GSTSTP oligonucleotides. The PCR fragment was digested with *Sma*I and inserted in frame into the *Sma*I site of pGEX-6P-1. This generates an N-terminal GST fusion of LIN-23. The amino acid sequence comprising the fusion 5'->3': GST tag - Precission Protease site - spacer (LGSPEFPG) - 2. amino acid of LIN-23.

pAS12 (pQE-80L-*lin-23(+)*): pGEX-6P-*lin-23* was cut with *Sma*I and the 1.9 kb *lin-23* cDNA fragment excised and inserted in frame into the *Sma*I-linearised pQE80L resulting in an N-terminal HIS_6 tag fusion. The sequence comprising the fusion site 5'->3': 6x HIS - spacer (GSACELGTPG) - 2. amino acid of LIN-23.

pAS13 (pQE-80L-*lin-23N)*: pQE80-*lin-23* was digested with *Pst*I and the 5.4 kb vector-backbone, containing the 764 bp N-terminal fragment of *lin-23*, religated. This results in *E. coli* expression of the first 254 amino acids of LIN-23.

pAS14 (pQE-80L-*lin-23C*): pQE80-*lin-23* was cut with *BamH*I, the 1.2 kb band released and the 5.5 kb vector religated. This results in the expression the last 265 amino acids of LIN-23 fused to six histidines at the N-terminus. Fusion site: HIS_6- codon 401 of *lin-23*.

2.2.2 Protein biochemistry

2.2.2.1 SDS-PAGE

SDS polyacrylamide gels were either purchased from Bio-Rad with the desired acrylamide concentration or prepared according to the following recipe (note for different acrylamide concentration the volumes of acrylamide and dH_2O were changed accordingly):

	10% running gel	stacking gel
30% Acrylamide/ Bisacrylamide (29:1)	17.1 ml	4 ml
10 % SDS	520 µl	200 µl
dH_20	21.2 ml	13.1 ml
1.5M Tris pH 8.7	13 ml	-
1M Tris pH 6.8	-	2.5 ml
10% Ammoniumpersulfate	500 µl	200 µl
TEMED	50 µl	20 µl

Table 2.13 SDS polyacrylamide gel composition.

Gels were assembled using the Minigel Cell / Transfer module (Bio-Rad) according to the manufacturer's instructions. Gels were run at 200 V for 45 to 50 min at room temperature.

2.2.2.2 Western blotting

SDS polyacrylamide gels and nitrocellulose membrane (Schleicher & Schuell) were soaked in 1x blotting buffer prior to transfer. Gels were assembled into the Minigel Transfer module (Bio-Rad), according to the manufacturer's instructions, and the protein transfer performed in 1x blotting buffer at 200 mAmp for 2 hr at 4°C. The membrane was subsequently soaked in 1x Ponceau solution (Sigma) for 2 min and immediately washed in 1x PBS-T, before incubation with blocking solution for 1 hr at room temperature. Primary antibody was added at the desired concentration (see Table 2.9) in blocking solution either for 2 hr at room temperature or overnight at 4°C. Following incubation, the blot was washed quickly three times in 1x PBS-T and three times for 10 min in blocking solution before addition of secondary antibody (in blocking solution). As secondary antibody either anti-rabbit (Amersham) or anti-mouse (Promega) IgG coupled to HRP were used at 1:2000 concentration for 45 min at room temperature (see Table 2.10). The blots were washed as above and after the third wash with blocking solution, rinsed three times in 1x PBS and subjected to ECL development. 2 ml of a 1:1 ECL solution (Amersham) was applied to 10 cm nitrocellulose membrane for 2 min at room temperature. The blot was routinely exposed to Kodak-film for 10 sec, 30 sec, 1 min, 2 min or 5 min or where necessary up to overnight.

2.2.2.3 Coomassie staining

SDS polyacrylamide gels were soaked for 30 min in Coomassie staining solution, washed once with dH_2O and soaked in destaining solution until bands became visible.

2.2.2.4 Recombinant expression of proteins in *E. coli*

Exact growth conditions are summarised in (Table 2.14). Typically, 0.5 µg of plasmid DNA was transformed into the BL21 Codonplus IRL strain (Stratagene) and the *E. coli* plated overnight on LB plates containing the desired antibiotics and 2% glucose. One inoculation loop of freshly grown colonies was scraped off the plate and added to 400 ml of liquid LB containing antibiotics and 2% glucose. The cultures were grown at 37°C to an OD_{600} 0.6. One ml of non-induced culture was collected by centrifugation at 13200 *g* for 30 sec at room temperature and the pellet suspended in 100 µl 2x SDS sample loading buffer

per one OD_{600} of cells (= non-induced sample). The non-induced sample was heated at 95°C for 4 min. The remaining culture was induced with IPTG and ethanol added to a final concentration of 3% for chaperon induction. Cultures were incubated for 4 hr at 20°C, the *E. coli* collected by centrifugation at 4000 *g* for 10 min at 4°C, and the *E. coli* pellets were frozen at -20°C until further usage. A 1 ml sample of the induced fraction was prepared in the same way as the non-induced sample. 0.1 OD_{600} of non-induced and induced sample were applied to SDS-PAGE, and protein induction was analysed by Coomassie staining (2.2.2.3) or Western blot (2.2.2.2).

Fusion protein	Plasmid	Antibiotics	IPTG (mM)
HIS_6::CDC25.1	pQE-30-*cdc-25.1(+)* pREP4	Ampicillin Kanamycin Chloramphenicol	0.5
GST::LIN-23	pGEX6P-*lin-23(+)*	Ampicillin Chloramphenicol	0.5
HIS_6::LIN-23	pQE-80L-*lin-23(+)*	Ampicillin Chloramphenicol	0.5
HIS_6::LIN-23N	pQE-80L-*lin-23N*	Ampicillin Chloramphenicol	0.5
HIS_6::LIN23C	pQE-80L-*lin-23C*	Ampicillin Chloramphenicol	0.5

Table 2.14 Growth conditions for protein expression in *E. coli*.

2.2.2.5 Purification of soluble fusion proteins from *E. coli*

The frozen and IPTG-induced *E. coli* pellets were resuspended on ice in the desired pre-chilled lysis buffer. Typically, 10 ml lysis buffer per 800 ml of starter culture were used. The cells were ruptured using an Ultrasonic Processor with a 5 mm microtip with 10 pulses for 10 seconds at 38% amplitude. The homogenate was lysed until it changed to a clear appearance. A 100 µl fraction of the homogenate was kept aside for test sample preparation. The total homogenate was centrifuged at 15000 *g* for 20 min at 4°C. During that time the homogenate test sample was centrifuged at 13200 *g* for 10 min at 4°C. After 10 min, 100 µl of 2x SDS sample loading buffer was added to the supernatant (soluble test fraction) of the test sample. The test sample pellet (insoluble test fraction) was suspended in 100 µl lysis buffer prior to addition of 100 µl 2x SDS sample buffer. Both samples were heated at 95°C for 4 min. Soluble and insoluble test fractions were applied to SDS-PAGE to estimate solubility of the fusion protein. For soluble proteins, the total supernatant was applied to the affinity resin, whereas the pellet was kept for purification of the insoluble fraction (see 2.2.2.6). Typically, 300 µl Ni-NTA agarose beads were used (Qiagen) for 10 ml supernatant of HIS_6-tagged fusion protein or 200 µl of Glutathione-Sepharose

(Amersham Biosciences) for 10 ml of supernatant of GST-tagged fusion protein. However, the amount was increased with elevated concentration of expressed fusion protein in the extract. Binding was performed using a 50 ml conical for 2 hr at 4°C with continuous end-over-end rotation. After 2 hr the beads were poured into a 10 ml Poly-Prep Column (Bio-Rad) and washed three times with 10 ml wash buffer. Proteins were eluted from the beads using five times one column volume of elution buffer and, where applicable, dialysed in 1x PBS-G overnight at 4°C.

Buffer	HIS_6 fusion	GST fusion
Lysis	50 mM Tris pH 7.5, 200 mM NaCl, 1 mM $MgCl_2$, 8.7% glycerol, 5 mM beta-mercaptoethanol, 15 mM Imidazole pH 7.5, 1x Protease inhibitor cocktail (PIC), 0.5 µg/µl Lysozyme	10 mM Tris pH 8, 150 mM NaCl, 1 mM EDTA, 5% glycerol, 1 mM DTT, 1x PIC, 0.5 µg/µl Lysozyme, 1% Triton X-100
Wash	50 mM Tris pH 7.5, 200 mM NaCl, 1 mM $MgCl_2$, 8.7% glycerol, 5 mM beta-mercaptoethanol	1x PBS, 8.7% glycerol
Elution	50 mM Tris pH 7.5, 200 mM NaCl, 1 mM $MgCl_2$, 8.7% glycerol, 5 mM beta-mercaptoethanol, 500 mM Imidazole pH 7.5	1x PBS, 40 mM Glutathione pH 7.5, 200 mM NaCl, 0.1% NP 40, 8.7% glycerol

Table 2.15 Buffers for HIS_6 and GST fusion proteins.

2.2.2.6 Purification of insoluble fusion proteins from *E. coli*

Typically, several growth conditions were chosen to improve the solubility of the fusion protein, such as different *E. coli* strains, low growth temperature, different IPTG concentrations or addition of ethanol to the culture. However, where only a small fraction of the fusion protein remained soluble, under any of the conditions tested, purification of the insoluble material was performed. This was the case for all proteins from (Table 2.16). After centrifugation of the homogenate from (2.2.2.5), the supernatant was removed and the pellet used for purification of the insoluble proteins from inclusion bodies. All further steps were carried out at room temperature to avoid precipitation of urea that was used as extraction reagent. The exact buffer conditions are summarised in (Table 2.16). 10 ml of lysis buffer was added to the insoluble fraction and sonicated for approximately 20 seconds to solubilise all proteins. The sample was clarified by centrifugation at 15000 *g* for 20 min and the supernatant applied to 300 µg Ni-NTA (Qiagen) per 800 ml starter culture (amount was increased for abundantly expressed fusion proteins). The mixture was incubated for 2 hr on a turning wheel with continuous end-over-end rotation. The sample was subsequently poured into a 10 ml Poly-Prep column (Bio-Rad), the beads were washed three times with 10 ml wash buffer and eluted with five column volumes of elution buffer. Where removal

of urea was essential, the eluted proteins were dialysed overnight in 1x PBS, containing 22% (v/v) glycerol, followed by a further dialysis step into 1x PBS-G. The dialysed sample was snap-frozen in liquid nitrogen and stored at -80°C. However, the dialysis step resulted in precipitation of LIN-23 fusion proteins and the precipitation could not be avoided by stepwise dialysis or extraction with guanidium chloride.

Fusion protein	Lysis buffer	Wash buffer	Elution buffer
HIS_6::CDC25.1	1x PBS, 8 M urea, 200 mM NaCl, 20 mM Imidazole pH 7.5, 8.7% glycerol, 1x PIC	1x PBS, 8 M urea, 200 mM NaCl, 20 mM Imidazole pH 7.5, 8.7% glycerol	1x PBS, 6 M urea, 500 mM Imidazole, 8.7% glycerol
GST::LIN-23	10 mM Tris pH 7.5, 4 M urea, 150 mM NaCl, 1 mM EDTA, 5% glycerol, 1 mM DTT, 1x PIC	not done, sample applied on polyacrylamide gel	not done, sample applied on polyacrylamide gel
HIS_6::LIN-23	1x PBS, 8 M urea, 200 mM NaCl, 20 mM Imidazole pH 7.5, 8.7% glycerol, 1x PIC	1x PBS, 8 M urea, 200 mM NaCl, 20 mM Imidazole pH 7.5, 8.7% glycerol	1x PBS, 6 M urea, 500 mM Imidazole, 8.7% glycerol
HIS_6::LIN-23N	1x PBS, 8 M urea, 200 mM NaCl, 20 mM Imidazole pH 7.5, 8.7% glycerol, 1x PIC	1x PBS, 8 M urea, 200 mM NaCl, 20 mM Imidazole pH 7.5, 8.7% glycerol	1x PBS, 6 M urea, 500 mM Imidazole, 8.7% glycerol
HIS_6::LIN23C	1x PBS, 8 M urea, 200 mM NaCl, 20 mM Imidazole pH 7.5, 8.7% glycerol, 1x PIC	1x PBS, 8 M urea, 200 mM NaCl, 20 mM Imidazole pH 7.5, 8.7% glycerol	1x PBS, 6 M urea, 500 mM Imidazole, 8.7% glycerol

Table 2.16 Lysis conditions for insoluble proteins.

2.2.2.7 Protein dialysis

Protein buffers were exchanged against the desired buffer (typically 1x PBS-G) overnight at 4°C using the Mini dialysis kit (1 kDa cut off, up to 500 µl, Amersham Biosciences) or for volumes up to 5 ml the Slide-A-Lyzer 3.5K MWCO dialysis cassettes (Pierce).

2.2.2.8 Peptide antibody production

Anti-LIN-23 peptide antibodies were generated by the company Covalab, according to the company's policy. Two peptides were synthesised by Covalab, according to the company's recommendations, these comprise the LIN-23 amino acids 18 - 31: CLTEGEHDEGKPLSI for peptide 1 and amino acids 194 - 207: CIIRDIHNIDNNWKR for peptide 2. Both peptides were utilised to immunise two rabbits. However, even after affinity purification of

the antisera these LIN-23 antibodies did not recognise any specific band on a Western blot. For the CDC-25.1A and CDC-25.1B antibodies see (Clucas, 2003; Clucas et al., 2002).

2.2.2.9 Antibody production against recombinant CDC-25.1 and LIN-23

GST::LIN-23 and HIS_6::CDC-25.1 were recombinantly expressed in *E. coli*. The proteins were purified according to (2.2.2.5) and (2.2.2.6). In case of CDC-25.1, one mg of full-length protein in 1x PBS-G was sent to SNBTS for immunisation of two rabbits. However, in the case of GST::LIN-23, slight modifications were necessary due to the low expression level and insolubility of the protein. The protein was first solubilised as in (2.2.2.5). However, the pellet was then further purified in a 4 M urea-containing lysis buffer (see 2.2.2.6), which retained 50% of the expressed protein in the insoluble pellet. This pellet fraction was substantially free of other contaminants and diluted in 2x SDS sample buffer. The sample was heated for 4 min at 95°C. In total, 500 µg of GST::LIN-23 protein was applied to SDS-PAGE (100 µg/gel), the SDS-gel stained with Coomassie and the correct size band cut out of the gel. The gel pieces were quick-frozen in liquid nitrogen and crushed into very small pieces using a pestle and mortar. 1x PBS-G was added to the pieces in order to obtain a thick slurry that was transferred into microcentrifuge tubes and concentrated overnight under vacuum pressure. The protein was sent to SNBTS Scotland for antibody production in one rabbit and one rat according to the company's regulations. A resulting first test bleed was analysed for expression of protein-specific antibodies by Western blotting against HIS_6::CDC-25.1 and HIS_6:: LIN-23N or HIS6::LIN-23C. For the LIN-23 antisera the rabbit serum only reacted to HIS_6::LIN-23C, suggesting it contained antibodies only against the C-terminus of LIN-23. The rat antibody did not react at all with recombinant LIN-23. Sera were affinity purified against recombinant HIS_6::CDC-25.1 or HIS_6::LIN-23C according to (2.2.2.12).

2.2.2.10 Crosslinking of recombinant CDC-25.1 and LIN-23 proteins to CNBr-Sepharose

This step was performed to provide an affinity matrix for purification of crude antisera that were raised against recombinant LIN-23 or CDC-25.1 as performed in (2.2.2.12). Purified recombinant HIS_6::LIN-23C and HIS_6::CDC-25.1 were dialysed in 4 M urea, 0.1 M sodium borate pH 8.3 overnight at 4°C. CNBr-Sepharose (Amersham Biosciences) was activated according to manufacturer's instruction. Briefly, 1 g CNBr-Sepharose 4B was added to 50 ml ice-cold 1 mM HCl in a 50 ml conical and allowed to swell for 2 min. The solution was poured into a 20 ml Economo column (Bio-Rad) and washed with an

additional 200 ml cold 1 mM HCl, followed by one wash with 80 ml wash buffer (100 mM sodium borate pH 8.3, 150 mM NaCl). 0.5 g of activated resin was used to immobilise 2.5 mg (LIN-23C) or 5 mg (CDC-25.1) recombinant protein in a total volume of 2.5 ml binding buffer (4 M urea, 0.1 M sodium borate pH 8.3) by batch-wise incubation for 2 hr at room temperature with continuous end-over-end rotation. The beads were spun at 700 *g* for 2 min and the flow-through collected for further analysis. The beads were washed once with 10 ml 100 mM sodium borate pH 8.3, 150 mM NaCl and once with 100 mM Tris pH 8.0, and collected by centrifugation between the washing steps. After the final wash, the beads were suspended in 10 ml of 100 mM Tris pH 8.0 and incubated at room temperature for 1 hr. Following this incubation, the beads were poured into a 10 ml Poly-Prep column (Bio-Rad) and washed with 7 ml of low pH wash buffer (100 mM sodium acetate pH 4, 150 mM NaCl), followed by an additional wash in 7 ml 100 mM Tris pH 8.0. This step was repeated three times and the protein beads were finally washed with 10 ml 1x PBS containing 0.01% sodium azide and stored at 4°C. A fraction (equivalent to 0.5 µg protein) of input, flow-through and crosslinked beads were analysed by SDS-PAGE to monitor binding and crosslinking efficiency of the proteins.

2.2.2.11 Affinity purification of CDC-25.1 and LIN-23 antisera against peptides

All peptides used to immunize the rabbits were coupled to Sepharose resin by the company Covalab (France) (see (Clucas, 2003; Clucas et al., 2002) for the anti-CDC-25.1A antibody, for the anti-CDC-25.1B antibody a peptide against amino acids 592 to 604 was used; see (2.2.2.8) for LIN-23). The LIN-23 antisera were affinity purified by Covalab. For CDC-25.1A and B antisera, 5 ml of immune serum was bound to 1 ml of coupled peptide resin for 90 min at room temperature. The flow-through was collected, the resin washed with 15 ml 1x PBS-T, followed by 30 ml 1x PBS. The antibody was eluted with 10 ml of elution buffer (0.1 M Glycine / 200 mM NaCl pH 2.2) and 1 ml fractions were collected on ice in microcentrifuge tubes containing 200 µl 1 M Tris pH 8.0. The column was re-equilibrated in 1x PBS / 50 mM Tris pH 8.0 and the flow-through re-bound to the beads. This step was repeated twice. A further 10 ml of fresh serum was utilised in case of the CDC-25.1B antiserum and purified twice as above. The OD_{280} was determined for all elution fractions and eluates with highest protein concentration were pooled and precipitated overnight on ice with 60% ammonium sulfate (ammonium sulfate powder was slowly added while stirring on ice). The sample was centrifuged at 4600 *g* for 30 min at 4°C, the pellet suspended in 500 µl 1x PBS-G and dialysed in 1x PBS-G for 10 hr at 4°C.

Protein concentration was determined by spectroscopy (5 µl in 100 µl dH_2O at OD_{280}) and SDS-PAGE analysis (final IgG concentration was 4.8 µg/µl for CDC-25.1A, 1.2 µg/µl for CDC-25.1B). The purified antibodies were kept at -20°C and specificity was analysed by Western blotting against *C. elegans* wild-type, *cdc-25.1* RNAi or *lin-23* RNAi extracts.

2.2.2.12 Affinity purification of CDC-25.1 and LIN-23 antisera against recombinant proteins

5 ml of the anti-CDC-25.1 first test bleed and 10 ml of anti-LIN-23 final bleed were diluted with 5 or 10 ml of 1x PBS, respectively. The anti-CDC-25.1 and anti-LIN-23 sera were bound to 4 mg HIS_6::CDC-25.1 and 1 mg HIS_6::LIN-23C proteins (that were crosslinked to CNBr-Sepharose as prepared in (2.2.2.10)), respectively. The samples were incubated overnight at 4°C in a 15 ml conical with continuous end-over-end rotation. The beads were subsequently poured into a 10 ml Poly-Prep column (Bio-Rad) and the flow-through collected. The antibody, bound to the beads, was washed once with 10 ml wash buffer (1x PBS-T), followed by three washes with 10 ml of 1x PBS. Bound antibody was eluted with 10 ml of elution buffer (100 mM Glycine, 200 mM NaCl pH 2.2), and 1 ml fractions were collected on ice in 1.5 ml microcentrifuge tubes, containing 200 µl 1 M Tris pH 8.0 to neutralise the acidic pH from the elution buffer. The beads were immediately neutralised by the addition of 10 ml 50 mM Tris pH 8.0 followed by one wash with 10 ml 1x PBS. The OD_{280} of all fractions was measured to determine the eluates with highest antibody concentration. Fractions with highest OD were kept on ice for further work. The flow-through of the serum was re-bound to the beads for 2 hr at room temperature and the beads washed and eluted as above. This step was repeated once or until no further antibody eluted from the beads. In case of anti-LIN-23 antibody purification, an additional 10 ml of fresh serum was added in a further purification step.

The fractions with highest antibody concentrations were pooled and subsequently diluted on ice to a final concentration of 50% ammonium sulfate, by slow addition of a concentrated (4.2 M) ammonium sulfate solution. This solution was incubated on ice overnight, followed by a centrifugation step at 4600 *g* for 30 min at 4°C to pellet the antibody. The pellet was suspended in an equal volume of 1x PBS-G and further dialysed against 1x PBS-G for 10 hr at 4°C. The antibody concentration was determined by spectroscopy (1 µl in 100 µl dH_2O at OD_{280}) and SDS-PAGE analysis against a known rabbit IgG standard (Sigma). The final concentration was 5 µg/µl for the anti-CDC-25.1f.l. antibody and 1.8 µg/µl for the anti-LIN-23 antibody. The purified antibodies were kept at

-20°C and the specificity tested by Western blotting against *C. elegans* extracts with or without *cdc-25.1* or *lin-23* RNAi as required. Additionally, a strain carrying GFP-tagged LIN-23 (OHT1707) was employed and the appearance of a high molecular weight band was detected with the anti-LIN-23 antibody that was also detected with an anti-GFP antibody.

2.2.2.13 Crosslinking of anti-CDC-25.1 and anti-LIN-23 peptide antibodies to Protein A-Sepharose

Crosslinking of affinity purified anti-CDC-25.1 and anti-LIN-23 peptide antibodies was done using the Seize X Protein A Immunoprecipitation Kit (Pierce), according to the manufacturer's instructions. In brief, 300 µl of Protein A beads suspension (= 150 µg beads) was washed in 400 µl 1x PBS and spun at 700 *g* using a microcentrifuge. This step was repeated three times and the equilibrated beads were added to 300 µg of affinity purified antibody, or as control rabbit IgG, in a total volume of 400 µl of 1x PBS (a fraction of the input material was kept for SDS-PAGE analysis). The mixture was rotated at room temperature for 1 hr and the beads spun down. The supernatant (= flow-through) was collected and the protein concentration compared to the input material using Bradford assay reagent (Pierce). The beads were washed three times in 1x PBS and resuspended in 400 µl 1x PBS, to which 25 µl of freshly dissolved Disuccinimidyl suberate (2 mg / 80 µl DMSO) was added. The beads were rotated at room temperature for 45 min, subsequently washed three times in 1x PBS and eluted using Pierce elution buffer. A fraction of the eluate was kept and the beads washed again three times with 1x PBS. A fraction of the input (3 µg protein) was compared to equal volume of flow-through and eluate on a 10% SDS polyacrylamide gel, to ensure that all antibody was crosslinked to the beads.

2.2.2.14 Crosslinking of anti-CDC-25.1 and anti-LIN-23 antibodies to Protein A-Agarose

Crosslinking of anti-CDC-25.1 and LIN-23 affinity purified antibodies (against full-length CDC-25.1 and the C-terminus of LIN-23, respectively), as prepared in (2.2.2.12), was done using 200 µg Protein A-Agarose (Bio-Rad), essentially as described in (Cheeseman and Desai, 2005). The Agarose was washed three times in 1 ml 1x PBS-T and 200 µg of affinity purified antibody was added in a final volume of 500 µl 1x PBS-G to each resin and incubated for 1 hr at room temperature with continuous rotation. The flow-through was kept and checked for binding efficiency, the beads were washed three times with 1 ml 1x

PBS-T followed by one wash in 1 ml 0.2 M sodiumborate pH 9.0. The beads were resuspended in 900 µl sodiumborate pH 9.0 to which 100 µl of 220 mM dimethylpimelimidate (freshly prepared) was added for 30 min at room temperature. This step was repeated once using fresh crosslinker, and the crosslinker quenched by washing the beads twice with 1 ml 0.2 M ethanolamine / 0.2 M NaCl pH 8.8. The beads were incubated in the same buffer for 1 hr at room temperature, followed by three washes with 1 ml 1x PBS and an elution with 500 µl 0.2 M Glycine pH 2.2 to remove any not-crosslinked antibodies.

2.2.3 C. elegans culturing and handling

C. elegans strains were grown on NGM plates seeded with a thin layer of OP50 according to standard procedures (Stiernagle, 1999; Sulston and Hodgkin, 1988).

2.2.3.1 Genetic crosses

Seven L4 males were picked onto 3.5 cm NGM plates, and allowed to grow to adulthood to mate with two adult hermaphrodites. After two to three days, the F1 generation was screened for the desired phenotype and the percentage of males recorded, as an indicator for mating efficiency. Individual F1 animals were transferred onto new plates to either observe the F2 generation after self-fertilization or where applicable to cross again into another strain.

2.2.3.2 Generation of males by heat shock

Around 80 L4 hermaphrodites were picked to four 3.5 cm OP50-seeded NGM plates, the plates sealed with parafilm and incubated at 33°C for 4 hr in a water bath. Occurrence of male progeny were scored after three days (typically four to five males were generated from 80 hermaphrodites) and backcrossed to hermaphrodites to maintain male progeny.

2.2.3.3 Growth of *C. elegans* in liquid culture

Growth of large *C. elegans* liquid cultures was essentially as described by (Cheeseman et al., 2004). Worms (for example JR1838 *cdc-25.1(+)* or IA530 *cdc-25.1(ij48)*) were axenized by adding 6 - 10 adult hermaphrodites into a drop of bleach solution (a mix of 12 µL 1 M NaOH and 6 µl 10-20% NaOCl) on the edge of a 5.5 cm OP50-seeded NGM growth plate. Cleaned embryos were allowed to hatch and grown until adulthood. 15

axenized adults were transferred onto 15 OP50-seeded 9 cm NGM growth plates (225 adults in total) for four further days to increase for L1 larvae among the population in freshly starved plates. About 5 - 6 plates, enriched with L1 larvae, were washed with 5 ml 1x M9 buffer and L1 larvae collected into a 50 ml conical and spun at 1000 *g* for 5 min at 4°C. The worms were washed once with 40 ml 1x M9 buffer, collected by centrifugation as above and the worm pellet resuspended in 5 ml 1x M9 buffer. The worms were then transferred to 500 ml of AB1157-seeded S-medium. This medium was obtained by overnight growth of AB1157 (kind gift from Prof. M. Stark, University of Glasgow) in 2 L LB, containing 50 µg/ml streptomycin, and the *E. coli* collected after centrifugation at 4000 *g* for 10 min at 4°C. The *E. coli* pellet was then added to a total of 2 L S-medium. Liquid worm cultures were grown at 20°C with continuous shaking (150 rpm) in baffled 2 L culture flasks (Fisher Scientific) to promote aeration of the cultures. Worms were grown until a maximum percentage reached adulthood and contained approximately ten embryos per hermaphrodite (usually after 3 or 3.5 days).

2.2.3.4 Harvesting embryos from large-scale liquid cultures

Adult worms, grown in liquid culture, were collected through settling them down the bottom of the 2 L flask for 1 hour on ice. Under this condition most *E. coli* remained in the supernatant. *C. elegans* adults were transferred to a 50 ml conical. The worms were allowed to settle for 10 min on ice and the worms were washed twice with 50 ml ice-cold 1x M9 buffer, allowing the worms to settle to the bottom of the tube between the washes. After the last wash, the worms were resuspended in 25 ml 1x M9 and 25 ml 60% ice-cold sucrose, mixed and spun at 1000 *g* for 5 min at 4°C. This step promoted the adult worms to float on top of the sucrose cushion, away from unwanted particles in the culture, and increased the efficiency of bleaching that subsequently followed. For this step, worms were taken from the top of the cushion, up to the 35 ml mark, transferred into a new 50 ml conical, washed once with 50 ml 1x M9 buffer and collected by centrifugation as above. Worms were resuspended in 10 ml 1x M9 buffer and split into 2 conicals to which 15 ml of freshly prepared bleach solution was added. Worms were vortexed for approximately 10 - 15 min until adults were bleached and only embryos remained. Bleaching of adults was monitored and stopped as soon as the majority of adults broke open. Embryos were spun at 4600 *g* for 5 min at 4°C, washed two times with 50 ml ice cold dH_2O, two times with 1 ml 1x M9 and resuspended in 100 µl 1x M9. Development of the intestine was measured under a fluorescence microscope. At this time usually about 50% of the embryos contained a fully developed intestine. Embryos were collected and a small fraction applied to a OP50-seeded NGM plate to monitor the hatch rate (usually about 70 - 80%). The

remaining embryos were washed in the desired lysis buffer (containing no detergent) and then resuspended in equal volume of desired lysis buffer containing 2x Protease inhibitor cocktail (Roche) and detergent (typically NP40 or as indicated otherwise). Embryos were snap-frozen in liquid nitrogen and kept at -80°C until further usage.

2.2.4 *C. elegans* transgenesis

2.2.4.1 Generation of *C. elegans* strains carrying extrachromosomal arrays

Microinjections to generate transformants were essentially done according to (Evans, 2006; Jin, 1999). pBS-*elt-2::LAP::cdc-25.1(+)*, pBS-*elt-2::LAP::cdc-25.1(ij48)* or pBS-*elt-2::cdc-25.1(+)* (10 ng/µl final concentration in 1x TE, purified with the Qiagen Maxi kit) were mixed with p76-16B *unc-76* (100 ng/µl final concentration) and microinjected into the gonads of DR96 *unc-76(e911)*. Prior to injection, the DNA mix was centrifuged at 13200 *g* in a microcentrifuge for 15 min at room temperature and loaded into a drawn out capillary (Clark Electromedical Instruments, http://www.harvardapparatus.co.uk/) using a mouth pipette (Sigma). Injection pads were prepared by adding a drop of liquefied 2% agarose in dH_2O on a 64 x 22 mm glass coverslip (Thickness 1, Menzel). The agarose was flattened through addition of a second coverslip placed on top of the agarose drop. After solidification, the top slide was removed and the pads dried in an 80°C oven for 15 min. Injection needles from aluminium silicate glass capillaries, containing inner filament (GC120F-15, Clark Electromedical Instruments), were pulled using an electrode puller (Model 773, Campden Instruments Ltd, http://www.campden-inst.com/).

Five young adult hermaphrodites were transferred to a drop of paraffin oil, placed on the injection pad, and allowed to adhere to the pad. Immobilised worms were placed on the stage of a Zeiss Axiovert100 inverted microscope using Nomarski optics and injected into their gonads at 400x magnification. The DNA was released into the gonad using nitrogen gas as a pressure source. Immediately after injection, the pad was removed to a dissecting microscope and a drop of 1x M9 buffer placed on top of the oil to release the worms from the bottom of the pad. The worms were then transferred to a drop of 1x M9 on an OP50-seeded NGM agar plate and allowed to recover at 20°C. Rescued animals were identified by analysing the F1 generation of injected animals for occurrence of non-Unc progeny. To maintain rescued animals, a piece of the growth agar containing the worm population was excised and placed onto a new plate away from the food source, selecting for wild-type animals that can move to the food source as opposed to uncoordinated non-rescued

animals. Rescued animals were analysed for GFP expression by fluorescence microscopy (in case of LAP-tagged CDC-25.1) or indirect immunofluorescence against CDC-25.1.

2.2.4.2 Chromosomal integration of LAP-tagged *cdc-25.1*

Chromosomal integration using γ-radiation was essentially as described in (Evans, 2006; Jin, 1999) Briefly, strains carrying an extrachromosomal array with a transmission frequency between 30 - 50% were chosen for integration to facilitate identification of integrated lines. Two lines were chosen for integration, IA522 *elt-2::LAP::cdc-25.1(+)* and IA524 *elt-2::LAP::cdc-25.1(ij48)* generating the strains IA535 and IA536, respectively.

Healthy worm cultures, containing a high proportion of L4 animals, were irradiated with 3800 rad using a ^{60}Co source (performed by Mrs A. Livingstone, Beatson Institute of Cancer Research, Glasgow; all subsequent steps were performed by A. Segref). The P_0 worms were allowed to recover for two hours. Eight L4 irradiated worms (for IA535) or five irradiated worms (for IA536) were picked each onto 20 OP50-seeded 9 cm plates (100 P_0 for IA536 and 160 P_0 for IA535) and the worms were allowed to grow to the F2 generation for six days at 20 degrees. 15 *unc-76* rescued worms from each medium plate were picked to individual 3.5 cm plates (the total number of F2's cloned in this case was 300). Integrated lines were selected from different F2 populations. This screen was repeated two times and two independently integrated lines were chosen for further analysis. The F2 animals were allowed to self-fertilise and the F3 progeny were screened for 100% segregation of the transgene. Individual lines were again selected to ten 3.5 cm plates to verify absence of Unc animals.

2.2.4.3 Microparticle bombardment to integrate *lin-23::FLAG-TY*

Microparticle bombardment was essentially as described in (Praitis et al., 2001) and performed by Jane Shingles (Hope laboratory, University of Leeds). As food source for liquid culture, the bacterial strain HB101 was grown overnight in 500 ml LB containing 12 μg/ml streptomycin. The next day the *E. coli* was pelleted and the pellet resuspended in an equal volume of 1x M9 buffer. 3 ml of HB101 pellet was used to inoculate 100 ml S-medium containing 50 μg/ml nystatin and 50 μg/ml streptomycin. The strain DP38 *unc-119(ed3)* was freshly grown on five OP50-seeded 6 cm NGM plates at 20°C until 100% confluent. The *unc-119(ed3)* renders worms unable to undergo dauer larvae formation, therefore care was taken not to starve the worms in order to prevent survival of rare revertants in the *unc-119* gene. The worms were collected and added to 100 ml HB101-

seeded S-medium. One culture was used for one hepta-shot of bombardment, however, several cultures were started to ensure that enough worms were available. Worms were grown at 200 rpm for four days at 20°C. Worms were collected in 50 ml sterile conicals and sedimented at room temperature for 10 min (pellet 1). The supernatant was collected and incubated on ice for 20 min to form a second pellet (pellet 2). Pellet 1 was used for bombardment, whereas pellet 2 was used to inoculate 100 ml of HB101-seeded S-medium to generate a continuous stock of worms for bombardment. The worms in the first pellet were kept on ice until further usage.

During this time the DNA was coated to the gold particles. To this end, gold particles were prepared by adding 60 mg of particles (0.3-3μm, Chempur) to 2 ml of 70% ethanol, vortexed for 5 min and then soaked for a further 15 min at room temperature. The particles were spun briefly in a microcentrifuge, the supernatant discarded and the gold particles washed three times with sterile water. The final gold pellet was resuspended in 1 ml 50% sterile glycerol and stored for up to 2 months at 4°C. 7 μg of *Not*I-linearised plasmid DNA (pBS-*unc-119-lin-23::FLAG-TY*) in 30 μl digestion reaction was added drop-wise to 70 μl of gold suspension with continuous vortexing. 300 μl of 2.5 M $CaCl_2$ and 112 μl of 0.1 M spermidine (Sigma) were also added drop-wise and the beads vortexed for a further 5 min at room temperature. The beads were centrifuged at 5000 *g* for 10 seconds using a microcentrifuge, the supernatant removed and the pellet suspended in 800 μl 70% ethanol. The beads were re-pelleted and suspended in 70 ml 100% ethanol and vortexed until just before use.

A Bio-Rad PDS-1000/He machine was used for the bombardment, according to the manufacturer's instruction. Seven macrocarriers were dipped in isopropanol and placed on a paper in the sterile hood to dry. 10 μl DNA gold particles were added to the centre of the macrocarriers, allowed to dry and inserted into the holder. Subsequently, the rupture disk (1350psi, Bio-Rad) and stopping screen (Bio-Rad) were inserted into the designated holder. The carrier containing the DNA was inserted into the top shelf of the Bio-Rad chamber. 1 ml of *C. elegans* pellet (equivalent to $5 \times 10^5 - 1 \times 10^6$ young adults) was subsequently distributed to seven target spots on a non-seeded 9 cm NGM plate, that were aligned to the spacing of the holes in the macrocarrier. The plate was inserted to the second shelf (from the bottom) and the worm target spots again adjusted to the exit holes of the macrocarrier. Bombardment was performed using 27 inches Hg according to the manufacturer's instruction. After bombardment 1 ml of 1x M9 buffer was added to the plate and the worms allowed to recover for 1 hr. Subsequently, the worms were suspended

in 4 ml 1x M9 buffer and distributed to seven 9 cm OP50-seeded NGM plates. Worms were incubated at 20°C for three to four weeks before screening for integrated non-Unc animals that were able to form dauer larvae (screening and selection process was done by A. Segref). Four non-Unc larvae were selected from each 9 cm plate and picked to single 3.5 cm OP50-seeded NGM plates to select for 100% transmission rate of non-Unc progeny. Subsequently, germline expression of LIN-23::FLAG-TY was confirmed by indirect immunofluorescence against the TY tag and Western blotting with anti-LIN-23 antibodies against adult extracts. All strains resulted in high death rates of embryonic progeny, but one strain that clearly displayed a visible correct size band by Western blotting was utilised for further experiments (IA582).

2.2.5 C. elegans RNAi

2.2.5.1 Feeding RNAi on NGM plates

RNAi was performed according to the bacterial feeding method (Kamath et al., 2000; Timmons et al., 2001). In brief, *E. coli* strain HT115 (DE3) carrying the T7 IPTG-inducible feeding vector L4440 was utilised, containing parts of the relevant target genes (Table 2.17) or for control the empty L4440 vector. Production of double-stranded RNA was induced overnight at 20°C on standard NGM plates containing 1 mM IPTG and 100 µg/ml Ampicillin. Ten embryos, L1-staged animals or late L4-to-adult hermaphrodites (see Table 2.17) were fed on RNA-induced plates (after hatching when embryos were applied on plates) until they reached adulthood (three days when embryos where applied on plates and for 24 hr when L4 animals were used). F1 embryos were analysed immediately under the microscope for the desired phenotype. In parallel, the hatch rate was determined by removing adults that had egg-layed on separate plates, and screening for hatched F1 progeny after 24 hr. When sterility was measured, 20 F1 survivors were placed on fresh RNAi-seeded plates and incubated at 25°C to avoid starvation. The number of embryos present on target RNAi and control RNAi plates was determined after three days of incubation at 25°C.

Gene (Sequence name)	Target fragment relative to genomic ATG (bp)	Source	Stage applied
lin-23 (K10B2.1)	685 - 1811	RNAi library	embryo or L1
lin-23 (K10B2.1)	1812 - 2686	this study	embryo or L1
cdc-25.1 (K06A5.7)	1175 - 2049	I. L. Johnstone	L4
gsk-3 (Y18D10A.5)	1266 - 2940	C. Clucas	L1 or L4
gsk-3 like (C44H4.6)	1319 - 3018	C. Clucas	L1
cullin-1 (D2045.6)	238 - 1234	RNAi library	L4
cullin-2 (ZK5204)	1990 - 3100	this study	L4
skr-1 (F46A9.5)	-234 - 785	RNAi library	embryo or L1
skr-3 (F44G3.6)	-158 - 889	RNAi library	embryo
sel-10 (F55B12.3)	796 - 3010	RNAi library	embryo
pop-1 (W10C8.2)	5171 - 6847	RNAi library	L4
apr-1 (K04G2.8)	2696 - 4615	this study	young adults, injection
wrm-1(B0336.1)	1095 - 2632	this study	young adults, injection
hmp-2 (K05C4.6)	1232 - 2349	RNAi library	embryo or L1
bar-1(C54D1.6)	1465 - 2595	this study and RNAi library	embryo or L1, young adults in case of injections

Table 2.17 *E. coli* RNAi clones.

2.2.5.2 Feeding RNAi in liquid culture

15 L1 animals of the desired strain were each placed on six large OP50-seeded NGM plates (or even more plates to ensure that four plates without contamination were available for each experiment) and incubated at 20°C for seven days. At this stage the plates were depleted of OP50 and contained freshly starved L1 animals. One day prior to starvation, fresh 100 ml liquid cultures of the *E. coli* strain HT115 (DE3) carrying a T7-inducible feeding vector L4440, containing parts of the gene-specific insert or as control no insert, were grown overnight at 37°C in LB containing 100 µg/ml Ampicillin. Only a small amount of starting material was chosen for inoculation to avoid overgrowth of the culture. The next morning, the cultures were diluted to an OD_{600} of 0.5 - 1 in a final volume of 400 ml LB containing 100 µg/ml Ampicillin and 1 mM IPTG (freshly added). After 4 hr induction at 37°C, the cultures were harvested by centrifugation at 4000 *g* at room temperature. The culture supernatant was removed and the pellet resuspended in the remaining supernatant. Each pellet was added to 250 ml of S-medium containing 100 µg/ml Ampicillin and 1 mM IPTG to produce RNAi S-medium. The freshly starved worms were collected from four large plates in a 15 ml conical using sterile 1x M9 buffer. The worms were spun down at 1000 *g* at room temperature and washed once in 15 ml 1x M9 buffer. 400 µl of 1x M9 buffer was added to the worm pellet (typically around 600 µl) and

400 µl of the worm suspension used to inoculate 250 ml RNAi S-medium. The cultures were placed at 25°C for three days and embryos harvested according to (2.2.3.4).

2.2.5.3 Double RNAi by feeding

In some cases double RNAi was performed in liquid culture according to (Lehner et al., 2006). Briefly, 1 ml of non-induced HT115 RNAi overnight culture was mixed with 1 ml of the second non-induced HT115 RNAi culture in a final volume of 12 ml and induced with 1 mM IPTG for 4 hr at 37°C. Single RNAi, that was necessary for comparison, was diluted using the control HT115 RNAi strain. The induced *E. coli* cultures were collected by centrifugation at 4000 *g* at room temperature and the pellet added to 10 ml S-medium in a 30 ml glass conical. One 3.5 cm plate of starved L1 worms was collected in 1x M9 buffer, quickly spun down using a microcentrifuge and the worm pellet suspended in 400 µl 1x M9 buffer. 100 µl of worm slurry was added to one 10 ml RNAi culture and incubated at 25°C for 3 days with continuous shaking at 200 rpm.

2.2.5.4 RNAi by microinjection

apr-1, *gsk-3*, *bar-1* and *wrm-1* RNAi were also performed by microinjection of double-stranded RNA into the gonads of young adult hermaphrodites. Double-stranded RNA was synthesised by *in vitro* transcription of 5 µg linearised-L4440 vector containing fragments of *apr-1* (*Pst*I, *Xho*I), *gsk-3* (*Spe*I, *Nco*I), *bar-1* (*Sal*I, *Pvu*I) or *wrm-1* (*Pst*I, *Hind*III). Special care was taken to avoid RNAse contamination. After restriction digest, the DNA was precipitated with equal volumes of sodium acetate and 2.5 volumes of 100% ethanol at -20°C for 30 min, followed by centrifugation at 13200 *g* for 30 min at 4°C. The precipitated DNA was washed with 75% ethanol, dried and suspended at a concentration of 1 µg/µl in RNAse free dH_2O (Gibco). 5 µg was used to *in vitro* transcribe the single-stranded RNA using the T7 RiboMax large-scale RNA production system (Promega) according to the manufacturer's instruction. The RNA was precipitated using one volume of sodium acetate, provided with the kit, and 2.5 volumes of 100% ethanol at -20°C for 30 min. The RNA was pelleted by centrifugation at 13200 *g* for 30 min at 4°C, and the pellet washed with 75% ethanol, air dried for 15 min at room temperature, and suspended in 50 µl RNAse free dH_2O. 20 µl of each single-stranded RNA was annealed in 1x annealing buffer (10 mM Tris pH 8.0/20 mM NaCl) for 2 min at 90°C and the mixture slowly cooled to room temperature in a heated metal block to produce double-stranded RNA. Single- and double-stranded RNA were separated on 1% agarose gels (see 2.2.1.2) to ensure production of double-stranded RNA. RNA was injected into the gonads of young adult

hermaphrodites and phenotypes observed 24 hr post-microinjection. For microinjection procedures see (2.2.4.1).

2.2.6 *C. elegans* molecular biology

2.2.6.1 Isolation of *C. elegans* genomic DNA

C. elegans genomic DNA was prepared according to (Johnstone, 1999). Mixed staged worms were grown on six 9 cm OP50-seeded NGM agarose plates until cultures reached a population density of 80 - 90%. Worms were washed off the plates with ice-cold 1x M9 buffer, collected in 15 ml conicals and allowed to settle on ice for 10 min (reduces *E. coli* contamination). Worms were transferred to a 1.5 ml microcentrifuge tube and spun for 1 min at 3000 *g*. The worm pellet was resuspended in five volumes of 1x WLB and incubated at 65°C for 1 hr with occasional mixing. The mixture was extracted with 1 volume of phenol (equilibrated with Tris pH 8.0), mixed carefully (note that vortexing would shear the DNA) and spun at 13200 *g* for 5 min at room temperature. Any remaining DNA that had not extracted at this stage was dissolved by addition of fresh lysis buffer. The extracted DNA, present in the top aqueous phase, was extracted two times with one volume of phenol/chloroform followed by one extraction with chloroform. The DNA was precipitated by addition of 0.1 volume of 3 M sodium acetate pH 5.2 and 0.7 volumes of isopropanol and gentle inversion for 5 min at room temperature. The DNA was spun at 13200 *g* for 10 min at room temperature and the pellet washed once with 70% ethanol. The DNA was carefully resuspended in 100 µl 1x TE and incubation for 1 hr at room temperature with occasional mixing using a 1 ml pipette tip. Subsequently, DNAse free RNAseA (Qiagen) was added at a final concentration of 100 µg/ml and incubated at 37°C for 1 hr to remove contaminating RNA. This step was followed by addition of 0.1 volume of sodium acetate pH 5.2 and 0.7 volume of isopropanol to precipitate the DNA. The DNA was dissolved in 20 - 40 µl 1x TE.

2.2.6.2 RNA isolation from *C. elegans*

To isolate RNA from *C. elegans,* mixed stage worms were grown on four OP50-seeded 9 cm NGM agar plates to a population density of 80 - 90%. Worms were washed off the plates using 10 ml chilled 1x M9 buffer, collected in 15 ml conicals and allowed to settle on ice for 10 min. The worm pellet (around 100 µl) was transferred to a 1.5 ml microcentrifuge tube. Around 30 µl of the worm pellet was lysed in 300 µl RNA lysis buffer and incubated at 55°C for 1 hr followed by incubation for 15 min at 95°C.

RNA was isolated using Total RNA Isolation Reagent TRIR (Abgene). This method is based on extraction with guanidine salts, urea and phenol. 750 µl of TRIR was added to 300 µl RNA lysate and the RNA isolated according to the manufacturer's instruction with slight modifications. In brief, the samples were vortexed, incubated at 4°C for 5 min before addition of 200 µl chloroform. The samples were mixed again, kept on ice for 5 min and spun at 12000 *g* for 15 min at 4°C. After centrifugation, the top phase was selected and the RNA precipitated with an equal volume of 100% isopropanol, incubated on ice for 10 min and spun at 12000 *g* for 10 min at 4°C. The pellet was washed twice with 1 ml 75% ethanol and allowed to air dry for 10 min at room temperature. The RNA was resuspended in 20 µl RNAse free dH_2O and kept at -80°C.

2.2.6.3 Single worm PCR from embryos and adults

Single adult hermaphrodites were picked in 10 µl SWLB, digested at 65°C for 1 hr and the Proteinase K subsequently inactivated at 95°C for 15 min. When embryos were to be analysed, single embryos were picked into 10 µl SWLB with a mouth-pipette containing 1x M9 buffer with 1 mg/ml chitinase to remove the eggshell. The 10 µl embryo solution was processed in the same way as done for adults. 3 µl of the lysed material was used for a 25 µl standard PCR reaction containing 100 ng gene specific primer, 1x reaction buffer, 500 µM dNTPs, 2.5 mM $MgCl_2$ and 5 units Taq Polymerase (Abgene). PCR parameters were according to (2.2.1.3).

2.2.6.4 *cdc-25.1(ij48)* restriction site polymorphism

The *cdc-25.1* genomic sequence was PCR-amplified from single worms as described in (2.2.6.3) using oligonucleotides A (5'->3'): TGATGGCTACCACCGGGG and B (5'->3'): CGCGCGGATCCTTACACTTCTAACGTTGGAGGAAGTTCAGAATC (provided by C. Clucas). These primers amplify a 903 bp *cdc-25.1* genomic sequence starting at position –2 relative to the *cdc-25.1* ATG. Additional 11 bp of unrelated sequence is added at the 3' end of the PCR product generating a 914 bp fragment. The *Hinf*I site present at position 136, relative to the first bp of the PCR fragment, is deleted through the *ij48* mutation (C to T mutation in the *Hinf*I site 5'GANTC3', (Clucas, 2003)) and used to detect a restriction site polymorphism at the mutation site. Typically, 8 µl of PCR reaction was digested with 1 µl of *Hinf*I in a total volume of 10 µl for 1 hr at 37°C, and the digested PCR fragments were applied on 1.8% agarose gel and stained with ethidium bromide. Images of the gel were taken using the Biorad Transilluminator and Quantity One software. Wild-type *cdc-25.1*

results in six fragments of 423, 187, 126, 94, 42 and 42 bp, whereas the *cdc-25.1(ij48)* allele produces fragments of 423, 187, 168, 94 and 42 bp. Note that the 42 bp band does not resolve well on the 1.8% agarose gel.

2.2.6.5 *lin-23(e1883)* restriction site polymorphism

The *lin-23* genomic DNA was PCR-amplified from single worms and embryos as described in (2.2.6.3) using the oligonucleotides *lin-23*tag5 and *lin-23*-GSTSTP (for sequence see Table 2.4). These oligonucleotides amplify a 1042 bp genomic sequence starting at position +1558 relative to the ATG. Due to the addition of 10 bp in the 3' oligonucleotide a 1052 bp fragment is generated. The *lin-23(e1883)* allele creates a TGG to TGA mutation (G to A mutant) at 1756 pb relative to the ATG creating a *Bgl*II restriction site (5'AGATCT 3') (Kipreos et al., 2000). This generates an additional *Bgl*II site at 198 bp in the amplified PCR fragment. PCR fragments were digested with *Bgl*II and processed as in (2.2.6.4). Wild-type *lin-23* produces fragments of 774 and 278 bp, whereas the homozygous *lin-23(e1883)* allele produces 199, 278 and 575 bp. When the genomic *lin-23(e1883)* allele was screened in the presence of the *lin-23::FLAG-TY* allele, the *lin-23*crssgen oligonucleotide was used at the 3' end to distinguish between *lin-23::FLAG-TY* and endogenous *lin-23*. This primer hybridises specifically at the 3' end of the *lin-23* genomic sequence and not the *lin-23::FLAG-TY* allele and amplifies 1054 bp of genomic *lin-23* DNA. After digestion of the amplified PCR fragment with *Bgl*II, fragments of 774 and 280 bp in wild-type *lin-23* and 199, 280 and 575 bp in *lin-23(e1883)* are produced.

2.2.7 C. elegans biochemistry

2.2.7.1 Preparation of embryo extracts

Embryos, prepared as in (2.2.3.4), were defrosted on ice and lysed using an Ultrasonic Processor with a 5 mm microtip (Jencons) with 10 pulses for 10 sec at 40% amplitude. Crude extracts were spun at 30 000 *g* (unless otherwise indicated in the main text) at 4°C for 20 min, and in some cases the supernatants were re-spun at 135000 *g* for 20 min at 4°C using ultracentrifugation (TLA100.4 rotor). The protein concentration was measured using the Bradford assay. 1 µl of extract was applied to 1 ml Bradford protein assay reagent to measure the OD at 595 nm. Extracts were quick-frozen in liquid nitrogen and kept at -80°C until further usage or used immediately for immunoprecipitation assays.

2.2.7.2 Preparation of L4-staged extracts

L1-staged worms were used to inoculate large-scale liquid cultures according to (2.2.3.3). Worms were collected before they reached adulthood at the early-to-late L4 stage and lysed in the appropriate lysis buffer in the same way as performed on embryos (see embryo extracts (2.2.7.1).

2.2.7.3 Preparation of adult worm extracts

For small-scale preparation of adult extracts, four to five OP50-seeded 9 cm NGM plates were inoculated with L1-staged worms and grown to adulthood. The worms were collected in 1x M9 buffer on ice and washed several times. The worms were allowed to settle on ice, the supernatant removed and the worm pellet suspended in an equal volume (around 100 µl) of lysis buffer (50 mM Tris pH 7.5, 150 mM NaCl, 1 mM EDTA, 10% glycerol, 1% NP40, 1 mM DTT and 1x Protease inhibitor tablet when worm extracts were prepared to remove cuticles). The worms were snap-frozen in liquid nitrogen, sonicated using an Ultrasonic Processor with a 5 mm microtip (Jencons) with 10 pulses for 10 sec at 40% amplitude. Crude extracts were spun at 30 000 *g* for 20 min at 4°C and the supernatant recovered. The extract was kept at -80°C until further usage.

2.2.7.4 Phosphatase treatment of adult and embryo extracts

Adult *C. elegans* extracts were prepared as in (2.2.7.3), except the worms were lysed in a buffer containing 50 mM Tris pH 7.5, 100 mM NaCl and 2x Protease inhibitor cocktail. Embryo extracts were prepared as in (2.2.7.1) and lysed in a buffer containing 50 mM Tris pH 7.5, 150 mM NaCl, 1 mM EDTA, 10% glycerol, 0.2% NP40, 1 mM DTT and 2 x Protease inhibitor cocktail. Typically, 5 µl of extract was incubated for 30 min at 30°C with either 1x λ–phosphatase reaction buffer alone (NEB) (final buffer concentration 50 mM Tris pH 7.5, 100 mM NaCl, 2 mM DTT, 0.1 mM EGTA, 0.01% Brij35, supplemented with 2 mM $MnCl_2$ and 1x Protease inhibitor cocktail) or λ-phosphatase buffer containing 800 units of λ–phosphatase (NEB) in a total volume of 20 µl. The samples were suspended in equal volumes of SDS sample buffer, heated for 4 min at 95°C and 12 µg (adult extract) or 15 µg total protein (embryo extract) applied to SDS-PAGE analysis using 8% SDS polyacrylamide gels (self-poured according to (2.2.2.1). As control the same amount of total protein was directly suspended in SDS sample buffer, heated and applied to SDS-PAGE.

2.2.7.5 Immunoprecipitation from embryo and L4 extracts

Unless otherwise stated, around 300 µg of total protein contained in an extract (obtained as in (2.2.7.1) and (2.2.7.2)) was diluted to 200 µl in lysis buffer (50 mM Tris pH 7.5, 100 mM KCl, 1 mM EDTA, 1 mM $MgCl_2$, 8.7% glycerol, 1% NP40, 2x protease inhibitor cocktail (Roche) and 1x phosphatase inhibitor cocktail I and II (Sigma)). The concentration of KCl and NP-40 was adjusted in several experiments and this buffer here displays the conditions that were used for immunoprecipitation of CDC-25.1 using the newly generated CDC-25.1f.l. affinity purified antibody. 40 µg of affinity purified CDC-25.1f.l. antibody, crosslinked to Protein A-Agarose (according to (2.2.2.14), was added to 200 µl of diluted extract in a 1.5 ml Mobicol tube (Mobitec, http://www.mobitec-us.com/) and rotated on a turning wheel for 1 hr at 4°C with continuous rotation. As control, rabbit IgG was used (Sigma) that had been crosslinked to Protein A-Agarose identical to the CDC-25.1f.l. antibody. During optimisation procedures (as indicated in the Chapter 4, (4.2.1.3)) sometimes higher concentrations of antibodies were employed. The beads were spun down at 700 *g* in a microcentrifuge and the flow-through recovered. The beads were washed three times with 400 µl of lysis buffer and finally eluted using 30 - 40 µl of elution buffer (100 mM Glycine, 200 mM NaCl pH 2.2) for 3 min at room temperature. The beads were again spun down, the eluate collected and an equal volume of SDS sample buffer was added to the flow-through and eluate and incubated at 95°C for 4 min. Samples were kept at -20°C.

2.2.7.6 Purification of LAP::CDC-25.1 on S-Protein Agarose

Embryonic extracts were prepared from large-scale liquid cultures of IA535, IA536 and JR1838 according to (2.2.7.1). Embryos were collected and lysed in lysis buffer (50 mM Tris pH 7.5, 300 mM KCl, 1 mM EDTA, 0.05 % NP40, 1 x Protease inhibitor cocktail (Roche) and 1x Phosphatase inhibitor cocktail I and II (Sigma). 60 µg of S-Protein Agarose (Novagen) were washed once with 400 µl of lysis buffer. 300 µg of total protein in lysis buffer were incubated with the washed S-Protein Agarose in a total volume of 200 µl. 10 µl was kept aside as input control. The mixture was incubated in a 1.5 ml Mobicol tube for 3 hr at 4°C with continuous end-over-end rotation, the flow-through collected, and the beads washed three times with 400 µl lysis buffer. The samples were eluted for 3 min at room temperature in 60 µl SDS sample buffer followed by 4 min incubation at 95°C. A fraction of the input and flow-through was suspended in equal volume of SDS sample buffer and heated at 95°C for 4 min. 5 µl of the input and flow-through and 20 µl of the

eluate were applied to 10% SDS-PAGE to probe against CDC-25.1, GFP or LIN-23. For probing of the Western blot against GFP slightly higher volumes had to be applied to SDS-PAGE for the LAP-tagged proteins and lower volumes for GFP::LacZ due to the difference in expression levels but the ratios of input, flow-through and eluate were kept constant.

2.2.8 Microscopy

2.2.8.1 Preparation of living specimen

Microscopy of embryos and worms was according to standard methods (Sulston and Hodgkin, 1988). Larvae or adults were mounted on a 4% agarose pad (containing 10 mM sodium azide if no real time imaging was performed) and a drop of 1x M9 buffer. Where embryos were to be imaged, around 20 adults were transferred to a watch glass that was filled with 1x M9 buffer. The adults were cut open using two 18-gauge needles and the embryos selected with a mouth pipette (a plastic tubing connected to a drawn out capillary glass). Embryos were transferred to a drop of 1x M9 buffer. A coverslip was carefully added on top of the adults or embryos and sealed with paraffin.

2.2.8.2 Preparation for fixed specimen

Prior to the collection of samples, one drop of 0.1% Poly-L-lysine solution (Sigma) was added on the centre of a glass slide and allowed to dry. Where larvae were to be analysed, several larvae were selected with a worm pick and placed in one drop of 1x M9 buffer that was added on top of the Poly-L-lysine-coated slide. Embryos were selected as in (2.2.8.1) and transferred to a drop of 1x M9 buffer that was placed on the surface of the Poly-L-lysine-coated slide. The samples were processed further as in (2.2.8.3).

2.2.8.3 Indirect immunofluorescence

Samples were prepared as in (2.2.8.2). A 22 x 22 mm coverslip (Menzel) was carefully added on to of the 1x M9 drop containing larvae or embryos. Excess liquid was removed by placing a tissue over the glass. Very slight pressure was applied to the coverslip during this procedure, to ensure direct contact of the coverslip and the specimen. The slide was immediately placed on top of a cold metal block that had been pre-chilled on dry ice for several minutes. Slides were allowed to freeze for several minutes and the coverslip quickly removed, with the aid of a scalpel blade, to crack open the eggshell or cuticle of

the embryo and worm, respectively. The slides were directly immersed in 100% methanol (pre-chilled at -20°C) and incubated at -20°C for 10 min before transfer into 100% acetone (pre-chilled at -20°C) for 10 min. Slides were removed from the acetone and allowed to air dry. 200 µl of 1x PBS/0.2% Tween 20 were added on top of the sample and incubated for 2 min. The sample was pre-blocked in 200 µl 1% dried milk in 1x PBS/0.2% Tween 20 for 20 min at room temperature. This was followed by an overnight incubation in the same blocking buffer containing the primary antibody in a humid chamber at 4°C (for antibody dilutions see Table 2.9). The next day, slides were washed quickly three times in 200 µl 1x PBS/0.2% Tween 20, followed by two 10 min washes in the same buffer, before incubation with secondary antibody at 1/200 dilution in 1x PBS/0.2% Tween 20 (for secondary antibodies used see Table 2.10). Samples were incubated in a humid chamber for 1 hr at room temperature protected from light. Identical wash steps, as done after the primary antibody incubation, were performed. The samples were allowed to air dry for several minutes, mounted in 10 µl of Vectashield (Vector Laboratories), containing 1.5 µg/ml DAPI, and sealed with clear nail polish. Slides were stored at 4°C in the dark.

2.2.8.4 Conventional microscopy for fluorescence and Nomarski imaging of fixed and living samples

Live or fixed embryos, larvae and adults were viewed using a Zeiss Axioplan 2 microscope (Carl Zeiss, http://www.zeiss.co.uk/) with Nomarski optics. For different magnifications either a 10x/0.3, 20x/0.5, 40x/0.75 Plan-Neofluar or 63x/1.4 and 100x/1.4 Plan-Apochromat lense were used. GFP, Alexa Fluor 488 or Alexa Fluor 543 fluorescence were viewed using a tungsten halogen lamp UV source at 488 or 543 nm, respectively. Images were taken with a Hamamatsu C4742-95 digital camera (Hamamatsu Photonics, http://www.hamamatsu.co.uk/) and Improvision Openlab 4.0.2. software. Images were processed with Adobe Photoshop 8.0 and Adobe Illustrator 12.0 for figure assembly.

2.2.8.5 Confocal microscopy of immunostained samples

Fixed samples were viewed using a Zeiss LSM 510 META Confocal microscope (Carl Zeiss) equipped with a Diode (405 nm), Argon 2 (458, 477, 488 and 514 nm), HeNe1 (543 nm) and HeNe2 Laser (633 nm). Samples were examined using the 63x/1.4 Plan Apochromat lens and two times optical zoom. Images were taken using the LSM 510 Meta version 3.2.SP2 imaging software (Carl Zeiss). When desired, the same settings were used for comparative imaging according to the manufacturer's instruction. For double staining the pinhole settings for the longer wavelength were adjusted to 1 airy unit and

subsequently the airy unit of the lower wavelength adjusted in order to keep the same optical slice. Typical settings for non-stacked images were: 1012 frame size, line-step: 1, maximum scan speed, 12 bit data depth, scan direction: single, mode: line, method: mean with average between 2-8 numbers. For comparison of fluorescence intensity, as in the case for CDC-25.1 abundance the embryo was first selected in the DAPI channel and the numbers of nuclei counted. The embryo was subsequently scanned for anti-CDC-25.1 and DAPI fluorescence in the middle focal plane and the images collected. The CDC-25.1 staining of all nuclei in the embryo was quantified by selection of the whole embryo using LSM 510 software tool, the fluorescence intensities extracted and the mean values of fluorescence intensities compared. All images were processed for figure assembly using Adobe Photoshop 8.0 and Adobe Illustrator 12.0 software.

2.2.9 Statistics

Datasets were analysed for normal distribution with the Normal quantile plot analysis function using the JMP 6.0 software. The mean value with standard deviation was determined using the average and standard deviation function in the Microsoft Excel (MS Office 2000) software. The p-value for the significance that two compared mean values are derived from the same mean was determined using the Students *t* test function in the Microsoft Excel (MS Office 2000) software. Where data followed non-normal distribution the nonparametric Kruskal-Wallis test (using the JMP 6.0 software) was performed to obtain the p-value for the significance whether the datasets were derived from the same median value.

2.2.9.1 Statistics for CDC-25.1 indirect immunofluorescence

The fluorescence intensities of anti-CDC-25.1 immunostained embryos were measured as described above (2.2.8.5) and analysed using standard statistical techniques by Sokal et al. (Sokal, 2000). Note that the staining of CDC-25.1 decreases from early to late stages of embryogenesis, which forced the use of different detector gains at different developmental stages (but kept identical between the two samples to be compared). Hence, the fold difference in staining intensity between for instance CDC-25.1 and CDC-25.1(S46F) was determined at each developmental stage with the help of Dr. Richard Wilson (University of Glasgow) and analysed in an Excel spreadsheet as indicated in the example below (see Table 2.19). Firstly, all data points were transformed into a log scale. The difference in fluorescence intensity of the mutant compared to the wild-type for each individual experiment was determined as the difference of the two mean values (Mutant fold increase,

Table 2.18). The difference between two means on a logarithmic scale corresponds to the logarithm of the fold difference of the two means and the fold difference can be obtained by back-transformation. The upper and lower confidence level in a 95% interval was calculated for each mean (Mutant fold increase, brackets Table 2.18) and the individual p-value for a two-tailed distribution determined through the Student's *t*-test in order to clarify, that the values of each dataset were derived from the same or different mean values (p-value). The combined difference (Combined fold increase), at each developmental stage from several separate experiments, was determined using the weighted means:

$$\Delta\mu_{comb}\ \frac{\Delta\mu_a\left(\frac{n_{1a} * n_{2a}}{n_{1a} + n_{2a}}\right) + \Delta\mu_b\left(\frac{n_{1b} * n_{2b}}{n_{1b} + n_{2b}}\right)}{\left(\frac{n_{1a} * n_{2a}}{n_{1a} + n_{2a}}\right) + \left(\frac{n_{1b} * n_{2b}}{n_{1b} + n_{2b}}\right)}$$

This takes into account the number of embryos underlying each individual difference of the mean in order to weight the contribution of each experiment to the overall fold difference of the mean. The significance of the combined dataset was obtained using the -2ln*P*:chi-squared method as in Sokal (Sokal, 2000) with one-tailed p-values being combined (combined p-value).

Comparison of CDC-25.1 with CDC-25.1(S46F)					
Stage	**No of Embryos (WT/*ij48*)**	**Mutant fold increase**	**p-value**	**Combined fold increase**	**Combined p-value**
30 - 40n	14/9	2.57 (3.62 - 1.83)	< 0.001		
	11/7	1.75 (2.67 - 1.15)	< 0.05	2.2	< 0.001

Table 2.18 Example of CDC-25.1 fluorescence intensity quantification.

A full Table with all fluorescence intensity quantifications is provided in the Appendix of this thesis (Table 8.1). Tables that display the combined fold increase are presented in Chapter 3 (Table 3.5 and Table 3.6).

Excel spreadsheet for CDC-25.1 fluorescence quantification				
	WT Experiment A	Mutant Experiment A	WT Experiment B	Mutant Experiment B
Values of fluorescence after transformation to LOG_{10}	2.654177 2.267172 2.181844 2.733999 2.374748 2.721811 2.350248 2.495544 2.639486 2.313867 2.588832 2.774517 2.31597 2.536558	2.843233 3.0187 3.008174 2.931966 2.723456 2.790988 2.859739 2.980003 3.002598	2.715167 2.681241 2.620136 2.690196 2.52763 2.700704 2.788875 2.770852 2.318063 2.513218 2.623249	2.64836 3.202216 2.663701 2.966611 3.031812 2.606381 3.010724
n	14	9	11	7
n-1	13	8	10	6
1/n	0.07143	0.11111	0.09091	0.14286
$n_1 * n_2$	126		77	
$n_1 + n_2$	23		18	
N-1 $\sum(n-1)$	21		16	
1/N $\sum(1/n)$	0.18254		0.23377	
Log Mean (μ) $\frac{\sum x}{n}$	2.49634	2.90654	2.63176	2.87569
Log fold difference ($\Delta\mu$) $\mu_{mt} - \mu_{wt}$	0.41020		0.24393	
Fold difference (backtransformed) $\Delta\mu$^10	**2.57158**		**1.75359**	
Standard Deviation σ (log) $\sqrt{\frac{n*\sum x^2 - (\sum x)^2}{n*(n-1)}}$	0.19487	0.10680	0.13606	0.23332
Deviation Square SS (log) $\sigma^2 * (n-1)$	0.49367	0.09125	0.18511	0.32664
Standard error of diff. Means SE (log) $\sqrt{\sum SS \frac{(N-1)}{(1/N)}}$	0.07130		0.08647	
tinv $t_{.05}$ (0.05, N-1)	2.07961		2.11990	

Excel spreadsheet for CDC-25.1 fluorescence quantification		
Upper 95% C.L (logscale) $\Delta\mu + (t_{.05} * SE)$	0.55848	0.42724
Lower 95% C.L. (logscale) $\Delta\mu - (t_{.05} * SE)$	0.26191	0.06062
Upper 95% C.L. (back transformed)	**3.61812**	**2.67446**
Lower 95% C.L. (back transformed)	**1.82774**	**1.14980**
p-value (two-tailed Student's *t*-test)	**1.03804×10^{-5}**	**0.01230**
p-value (*P*1) (one-tailed Student's *t*-test)	5.19018×10^{-6}	0.00615
ChiSqTerm $-2\ln P1$	24.33749	10.18314
Combined ChiSqTerm χ^2 $-2\sum \ln P1$	34.52063	
d.f.	4	
Combined p-value CHIDIST (χ^2, d.f.)	**5.82706×10^{-7}**	
Log combined fold increase ($\Delta\mu_{comb}$): $\frac{\Delta\mu_a\left(\frac{n_{1a} * n_{2a}}{n_{1a} + n_{2a}}\right) + \Delta\mu_b\left(\frac{n_{1b} * n_{2b}}{n_{1b} + n_{2b}}\right)}{\left(\frac{n_{1a} * n_{2a}}{n_{1a} + n_{2a}}\right) + \left(\frac{n_{1b} * n_{2b}}{n_{1b} + n_{2b}}\right)}$	0.33750	
Combined fold increase ($\Delta\mu_{comb}$ ^10)	**2.17522**	

Table 2.19 Spreadsheet for analysis of CDC-25.1 fluorescence intensities.

2.2.10 Bioinformatics

Wormbase (http://www.wormbase.org/) was preferentially used to acquire *C. elegans* genomic and cDNAs as well as protein sequences. Sequence analysis such as sequence similarity searches were performed with Wormbase (http://www.wormbase.org/) or NCBI Blast (http://www.ncbi.nlm.nih.gov/BLAST). For identification of phosphorylation and other motif sites, NetphosK1.0 (http://www.cbs.dtu.dk/services/NetPhosK), the Eukaryotic Linear Motif Resource for Functional Sites in Proteins (ELM) (http://elm.eu.org/) or PSORTII (http://psort.nibb.ac.jp/form2.html) were utilised. For oligonucleotide design, DNA analysis of restriction digests, DNA sequence comparisons as well as multiple protein alignments Vector NTI Advance10 (free version, Invitrogen) was preferentially utilised.

Chapter 3

Identification of CDC-25.1 regulators

3 Identification of CDC-25.1 regulators

3.1 Introduction

C. elegans embryogenesis offers an attractive system to study the integration of the cell cycle with developmental decisions, because all divisions follow a precise pattern that is invariant between individual animals. The identification of a *cdc-25.1(ij48)* mutant allele that causes a S46F mutation in the general cell cycle regulator CDC-25.1 has demonstrated the advantages of using this model system (Clucas, 2003; Clucas et al., 2002). Identification of this mutant was rather intriguing as it caused a tissue-specific hyperproliferation of intestinal cells, albeit removal of *cdc-25.1* by RNAi resulted in embryonic death (Ashcroft et al., 1999; Clucas, 2003; Clucas et al., 2002; Kostic and Roy, 2002) with decreased proliferation of several tissues implicating a general function for CDC-25.1 to driving the cell cycle in all or several other embryonic tissues (Clucas, 2003; Clucas et al., 2002). CDC25 proteins have been identified in many eukaryotic systems and their role as positive regulators of the cell cycle is well established (see Chapter 1).

Consistently, the S46F mutation in *C. elegans* CDC-25.1 has been proposed to elicit a gain-of-function of the CDC-25.1 molecule (Clucas, 2003; Clucas et al., 2002). Hence, this suggests the loss of negative regulation of CDC-25.1 through the S46F mutation in CDC-25.1 ultimately resulting in intestinal hyperproliferation. This strongly argues for the presence of a negative regulator acting through S46 in CDC-25.1 possibly in a tissue-specific fashion. Deciphering the molecular mechanism underlying the tissue-specific phenotype of the CDC-25.1(S46F) mutant was therefore an important task in order to shed light into the tissue-specific regulation of the *C. elegans* cell cycle.

3.1.1 Conservation of the DSG consensus in CDC-25.1

Apart from the tissue specificity reported for the *cdc-25.1(ij48)* allele, no obvious differences have been reported that would facilitate the identification of a molecular pathway underlying the tissue-specific regulation of the CDC-25.1 protein. Immunostaining against CDC-25.1 using anti-CDC-25.1 specific antibodies revealed no difference in the CDC-25.1(S46F) localisation compared to wild-type CDC-25.1. Furthermore, no difference for the CDC-25.1(S46F) protein level was detected as compared to CDC-25.1 (Clucas, 2003; Clucas et al., 2002) and see Chapter 1, (1.3.5)). Hence, the only clue for a molecular mechanism underlying the *cdc-25.1(ij48)* mutation

was provided by the nature of the S46F mutation site. This serine falls into a conserved motif present in *C. elegans cdc-25.2* and *C. briggsae cdc-25.1* (Clucas et al., 2002). Interestingly, sequence conservation of this motif is not restricted to nematode species and the similarity to the DSG consensus motif in human β–catenin and CDC25A has been previously suggested (Busino et al., 2003; Clucas, 2003).

The DSG motif has been extensively studied and most data arose from the original identification of this motif in β–catenin and the human NFκB pathway (see Figure 3.1, A, for an alignment of the DSG motif in *C. elegans* CDC-25.1 with several DSG motifs found in higher eukaryotes). Early studies from several laboratories revealed that a DpSGΦXpS phosphodegron sequence (where pS denotes serine phosphorylation, Φ any hydrophobic residue and X any amino acid) was important for ubiquitin-dependent degradation of IκB (Yaron et al., 1997) and human β–catenin (Aberle et al., 1997; Orford et al., 1997). Phosphorylation of the serines has proven important for the ubiquitin-mediated degradation of these molecules. Interestingly, phosphorylation of the serine adjacent to the aspartic acid in the DSG consensus of β–catenin requires the kinase GSK3β in complex with Axin and APC (adenomatous polyposis coli) (Aberle et al., 1997; Hart et al., 1998; Ikeda et al., 1998; Kitagawa et al., 1999; Liu et al., 2002; Orford et al., 1997).

Intriguingly, inactivating mutations in human APC and in the DSG consensus motif of β–catenin have been frequently associated with human primary cancers such as colorectal carcinomas (Polakis, 2000). Thus, could this provide a potential link to the tissue-specific hyperplasia observed in the *C. elegans* CDC-25.1 putative DSG phosphodegron mutant CDC-25.1(S46F)? In this chapter I set out to answer this question by identifying whether there are common negative regulators that are conserved between *C. elegans* and higher eukaryotes that can regulate S46 in the DSG consensus of *C. elegans* CDC-25.1. A brief introduction into the molecules regulating the DSG consensus in higher eukaryotes is given below, and known roles of their respective *C. elegans* counterparts during *C. elegans* development are highlighted.

3.1.2 Mechanisms of DSG-mediated regulation in higher eukaryotes

The DSG motif has been identified in many diverse target genes. Figure 3.1 (panel A) depicts an alignment of the DSG site in *C. elegans* CDC-25.1 with several studied DSG motifs in eukaryotic systems (according to (Fuchs et al., 2004; Nakayama and Nakayama,

2006), details of some target interactions will be discussed below). Original data suggested that this motif is important for the degradation of β–catenin (Aberle et al., 1997; Orford et al., 1997) and NFκB pathway components such as p105 and IκBα-ε (Yaron et al., 1997). However, since there is no indication of the presence of NFκB pathway components in *C. elegans*, this pathway will not be elucidated further here (Manning, 2005; Wang et al., 2006). What has become evident from many independent studies is that the DSG consensus is also present in several cell cycle regulators such as CDC25A, CDC25B, WEE1A and EMI1 and serves as a recognition site for an F-box molecule β-TrCP (discussed below). Humans have two β-TrCP genes named β-TrCP1 and β-TrCP2 located on chromosome 10 and 5, respectively (Fuchs et al., 2004). Since both genes have been implicated in the regulation of the DSG consensus, the term β-TrCP will be utilised here unless significant differences in their functions require highlighting the specific molecule. β-TrCP belongs to a large family of Fbw proteins containing an N-terminal F-box motif and a C-terminal WD40 domain. The protein is part of a large multisubunit E3 ubiquitin ligase complex SCF named after its members SKIP1, CULLIN1 and the F-box protein. The SCF complex mediates the transfer of ubiquitin molecules from the E2 conjugating enzymes to the substrate, thereby targeting the substrate for ubiquitin-mediated proteasomal degradation ((Pickart and Eddins, 2004) and Chapter 4, (4.1)). The F-box molecule β-TrCP interacts via the WD40 domain found in its C-terminus to the phosphorylated DSG consensus sequence present in diverse target substrates. In this regard the recognition of β–catenin has been extensively studied and will be introduced below, as well as the interaction of β-TrCP with known cell cycle related molecules.

3.1.2.1 β-TrCP recognition of β–catenin and other substrates

In the canonical Wnt signalling pathway, secreted cysteine-rich ligands act on cell surface receptors, such as Frizzled, which mediate the stabilisation of β–catenin. Stabilised β–catenin then moves to the nucleus and binds to the transcription T-cell factor (TCF) releasing the transcriptional repression of TCF target genes such as c-myc, c-jun or cyclin D1 (Kikuchi et al., 2006; Logan and Nusse, 2004). In the absence of Wnt signalling β–catenin is degraded through the APC/Axin/GSK3β/CK1α complex and β-TrCP (for a recent review see (Kikuchi et al., 2006)). β-TrCP recognises β–catenin phosphorylated by GSK3β on S33, S37 and T41 at the DSG consensus (where S33 represents $D(S_{33})G$) (Fuchs et al., 2004; Kikuchi et al., 2006; Kitagawa et al., 1999; Liu et al., 2002). Phosphorylation of S45 by CK1α is a priming event for the subsequent phosphorylation of S33, S37 and T41 by GSK3β (Liu et al., 2002). Thus, binding of β-TrCP to β–catenin

follows a two-step phosphorylation mechanism on β–catenin mediated by the kinases GSK3β and CK1α. Interestingly, GSK3β and CK1α exert their function as a multisubunit complex. Central to it are the two molecules Axin and APC. In this complex the scaffolding molecule Axin binds via its G-protein signalling (RGS) domain to the central domain of APC (Behrens et al., 1998; Kishida et al., 1998) and via separate central domains to GSK3β, β–catenin (Ikeda et al., 1998; Liu et al., 2002) and CK1α (Liu et al., 2002). The binding of APC to β–catenin as well as to Axin is necessary for β–catenin degradation (Kawahara et al., 2000; Kikuchi et al., 2006).

3.1.2.2 Diverse kinases implicated in DSG phosphorylation

The DSG consensus site is also found in other proteins, for example in HIV Vpu, human EMI1, human PERIOD and human WEE1A, and is important for β-TrCP-mediated protein degradation (Nakayama and Nakayama, 2006). Though HIV Vpu and EMI1 conform to the strict DSG consensus, WEE1A and PERIOD show slight alterations of the DSG motif site (Figure 3.1, A). The serine residues within the DSG motif in HIV Vpu and human EMI1 were suggested to be casein kinase 2 (CK2) (Schubert et al., 1994) and polo-like kinase 1 (PLK1) (Moshe et al., 2004) target sites, respectively. Similarly, phosphorylation of the serine (S53) in the DSG site of WEE1A implicated PLK1 function as revealed by *in vitro* analysis of a peptide comprising this region (Watanabe et al., 2004). Thus, multiple kinases have been implicated in phosphorylation of the serine within the DSG motif in different target molecules.

3.1.2.3 β-TrCP recognition of CDC25

Interestingly, the DSG motif is also found in human CDC25A, a homologue of *C. elegans* CDC-25.1. As already discussed in the general introduction, CDC25 proteins are phosphatases that regulate the cell cycle by dephosphorylating inhibitory phosphates present on threonine14 and tyrosine15 in cyclin-dependent kinases and thereby stimulating cell cycle progression. The fine-tuning of CDC25A protein levels during different stages of the cell cycle can therefore mediate a control for cell cycle progression. Hence, CDC25A protein levels fluctuate during the mammalian cell cycle, which is the result of a balance between *de novo* protein synthesis and protein degradation during mitosis and S phase (see review by (Busino et al., 2004)). While the anaphase-promoting complex/cyclosome (APC/C) orchestrates the degradation of CDC25A at the exit of mitosis (Donzelli et al.,

2002), S phase degradation of CDC25A is carried out by the $SCF^{\beta\text{-}TrCP}$ complex (Busino et al., 2003; Donzelli et al., 2004; Donzelli et al., 2002; Jin et al., 2003).

Binding of β-TrCP to CDC25A has been demonstrated *in vivo* and it requires phosphorylation of S82 in the DSG consensus site of human CDC25A. Interaction between β-TrCP and the DSG consensus of CDC25A is essential for CDC25A degradation during the normal cell cycle and in response to DNA damage in human tissue culture cells (Busino et al., 2003; Jin et al., 2003). Removal of β-TrCP by RNAi resulted in increased CDC25A protein levels during S phase of the cell cycle or in response to DNA damage. A double mutation in the DSG consensus site of CDC25A (S82/S88, where S82 is the residue adjacent to D in the DSG site) abolished binding of β-TrCP to CDC25A and increased CDC25A protein levels (Busino et al., 2003). Similarly, Jin et al. (2003) reported that single mutations of S82 abolished β-TrCP binding *in vivo*. Phosphorylation of S76 as well as S79 preceding the S82 in the DSG consensus of human CDC25A is also necessary for β-TrCP-mediated *in vitro* ubiquitination (Donzelli et al., 2004; Jin et al., 2003). However, S76 is not directly required for binding of β-TrCP to CDC25A. *In vivo* data revealed that a single S76A mutant could still bind to β-TrCP, but a S79A mutant was abolished in β-TrCP binding (Jin et al., 2003). Furthermore, a synthetic peptide spanning the DSG region (comprising S76, S79 and S82) of CDC25A was able to bind to β-TrCP *in vitro* when only S82 was phosphorylated, but it did not bind to β-TrCP when only S76 was phosphorylated (Donzelli et al., 2004; Jin et al., 2003). Single alanine mutations in S76 or S82 resulted in a strong decrease of the CDC25A polyubiquitination rate, whereas mutations of surrounding S residues such as S88 or S124 to alanine only caused a slight reduction of CDC25A polyubiquitination (Donzelli et al., 2004; Jin et al., 2003). Similarly, S79A abolished CDC25A polyubiquitination *in vitro* (Jin et al., 2003).

Thus, these data indicate that S76, S79 and S82 are the prime target sites of human CDC25A interaction with β-TrCP mediated through the DSG motif. Phosphorylation of S76 in human CDC25A is mediated by checkpoint kinase 1 (CHK1) *in vitro* (Hassepass et al., 2003). Furthermore, this group showed that UV-induced DNA damage could induce S76 phosphorylation *in vivo*, indicative of an activated CHK1/CHK2 kinase pathway. Moreover, CDC25A S76 can be phosphorylated by CHK1 or p38 kinase probably as a response to UV-mediated DNA damage and osmotic stress (Goloudina et al., 2003). However, during the normal cell cycle knockdown of CHK1 kinase by RNAi did not affect the degradation of CDC25A, indicating that in unperturbed cells another kinase is acting through this site (Ray et al., 2005). Importantly, the kinases responsible for

phosphorylation of S79 and S82 have not been identified to date. Thus, β-TrCP-mediated degradation of human CDC25A requires a two-step mechanism; phosphorylation of S76 maybe through CHK1 kinase which is surmised to act as a priming event to phosphorylate S82 at the DSG consensus site by an unknown kinase, and subsequent recognition through the $SCF^{\beta TrCP}$ complex (Donzelli et al., 2004; Jin et al., 2003).

3.1.2.4 β-TrCP also recognises DSG-like motifs

Intriguingly, given the high conservation of the DSG motif between *C. elegans* and human, it has recently become apparent that phosphorylation of the strict consensus motif is not vital for interaction and degradation of substrates with β-TrCP. A DSG-like motif (DDGΦXD) present in *Xenopus* CDC25A and human CDC25B (see Figure 3.1, A) can act to recruit β-TrCP in *Xenopus* egg extracts (Kanemori et al., 2005). Mutational analysis of *Xenopus* CDC25A revealed that within this motif all residues except for the non-conserved (X) residue were important to interact with β-TrCP. Alanine mutations of at least two residues DDAΦXD and DDGΦXA resulted in increased CDC25A protein levels and, as demonstrated for DDGΦXA, a concomitant decrease of the CDC25A polyubiquitination rate (Kanemori et al., 2005). Furthermore, these authors demonstrated that a DDAΦXA mutant present in human CDC25B was unable to bind to β-TrCP, resulting in decreased polyubiquitination rate and increased CDC25B stability in *Xenopus* eggs. Additionally, mutational analysis of serine or aspartic acid residues within six to seven amino acids upstream of this DDG motif site revealed an important function for negatively charged residues as being important for β-TrCP interaction and CDC25A or CDC25B stability.

3.1.3 Conservation of mammalian DSG regulators in C. elegans

In summary, analysis of the general mechanism underlying the control of DSG motifs in higher eukaryotes implicated a central role for the $SCF^{\beta\text{-}TrCP}$ complex in the regulation of this target site. Interestingly, several components of the $SCF^{\beta\text{-}TrCP}$ complex have already been identified in *C. elegans* with CUL-1, the scaffolding protein of the SCF complex being the founding member of the human CULLIN family (Kipreos et al., 1996). Additionally, out of 326 predicted *C. elegans* F-box molecules, LIN-23 has been identified as the *C. elegans* orthologue of human β-TrCP, displaying 81-83% identity to β-TrCP1 and β-TrCP2 in the WD region (Kipreos, 2005; Kipreos et al., 2000; Kipreos and Pagano, 2000). Whereas, of 21 SKP1 related genes (SKR) present in the *C. elegans* genome, the *C. elegans* SKR-1 displays highest homology to the human SKP1 gene (64% overall identity)

(Nayak et al., 2002; Yamanaka et al., 2002). Interestingly, analysis of the *C. elegans* CDC-25.1 DSG consensus site revealed that it resembles a potential GSK3β phosphorylation site similar to the one identified in human β-catenin. The *C. elegans* genome contains seven potential GSK-3 kinases, and recently GSK-3 (previously called SGG-1) was shown to display high homology to other eukaryotic GSK3β kinases (Schlesinger et al., 1999). Among all members of the *C. elegans* GSK-3 family, GSK-3 (SGG-1) displays the highest homology to human GSK3β (Figure 3.1 (panel B), *Ce* GSK-3, 71% overall identity), and GSK-3 will hereafter refer to this *C. elegans* GSK-3 kinase. The *C. elegans* genome contains one single APC homologue APR-1, that shares 31% identity to the human APC gene in the arm repeat region (Rocheleau et al., 1997). Interestingly, a role for *C. elegans* cell proliferation had already been assigned for LIN-23, CUL-1 and SKR-1, whereas GSK-3 and APR-1 play a vital role in the specification of intestinal cells. Hence, these molecules could well be involved in the regulation of intestinal cell proliferation.

A

Ce CDC-25.1	(40)	DGSSRDSGVSMT
Ce CDC-25.2	(29)	DSMSRDSGICEL
Hs CDC25 A	(76)	SSESTDSGFCLD
Hs IκBα	(26)	LDDRHDSGLDSM
Hs IκBβ	(13)	ADEWCDSGLGSL
Hs IκBε	(151)	EESQYDSGIESL
Hs p105	(921)	SDSVCDSGVETS
Hs β-CAT	(27)	QQSYLDSGIHSG
Hs EMI 1	(139)	SRLYEDSGYSSF
HIV Vpu	(47)	RERAEDSGNESE
Xl CDC25 A	(221)	STEGSDDGFLDM
Hs CDC25 B	(151)	GDTEEDDGFVDI
Hs PER1	(116)	QDNPSTSGCSSE
Hs WEE1 A	(47)	HSTGEDSAFQEP
Consensus		DSGΦ S

B

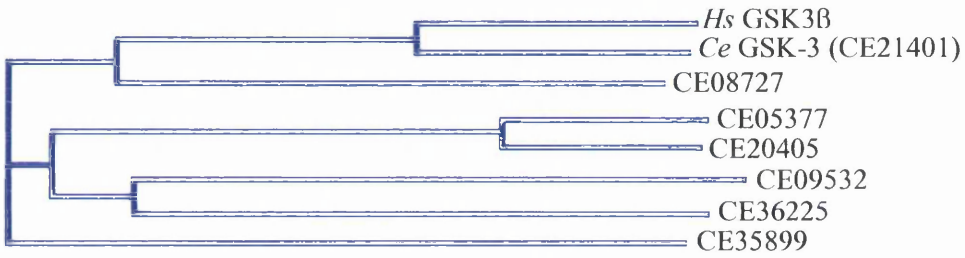

	Ce GSK-3	CE08727	CE05377	CE20405	CE09532	CE36225	CE35899
***Hs* GSK3β**	**71**	**40**	**30**	**30**	**25**	**25**	**29**
Ce GSK-3		41	28	30	25	26	28
CE08727			29	29	27	27	30
CE05377				78	29	32	26
CE20405					29	32	28
CE09532						38	26
CE36225							29

Figure 3.1 CDC-25.1 and GSK-3 protein alignments. A) Alignment of the DSG consensus sequence in β-TrCP targets. Proteins of accession numbers NP_491862, NP_503446, NP_001780, CAB 65556, NP_002494, NP_004547, P19838, NP_001895, AAL86610, AAF35359, AAF09263, CAI18849, NP_002607, NP_003381 were aligned using the Vector NTI program. **B)** Top: phylogenetic tree of human GSK3β (*Hs* GSK3β, swissprot accession number: P49841) aligned with *C. elegans* GSK-3 family members. Wormbase protein accession numbers are indicated (for *Ce* GSK-3 in brackets). Bottom: amino acid identity (%) of the proteins analysed in the top panel. Data are derived from multiple protein alignment analysis using the Vector NTI program.

3.1.3.1 LIN-23 and CUL-1 function during cell proliferation in *C. elegans*

lin-23 and *cul-1* null mutants have recently been characterised by (Kipreos et al., 2000) and (Kipreos et al., 1996), respectively. Their proliferation phenotypes are illustrated below. Homozygous *lin-23* or *cul-1* null mutants show hyperplasia of many proliferating tissues during their post-embryonic development, indicating that loss of either gene causes a delay in cell cycle exit. The onset of the proliferation defect differs slightly, starting at the L1 larval stage for the *lin-23* mutant and at around the L2 larval stage for the *cul-1* mutant, which is probably caused by the difference of the longevity of maternally provided LIN-23 and CUL-1. *lin-23* and *cul-1* heterozygous hermaphrodites proceed normally through embryogenesis, suggesting that the half gene-dose from the mother is sufficient for normal embryogenesis. Interestingly, *lin-23* homozygous null mutants are almost sterile and the few embryos produced are not viable. Mosaic analysis of *cul-1* null hermaphrodites also reveals dying embryos. These embryos arrest without any overt morphogenesis and show increased numbers of nuclei as examined by DNA squashes suggesting a hyperproliferation defect in the embryo. Thus, maternally provided *lin-23* and *cul-1* may be implicated in restraining normal proliferation of several tissues during embryogenesis.

lin-23 homozygous null hermaphrodites produce the wild-type number of intestinal cells, indicating that cells, that have exited the mitotic cycle during embryogenesis remain quiescent during post-embryonic development, even without *lin-23* present. Unfortunately, examination of intestinal cell proliferation during post-embryonic development was lacking for the *cul-1* mutant. Similarly, the Hobert laboratory recently presented further evidence for a proliferative function for *lin-23* null mutants during proliferation of post-embryonic motor and touch neurons (Mehta et al., 2004). Interestingly, this study identified a *lin-23(ot1)* point mutant that showed axonal outgrowth defects of several motor and sensory neurons. However, though this point mutation was able to rescue the *lin-23* null mutant, homozygous *lin-23(ot1)* showed no proliferation defects of the neurons whose proliferation was clearly affected in the homozygous *lin-23* null mutant. The *ot1* allele results in a P610S mutation in a conserved C-terminal PAPP motif; thus these authors concluded that the C-terminus can have distinct roles from the cell proliferative function of the N-terminus (comprising the F-box) and the middle domain (comprising the WD40 domain).

3.1.3.2 SKR-1 functions during cell proliferation in *C. elegans*

Interestingly, SKR-1, the *C. elegans* SKP1 homologue, has also been shown to display a hyperproliferation phenotype. Removal of SKR-1 by RNAi causes hermaphrodites to produce dying embryos that arrest between gastrulation and the two-fold stage. DNA analysis by DAPI staining revealed a strong increase in the number of nuclei generated in those embryos, suggesting that they produce too many cells (Nayak et al., 2002; Yamanaka et al., 2002).

Thus, several *C. elegans* SCF members, such as LIN-23, CUL-1 or SKR-1, homologous to the human $SCF^{\beta\text{-}TrCP}$ complex can be identified. In higher eukaryotes $SCF^{\beta\text{-}TrCP}$ is critically involved in the negative regulation of the DSG motif present in many proteins including CDC25A. Intriguingly, loss-of-function of *lin-23*, *cul-1* and *skr-1* show proliferation defects during post-embryonic and maybe embryonic development of several tissues and hence their phenotypes fit well with the expected phenotype of a loss of a negative regulator during cell proliferation, namely the failure to induce cell cyle exit.

Additionally, GSK-3 and the APC homologue APR-1 have been shown to specify the production of intestinal cells in a non-canonical Wnt signalling pathway requiring the action of a β–catenin homologue WRM-1. Unlike the canonical Wnt signalling pathway GSK-3 is required to activate WRM-1 (rather than down-regulate it as in the absence of the canonical Wnt signal of human β–catenin; see Chapter 1 (1.2.2) for details). Nevertheless, it is intriguing to note that *C. elegans* GSK-3 can act in concert with the human APC homologue APR-1 to specify intestinal cells. The DSG consensus in CDC-25.1 comprises a potential GSK-3 phosphorylation site. Thus, the question whether GSK-3 together with APC could act similarly to the canonical Wnt signalling pathway on the stability of CDC-25.1 once intestinal cells are born became apparent. In this case, GSK-3 should be able to act together with APR-1 to down-regulate CDC-25.1 through S46 once intestinal cells are specified. Unfortunately, so far there were no data regarding the proliferation of intestinal cells in embryos that still specify the intestine after removal of GSK-3 (Bei et al., 2002; Maduro et al., 2001; Schlesinger et al., 1999) or APR-1 (Bei et al., 2002; Rocheleau et al., 1997; Rocheleau et al., 1999).

3.1.4 Hypothesis and aims

It was hypothesised in the Johnstone lab that CDC-25.1 is negatively regulated through S46, possibly only in intestinal cells during embryogenesis. Possible candidates that might

act as negative regulators are LIN-23, CUL-1, SKR-1 or GSK-3 and APR-1. Preliminary RNAi data obtained in the Johnstone laboratory prior to this study implicated a role for LIN-23 and GSK-3 in proliferation of intestinal cells as *lin-23* and *gsk-3* RNAi caused extra intestinal cells (I. L. Johnstone, pers. comm.). Hence, experiments were set up to test whether members of the *C. elegans* SCF complex such as LIN-23, CUL-1 or SKR-1 as well as GSK-3 and APR-1 can act as negative regulators on S46 of CDC-25.1 in embryos. Removal of the negative regulator was predicted to cause intestinal hyperplasia during embryogenesis, similar to the phenotype observed for the *cdc-25.1(ij48)* allele. To this end, RNAi was to be utilised to down-regulate the protein levels of potential candidates in embryos. The embryos would then be examined for intestinal hyperplasia. Genes with RNAi phenotypes were to be further examined to analyse whether they can act through the *ij48* allele on *cdc-25.1* by comparison of RNAi in wild-type and *cdc-25.1(ij48)* mutants. In order to see whether the negative regulator can act in a tissue-specific fashion, the cell numbers of other tissues were to be examined, by utilising strains that express tissue-specific GFP markers.

3.1.4.1 Introduction to RNAi in *C. elegans*

Here, a reverse genetic approach, termed RNA-mediated interference (RNAi), is utilised to study negative regulators of CDC-25.1 function during embryonic development. In order to facilitate the understanding of the method, a short introduction to the RNAi methods utilised in *C. elegans* is given below. RNAi was first discovered and characterised in *C. elegans* (Fire et al., 1998). It has also been demonstrated to act in a variety of systems including plants, fungi, *Drosophila* and mammalian tissue culture cells (Grishok, 2005). In *C. elegans* Fire et al. first reported that RNA expressed from a transgene could mimic a null mutation of that gene (Fire et al., 1991). Subsequently Guo and Kemphues showed that both sense or antisense RNA caused downregulation of gene expression in the germline (Guo and Kemphues, 1995). Fire et al. termed this mechanism RNAi and established that it is induced by double-stranded RNA and that in *C. elegans* this process is systemic and heritable. In *C. elegans*, RNAi can be applied by injection (Fire et al., 1998) or soaking (Tabara et al., 1998) worms with dsRNA, or by feeding worms *E. coli* that expresses double-stranded RNA from an IPTG-inducible T7 promoter (Timmons et al., 2001; Timmons and Fire, 1998).

It has become evident that RNAi mediates the post-transcriptional silencing of endogenous genes. Induction of RNAi in *C. elegans* by injection of double-stranded RNA caused downregulation of a gene downstream of the RNAi target gene present in a single operon.

RNAi against the target gene resulted in embryonic lethality indicative of a loss-of-function phenotype of the downstream gene, whereas a null mutant of the target gene was viable. This indicated that RNAi can target pre-mRNA of two genes that are expressed from a single transcript (Bosher et al., 1999). The RNAi mechanism has been the object of intensive studies from many laboratories, and identification of *C. elegans* mutant alleles defective in RNAi have contributed to our knowledge of how RNAi functions. During post-transcriptional gene silencing, double-stranded RNA is cleaved into 21-23 nt short interfering RNAs (siRNAs) by the DICER complex, and subsequently endogenous mRNA levels are degraded through the RNAi-induced silencing complex (RISC) that utilises a single-stranded siRNA as a primer to anneal to the mRNA and induce degradation of the mRNA (see (Grishok, 2005) for review).

Interestingly, if RNAi is applied in *C. elegans* it causes the spread of the RNAi signal throughout the animal, thus indicating that RNAi is systemic. Furthermore, when adults are subjected to RNAi, an RNAi phenotype can be observed in the treated adult. Besides, a transfer of the RNAi signal to their offspring is evident resulting in offspring that can display a phenotype indicative of a null mutation or loss-of-function mutation of the target gene (Fire et al., 1998). This systemic and heritable RNAi phenotype can be induced by exogenous dsRNA independent of the method applied (Fire et al., 1998; Tabara et al., 1998; Timmons et al., 2001; Timmons and Fire, 1998). However, the strongest phenotypes are observed after RNAi by injection when compared to the soaking or feeding method (Tabara et al., 1998). Genes involved in the spread of systemic RNAi have been identified in *C. elegans* and involve a transmembrane protein SID-1 which is surmised to act as a channel protein facilitating the uptake of cellular dsRNA (Feinberg and Hunter, 2003; Winston et al., 2002). Expression of the SID-1 protein in *Drosophila* cells, that do not normally express a SID-1 protein, facilitates the uptake of dsRNA. Interestingly, the uptake of dsRNA was increased with target size, indicating that systemic RNAi in *C. elegans* requires at least several hundred base pairs in order to function throughout the animal. Consistently, longer dsRNAs were shown to function as preferred substrates for systemic RNAi in *C. elegans* (Feinberg and Hunter, 2003). The precise mechanism of systemic RNAi uptake and inheritance signals is still under investigation and is not the focus of this study.

3.2 Results

3.2.1 RNAi to identify negative regulators of CDC-25.1

In order to determine whether members of the *C. elegans* SCF complex such as LIN-23, CUL-1 or SKR-1 are involved in the regulation of CDC-25.1, RNAi was performed by feeding worms bacteria that express double-stranded RNA against the target genes, synthesised from a vector that carries the target gene between two IPTG-inducible T7 promoters. The exact size and position of the double-stranded target RNAs are displayed in (Table 2.17, Chapter 2). As control, bacteria were utilised that contain only the empty vector. It was proposed that removal of a negative regulator would result in intestinal hyperplasia similar to the phenotype observed with *cdc-25.1(ij48)*.

Thus, the *C. elegans* strain JR1838 that carries an intestinal-specific marker was utilised for this purpose. JR1838 carries a chromosomally integrated *GFP* transgene fused to *LacZ* under the expression of the *elt-2* promoter (*elt-2::GFP::LacZ*, termed *elt-2::GFP* hereafter for simplicity). This strain is otherwise like wild-type and induces tight expression of the GFP in the nuclei of intestinal cells (when 2 E cells are born in the embryo until adulthood) due to the presence of a nuclear localisation signal present in the GFP (Clucas, 2003; Clucas et al., 2002). The *C. elegans* intestine consists of 20 cells that are generated in the embryo and are manifested in the hatching larva. Cell lineage analysis and the expression of an intestinal-specific *elt-2::GFP* reporter previously revealed that the *cdc-25.1(ij48)* gain-of-function allele promotes a tissue-specific hyperplasia of intestinal cells (Clucas, 2003; Clucas et al., 2002). Thus the *elt-2::GFP* transgene can act as an indicator for the proliferation of intestinal cells in the embryo.

Interestingly, here it is shown that when worms were fed on plates with bacteria expressing double-stranded RNA against *lin-23*, *cul-1* and *skr-1*, a strong increase in the number of intestinal nuclei became evident in the embryos derived from RNAi-fed mothers (Figure 3.2, Table 3.2). *lin-23* RNAi embryos show otherwise no developmental abnormality as compared to the control embryos under these RNAi conditions when visualised in Nomarski optics. However, embryos depleted for *cul-1* and *skr-1* arrest at around the comma stage, similar to previous results (Kipreos et al., 1996; Nayak et al., 2002; Yamanaka et al., 2002). To ensure that the RNAi was specific to the genes investigated, several controls were carried out. Firstly, RNAi was performed against close homologues

of the genes investigated. SEL-10 has been demonstrated to display closest homology to LIN-23 (Kipreos et al., 2000). However, when RNAi was performed against *sel-10* all embryos displayed the wild-type number of intestinal cells (19.3 ± 1.5 cells, (mean ± s.d.), n=50, two independent experiments).

Similarly, RNAi against the *cul-1* paralogue *cul-2* (Kipreos et al., 1996) resulted in embryonic arrest in around 100 embryos analysed, but none of those embryos showed an increase in the numbers of intestinal nuclei (exact numbers of intestinal cells were not determined, but were clearly not above 20). Furthermore, when RNAi was performed against the *skr-1* homologue *skr-3,* that has been shown to interact with *cul-1* in a yeast two-hybrid system (Nayak et al., 2002; Yamanaka et al., 2002), embryos showed the wild-type number of intestinal nuclei (20.1 ± 0.5, (mean ± s.d.), n=53, one experiment). Thus, this indicated that the hyperplasia seen is not due to non-specific knockdown of unrelated genes. Another control experiment was carried out that targets a different part of the *lin-23* mRNA. The *lin-23* RNAi displayed in Figure 3.2 targets a 1126 bp fragment of the pre-mRNA starting at position +685 relative to the genomic ATG. A second *lin-23* RNAi clone was designed (*lin-23* RNAi 2) that targets 874 bp of the pre-mRNA starting at position +1812, creating no overlap to the first target *lin-23* RNAi. Analysis of embryos derived from hermaphrodites treated with *lin-23* RNAi or *lin-23* RNAi 2 revealed that both displayed a similar increase in the number of intestinal cells compared to wild-type (intestinal nuclei: 31.4 ± 3.4 for *lin-23* RNAi (n=62 embryos), 32.6 ± 4.3 for *lin-23* RNAi 2 (n=81), 19.8 ± 0.8 for control RNAi (n=66), numbers display mean ± s.d., two independent experiments). Thus, it can be concluded that the hyperplasia phenotype observed through *lin-23* is specific to the *lin-23* knockdown.

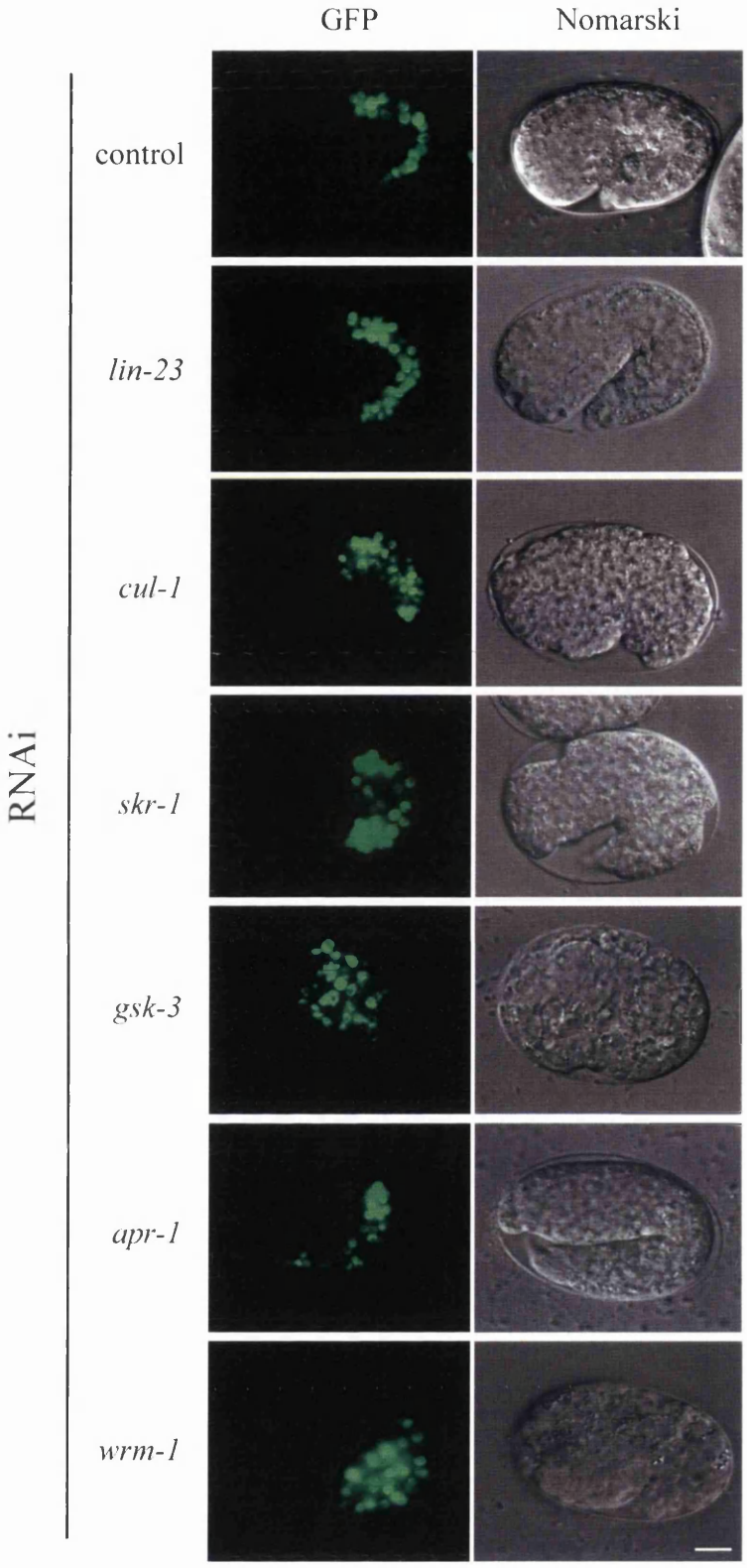

Figure 3.2 *C. elegans* excess endoderm phenotypes. Left panel: GFP fluorescence of the JR1838 strain carrying the *elt-2::GFP* transgene, expressed in intestinal nuclei, was analysed at the comma stage (control, *skr-1*, *wrm-1*), 1.5-fold stage (*lin-23*), 2-fold stage (*apr-1*) or early arrested embryos (*cul-1*, *gsk-3*) after control, *lin-23*, *cul-1*, *skr-1*, *gsk-3*, *apr-1* or *wrm-1* RNAi, right panel: corresponding Nomarski counterparts. For quantification of cell numbers see Table 3.2. Scale bar: 10 μm.

To further elucidate the role of *gsk-3* to act as a potential kinase negatively regulating CDC-25.1, the intestinal cell proliferation phenotype was analysed after *gsk-3* RNAi. When RNAi was performed by feeding worms on plates with *E. coli* expressing double-stranded RNA against the *C. elegans gsk-3*, a percentage of embryos did not express the intestinal-specific GFP marker, indicating that the RNAi was specific to *gsk-3* because it was previously established that removal of *gsk-3* caused a loss of endoderm in RNAi-treated embryos (Schlesinger et al., 1999), a phenotype later also observed by (Bei et al., 2002). However, embryos arresting at an early stage of development and expressing the intestinal fate marker showed a mixed number of intestinal cells, with many embryos displaying clearly above 20 intestinal cells (Figure 3.2, Table 3.2). In a control experiment targeting the closest *C. elegans* GSK-3 homologue (Figure 3.1, CE08727), all embryos displayed wild-type numbers of intestinal cells (20, exact number not determined ($n > 400$), two independent experiments).

Thus, this experiment suggested that *gsk-3* might be involved in the proliferation of intestinal cells once the intestine is specified. Since in the mammalian system, GSK3β can act together with APC to phosphorylate β–catenin (see introduction this chapter), the role of the *C. elegans* APC homologue APR-1 in proliferation of intestinal cells was investigated. RNAi against *apr-1* was performed by microinjection of double-stranded RNA targeting the *apr-1* mRNA. Microinjection was necessary since feeding resulted in only a very mild phenotype. Similar to the *gsk-3* RNAi experiments, a percentage of embryos did not express the intestinal fate marker *elt-2::GFP*, suggesting that the RNAi was specific to APR-1 since previous experiments had shown that *apr-1* is required for endoderm specification (Bei et al., 2002; Rocheleau et al., 1997; Rocheleau et al., 1999). Interestingly, among those embryos expressing the intestinal fate marker *elt-2::GFP* several embryos displayed excess numbers of intestinal nuclei (Figure 3.2, Table 3.2).The precise number of embryos displaying hyperplasia among the total population was not quantified since in the experiments a spectrum of the severity of the RNAi phenotype was observed ranging from embryos without *elt-2::GFP* expression, or with *elt-2::GFP* expression in less or more than 20 nuclei. This phenotype was also observed after *gsk-3* and *wrm-1* RNAi and in all cases only embryos without *elt-2::GFP* expression or with an *elt-2::GFP* expression in 20 or above 20 nuclei were counted. The percentage of no E expression was derived from all embryos counted. Among the F1 escapers of *apr-1* RNAi, none showed an increase in the number of intestinal nuclei, suggesting that the embryos that possess extra nuclei are not viable. In order to identify whether the nuclei analysed were the result of extra intestinal cells being born in the embryo, cell lineage analysis was

carried out by Dr. J. Cabello using the JR1838 strain and RNAi conditions established in this study (for details see (3.2.5)). Several embryos depleted by RNAi against *gsk-3* or *lin-23* were analysed. It was shown that RNAi against both genes resulted in extra cells that were generated from extra divisions of the E blastomere in the embryo. Hence, the number of intestinal nuclei observed with the expression of the intestinal-specific *elt-2::GFP* marker reflects the number of intestinal cells generated in the embryos and are not additional nuclei evolved through extra rounds of karyokinesis. Thus, these data established that members of the *C. elegans* SCF complex LIN-23, CUL-1 and SKR-1 as well as GSK-3 and APR-1 are necessary to control the numbers of intestinal cells being born in the embryo, implying they could act to negatively regulate CDC-25.1 in the embryo.

3.2.2 lin-23 RNAi mimics the tissue-specific phenotype of cdc-25.1(ij48)

Since embryos derived after *lin-23* RNAi seemed to develop relatively normally compared to embryos in all other RNAi experiments investigated here, these embryos were examined further in order to determine whether the removal of *lin-23* would affect proliferation of other tissues. RNAi was compared directly in three strains carrying tissue-specific GFP markers: JR1838 *wIs84* carrying the intestinal-specific GFP, JR667 *wIs51* carrying a seam cell reporter GFP and IA105 *wIs12* carrying a GFP reporter that is expressed in hypodermal nuclei (for strain genotypes see Chapter 2, Table 2.7). Under conditions where *lin-23* RNAi resulted in a strong hyperplasia of intestinal cells as analysed in embryos that reached a stage prior to hatching, no increase in the number of seam cell or hypodermal cell nuclei was seen (Figure 3.3, top). It should be noted that *lin-23* RNAi resulted in 100% of the embryos displaying the intestinal hyperplasia phenotype to a variable degree with normal-appearing embryos displaying the milder phenotype. The numbers of GFP-positive nuclei were quantified in three-fold stage embryos, and whereas there was a clear increase in the number of intestinal nuclei after *lin-23* RNAi compared to the control RNAi, no increase was observed for the seam cells or hypodermal cell nuclei (see Figure 3.3, bottom). All three strains were affected by removal of *lin-23*, because they displayed a similar hatch rate after *lin-23* RNAi (Table 3.1).

	% hatch rate control RNAi	% hatch rate *lin-23* RNAi	p-value	mean % decrease *lin-23* RNAi
elt-2::GFP	98.0 ± 2.6 (n=186)	80.7 ± 8.9 (n=198)	< 0.05	17.7
scm::GFP	94.1 ± 6.1 (n=437)	66.6 ± 10.9 (n=611)	< 0.05	29.2
dpy-7::GFP	99.1 ± 1.0 (n=415)	73.5 ± 5.9 (n=447)	< 0.01	25.6

Table 3.1 *lin-23* RNAi affects different *C. elegans* strain backgrounds equally. JR1838 *wIs84* (*elt-2::GFP*, intestinal GFP), JR667 *wIs51* (*scm::GFP*, seam cell GFP) and IA105 *wIs12* (*dpy-7::GFP*, hypodermal GFP) are all sensitive to *lin-23* RNAi by feeding on plates. mean ± s.d., p-value: two-tailed Student's *t*-test, n= number of embryos from three independent experiments.

Hence, around 80% of the animals depleted by *lin-23* through RNAi can hatch and have a normal body morphology. They are viable and can reach adulthood, although they become sterile as adults. F1 animals that survived *lin-23* RNAi show on average 4.2 ± 3.3% F2 offspring compared to 100% offspring that is produced from F1 animals when treated with control RNAi when analysed 24 hrs after RNAi-treated F1 animals reached adulthood (25 JR1838 F1 each, three independent experiments, the total brood size was not determined). However, embryos with a very strong hyperplasia were also observed which did not undergo any morphogenesis and probably represent the approximately 20% of embryos that are dying (Table 3.1) Thus, it was possible to establish conditions where knockdown of LIN-23 from the embryos affected primarily the proliferation of intestinal cells, but cell lineages such as the hypodermal and seam cells (depicted in Figure 3.3) remained unaffected. Thus, removal of *lin-23* by RNAi mimics the tissue-specific hyperproliferation phenotype of *cdc-25.1(ij48)*.

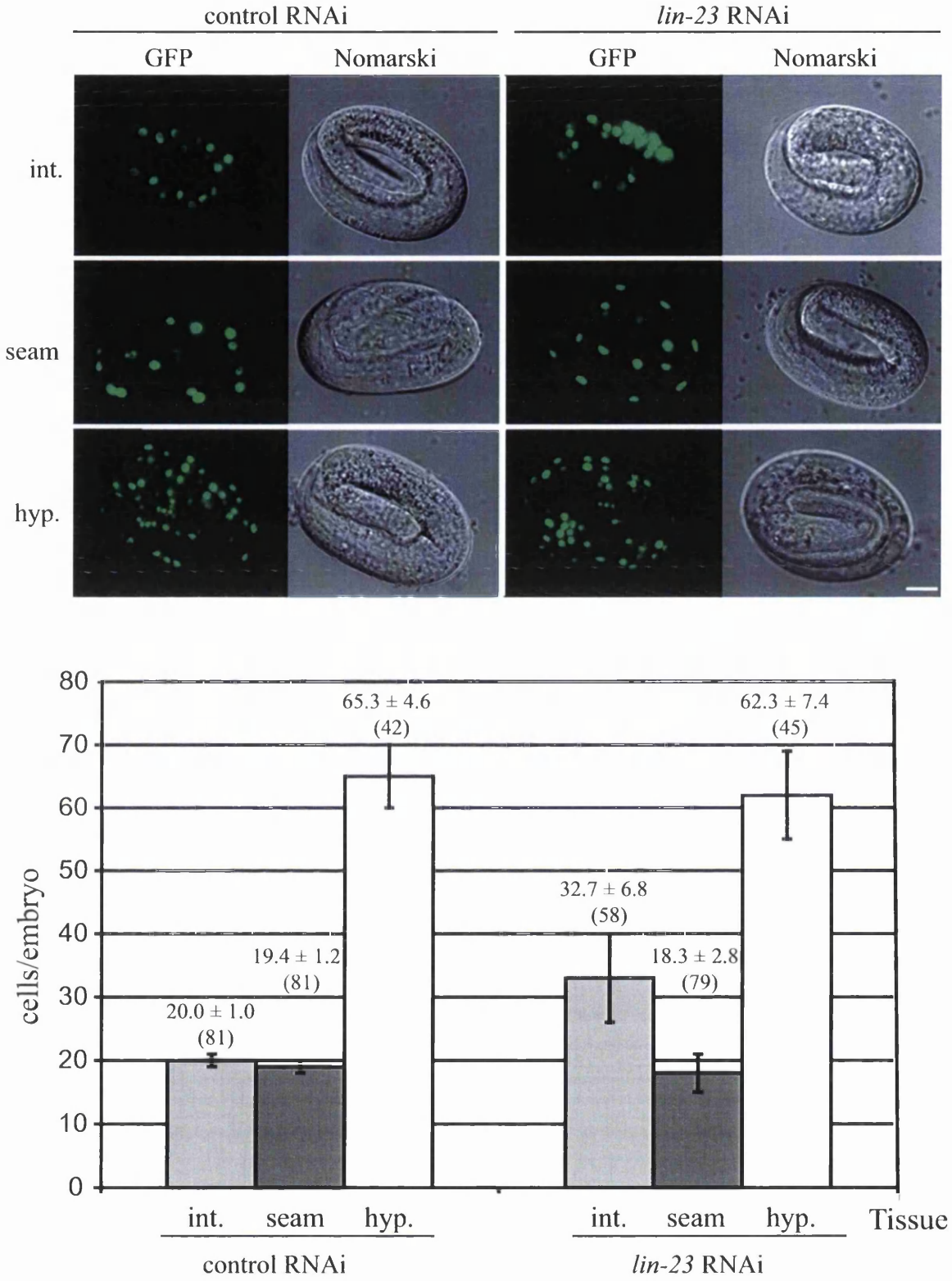

Figure 3.3 *lin-23* RNAi mimics the *cdc-25.1(ij48)* intestine-specific hyperproliferation phenotype. Top: GFP fluorescence phenotypes and corresponding Nomarski counterparts of strain JR1838 carrying *elt-2::GFP* expressed in intestinal nuclei (int.), JR667 *wIs51* carrying a seam cell reporter (seam) and IA105 carrying the hypodermal *dpy-7::GFP* (hyp.) in control or *lin-23* RNAi embryos at the three-fold stage. Scale bar: 10 µm. Bottom: Quantification of GFP-positive nuclei from the experiments performed as above (mean ± s.d., in brackets number of embryos from two independent experiments).

3.2.3 SCF members control proliferation of intestinal cells through S46 in CDC-25.1

The tissue-specific nature of the *lin-23* RNAi phenotype suggested that *lin-23* might act through S46 in CDC-25.1 to control the proliferation of the intestine. In order to clarify this point the following experiment was carried out. If LIN-23 can act through S46 of CDC-25.1, it would be anticipated that removal of *lin-23* in a *cdc-25.1(ij48)* mutant background would not result in an additional increase of intestinal cells as compared to removal of *lin-23* by RNAi in a wild-type strain (i.e. the effects of *lin-23* RNAi and the *cdc-25.1(ij48)* mutation would not be additive).

3.2.3.1 Strain generation to visualize intestinal cells

Therefore, a new strain was generated in order to visualize the number of intestinal cells in *cdc-25.1(ij48)* mutants. This strain was derived by crossing heterozygous IA268 *cdc-25.1(ij48)* males into JR1838 *wIs84* carrying the intestinal-specific *elt-2::GFP* transgene. GFP-positive F2 progeny displaying strong intestinal hyperplasia were picked and checked for homozygosity of the *cdc-25.1(ij48)* allele, by single worm PCR and using restriction enzyme digestion to check for restriction site polymorphism that is introduced through the mutation in *cdc-25.1* (data not shown, for an example see Chapter 7, Figure 7.2). The resulting strain, IA530 *cdc-25.1(ij48) wIs84*, was utilised for most applications throughout this study.

3.2.3.2 Analysis of intestinal cell numbers

Analysis of the average number of intestinal cells in the embryos of a wild-type strain JR1838 compared to IA530 *cdc-25.1(ij48)* revealed an increase from 19.7 to 29.5 intestinal cells when the control RNAi was applied at 20°C similar to results previously reported (Table 3.2) (Clucas, 2003; Clucas et al., 2002). However, at 25°C, on average 19.9 nuclei were detected after control RNAi in JR1838, increasing to only 24.1 nuclei in IA530 *cdc-25.1(ij48)*, indicating that the *cdc-25.1(ij48)* allele is temperature-sensitive. Nevertheless, to ensure a visible phenotype the *lin-23* RNAi had to be carried out at 25°C. In a control experiment, removal of the transcription factor *pop-1* was performed. This causes a switch of the anterior mesodermal sister-cell (MS) of the intestinal precursor (E) to adopt an E fate, such that EMS produces two E cells instead of MS and E (Lin et al., 1995; Thorpe et al., 1997). This mechanism is distinct from the mechanism of CDC-25.1-mediated proliferation, and thus *pop-1* RNAi results in double the numbers of intestinal cells (Table

3.2). Consistent with the two genes acting in separate pathways, when *pop-1* RNAi is performed in the *cdc-25.1(ij48)* background, a significant 1.2-fold synergistic increase of intestinal cells was detected (Table 3.2). In contrast, *lin-23* RNAi performed in the wild-type strain JR1838 caused on average 36.9 intestinal cells to be born, but no significant difference was detected when *lin-23* RNAi was performed in IA530 *cdc-25.1(ij48)* (Table 3.2) suggesting that *lin-23* may act through the *ij48* site of *cdc-25.1*. Similarly, *cul-1* RNAi did not result in any synergistic effect on the intestinal cell numbers when combined with *cdc-25.1(ij48)* (Table 3.2). A slight, but significant increase in the numbers of intestinal cells was detected when *skr-1* RNAi was performed in a wild-type compared to *cdc-25.1(ij48)* mutant background (Table 3.2). The possible reason for the slight additive effect will be discussed below (3.3.1.1). In summary, these data suggest that members of the *C. elegans* SCF complex such as LIN-23 or CUL-1 can act through the *ij48* site on *cdc-25.1* because knockdown of these proteins by RNAi does not result in an additive phenotype when performed in the *cdc-25.1(ij48)* mutant background.

RNAi	JR1838 *cdc-25.1(+)*	IA530 *cdc-25.1(ij48)*	p-value	Fold increase	% Hatch (JR1838 / IA530)
control 25°C	19.9 ± 0.9 (n=176/6)	24.1 ± 3.9 (n=298/6)	< 0.001	1.2	98.8 ± 0.4 98.4 ± 1.5
pop-1	41.9 ± 7.8 (n=175/3)	49.2 ± 11.1 (n=152/3)	< 0.001	1.2	< 1 < 1
lin-23	36.9 ± 7.8 (n=154/4)	35.4 ± 6.8 (n=156/4)	n.s.	1.0	73.2 ± 10.8 69.8 ± 13.2
skr-1	35.7 ± 7.5 (n=130/3)	38.6 ± 9.2 (n=133/3)	< 0.01	1.1	2.9 ± 1.1 1.2 ± 1.2
cul-1	32.6 ± 5.3 (n=129/2)	32.9 ± 5.0 (n=134/2)	n.s.	1.0	56.0 ± 4.2 44.7 ± 20.1
gsk-3	27.5 ± 5.8 (n=176/3)	34.6 ± 8.7 (n=187/3)	< 0.001	1.3	27.2 ± 5.4 20.8 ± 10.2
control 20°C	19.7 ± 0.6 (n=22/1)	29.5 ± 3.2 (n=60/1)	< 0.001	1.5	n.d.
apr-1	27.1 ± 4.9 (n=47/3)	34.9 ± 5.9 (n=76/3)	< 0.001	1.3	n.d.*
wrm-1	23.4 ± 5.3 (n=146/2)	34.2 ± 7.6 (n=77/2)	< 0.001	1.5	n.d.*

Table 3.2 Quantification of intestinal nuclei in *cdc-25.1(+)* (JR1838) and *cdc-25.1(ij48)* (IA530) strains with or without gene-specific RNAi. RNAi was performed as indicated. For *lin-23* RNAi the embryos display the mild RNAi phenotype, all embryos with *elt-2::GFP* expression in above 19 nuclei were counted in all cases. For RNAi by injection (control 20°C, *apr-1* and *wrm-1*): *apr-1* RNA was very diluted (0.2 µg/µl) compared to later experiments, only a few embryos showed a phenotype but that was stronger compared to later experiments, *wrm-1* dsRNA was diluted to 0.5 µg/µl prior to injection. For RNAi by injection the loss of endoderm served as internal control for functional RNAi. * = % no E phenotype: 17.4 ± 10 and 16.0 ± 15.0 for *apr-1*, 74,6 ± 7.5 and 69.7 ± 7.0 for *wrm-1* in JR1838 or IA530, respectively. n.d.= not determined, mean ± s.d., p-value: two-tailed Students *t*-test of wild-type compared to *cdc-25.1(ij48)*, n.s.: p >0.05, n= number of embryos with *elt-2::GFP* expression in 19 nuclei and above/independent experiments.

3.2.4 gsk-3 and apr-1 act independently of cdc-25.1(ij48)

To determine whether GSK-3 could be the kinase phosphorylating S46 in CDC-25.1, a comparison of *gsk-3* RNAi in JR1838 compared to IA530 *cdc-25.1(ij48)* was performed. However, the combination of *gsk-3* RNAi and the *cdc-25.1(ij48)* lesion was found to be additive, with a significant 1.3-fold increase in the number of intestinal cells being evident (Table 3.2). This implies that removal of *gsk-3* acts independently of the *ij48* site of *cdc-25.1*. A similar result was detected for the *apr-1* RNAi. This experiment was performed by microinjection of *apr-1* dsRNA into the gonads of adult hermaphrodites. Offspring were analysed after incubation at 20°C for 24 hours. A significant 1.3-fold increase from 27.1 intestinal cells in JR1838 to 34.9 intestinal cells in IA530 *cdc-25.1(ij48)* was detected after *apr-1* RNAi. Thus, *gsk-3* and *apr-1* function independently of the *ij48* site in *cdc-25.1*.

3.2.5 Cell lineage analysis (by Dr. J. Cabello)

In order to determine whether the GFP-positive nuclei analysed were indeed the result of extra cells being born in the embryo, a cell lineage analysis was carried out in collaboration with Dr. J. Cabello (Prof. Dr. R. Schnabel laboratory, Germany) who performed the experiments. The transparency of the *C. elegans* embryo permits the precise tracking of cell divisions of all embryonic cells over time with the aid of four-dimensional microscopy (Schnabel et al., 1997). The two strains JR1838 *cdc-25.1(+)* and IA530 *cdc-25.1(ij48)* were analysed (under RNAi conditions established in this study) for the proliferation of the E (intestine) and C (hypodermis and body muscle) lineage, and the fate determination of intestinal cells was followed by the expression of the *elt-2::GFP* marker present in both strains (indicated by green vertical lines). A representative result is depicted in Figure 3.4 in each case the two lineages (E (top) and C (bottom) are derived from the same embryo. In a wild-type strain (JR1838), the progenitor cell E divides over time, resulting in 16 intestinal cells that are born after the fourth division at around 200 minutes post-fertilisation, of these only four cells undergo a further fifth round of division at about 330 minutes post-fertilisation generating 20 intestinal cells that all express the intestinal fate *elt-2::GFP* marker (Figure 3.4, Wild-type).

3.2.5.1 Cell lineage after *lin-23* RNAi

Interestingly, when *lin-23* RNAi was performed in this strain a general shortening of the cell cycle was observed such that the fourth and fifth divisions take place at 160 and 250 minutes, respectively (Figure 3.4, Wild-type, *lin-23* RNAi). Unlike in the wild-type, all

cells born after the fourth cleavage undergo a further fifth division leading to excess intestinal cells. The shortened cell cycle and hyperplasia is indistinguishable from that previously shown for the *cdc-25.1(ij48)* allele (Clucas, 2003; Clucas et al., 2002). However, *lin-23* RNAi causes a more robust failure to exit the cell cycle than the variable effect previously observed for the *cdc-25.1(ij48)* allele. The embryo analysed here displays a strong *lin-23* RNAi phenotype because the embryo does not undergo morphogenesis (J. Cabello pers. communication). In this embryo *lin-23* RNAi causes a fate-change in Cp, the posterior daughter of C, which develops ectopically as endoderm expressing *elt-2::GFP* fate (Figure 3.4, Wild-type, *lin-23* RNAi bottom). Note that the timing of the Cp divisions is enhanced compared to a wild-type E lineage. The *cdc-25.1(ij48)* mutant does not enhance the effect of *lin-23* RNAi when *lin-23* RNAi is performed in a *cdc-25.1(ij48)* mutant background; both the timing and numbers of E and the Cp-transformed E cells appear indistinguishable from the *lin-23* RNAi alone (*cdc-25.1(ij48)*, *lin-23* RNAi). Thus, removal of *lin-23* causes a true hyperplasia of endodermal cells through a shortening of the cell cycle and a cell cycle exit defect after the fourth division. Under strong RNAi conditions a Cp to E fate switch is observed, that is not apparent in embryos with mild RNAi phenotype that undergo morphogenesis and display only hyperplasia of E (J. Cabello, pers. comm.).

3.2.5.2 Cell lineage after *gsk-3* RNAi

A similar lineage analysis was carried out to study *gsk-3* function. *gsk-3* RNAi causes Ea, the anterior daughter of E, to develop with non-endodermal fate (cells do not express the *elt-2::GFP* marker), while Ep, the posterior daughter develops as endoderm (Figure 3.4) similar to previous reports (Bei et al., 2002; Schlesinger et al., 1999). But no lineage data was available previously. Interestingly, whereas in the wild-type a lengthened cell cycle is incorporated when Ea and Ep divide (Figure 3.4, see first to second division in Wild-type), after *gsk-3* RNAi the first cleavage of Ep is faster than in the wild-type (see first to second division in wild-type, *gsk-3* RNAi) and the first long cell division occurs after Ep divides (Figure 3.4, see second to third division in Wild-type, *gsk-3* RNAi). Furthermore, after *gsk-3* RNAi all cells undergo further divisions in subsequent cleavages and in the embryo recorded no exit of the cell cycle was observed. Thus, *gsk-3* RNAi results in an aberrant Ep lineage with more cells born than in wild-type. Also, in more severe cases it was observed that Epl developed as non-endoderm with only Epr developing as endoderm. However, unlike for *lin-23* RNAi, no severe shortening of the cell cycle was observed. Interestingly, the Cp cell develops with endodermal fate after removal of *gsk-3*. A similar result was previously demonstrated but no cell lineage analysis was performed in those studies

(Maduro et al., 2001; Schlesinger et al., 1999). Intriguingly, the cell cycle length in the Cp to E transformed lineage is comparable to the cell cycle length of a wild-type E lineage (Figure 3.4, compare Wild-type E with Wild-type, *gsk-3* RNAi in C). Clearly, this cell cycle length is different from the shortened Cp to E transformed lineage after *lin-23* RNAi (Figure 3.4, compare Wild-type, *lin-23* RNAi with *gsk-3* RNAi in C). Significantly, when *gsk-3* RNAi is performed in the *cdc-25.1(ij48)* mutant, a further shortening of the cell cycle is observed for both the E and the Cp to E transformed lineage as compared to *gsk-3* RNAi in the wild-type (Figure 3.4).

3.2.5.3 Cell lineage summary

Hence, these data provide significant evidence for a *lin-23* function to restrain proliferation of intestinal cells. Most cells undergo a fifth or sometimes even sixth (not shown) division through a major shortening of the cell cycle that is mediated through *cdc-25.1(ij48),* since no additive effect has been observed in the mutant background, consistent with *lin-23* acting through the site of the *ij48* lesion. Removal of *gsk-3* causes a phenotype different from that observed by loss of *lin-23*. GSK-3 knockdown causes a shortening of the first cell cycle length in E, a phenotype not observed after LIN-23 knockdown. However, subsequent cell divisions of both the E and the Cp to E transformed lineage are similar to a wild-type E lineage, but all cells expressing endodermal-fate fail to exit the cell cycle after the fourth cleavage. The cell cycles of both lineages remain sensitive to the presence of the *cdc-25.1(ij48)* mutant causing a further shorting of the cell cycle when combined with *gsk-3* RNAi. Thus, *gsk-3* does not promote cell cycle transition through the *ij48* lesion of *cdc-25.1*.

Figure 3.4 *C. elegans* cell lineage analysis.

Cell lineage analysis of the E and C blastomeres. Embryos were cultured at 25°C. Lineages are derived from wild-type or *cdc-25(ij48)* embryos with or without *lin-23* or *gsk-3* RNAi, as indicated. The E (top) and C (bottom) lineages are derived from the same embryo for each condition tested. Branches of the cell lineages expressing the endodermal cell-fate marker *elt-2::GFP* are indicated in green; the wild-type C lineage in black and aberrant, undetermined fates in blue. Time-scale: minutes post first cleavage. The various lineages were followed up to the time indicated by the ends of the vertical lineage lines. Three embryos were analysed in case of (Wild-type, *lin-23* RNAi; Wild-type, *gsk-3* RNAi and *cdc-25.1, gsk-3* RNAi) and two embryos in case of (*cdc-25.1(ij48)*, *lin-23* RNAi). Figure assembly by I.L. Johnstone, edited by A. Segref.

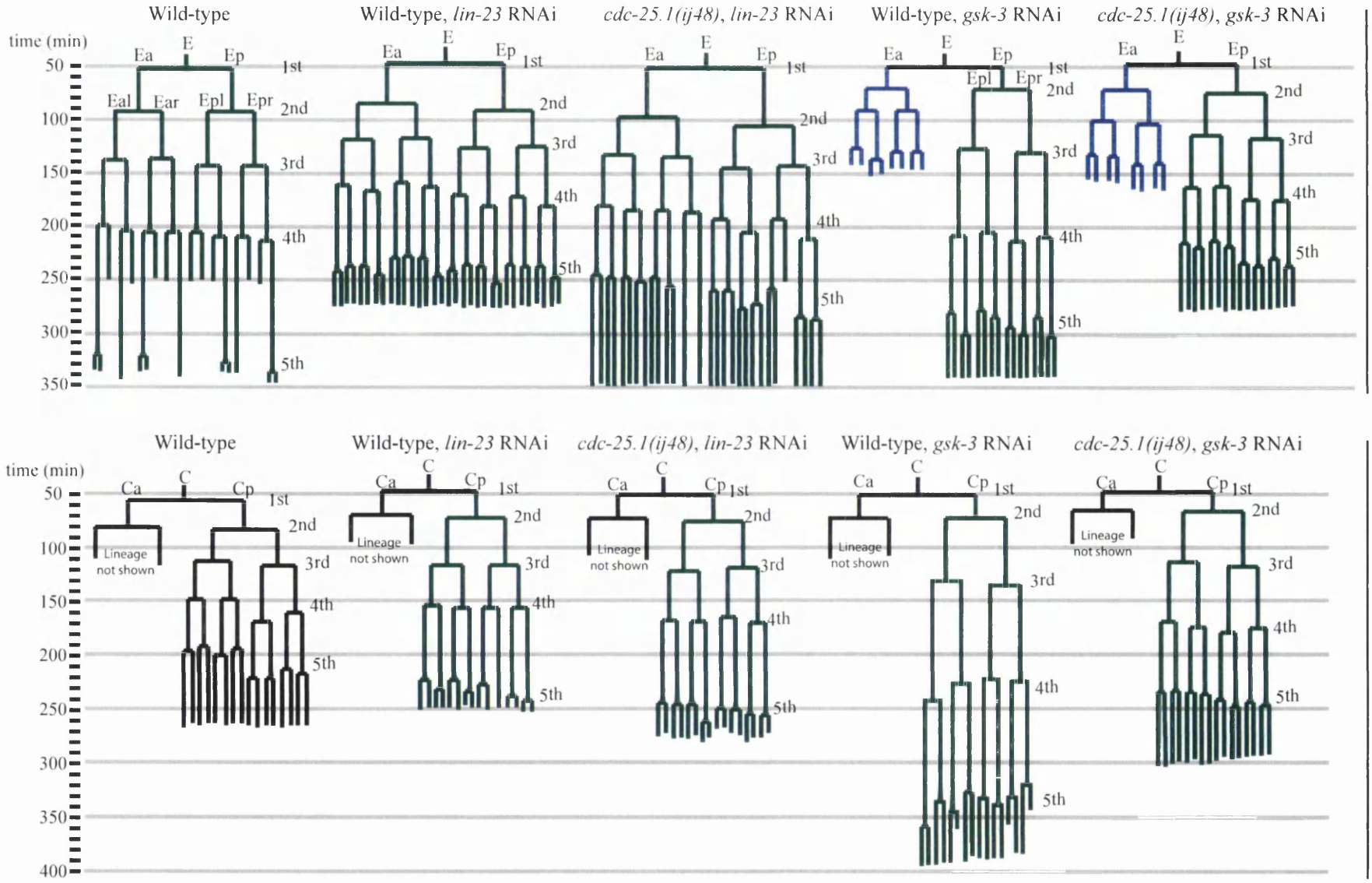

Figure 3.4
Cell lineage.

3.2.6 *gsk-3*-mediated extra intestinal cells requires *wrm-1*

Since knockdown of GSK-3 and APR-1 caused an additive effect when RNAi was performed in *cdc-25.1(ij48)* mutants, it suggested that GSK-3 and APR-1 cause extra intestinal cells through a pathway independent of CDC-25.1. During the specification of intestinal cells via a non-canonical Wnt signalling pathway, these two genes act in concert on *wrm-1,* the *C. elegans* homologue of human β–catenin (Rocheleau et al., 1997). In this pathway, WRM-1 levels are required in E in order to specify intestinal cells. However, it remained to be established whether proliferation of intestinal cells, once specified, requires the presence of *wrm-1*. Interestingly, *wrm-1* RNAi results in 74.6% of embryos not expressing the intestinal fate marker *elt-2::GFP* (Table 3.3). However, embryos that do express the intestinal fate show a variable number of intestinal cells, including embryos with excess endoderm phenotype (Figure 3.2). Similar to *gsk-3* RNAi, *wrm-1* RNAi caused a significant 1.5-fold increase of intestinal cells in JR1838 compared with IA530 *cdc-25.1(ij48)* (Table 3.2, only embryos with extra intestinal cells were counted).

A combined approach of RNAi was performed in order to test whether *gsk-3*, *apr-1* and *wrm-1* act independently to promote the increased numbers in intestinal cells. Here, dsRNA against a single gene or two genes was injected at equal concentrations into the gonad of adult hermaphrodites, and the F1 embryos examined after 24 hours of incubation at 20°C and only embryos with more than 19 intestinal cells were counted. Although all RNAi resulted in extra intestinal cells, no significant increase could be detected for any of the combinations tested (Table 3.3). Hence, *gsk-3* appears to act together with *wrm-1* and *apr-1* to induce extra intestinal cells.

RNAi	Number of E	p-value	% no E
gsk-3	24.2 ± 3.9 (n=141)	n.s.	18.5 ± 1.7
wrm-1	23.4 ± 5.3 (n=146)	n.s.	74.6 ± 7.5
apr-1	23.2 ± 3.0 (n=182)	n.s.	12.6 ± 5.1
wrm-1 gsk-3	23.3 ± 4.5 (n=126)	n.s.	74.0 ± 4.2
gsk-3 apr-1	23.4 ± 2.7 (n=103)	n.s.	21.7 ± 1.8
wrm-1 apr-1	23.6 ± 4.7 (n=98)	n.s.	70.9 ± 2.2

Table 3.3 *gsk-3* double RNAi with *apr-1* and *wrm-1* in a *cdc-25.1(+)* (JR1838) strain. RNAi was performed by injection of ds RNA against the indicated genes. dsRNA was diluted to 0.5 μg/μl (*wrm-1*) and 2 μg/μl (*gsk-3, apr-1*) prior to injection, two independent experiments for each double RNAi, three independent experiments for each single RNAi. mean ± s.d., n= number of embryos expressing *elt-2::GFP* in more than 19 cells, p-value: Kruskal-Wallis test, n.s.: $p > 0.05$.

To validate this experiment further, RNAi was carried out against the two other *wrm-1* homologues *bar-1* and *hmp-2* (Eisenmann et al., 1998; Natarajan et al., 2001). RNAi against *bar-1* resulted in no visible embryonic phenotype when applied by feeding (Table 3.4) or microinjection of dsRNA (data not shown). A weak decrease in the embryonic hatch rate was observed and several mothers displayed a post-embryonic ruptured-vulva phenotype when observed under the microscope, similar to previous reports, indicating that the RNAi was indeed targeting *bar-1* (Kamath et al., 2003; Simmer et al., 2003). However, RNAi against *hmp-2* caused a strong embryonic lethality (Table 3.4), similar to previous reports (Fraser et al., 2000; Lehner et al., 2006; Piano et al., 2002; Sonnichsen et al., 2005) and indicating that the RNAi is functioning. However, all embryos analysed exhibited a wild-type number of intestinal cells and *hmp-2* RNAi did not suppress the *gsk-3*-mediated extra intestinal cells (Table 3.4). Knockdown of GSK-3 by RNAi in some animals results in birth of additional intestinal cells, and in others there is a loss of intestinal cells. But no significant difference was detected when *gsk-3* RNAi was combined with *bar-1* or *hmp-2* (Table 3.4). Thus, the increase in intestinal cells caused through RNAi of *gsk-3* does require *wrm-1* and is independent of the *ij48* lesion in *cdc-25.1*.

RNAi	number of E	p-value	% no E	% hatch
gsk-3	26.1 ± 8.6 (n=369)	-	15.8 ± 4.3	0
bar-1	19.3 ± 1.5 (n=121)	-	0	87.7 ± 1.8
hmp-2	19.8 ± 1.3 (n=96)	-	0	21.0 ± 13.4
bar-1 gsk3	26.4 ± 9.2 (n=128)	n.s.	14.6 ± 0.6	0
hmp-2 gsk-3	25.6 ± 7.9 (n=119)	n.s.	20.2 ± 0.2	0

Table 3.4 *gsk-3* double RNAi with *bar-1* and *hmp-2* in a *cdc-25.1(+)* (JR1838) strain. Double RNAi was performed by feeding worms in liquid cultures, see Chapter 2, (2.2.5.3). Under these conditions only two major phenotypes were observed, loss of intestinal cells or expression of the *elt-2::GFP* marker in at least 18 intestinal cells. Two independent experiments each (six in case of *gsk-3* RNAi), mean ± s.d., p-value: two-tailed Students *t*-test compared to *gsk-3* RNAi only, n= number of embryos expressing the *elt-2::GFP* marker, n.s.: p> 0.05.

3.2.7 CDC-25.1 protein levels in the embryo are dependent on S46

It had become evident through the experiments above that removal of *lin-23* and *cul-1* seemed to act on S46 in CDC-25.1, and *lin-23* RNAi primarily affected proliferation of intestinal cells as compared to other tissues. These observations posed the question whether LIN-23 in complex with CUL-1 could act on the CDC-25.1 protein levels in the embryo. It was decided to focus the efforts on LIN-23 as in an SCF complex this protein would be expected to act as the direct binding partner of CDC-25.1. Previous experiments

by Dr. C. Clucas revealed no difference for the CDC-25.1 protein levels compared to CDC-25.1(S46F) in protein extracts from whole animal cultures (Clucas, 2003; Clucas et al., 2002); however the *cdc-25.1(ij48)* allele causes aberrant proliferation in the embryo suggesting that the protein malfunction should be evident in embryos.

Thus, embryos were analysed for the amount of CDC-25.1 protein levels. In *C. elegans* a relatively pure embryo preparation can be obtained by treating adult worms grown in large liquid cultures in a standard bleach solution, which removes the rest of the worms, but does not penetrate the embryos due to the presence of the eggshell. Interestingly, when embryonic extracts were prepared of the strain IA530 *cdc-25.1(ij48)* derived from control RNAi-treated worms an increase in the CDC-25.1(S46F) protein levels can be detected on a Western blot compared to CDC-25.1 (Figure 3.5, A, compare lane 2 with 4). The antibody utilised to detect CDC-25.1 was previously developed and demonstrated to specifically recognise CDC-25.1 in immunocytochemistry and Western blotting (Clucas, 2003; Clucas et al., 2002). For clarity, this antibody will be referred to as anti-CDC-25.1A antibody throughout this study and is characterized in more detail in Chapter 4. Equal amounts of protein were loaded on the SDS-polyacrylamide gel as examined by β-ACTIN protein levels.

Furthermore, an increase of CDC-25.1 protein levels can be detected in embryos derived from mothers that were fed with dsRNA against *lin-23* (Figure 3.5, A, lanes 1 and 2). Removal of the LIN-23 protein was evident by probing the Western blots with a newly generated antibody against LIN-23 (this antibody is further characterised in Chapter 4, (4.2.3). The samples were separated multiple times on SDS polyacrylamide gels, and since CDC-25.1 and LIN-23 protein run at almost identical size, they were probed independently (including β-ACTIN as internal control). Only one typical representative for each sample loading and the internal control is depicted here and in subsequent figures that required double probing of CDC-25.1 and LIN-23. Importantly, no increase in CDC-25.1(S46F) mutant protein was detected after *lin-23* RNAi as compared to the control (Figure 3.5, A, compare lanes 3 and 4). Thus, consistent with the results above, LIN-23 may act through S46 to control the CDC-25.1 protein levels in embryos. In contrast, *gsk-3* RNAi does not increase CDC-25.1 protein levels in embryos (Figure 3.5, B, compare lanes 1 with 2). However, a decrease is detected in CDC-25.1 protein levels, which could be due to the high lethality rate evident after *gsk-3* RNAi as compared to *lin-23* RNAi (Table 3.2). Nevertheless, a difference between the CDC-25.1 and CDC-25.1(S46F) protein levels is still apparent after *gsk-3* RNAi (Figure 3.5, B, compare lanes 1 and 3), indicating that removal of *gsk-3* does not act to stabilise CDC-25.1 through S46. Knockdown of the GSK-

3 protein was confirmed with a commercial anti-GSK3β antibody, that recognises the correct size band (40.9 kDa) on the Western blot.

3.2.8 CDC-25.1(S46F) protein levels are increased in all early embryonic blast cells

Previous work had established that CDC-25.1 is maternally provided to the embryo and that the protein levels decrease and become undetectable after the 28-cell stage (Ashcroft et al., 1999; Kostic and Roy, 2002) or the 100-cell stage (Clucas, 2003; Clucas et al., 2002) during embryogenesis. The increase of CDC-25.1(S46F) protein levels compared to CDC-25.1 in early embryos by Western blotting strongly argues that CDC-25.1 abundance is regulated through S46. This could be due to an increase in the longevity of CDC-25.1(S46F) in only intestinal cells, or an increase in CDC-25.1(S46F) abundance in all blast cells. In order to address this point, indirect immunofluorescence was carried out using the anti-CDC-25.1A antibody which has been previously demonstrated to specifically recognise CDC-25.1 (Clucas, 2003; Clucas et al., 2002). However, unlike in the previous work, the primary antibody was used at a slightly lower concentration 1:150 instead of 1:50 (for dilutions see also Chapter 2, Table 2.9) to prevent saturation of the signal. Furthermore, confocal microscopy was utilised to facilitate quantification of the signal. As can be seen in Figure 3.6 (panel A), CDC25.1 protein levels decrease from early to late stages of embryogenesis. The cell stage of the embryo was determined by counting the numbers of nuclei after DAPI staining. Note that the signal detected here is rather an under-representation of the fast decline of CDC-25.1 protein levels. In order to keep the signal linear for quantification purposes, each developmental stage was imaged at the appropriate detector gain (kept identical between wild-type and mutant for each stage). Interestingly, CDC-25.1(S46F) protein levels are increased at the early stages of development as compared to CDC-25.1. However, both protein levels decrease at later stages and become almost undetectable when the embryo contains between 100 and 200 blast cells (Figure 3.6, A).

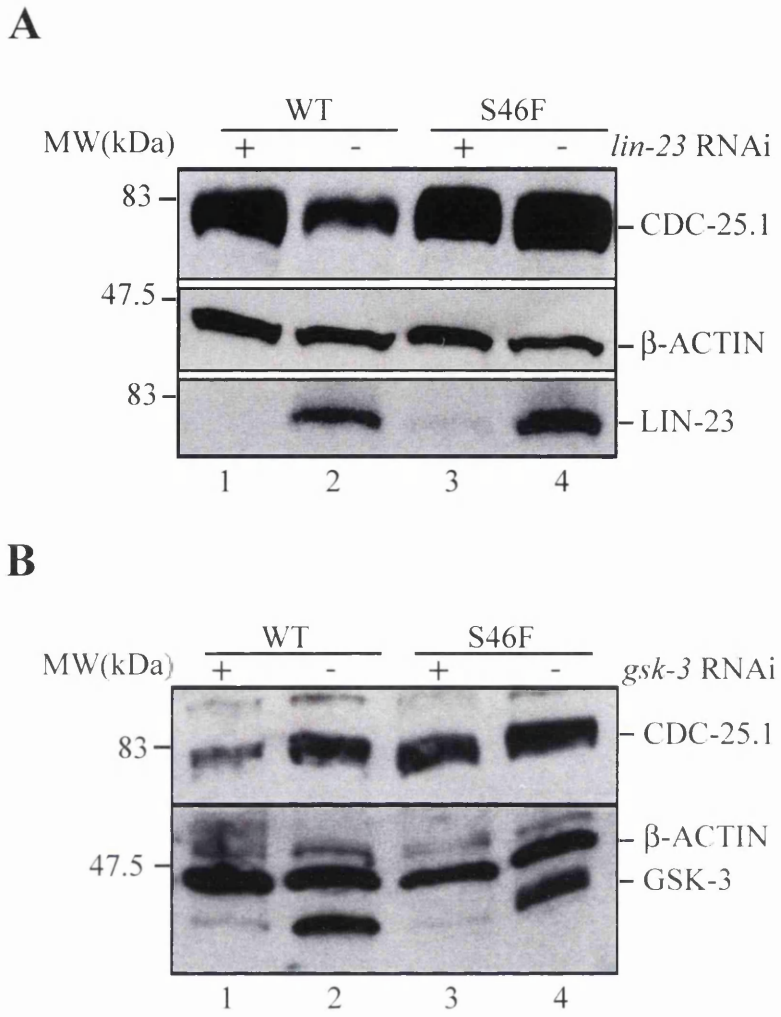

Figure 3.5 *lin-23* but not *gsk-3* RNAi enhances CDC-25.1 stability in *C. elegans* embryos. A) Embryonic extracts derived from adult strains JR1838 (WT, lanes 1 and 2) or IA530 *cdc-25.1 (ij48)* (S46F, lanes 3 and 4) that were grown in liquid culture at 25°C after control (-) or *lin-23* (+) RNAi. The same amount of total proteins for each sample were applied to SDS-PAGE followed by Western blotting. The blots were cut and individually probed against CDC-25.1 (anti-CDC-25.1A), LIN-23 (this study) or β- ACTIN (Sigma) as loading control. **B)** Essentially as (A) but RNAi was performed against *gsk-3* followed by Western blotting against CDC-25.1, GSK3β (Sigma) and β-ACTIN.

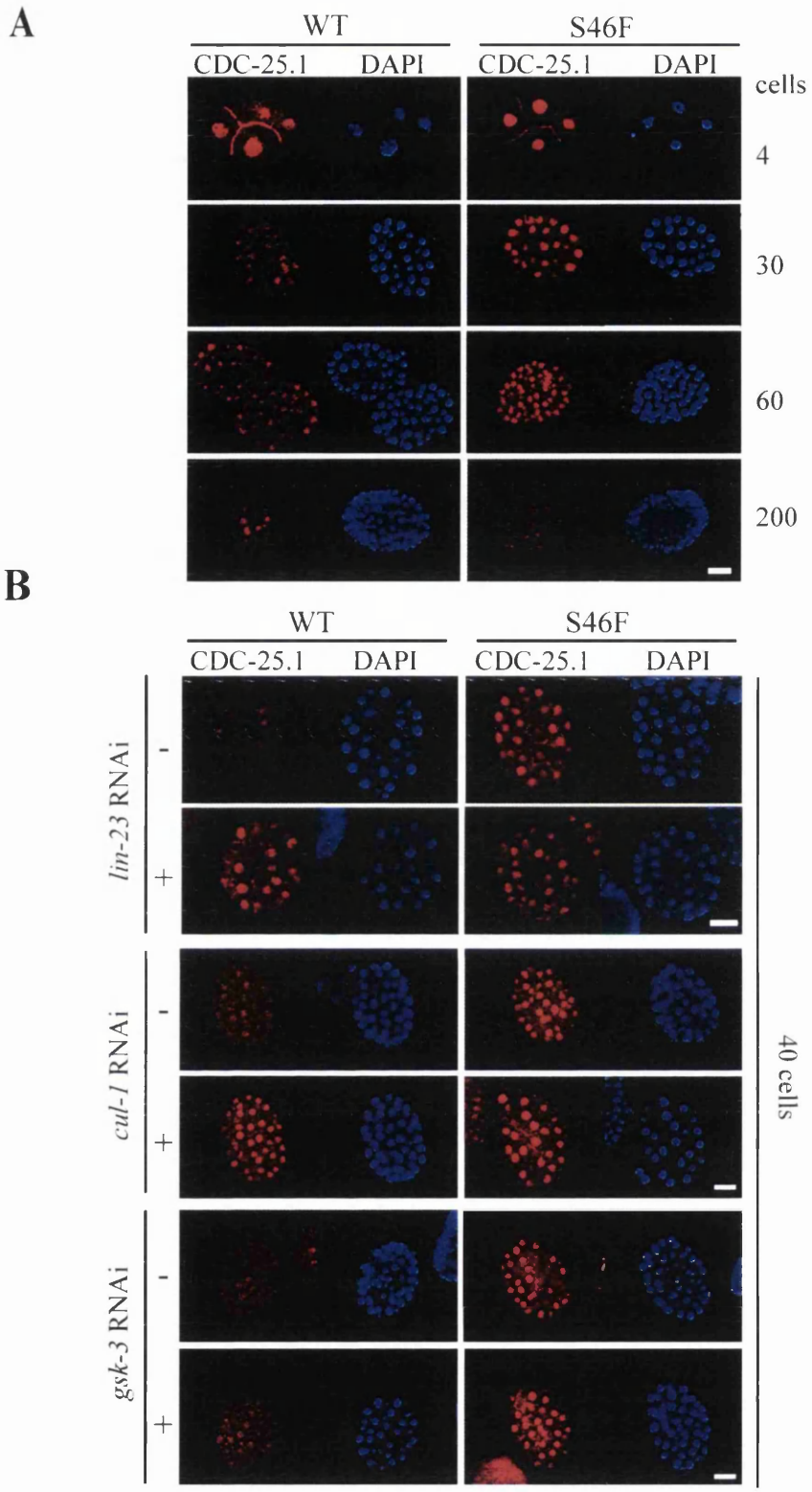

Figure 3.6 Elevated CDC-25.1 protein levels in the early embryo. A) Indirect immunofluorescence of CDC-25.1 using CDC-25.1A antibodies (red panels) with corresponding DAPI counterparts (blue panels) in JR1838 (WT) or IA530 *cdc-25.1(ij48)* (S46F) at approximately the 4-, 30-, 60- or 200-cell stage. Scale bar: 10 μm. **B**) Indirect immunofluorescence as in (A) at the 40-cell stage of JR1838 (WT) or IA530 *cdc-25.1(ij48)* (S46F) after control, *lin-23*, *cul-1* or *gsk-3* RNAi. Note that each gene-specific RNAi is compared with its corresponding control RNAi. Scale bar: 10 μm.

A quantification of the signal was carried out (for a detailed description of this method please see Chapter 2, (2.2.8.4)). The fluorescence signal of early and late embryos derived from strain JR1838 and IA530 *cdc-25.1(ij48)* was quantified in individual embryos. Here, the developmental stage of the embryo was determined by DAPI staining through counting the number of nuclei present in the embryos (Table 3.5, Stage). The fold increase in fluorescence intensity was determined according to statistical methods that are described in detail in (Chapter 2, (2.2.9.1). The overall fold increase was calculated by combining several individual datasets and the statistical significance was revealed by the determination of the p-value for the overall fold increase (Table 3.5, p-value). Interestingly, analysis from several experiments showed that CDC-25.1(S46F) protein levels were significantly increased between the 10- to 60-cell stage of embryogenesis (Table 3.5). However, at later stages no significant increase was detected between CDC-25.1 and CDC-25.1(S46F) (Table 3.5).

Stage (nuclei)	Embryos CDC-25.1	Embryos CDC-25.1(S46F)	CDC-25.1 (S46F) fold increase	p-value
10 - 20	22 (3)	22 (3)	**1.4**	< 0.001
30 - 40	25 (2)	16 (2)	**2.2**	< 0.001
50 - 60	24 (3)	24 (3)	**1.9**	< 0.001
100 - 200	19 (3)	19 (3)	**1.4**	n.s.

Table 3.5 Comparative analysis of CDC-25.1 protein levels in the early embryo by immunostaining. Average fold increase of CDC-25.1 levels was determined by indirect immunofluorescence in embryos of the wild-type strain JR1838 compared to IA530 *cdc-25.1(ij48)*. Embryos: number of embryos (experiments). p-value: two-tailed Student's *t*-test, n.s.: p-value > 0.05.

As an independent approach to validate the statistics, the individual fluorescence intensities determined from single experiments were directly compared for CDC-25.1 and CDC-25.1(S46F) without any sophisticated calculations. Figure 3.7 (top panel) displays an example of the comparisons of CDC-25.1 and CDC-25.1(S46F) at the 30- to 40-cell stage when raw fluorescence intensities from all individual experiments were combined. Clearly, there is an increase in the CDC-25.1(S46F) protein levels compared to CDC-25.1. In summary, here it is shown that the CDC-25.1(S46F) protein levels remain at higher levels compared to CDC-25.1 in all early blast cells of the embryo, but both proteins are eventually degraded and become undetectable at later stages of development.

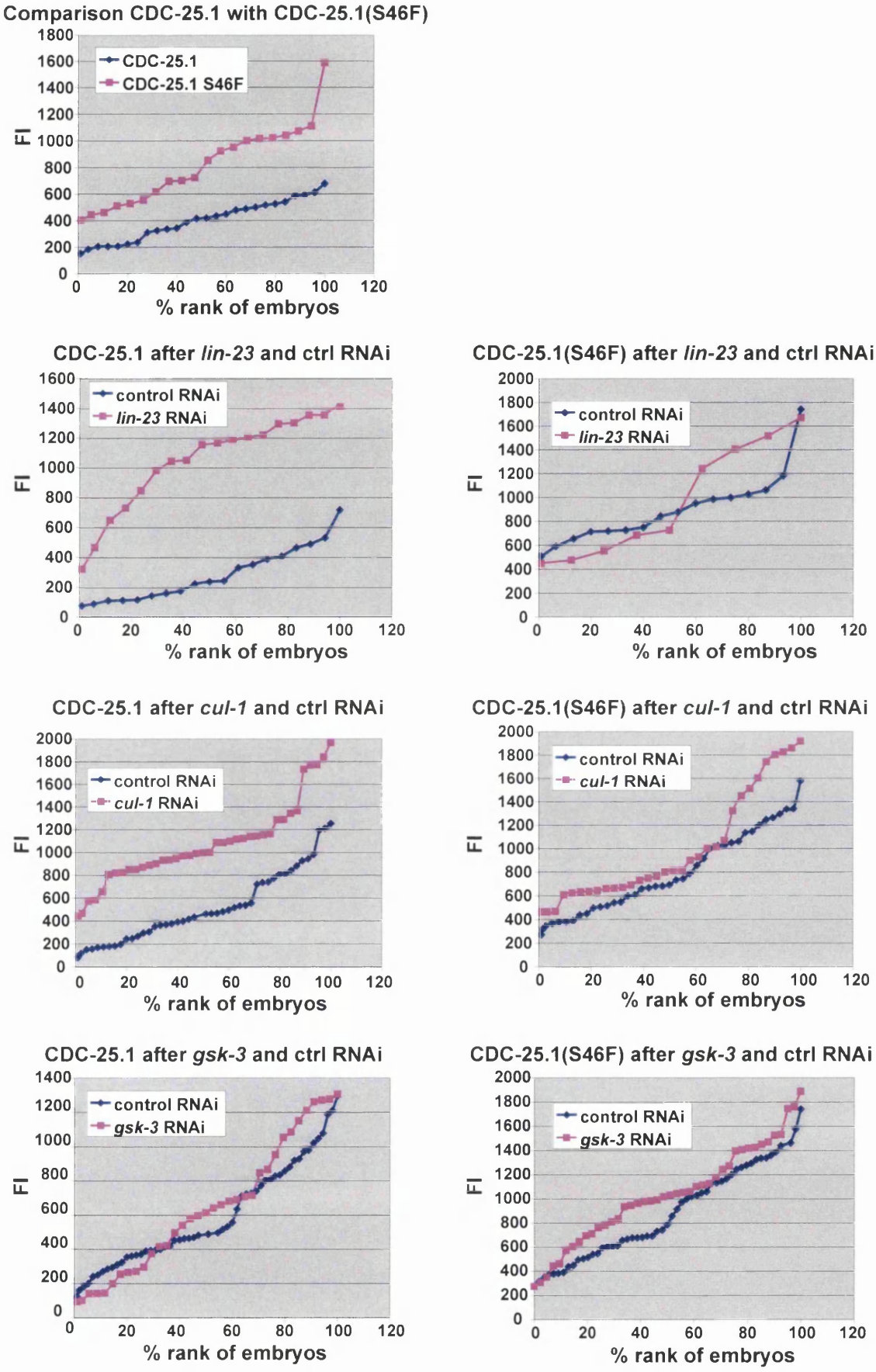

Figure 3.7 Quantification of CDC-25.1 fluorescence in embryos after indirect immunostaining against CDC-25.1. Combined raw data of CDC-25.1 fluorescence intensities (FI) for immunostaining experiments at the 30- to 40-cell stage of JR1838 (CDC-25.1) and IA530 (CDC-25.1(S46F)) alone or after control (ctrl) or gene-specific RNAi, as indicated. Each point represents one embryo and fluorescence intensities (FI) were plotted by rank. Two (*lin-23* RNAi), three (without and *cul-1* RNAi) and four (*gsk-3* RNAi) independent experiments.

3.2.9 LIN-23 and CUL-1 regulate CDC-25.1 abundance in all blast cells through S46

The protein levels of CDC-25.1 in the strain JR1838 were compared by indirect immunofluorescence after control and *lin-23* RNAi treatment. Quantification revealed a significant increase in CDC-25.1 protein levels after *lin-23* RNAi (Table 3.6). At later stages the signal became too weak for the CDC-25.1 control experiment, and therefore quantification was omitted at later stages. Figure 3.7 depicts an example of the comparison at the 30- to 40-cell stage after analysis of the raw data and demonstrates the clear increase observed for the protein levels after *lin-23* RNAi compared to the control RNAi. Importantly, CDC-25.1 protein levels are elevated in all blast cells similar to CDC-25.1(S46F) (Figure 3.6, B). Additionally, knockdown of LIN-23 was performed in the IA530 *cdc-25.1(ij48)* strain. *lin-23* RNAi did not cause any significant increase in the CDC-25.1(S46F) protein levels (Table 3.6, see also Figure 3.7 for analysis of raw data and Figure 3.6, (panel B) for immunostaining picture). Hence, knockdown of LIN-23 from the early embryo increases CDC-25.1 but not CDC-25.1(S46F) protein levels in all blast cells. Since *cul-1* RNAi showed no synergism for the number of intestinal cells in a wild-type compared to *cdc-25.1(ij48)* allele, it was surmised that depletion of CUL-1 would result in a similar stabilisation of the CDC-25.1 protein. Consistently, comparison of CDC-25.1 protein levels after *cul-1* and control RNAi revealed a significant increase in CDC-25.1 protein levels (Table 3.6). However, no significant increase of CDC-25.1(S46F) in all blast cells was detected when *cul-1* RNAi was compared to control RNAi (Table 3.6). See also Figure 3.6 (panel B) for a staining image and comparison of the raw data. In summary, LIN-23 and CUL-1 can act through S46 in CDC-25.1 to control the protein abundance in all blast cells in the early embryo.

3.2.10 GSK-3 does not stabilise CDC-25.1 through S46

Detection of CDC-25.1 by Western blotting suggested that GSK-3 does not act to stabilise CDC-25.1 through S46. However, a small decrease in the CDC-25.1 protein levels was detected after *gsk-3* RNAi. This could be due to an increased death rate of the overall embryo population. Thus, CDC-25.1 protein levels were also quantified by immunostaining of embryos at the 30- to 40-cell stage after control or *gsk-3* RNAi. The CDC-25.1 protein levels remain similar in the control and *gsk-3* RNAi-treated sample (Table 3.6). A similar result was obtained when *gsk-3* RNAi was performed in the *cdc-25.1(ij48)* strain (Table 3.6). Analysis of the raw data clearly demonstrates that all

fluorescence intensities measured are derived from similar readings (Figure 3.7) and no increase of CDC-25.1 or CDC-25.1(S46F) was detected in the 30- to 40-cell stage (Figure 3.6). Thus, GSK-3 does not act to regulate the stability of CDC-25.1 through S46 in early embryos.

RNAi	Stage (nuclei)	CDC-25.1	Embryos control /gene-specific RNAi	Fold increase	p-value
lin-23	10 - 20	WT	15/18 (2)	1.7	< 0.001
lin-23	30 - 40	WT	19/18 (2)	2.8	< 0.001
lin-23	50 - 60	WT	13/15 (2)	2.3	< 0.001
lin-23	10 - 20	S46F	15/16 (2)	1.1	n.s.
lin-23	30 - 40	S46F	16/ 9 (2)	1.0	n.s.
lin-23	50 - 60	S46F	14/16 (2)	1.0	n.s.
cul-1	30 - 40	WT	46/39 (3)	2.2	< 0.001
cul-1	30 - 40	S46F	40/33 (3)	1.1	n.s.
gsk-3	30 - 40	WT	56/35 (3)	0.9	n.s.
gsk-3	30 - 40	S46F	56/42 (4)	1.1	n.s.

Table 3.6 CDC-25.1 protein levels by immunostaining after gene-specific RNAi compared to control RNAi. CDC-25.1 protein levels were compared by indirect immunofluorescence in the JR1838 strain (WT) or in IA530 *cdc-25.1(ij48)* (S46F) after gene-specific RNAi compared to control RNAi-treated embryos. Embryos: number of embryos (experiments). p-value: two-tailed Student's *t*-test, n.s.: p-value > 0.05.

3.3 Discussion

Based on information on DSG motifs present in higher eukaryotes it was hypothesised that the DSG motif in *C. elegans* CDC-25.1 is regulated through members of the *C. elegans* SCF complex. Furthermore, the S46 residue within the CDC-25.1 DSG consensus could possibly resemble a GSK3β phosphorylation site and thus implicate the *C. elegans* GSK-3 and APR-1 in phosphorylation of this residue. Here, data are presented showing that LIN-23 and CUL-1 act to negatively regulate CDC-25.1 through S46 in all blast cells of the early *C. elegans* embryo. Interestingly, GSK-3 and APR-1 are not involved in the regulation of CDC-25.1 through S46, though knockdown of both proteins causes a hyperproliferation of intestinal cells. Several experiments were performed that reinforce this conclusion and are discussed below.

3.3.1 lin-23 and cul-1 act through the cdc-25.1(ij48) allele

RNAi against LIN-23, SKR-1 and CUL-1 resulted in a hyperproliferation of intestinal cells in the *C. elegans* embryo. This clearly implicated a role for these proteins in the negative regulation of cell cycle exit in intestinal cells during *C. elegans* embryogenesis. The result fits well with previous studies that show that a few dying embryos generated in *lin-23*

(Kipreos et al., 2000) and *cul-1* (Kipreos et al., 1996) null hermaphrodites show an increased number of embryonic nuclei, possibly representing embryonic hyperplasia of unknown origin. Similarly, *skr-1* RNAi was shown to cause embryonic arrest with increased numbers of nuclei (Nayak et al., 2002; Yamanaka et al., 2002). Interestingly, here it is shown that when the RNAi was performed in a *cdc-25.1(ij48)* mutant background compared to wild-type *cdc-25.1(+)*, no synergistic increase for the number of intestinal cells was detected when LIN-23 or CUL-1 were removed. This proposed that knockdown of either protein causes the hyperplasia by the same pathway as CDC-25.1(S46F). Specificity of the experiments was evident by the fact that no RNAi effect was seen after control RNAi or when SEL-10, the close homologue of LIN-23, was targeted. Most importantly, a second RNAi experiment, targeting a separate part of the *lin-23* mRNA, resulted in an identical hyperplasia phenotype. Furthermore, the LIN-23 protein knockdown in embryos was clearly demonstrated by Western blotting. Here, the expected 75.9 kDa band is deleted after *lin-23* RNAi as detected using a newly synthesised anti-LIN-23 antibody (this antibody is also characterised in Chapter 4, (4.2.3)) and compared to an internal protein loading control. Additionally, an RNAi experiment against the *cul-1* paralogue *cul-2* displayed no intestinal hyperproliferation phenotype. Thus, it can be concluded that the RNAi against *cul-1* and *lin-23* is specific for both genes. This was also strengthened by the fact that RNAi against *skr-1*, another member of the SCF complex, also resulted in hyperplasia of the intestine. Furthermore, RNAi against *skr-3*, a homologue of *skr-1* but no member of the SCF complex, did not reveal this phenotype.

Thus, targeting of three molecules with homology to known SCF components resulted in an identical hyperproliferation of the intestine, suggesting that all molecules can act as one entity in the negative control of the proliferation of the intestine. In fact, physical interaction of SKR-1 with CUL-1 has been demonstrated by two independent groups (Nayak et al., 2002; Yamanaka et al., 2002). Furthermore, one study reported that binding of LIN-23 to SKR-1 and the paralogue SKR-2 was detected using the yeast two-hybrid assay (Nayak et al., 2002). This is highly indicative of a ternary complex formation including LIN-23, SKR-1 or SKR-2 and CUL-1.

3.3.1.1 *skr-1* RNAi is synergistic to the *cdc-25.1(ij48)* allele

Surprisingly, when *skr-1* RNAi was performed in a *cdc-25.1(ij48)* mutant background (compared to *cdc-25.1(+)*) a slight synergism in the number of intestinal cells was evident after removal of *skr-1*. One possible reason is that *skr-1* is highly homologous to *skr-2* (83% nucleotide identity), and thus it is likely that the *skr-1* RNAi is targeting both genes

at the same time as previously suggested (Nayak et al., 2002; Yamanaka et al., 2002). However, two-hybrid analysis revealed that SKR-2 interacts with CUL-1 and LIN-23 as well (Nayak et al., 2002; Yamanaka et al., 2002), thus making it unlikely that the slight additive effect is mediated through additional downregulation of SKR-2 in complex with CUL-1. Knockdown of SKR-2 should then also mimic the RNAi phenotype of CUL-1 knockdown. But *cul-1* RNAi does not cause an additive effect when performed in a *cdc-25.1(ij48)* strain. However, it remains to be established whether both SKR-1 and SKR-2 binding is specific to CUL-1 only. The experiments performed previously were mainly based on yeast two-hybrid assays and may not reflect the natural binding properties of both proteins.

Consistently, it was demonstrated that the human homologue SKP1 could act independently of CUL-1 to down-regulate β-catenin levels (Matsuzawa and Reed, 2001). There is no evidence so far for a secondary target interaction of SKR-1 or SKR-2 independent of CUL-1. Nevertheless, if SKR-1 or SKR-2 were able to negatively regulate a factor involved in intestinal cell proliferation independently of CUL-1, this would explain the additive effect when *skr-1* RNAi is performed in a *cdc-25.1(ij48)* mutant background.

In order to identify whether *skr-1* RNAi targets *skr-1* and *skr-2*, the mRNA levels could be analysed by RT-PCR. However, measurement of mRNA levels is not always an indicator for the protein levels, as proteins can have a long half-life and be supplied maternally to the embryo. Specific peptide antibodies could be employed to distinguish between SKR-1 or SKR-2 downregulation by Western blotting. Additionally, pull-down of SKR-1 or SKR-2 from *C. elegans* embryos and analysis of their binding partners could serve to identify additional regulatory molecules and decipher between SKR-1- and SKR-2-mediated phenotypes. These are major experiments and would require either the preparation of protein-specific antibodies or the expression of tagged versions of SKR-1 and SKR-2 in *C. elegans* embryos. None of the experiments have been attempted here, because the primary focus was directed towards identifying the physical interaction between CDC-25.1 and its possible direct binding partner LIN-23.

In summary, it is concluded that LIN-23 together with CUL-1 and possibly SKR-1 or SKR-2 regulates the proliferation of intestinal cells during *C. elegans* embryogenesis through S46 in CDC-25.1.

3.3.2 lin-23 RNAi mimics the cdc-25.1(ij48) allele

Intriguingly, whereas *cul-1* RNAi resulted in a robust early embryonic arrest similar to a previous report (Yamanaka et al., 2002), a high percentage of embryos derived from *lin-23* RNAi-treated mothers (80%) did hatch with no obvious morphological defects. Analysis for the intestinal-specific *elt-2::GFP* marker revealed that almost all *lin-23* RNAi embryos analysed displayed a strong hyperplasia of the intestine. This was also confirmed by a cell lineage analysis that revealed additional numbers of E cells being born that express the GFP marker in embryos that undergo normal morphogenesis. Cell divisions of the C lineage, giving rise to hypodermis, body muscle and neurons appeared normal in those embryos (J. Cabello, pers. comm.). In this study, quantification of intestinal nuclei in embryos at the three-fold stage revealed about 32-36 intestinal nuclei. The difference in numbers between independent experiments is probably due to the difference in batches of IPTG being used, consistent with the notion that lowering IPTG concentrations can lead to less severe RNAi phenotypes (Kamath et al., 2000). Thus, each experiment was analysed with its internal control on its own. Importantly, abnormal looking embryos with many intestinal cells (up to around 60) were also detected, which most likely represent the 20% dying embryos. Indeed cell lineage analysis carried out by Dr. Cabello confirmed that *lin-23* RNAi-treated embryos that do not undergo morphogenesis (and probably die) have a strong hyperplasia of endodermal cells and additionally the neighbouring C lineage (in particular Cp) expressed the intestinal fate *elt-2::GFP* marker in those embryos. These differences in phenotype are probably caused through differences in the severity of the RNAi effect. Such an effect has been reported previously and it was suggested that embryos can escape the severity of the RNAi depending on their developmental stage when the RNAi is applied (Clucas et al., 2002; Grishok et al., 2000; Tijsterman et al., 2004; Timmons et al., 2001; Timmons and Fire, 1998). Mild RNAi affected embryos are able to reach adulthood, whereas severely affected *lin-23* RNAi embryos, probably representing the almost complete knockdown of the LIN-23 protein, arrest during their embryogenesis. This is also consistent with the fact that embryos derived from *lin-23* null mutants are not viable, whereas embryos from heterozygous *lin-23* mutants grow up to adulthood and produce a sterile phenotype (Kipreos et al., 2000). This is probably due to the presence of maternal LIN-23 product coming from heterozygous *lin-23* mothers (the maternal function of *lin-23* is discussed in Chapter 5). Consistently, *lin-23* RNAi escapers analysed here reach adulthood and produce a 100% sterile phenotype, phenocopying a *lin-23* null mutant.

3.3.2.1 Mild *lin-23* RNAi affects primarily intestinal cell proliferation

Intriguingly, unlike the severe *cul-1* RNAi phenotype, it was possible to generate conditions for *lin-23* RNAi that resulted in embryos displaying only an intestinal-specific phenotype. Given the role of both proteins, LIN-23 is assumed to confer target specificity due to its homology to known F-box proteins (Kipreos et al., 2000; Kipreos and Pagano, 2000). CUL-1 however is surmised to act as a scaffolding protein, possibly mediating the regulation of many target genes unrelated to CDC-25.1 (Kipreos, 2005; Kipreos et al., 1996). Quantitative analysis of other tissues through expression of tissue-specific markers in embryos with mild *lin-23* RNAi phenotype revealed that those tissues were unaffected by *lin-23* RNAi under conditions where the intestine displayed a strong hyperplasia. It was evident that all strains were targeted by *lin-23* RNAi because they showed a similar decrease in their hatch rate after LIN-23 knockdown.

Thus, knockdown of LIN-23 affects primarily the proliferation of intestinal cells and mimics the *cdc-25.1(ij48)* phenotype. Cell lineage analysis revealed that knockdown of LIN-23 resulted in increase of intestinal cells by two mechanisms: and a severe shortening of the cell cycle in cells expressing the intestinal fate marker and a robust failure to exit the cell cycle after the fourth division. These phenotypes are similar to the lineage described for *cdc-25.1(ij48)*, though the failure to exit the cell cycle is more variable in this mutant (Clucas, 2003; Clucas et al., 2002). Intriguingly, when *lin-23* RNAi was performed in a *cdc-25.1(ij48)* background, no further shortening of the cell cycle in cells expressing endodermal fate such as the E and even a Cp to E transformed lineage was detected by cell lineage analysis consistent with the fact that LIN-23 acts through S46 in CDC-25.1 described in this study.

3.3.2.2 LIN-23 regulates CDC-25.1 protein levels through S46

In agreement with the results above, *lin-23* RNAi causes elevated CDC-25.1 protein levels during early embryonic development in all tissues in accordance with the nature of the *cdc-25.1(ij48)* allele (discussed below). This was examined by Western blotting and indirect immunostaining against CDC-25.1. Consistent with the action of LIN-23 through S46 in CDC-25.1, no increase in protein abundance was detected when *lin-23* RNAi was performed in the *cdc-25.1(ij48)* strain. This result was confirmed by RNAi against *cul-1* and thus complements the *lin-23* RNAi phenotype. The results reinforce the importance for the LIN-23 and CDC-25.1 interaction in *C. elegans* embryos and suggest that abrogation of

the interaction through knockdown of LIN-23 or mutation of a possible LIN-23 binding site in CDC-25.1 primarily affects proliferation of the intestine.

3.3.3 CDC-25.1(S46F) is elevated in all embryonic blast cells

Novel data presented here establish that CDC-25.1(S46F) protein levels are elevated compared to CDC-25.1 during early stages of embryogenesis as examined by Western blotting and indirect immunofluorescence. This conclusion contradicts previous work that did not detect any differences in CDC-25.1(S46F) abundance by Western blotting and indirect immunofluorescence (Clucas, 2003; Clucas et al., 2002). The discrepancy in the data obtained is explained by the difference in the methodology applied. In this study Western blotting was performed using purified embryonic extracts reflecting the stage when CDC-25.1(S46F) exerts its cell-proliferative effects. The previous studies however examined an adult worm culture where the majority of CDC-25.1(S46F) protein might be reflecting the protein expressed in the germline, which is differentially regulated. Data supporting this idea are presented in Chapter 5. Thus, in adult cultures the embryonic CDC-25.1 protein levels might be underrepresented. Additionally, here indirect immunostaining against CDC-25.1 was performed using less primary antibody though the same antibody preparation as used by (Clucas, 2003; Clucas et al., 2002) was employed. Down-titration of the antibody ensured less saturation of the signal, and confocal microscopy facilitated the fast scanning and therefore less bleaching of the signal.

In summary, from the data presented in this study it can be concluded that CDC-25.1(S46F) protein levels are elevated in all blastomeres during the 10- to 60-cell stage of embryogenesis. In accordance with this conclusion, a CDC-25.1(G47D) mutant was demonstrated to persist longer in all blast cells in *C. elegans* embryos (Kostic and Roy, 2002). This mutant was demonstrated to exhibit a similar intestinal hyperplasia phenotype as compared to CDC-25.1(S46F). The authors concluded that CDC-25.1 protein levels become undetectable after the 28-cell stage of embryogenesis, whereas CDC-25.1(G47D) longevity is increased up to the 100-cell stage. However, previous work (Clucas, 2003; Clucas et al., 2002) and data presented here clearly show that CDC-25.1 is present up to the 100-cell stage of embryogenesis. This elementary difference is probably the result of different antibodies employed in the studies.

Importantly, the immunostaining results presented here argue strongly that CDC-25.1(S46F) protein is elevated compared to CDC-25.1 at a time when CDC-25.1 would also normally be present. This conclusion differs from the statement by Kostic and Roy

(2002) who proposed that CDC-25.1(G47D) persists longer at a time when CDC-25.1 would not normally be present in the embryo (i.e. after the 28-cell stage) (Kostic and Roy, 2002). This would suggest that the presence of CDC-25.1 in cells that would normally be depleted from this cell cycle regulator remain sensitive to the presence of CDC-25.1 following an all or nothing principle. However, the data here argue that intestinal cells normally still possessing CDC-25.1 protein levels are more sensitive to slightly elevated CDC-25.1 protein levels when degradation of CDC-25.1 is reduced.

3.3.4 CDC-25.1 S46 regulation is not tissue-specific

3.3.4.1 Is a downstream molecule limiting in non-intestinal tissues?

Intriguingly, the CDC-25.1(S46F) protein increase is not restricted to intestinal cells, but affects all tissues, similar to the CDC-25.1(G47D) phenotype (Kostic and Roy, 2002). It is conceivable that a downstream regulator such as a cyclin-dependent kinase becomes limiting in non-intestinal cells as compared to the intestine. The *C. elegans* genome contains twelve genes related to cyclin-dependent kinases (Manning, 2005) and at least seven show embryonic lethality in RNAi screens (Fernandez et al., 2005; Gonczy et al., 2000; Kamath et al., 2003; Lehner et al., 2006; Maeda et al., 2001; Piano et al., 2002; Rual et al., 2004; Simmer et al., 2003; Sonnichsen et al., 2005). Furthermore, at least ten cyclin-related genes are present in the *C. elegans* genome and for seven of those an embryonic lethal phenotype has been described in RNAi screens (Kamath et al., 2003; Maeda et al., 2001; Piano et al., 2002; Rual et al., 2004; Simmer et al., 2003; Sonnichsen et al., 2005). In particular cyclin E could be of potential interest as it has recently been implicated as a downstream partner of CDC-25.1 in embryos (Kostic and Roy, 2002). In other metazoans, CDK2 interacts with cyclin E (van den Heuvel, 2005). By sequence homology, *C. elegans* has one putative *cdk-2* gene that is required during embryogenesis (Boxem et al., 1999) and could be another downstream target of CDC-25.1. However, in the (Kostic and Roy, 2002) study no cyclins that may act at distinct cell cycle stages and which have known implications for early embryonic development were tested (such as B type cyclins that would be surmised to act at the G_2/M transition). This is particularly important given the fact that intestinal cells are the primary cells in the embryo that initiate a G_2 phase. During intestinal development, after the first intestinal Ea to Ep division a first G_2 phase is initiated (Edgar and McGhee, 1988), thus indicating that factors acting at this cell cycle stage might become important downstream targets of CDC-25.1. Further indications that CDC-25.1 may also be able to act at the G_2/M transition are given by the fact that the G_2/M phase kinase CDK-1 is expressed in the early embryo (Boxem et al., 1999). Furthermore,

knockdown of CDK-1 results in embryonic lethality (Boxem et al., 1999) and a *cdk-1* mutant produces excess endoderm through aberrant C specification; however E cell proliferation was not analysed (Shirayama et al., 2006). Thus, it remains to be elucidated whether *cdk-1* might also be functioning in the intestine.

Another downstream candidate of CDC-25.1 could be cyclin D (*cyd-1*), because a *cyd-1* loss-of-function mutant was previously shown to produce only 16 intestinal cells (Boxem and van den Heuvel, 2001). This could indicate that at least the final four divisions of intestinal cells might require *cyd-1* function. However, this phenotype was not observed by *cyd-1* RNAi, indicating that *cyd-1* RNAi is not effective in the embryo under the conditions examined. A previous study by (Kostic and Roy, 2002) proposed that CDC-25.1 does not act through CYD-1 because *cyd-1* RNAi could not suppress CDC-25.1(G47D) mediated hyperplasia, but it remains to be established whether the *cyd-1* loss-of-function allele can suppress the intestinal hyperplasia of *cdc-25.1(ij48)* or *cdc-25.1(rr31)*.

3.3.4.2 Identification of CDC-25.1 downstream partners

Hence, if a downstream regulator of CDC-25.1 becomes limiting in other tissues but not the intestine, removal of that factor might primarily result in abrogation of the cell cycle in tissues other than the intestine (see Figure 3.8). Removal of kinases for which an embryonic lethal phenotype has been described (*cdk-1*, *cdk-2*, *cdk-5*, *cdk-7*, *cdk-9*, B0285.1 or B0495.2) or a cyclin (*cyb-1*, *cyb-2.1*, *cyb-2.2*, *cyb-3*, *cye-1*, *cyh-1*, *cyl-1*) (Fernandez et al., 2005; Gonczy et al., 2000; Kamath et al., 2003; Lehner et al., 2006; Maeda et al., 2001; Piano et al., 2002; Rual et al., 2004; Simmer et al., 2003; Sonnichsen et al., 2005) with priority given to the *cdk-1*, *cdk-2* and *cyb* and *cye* genes (see above) could be performed in strains expressing tissue-specific GFP markers as done for *lin-23* RNAi in this study. Unfortunately, this experiment would not be easily performed with *cyd-1* because *cyd-1* RNAi is not very effective (see above). However, for the other genes analysed this would reveal whether it is possible to obtain conditions where removal of any kinase or cyclin affects proliferation of other tissues more easily. Such tissue might be more sensitive due to its limiting pool of the kinase or cyclin and thus would be more sensitive to depletion. Such experiments would establish whether the 'limiting pool' theory could indeed be true. Any candidate could be further tested for suppression of the *cdc-25.1(ij48)* phenotype, thus implicating it as a downstream target for *cdc-25.1*. Overexpression of any candidate could then be performed in the *cdc-25.1(ij48)* mutant, to determine whether it triggers a hyperplasia of that tissue.

Figure 3.8 The 'limiting pool' model.

The downstream target of CDC-25.1 is limiting in other tissues compared to the intestine. The circle represents the pool of the cyclin-dependent kinase (CDK) or cyclin. Under normal conditions, CDC-25.1 activates (arrow) a certain pool of its downstream kinase. Overexpression of CDC-25.1 through S46F mutation results in increase of the levels of active kinase in the intestine but not other tissues, because other tissues do not possess more molecules that can be activated.

3.3.4.3 Are additional negative regulators present in non-intestinal tissues?

As an alternative model, the amounts of downstream target might not be limiting but an additional negative regulator might be missing from intestinal cells (for a model see Chapter 7, Figure 7.1). In that regard the observation that CDC-25.1(S46F) (this study) as well as CDC-25.1(G47D) (Kostic and Roy, 2002) render cells sensitive to the protein levels once E is specified is rather intriguing. Removal of the transcription factor *pop-1* by RNAi causes the progenitor of endoderm, the EMS blastomere, to produce two E cells rather than MS and E (Lin et al., 1995; Thorpe et al., 1997), probably due to the release of endoderm repression in MS. A hyperplasia of the MS to E transformed cells was detected when *pop-1* RNAi was performed in *cdc-25.1(ij48)* (this study) or *cdc-25.1(rr31)* (Kostic and Roy, 2002) mutant backgrounds, resulting in a synergistic increase of intestinal cells. This suggests that zygotic transcription might be important to confer the enhanced sensitivity of intestinal cells to increased CDC-25.1 levels. This could be achieved either by *de novo* synthesis of additional negative regulators in non-intestinal tissues but not transcribed in E. Alternatively, *de novo* synthesis of a downstream molecule in E that is not expressed in MS or other tissues could account for the tissue-specific phenotype (see limiting pool theory above). If an additional negative regulator is present in non-intestinal tissues, a combination of an inactivating mutation in a negative regulator, present in other tissues but not in the intestine, with *cdc-25.1(ij48)* might result in hyperproliferation of other tissues and cause embryonic lethality. A genome-wide RNAi screen could identify negative regulators that enhance the CDC-25.1(S46F) phenotype (details on how to perform such experiment are described in the Chapter 7, (7.1.1)).

3.3.5 GSK-3 is not the kinase acting on S46 in CDC-25.1

The experiments performed in this chapter suggest that GSK-3 acts independently of S46 in CDC-25.1. Firstly, *gsk-3* RNAi results in a synergistic increase of intestinal cells when performed in the *cdc-25.1(ij48)* strain. Secondly, cell lineage analysis (by J. Cabello) demonstrated that knockdown of GSK-3 caused no shortening of the cell cycle, a phenotype that was observed after LIN-23 knockdown or in the *cdc-25.1(ij48)* mutant. When the *gsk-3* RNAi was performed in the *cdc-25.1(ij48)* mutant, a further shortening of the cell cycle was observed compared to *gsk-3* RNAi in the *cdc-25.1(+)* background. This was evident for intestinal cells expressing the *elt-2::GFP* marker generated from Ep and Cp. Hence, the shortening of the cell cycle mediated through *cdc-25.1(ij48)* is additive to the removal of *gsk-3* and thus might reflect the further increase in the number of intestinal cells observed in this study. Thirdly, RNAi against *gsk-3* does not increase CDC-25.1 protein levels, either on Western blot or as examined by indirect immunofluorescence in embryos. Clearly, GSK-3 is depleted under these conditions as examined by Western blotting against GSK-3. Furthermore, the fact that around 15 - 18% of the embryos fail to express intestinal cells is consistent with the down-regulation of GSK-3 (Bei et al., 2002; Schlesinger et al., 1999).

3.3.5.1 *gsk-3* RNAi phenotype is novel

The extra intestinal cell phenotype detected in these and preliminary experiments (earlier performed in the Johnstone lab) is novel, since previous reports mostly addressed the specification of intestinal cells (Bei et al., 2002; Schlesinger et al., 1999). None of the studies analysed the expression of an intestinal-specific marker. Furthermore, the cell lineage demonstrated that the posterior E cell Ep generates at least 16 intestinal cells (thus six more than it would normally do). Here, knockdown of GSK-3 causes Ea to express non-endodermal fate, suggesting a fate switch similar to a previous report that demonstrated that E in isolation is able to express a pharyngeal marker after *gsk-3* RNAi (Schlesinger et al., 1999). Furthermore, cell lineage analysis revealed that the Cp blastomere produces intestinal cells, in agreement with previous reports showing that Cp or P2 in isolation can produce intestinal cells after *gsk-3* RNAi (Maduro et al., 2001; Schlesinger et al., 1999). Interestingly, *lin-23* RNAi also causes a Cp to E transformation, which could suggest that both GSK-3 and LIN-23 might have a common function in the suppression of endodermal fate in C. However, the fate specification was not the primary focus of this study. To sum up, the intestinal cells that are quantified after *gsk-3* RNAi are the results of more cells generated in Ep and Cp.

3.3.5.2 *apr-1* and *wrm-1* RNAi induce extra intestinal cells similar to *gsk-3* RNAi

Interestingly, *apr-1* and *wrm-1* RNAi show a similar phenotype to GSK-3 knockdown. During the non-canonical Wnt signalling pathway, the development of the intestine requires the action of *gsk-3* (Bei et al., 2002; Schlesinger et al., 1999), *apr-1* and *wrm-1* (Bei et al., 2002; Rocheleau et al., 1997; Rocheleau et al., 1999). Thus, the hyperplasia generated through *apr-1* and *wrm-1* RNAi might be by the same mechanism as *gsk-3* RNAi, because when RNAi was performed in combination no synergism could be detected. However, without a lineage analysis after *apr-1* or *wrm-1* RNAi it is unclear whether the intestinal cells are derived from the same tissues as those obtained after *gsk-3* RNAi. It is interesting to see that the wrong specification of E results in excess numbers of intestinal cells. A possible reason could be that *gsk-3* RNAi can delay the specification of the E blastomere and therefore the terminal differentiation of the intestine, such that E behaves as EMS and can give rise to a MS and E complement (with Ea generating MS and Ep generating a complete E lineage; I. L. Johnstone pers. comm.). The fact that GSK-3 knockdown results in a shortened cell cycle when the putative Ep cell divides for the first time compared to wild-type is also in agreement with this hypothesis. In this case the fifth division indicated after *gsk-3* RNAi would be comparable to the fourth division in the wild-type, due to the delay of E specification for one cell cycle. One way to test if the E cell has retained an EMS potential for another division (such that E is actually EMS) would be to isolate the EMS blast cell after *gsk-3* RNAi in the four-cell stage embryo, but prior to P2 signalling. In the wild type, EMS loses its ability to react to the P2 derived signal if the contact is provided less than three minutes prior to EMS cytokinesis (Goldstein, 1995). Placing the EMS blastomere in contact with P2 after it has divided will identify, if the posterior cell can induce endoderm by *elt-2*::GFP expression. If so, than E has retained the EMS potential.

Unfortunately, it is presently unknown whether all of the intestinal cells after *gsk-3* RNAi undergo one further division or if only four cells continue dividing. Importantly, the *gsk-3* RNAi phenotype seems different from the cell proliferative function of LIN-23 or CDC-25.1 in the intestine. It will be interesting to determine whether a cell lineage analysis of *apr-1* or *wrm-1* RNAi-treated embryos results in an identical phenotype to the *gsk-3* RNAi. However, cell lineage analysis of *wrm-1* RNAi-treated embryos is quite difficult to perform due to the high percentage of embryos lacking endoderm.

Most importantly, here it is shown that the *gsk-3*-mediated extra intestinal cells are not generated through the same mechanism as the hyperplasia mediated through *cdc-25.1(ij48)*. In fact, the synergism observed by *gsk-3* RNAi in *cdc-25.1(ij48)* shows clearly that both phenotypes are caused by separate mechanisms. Together, these data suggest that the *C. elegans* GSK-3 does not act through S46 in CDC-25.1. Nevertheless, it does not exclude the possibility that another member of the *C. elegans* GSK-3 family is able to negatively regulate this site or that GSK-3 may be able to act on another site of CDC-25.1.

3.3.6 Conclusion

Novel data presented in this chapter provide significant insight into the mechanism underlying the *cdc-25.1(ij48)* mutant phenotype. For the first time LIN-23 is shown to act as a negative regulator of CDC-25.1, mediating its effect through S46 and thus controlling the intestinal cell proliferation in a whole model organism. LIN-23 is necessary in the *C. elegans* embryo to restrain CDC-25.1 protein levels in all blast cells during early embryogenesis. In human tissue culture experiments an interaction between CDC25A or CDC25B and β-TrCP is necessary to control progression of the cell cycle under normal conditions and in response to DNA damage (see Introduction to this chapter, (3.1.2.3)). Thus, the data displayed here exemplify the high conservation of the regulation of the DSG consensus of CDC25 from *C. elegans* to humans. Phosphorylation of S46 is not achieved through the closest GSK3β homologue GSK-3. But interestingly, GSK-3 influences the number of intestinal cells in a mechanism distinct from S46 in CDC-25.1.

Chapter 4

CDC-25.1 S46 is crucial for LIN-23 binding

4 CDC-25.1 S46 is crucial for LIN-23 binding

4.1 Introduction

The work presented in Chapter 3 clearly delineates a role for LIN-23 in the regulation of CDC-25.1 through the S46 residue in the DSG consensus sequence. In mammalian cells the LIN-23 orthologue β-TrCP forms part of the E3 ubiquitin ligase complex, termed SCF (SKP1, CULLIN1, F-box), and participates in the ubiquitination of target substrates. Ubiquitin-mediated delivery to the substrates is a multistep process requiring the E1, E2 and E3 enzymes. The activating enzyme E1 utilises ATP to transfer ubiquitin to the E2 conjugating enzyme. The E2 enzyme then transfers the ubiquitin to the target substrate with the aid of the E3 ubiquitin ligase. In the SCF ligase complex the transfer of ubiquitin occurs directly from the E2 ligase to the substrate. Ubiquitination is achieved by the covalent attachment of ubiquitin between the C-terminal glycine of ubiquitin and the ε-amino group of the lysine in the target protein or another ubiquitin. Attachment of multiple ubiquitins to the lysine-48 or lysine-29 residue of ubiquitin results in proteasome-dependent degradation of the target substrate (Nandi et al., 2006; Pickart and Eddins, 2004).

In the E3 ligase SCF complex the CULLIN1 (also termed CUL1 hereafter) protein acts as a scaffold molecule whose C-terminus binds the RING finger (Really Interesting New Gene) molecule RBX1 that is bound to the E2 ubiquitin conjugating enzyme. The N-terminus of CUL1 interacts with the SKP1 protein bound to the F-box region of the substrate recognition particle such as β-TrCP. Association of the SCF core subunit with multiple F-box molecules allows for the distinct targeting of substrate molecules for ubiquitin linkage. The F-box molecule β-TrCP interacts via its C-terminal WD40 domain with the phosphorylated DSG consensus sequence present in diverse target substrates and positions the substrate to the ubiquitin conjugating enzyme E2, which covalently attaches ubiquitin to the lysine residues on the substrate molecule (Ang and Wade Harper, 2005).

4.1.1 C. elegans SCF components

Based on homology searches members of the *C. elegans* SCF complex have been identified (Kipreos, 2005). The *C. elegans* genome contains 326 F-box molecules compared to only 68 in humans. These are subdivided into several distinct categories based on their motif domain in their C-terminus. The FBXW proteins contain the WD40 motif,

FBXL proteins the leucine rich repeats (LRR) and FBXO denotes proteins with another or no other motif (Kipreos and Pagano, 2000). Common to all these molecules is an approximately 50 residue F-box motif that has been demonstrated to bind to the SKP1 protein and was named after its presence in cyclin F (Bai et al., 1996). Only three members, LIN-23, SEL-10 and the so far unnamed protein WP:CE02308 (Wormbase accession number) form the FBXW family of proteins in *C. elegans* as compared to five family members in humans (Kipreos and Pagano, 2000). Furthermore, 21 SKP-related (SKR) proteins have been identified in *C. elegans* compared to a single SKP1 gene in humans. Seven of the SKR genes (SKR-1,-2,-3,-7,-8,-9 and 10) were found to interact with the *C. elegans* CULLIN1 orthologue CUL-1 (Nayak et al., 2002; Yamanaka et al., 2002). An interaction of LIN-23 with CUL-1 and SKR-1 and SKR-2 has been reported making it likely that LIN-23, CUL-1 and SKR-1 or SKR-2 form a SCF complex in *C. elegans* (Nayak et al., 2002). So far only BAR-1, another *C. elegans* homologue of human β–catenin (Eisenmann et al., 1998; Natarajan et al., 2001), has been identified as a downstream target of LIN-23 during *C. elegans* post-embryonic development (Dreier et al., 2005). Dreier et al. demonstrated binding of LIN-23 to BAR-1 in mammalian tissue culture cells and the dependence of the BAR-1 ubiquitination state on LIN-23 function in *C. elegans*.

In the previous chapter it was established that LIN-23 and CUL-1 influence the stability of CDC-25.1 through residue S46 in *C. elegans* embryos. However, it remained to be determined whether this is due to a direct effect on CDC-25.1 or caused through a secondary effect on the stability of another molecule. Since LIN-23 is surmised to act as a direct binding partner of CDC-25.1 its function was further elucidated. The LIN-23 protein consists of 665 amino acids (Kipreos et al., 2000; Mehta et al., 2004). The F-box domain comprises amino acids 87 to 127, whereas the WD40 domain is found between amino acid 207 to 500 (Kipreos et al., 2000; Mehta et al., 2004). High mRNA levels were detected in embryos and the germline of gravid adults, indicating that the LIN-23 protein might be expressed at higher levels during these developmental stages (Kipreos et al., 2000).

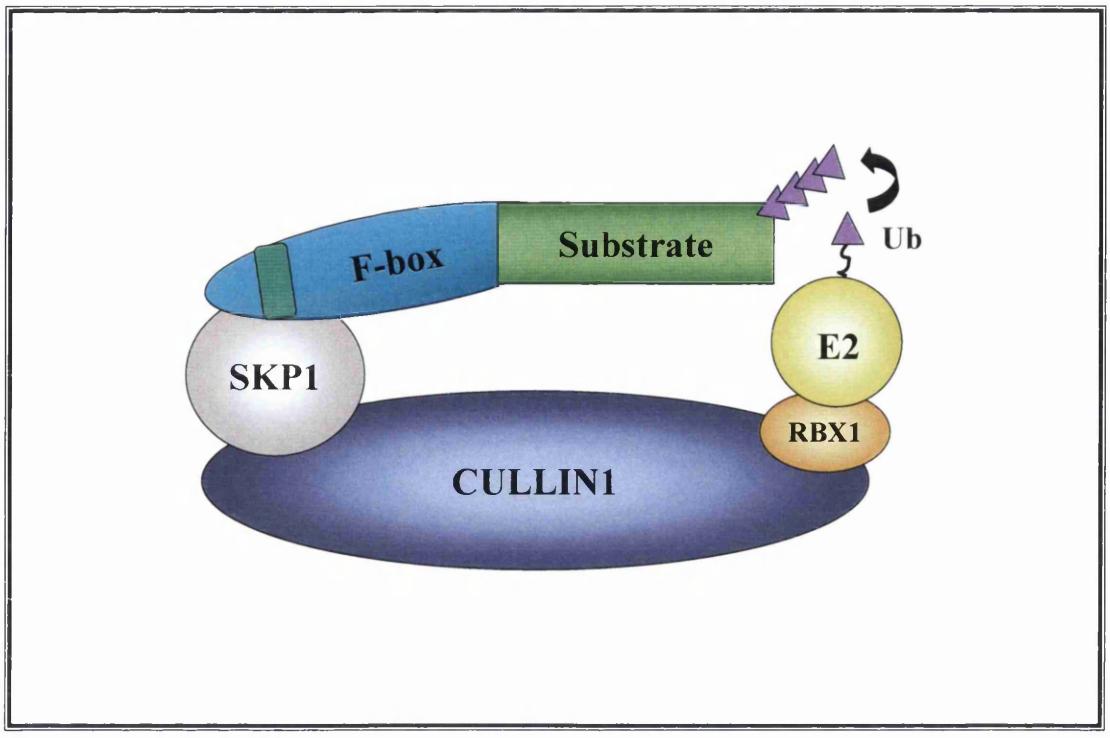

Figure 4.1 Schematic representation of the SCF complex. Adapted from (Kipreos, 2005, Pickart and Eddins, 2004). The N-terminus of CUL1 (CULLIN1) binds the adaptor SKP1 (SKR in *C. elegans*), while the C-terminus binds RBX1 in complex with the E2 ubiquitin-conjugating enzyme. The F-box-containing protein β-TrCP (LIN-23 in *C. elegans*) binds via its F-box domain to SKP1 and its WD40 domain to the target substrate. Ubiquitin (Ub) is directly transferred from E2 to the substrate.

4.1.2 Hypothesis and aims

Since LIN-23 function is required to restrain CDC-25.1 protein levels in the early *C. elegans* embryo, I surmised that LIN-23 might physically interact with CDC-25.1 in the *C. elegans* embryo. Furthermore, the interaction may be disrupted through the S46F mutation in CDC-25.1. To address these questions binding studies were to be employed to determine whether CDC-25.1 physically interacts with LIN-23 in *C. elegans* embryos and whether this binding is reduced in CDC-25.1(S46F) mutant embryos. To this end, a biochemical system that utilises embryonic extracts to analyse the binding between CDC-25.1 and LIN-23 was to be set up. The principle of this methodology is rather straightforward.

However, the *C. elegans* system is not as simple as other purification systems such as human tissue culture cells or *Xenopus* eggs where the harvesting of samples can be performed at distinct cell cycle stages when the interaction between SCF components and CDC25 is maximal (Jin et al., 2003; Kanemori et al., 2005). Additionally, in *C. elegans* obtaining sufficient material from embryos to undertake several experiments is not straightforward and requires growth of large-scale cultures that can take several weeks (discussed below). Due to the multicellular nature, the *C. elegans* embryos comprise several tissues that are found at different cell cycle and developmental stages and cell cycle synchronisation is not an option. A previously developed method is to feed adults a deoxynucleoside analogue fluorodeoxyuridine that can block the development of the embryos at the 200-cell stage (Mains, 1999). But as demonstrated in the previous chapter, the interaction between CDC-25.1 and LIN-23 occurs at a narrow time window during *C. elegans* embryogenesis (between the 10- to 60 -cell stage) and it is therefore difficult to enhance for embryos that are present at these early developmental stages. Additionally, the LIN-23 interaction with CDC-25.1 may be rather dynamic. Once CDC-25.1 is bound to LIN-23 the protein will be released and degraded by the proteasome after addition of sufficient ubiquitin moieties. The transient nature of the binding may therefore be difficult to detect. Finally, the methodology for obtaining embryos that can be utilised for binding studies is tricky. Many adults have to be harvested to generate enough embryos that allow purification of cellular components. Adult worms containing sufficient amounts of embryos have to be treated with a solution containing sodium hypochloride and sodium- or potassium-hydroxide (Mains, 1999; Sulston and Hodgkin, 1988). Bleaching of the adults has to be sufficient enough to release all embryos and remove the surrounding adult worms. However, extended incubation with bleach solution can ultimately penetrate the eggshell of the embryo and therefore destroy them.

Thus, *C. elegans* culture conditions were to be set up to enhance for adult worms and a relatively pure and healthy embryo population in order to perform purification assays. Experiments were set up to precipitate endogenous CDC-25.1 and determine the binding of LIN-23. To this end, the anti-CDC-25.1A antibody utilised for indirect immunofluorescence and Western blotting in previous work (Clucas, 2003; Clucas et al., 2002) and this study was to be used in order to identify conditions to pull down endogenous CDC-25.1 or CDC-25.1(S46F) from embryonic extracts. Furthermore, a new antibody against LIN-23 was required in order to detect LIN-23 and to analyse binding of CDC-25.1 to endogenous LIN-23. However, in other systems overexpression studies of tagged proteins were frequently used to detect binding between β-TrCP and CDC25, indicating that it may be difficult to detect physical interaction between the endogenous molecules, because either of them may be limiting in abundance (Busino et al., 2003; Jin et al., 2003; Kanemori et al., 2005; Ray et al., 2005). Hence, as a second approach the expression of a LAP-tagged version of CDC-25.1 was to be employed in order to enrich for the substrate molecule. CDC-25.1 was to be fused under the control of the *elt-2* promoter allowing expression of CDC-25.1 in the intestine. This promoter enriches for CDC-25.1 in the tissue that is of primary interest, since overexpression in all tissues may lead to an increase in embryonic lethality. The *elt-2* promoter allows expression of the CDC-25.1 protein starting from the 2E cell stage that persists until adulthood. Thus, the CDC-25.1 is present at a time when most of the endogenous CDC-25.1 is no longer expressed because endogenous CDC-25.1 is degraded after the 100-cell stage and is not expressed in the adult intestine (Ashcroft et al., 1999; Clucas, 2003; Clucas et al., 2002; Kostic and Roy, 2002). The CDC-25.1 protein was to be tagged using the previously established LAP tag method (localisation and affinity purification) (Cheeseman and Desai, 2005; Cheeseman et al., 2004). Here, a GFP tag is fused to a TEV cleavage site followed by an S-peptide tag, which allows a tandem purification of the fusion protein. As a first purification step an anti-GFP antibody bound to a Sepharose resin can be used, the protein cleaved off the beads using TEV protease and subsequently purified on S-Protein Agarose through the S-peptide tag. The advantage of this double system is the purity of the resultant eluate compared to single-step purifications. The experiments will allow to determine whether CDC-25.1 physically interacts with LIN-23 and whether this interaction is weakened or abolished in the *cdc-25.1(ij48)* mutant background.

4.2 Results

4.2.1 Characterisation of CDC-25.1A and B antibodies

Previous work had established that the anti-CDC-25.1A antibody raised against peptide 495 - 509 of CDC-25.1 utilised in the lab detects endogenous CDC-25.1 on Western blots and in indirect immunofluorescence (Clucas, 2003; Clucas et al., 2002). A second anti-peptide antibody raised against amino-acids 592 - 604 and thus the very C-terminus of CDC-25.1 (termed CDC-25.1B hereafter) had also been generated in our laboratory but the specificity not tested. In order to determine whether either or both antibodies could precipitate CDC-25.1 from *C. elegans* embryos, both antibodies were first affinity purified against the corresponding peptide and analysed for specificity by Western blotting. The experiments were performed side by side to ensure a correct purification procedure by utilising the CDC-25.1A antibody as a positive control.

Whole adult worms were lysed, sonicated, the cuticles removed by centrifugation and the soluble fraction applied to SDS-PAGE. Indeed, both the newly affinity purified anti-CDC-25.1A antibody as well as the previously established one recognise a specific band of around 83 kDa on Western blots that is depleted when adult worms were fed with RNAi against *cdc-25.1* (Figure 4.2, A, lanes 1 and 2, only one condition is depicted for simplicity). The similar size band was also detected with the CDC-25.1B antibody that was run side by side (although to a much lesser extent) that disappeared after *cdc-25.1* RNAi (Figure 4.2, A, lanes 4 and 5, note that due to the weak signal a different exposure had to be utilised for figure assembly). Thus, both antibodies can recognise CDC-25.1 by Western blotting of proteins extracted from adult hermaphrodites.

4.2.1.1 Setting up healthy embryo preparations

To determine whether this band could be detected in embryos, adult worms were grown in liquid cultures and the embryos harvested by the bleach method. To obtain enough healthy embryos new growth conditions were set up. Here, *C. elegans* worms were fed with the AB1157 strain that is not uracil auxotroph compared to the regular OP50 strain and can be grown to high densities in order to avoid starvation of worms in the culture which could result in dauer larvae formation. Growth conditions were optimised to obtain the maximum number of adults that carry enough embryos. Several bleach methods were also tested in order to define the optimal condition that could be utilised for further studies. The amount of embryonic viability obtained was therefore tested each time when embryos were

extracted and under optimal conditions found to be around 70 to 80%. The final conditions used are summarised in (Chapter 2, (2.2.7.1)).

4.2.1.2 CDC-25.1 is phosphorylated in embryos

As depicted in Figure 4.2 (panel A), both antibodies recognise the 83 kDa band in embryos. Interestingly, the size of this band does not correlate with the predicted molecular weight of 67.9 kDa (WormBase, 2007). When the samples were applied to 8% SDS-PAGE and electrophoresed for a longer time (70 min) to obtain a higher resolution, it was obvious that the original band detected in adult worms (and also in embryos, see Figure 4.2, E) was in fact derived from at least three distinct bands with slightly different molecular weights (Figure 4.2, A lanes 1 and 2 bottom). Thus, it became apparent that CDC-25.1 could be a target of post-translational modifications or alternative splicing. Previous work established the presence of only a single *cdc-25.1* mRNA transcript (Ashcroft et al., 1999) and in other model systems CDC25 proteins are the target of extensive phosphorylations (for a review see (Busino et al., 2004)).

Hence, the phosphorylation state of CDC-25.1 was determined in *C. elegans* adults and embryos. Treatment of embryonic extracts with lambda phosphatase results in downshift of all bands to one lower migrating form at around 70 to 75 kDa (Figure 4.2, B, compare lanes 1 and 5). The same result was obtained when adult extracts were analysed (data not shown). This result was obtained in a wild-type and in the *cdc-25.1(ij48)* mutant background (compare lanes 2 and 6), indicating that there is no difference in phosphorylation detectable between CDC-25.1 and CDC-25.1(S46F). Note that due to differences in signal intensity the top CDC-25.1 band is not visible at this exposure. A partial downshift of the three bands was also apparent when the extracts were incubated with buffer alone, probably reflecting the endogenous phosphatase activity in the extracts (Figure 4.2, B, compare lanes 1 and 2 with 3 and 4). Thus, CDC-25.1 and CDC-25.1(S46F) protein levels are highly phosphorylated in embryos (and adults). At this resolution there was no consistent difference detectable between CDC-25.1 and CDC-25.1(S46F) when different extracts were analysed. Note however that in accordance with the results in the previous chapter, an increase in the CDC-25.1(S46F) protein levels compared to CDC-25.1 is clearly detectable (Figure 4.2, B). Interestingly, removal of *lin-23* by RNAi results in an increase of all three detectable phosphorylation forms (Figure 4.2, E, compare lanes1 and 2).

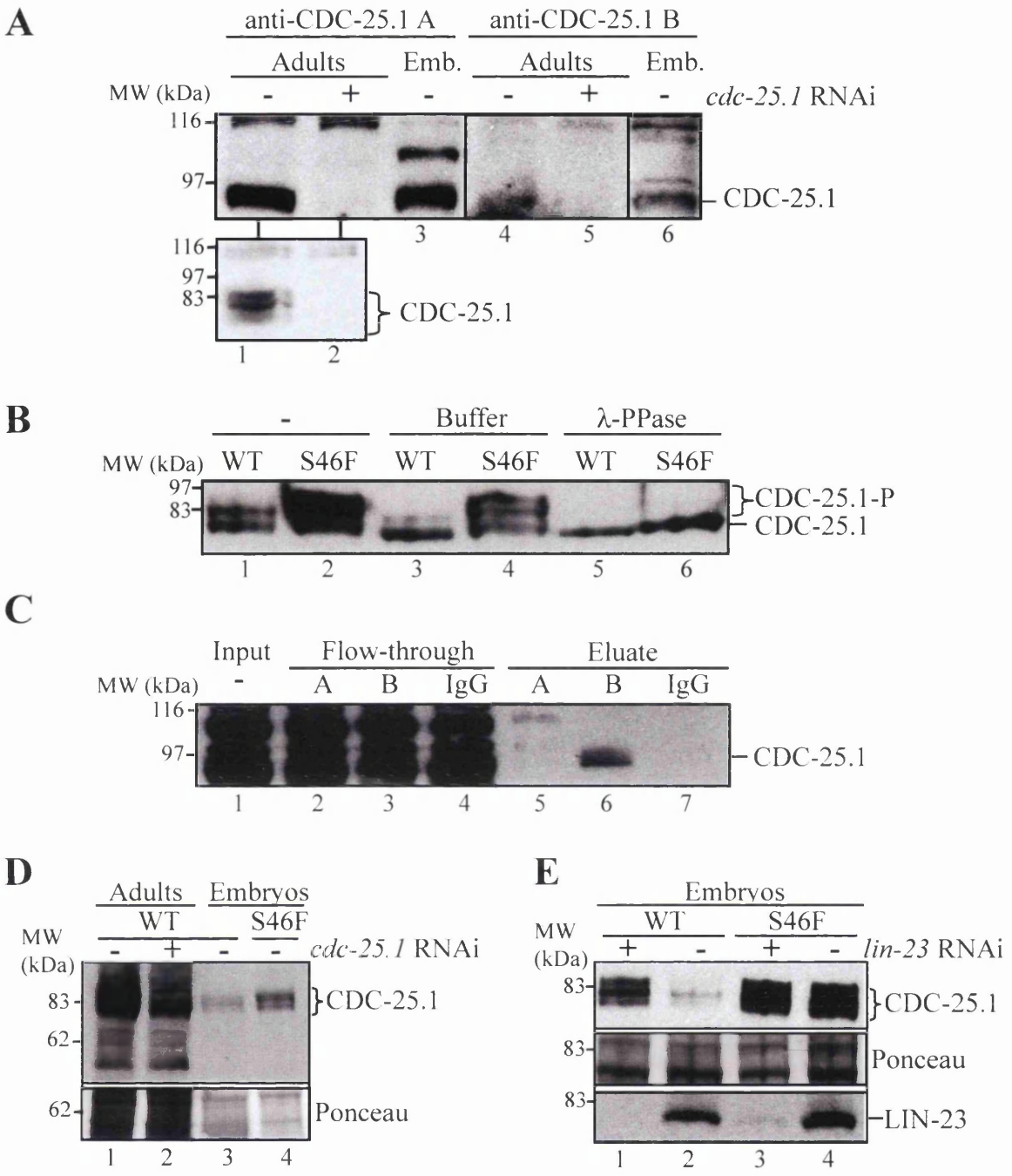

Figure 4.2 Characterisation of CDC-25.1 and LIN-23 antibodies. A) Extracts of wild-type adults (lanes 1, 2, 4 and 5) or embryos (lanes 3 and 6) with (+) or without (-) *cdc-25.1* RNAi (lanes 1, 2, 4 and 5) were applied to 10% SDS-PAGE and Western blotted with anti-CDC-25.1A or anti-CDC-25.1B antibodies, 20 µg of total protein were applied per lane, bottom: same as top lanes 1-2 but samples were applied to 8% SDS-PAGE. **B)** CDC-25.1 is regulated through phosphorylation in embryos. Embryonic extracts from wild-type JR1838 (WT) or IA530 *cdc-25.1(ij48)* (S46F) strains were either suspended in SDS sample buffer (lanes 1, 2), incubated at 30°C in phosphate buffer (lanes 3, 4) or in phosphate buffer containing 800 U of λ-phosphatase (lanes 5, 6) and 15 µg total protein applied to 8% SDS-PAGE followed by Western blotting against CDC-25.1 (anti-CDC-25.1A). **C)** Immunoprecipitation of CDC-25.1 from embryonic extracts using anti-CDC-25.1A, or B antibodies or rabbit IgG. Input and flow-through represent 3%, the eluate 30% of the total fraction. The Western blot was probed against CDC-25.1 using anti-CDC-25.1A. **D)** Similar to (A), but the anti- CDC-25.1f.l. antibody was used, 100 adults were lysed in sample buffer and applied per lane, 2.5 µg of embryos were lysed in an equal volume of sample buffer and applied per lane, Ponceau staining to show equal loading of proteins (bottom). **E)** Embryonic extract of JR1838 strain (WT) or IA530 (S46F) with (+) or without (-) *lin-23* RNAi were applied to 8% or 10% SDS-PAGE (same amount as D) and probed against CDC-25.1 (anti-CDC-25.1A) or LIN-23, Ponceau staining to show equal protein loading, (same samples as Chapter 3). Two (A, B, D, E *lin-23* RNAi) and three (E, (-) *lin-23* RNAi) independent experiments each.

4.2.1.3 Characterisation of anti-CDC-25.1 antibodies for immunoprecipitation

Western blotting confirmed that both anti-peptide antibodies A and B raised against CDC-25.1 could recognise CDC-25.1 and CDC-25.1(S46F). However, the signal intensity derived of the A antibody was slightly higher on Western blots (also when almost identical antibody concentrations were tested). However, this result could suggest that the B antibody shows a lower affinity to the target peptide under denaturing conditions, but it might be able to recognise the native CDC-25.1. Conditions were set up to purify endogenous CDC-25.1 from embryonic extracts.

To this end, lysis conditions were to be established, to allow purification of the CDC-25.1 protein from embryos. As a starting point a lysis buffer was utilised that closely resembles the conditions previously published for CDC-25.1 (Ashcroft et al., 1999) or β-TrCP purifications (Busino et al., 2003; Donzelli et al., 2002). However, ionic detergents were omitted and a low concentration of non-ionic detergent was utilised in order to start with mild buffer conditions. Firstly, embryos were lysed in 50 mM Tris, 100 mM NaCl, 1 mM EDTA, 10% glycerol, 0.2% NP40, 1 mM DTT and 1 x protease inhibitor cocktail. 50 μg of affinity purified anti-CDC-25.1 antibody A or B were crosslinked to Protein A-Sepharose and incubated with the embryo extract (Table 4.1, 1). As seen in Figure 4.2 (panel C), only antibody B precipitated CDC-25.1 as compared to rabbit IgG that was used as negative control (compare lane 6 and 7) under this experimental condition. However, the amount precipitated was minor compared to the amount present in the flow-through (bottom band lanes 2-4). Thus, the flow-through (FT) was utilised to determine whether the antibody was limiting. Increasing the antibody concentration and lowering the amount of total protein did not precipitate more CDC-25.1 (Table 4.1, FT1, a), indicating that the antibody was not limiting. Additionally, different salt and non-ionic detergent conditions were utilised to precipitate the FT with antibody B only (Table 4.1, FT1, b-d). None of these conditions purified more CDC-25.1 protein, though the initial control conditions remained positive. Thus, the remaining CDC-25.1 protein was not extractable with different salt conditions. New extracts were generated and extracted with a buffer with constant salt concentration and slightly higher centrifugal force applied to further clarify the supernatant (Table 4.1, 2-5).

Experiment	Salt (mM)	Detergent (%)	Centrifugal force (*g*)	Antibody (µg)	Total protein
1	100 NaCl	0.2 NP40	30000	50 (A/B)	3200
FT 1a	100 NaCl	0.2 NP40	30000	100 (A/B)	600
FT 1b	100 KCl	0.05 NP40	30000	50 (B)	600
FT 1c	300 KCl	0.05 NP40	30000	50 (B)	600
FT 1d	300 KCl	0.2 NP40	30000	50 (B)	600
2	300 KCl	0.1 NP40	30000 135000	75 (B)	600
3	300 KCl	0.1 NP40	30000 135000	75 not crosslinked (B)	700
4	300 KCl	1 NP40 0.5 DOC 0.1 SDS	30000 135000	75 (B)	500
5	300 KCl	1 NP40 0.5 DOC	30000 135000	75 (B)	500

Table 4.1 Various experimental conditions to precipitate endogenous CDC-25.1 from embryonic extracts using anti-CDC-25.1A or B antibody.

The precipitation efficiency of CDC-25.1 was compared with and without crosslinking of the B antibody (2 and 3) and DTT omitted to ensure that the crosslinking or the DTT did not inactivate the antibody, but no difference to the initial binding was obtained. Furthermore, more stringent lysis conditions using higher NP40 concentrations, SDS or sodium deoxycholate did not increase the binding.

Thus, it was concluded that the antibodies A and B available in the laboratory were not suitable for precipitation studies to analyse for potential binding partners such as LIN-23. Only a minor fraction of the total CDC-25.1 protein could be precipitated. Though given the anticipation that not all the protein might interact with LIN-23, this amount was clearly not enough.

4.2.2 Generation of a new anti-CDC-25.1 antibody

Since the CDC-25.1A and B antibodies were not able to precipitate sufficient amounts of CDC-25.1 a new antibody against CDC-25.1 was generated. I decided to generate an antibody that can recognise multiple epitopes of the full-length protein and might provide a better tool for immunoprecipitation studies. To this end, conditions were set up to express and purify HIS_6-tagged CDC-25.1. The *cdc-25.1* cDNA was cloned into the pQE-30 expression vector allowing the N-terminal fusion of six histidines to CDC-25.1. After initial difficulties in obtaining any expressed protein, conditions were finally established that produced reasonable amounts of CDC-25.1 protein (600 µg/400 ml culture was obtained after purification from the insoluble fraction and protein dialysis). This protein

was utilised to immunise one rabbit (performed by SNBTS) and the obtained serum affinity purified against recombinant CDC-25.1. The affinity purified antibody was tested against wild-type adult extracts and recognises multiple specific bands of around 83 kDa on Western blot that are reduced after *cdc-25.1* RNAi (Figure 4.2, D, lanes 1 and 2). The same bands are detected in *C. elegans* embryonic extracts and are increased in embryos derived from the *cdc-25.1(ij48)* strain, similar to the result obtained with the anti-CDC-25.1A antibody (Figure 4.2, D, lanes 3 and 4). The exact conditions for protein expression and affinity purification of the serum are depicted in (Chapter 2, (2.2.2.5), (2.2.2.6) and (2.2.2.12)). Consequently, the new antibody generated against CDC-25.1 (hereafter named CDC-25.1f.l.) specifically recognises both CDC-25.1 and CDC-25.1(S46F) on Western blots.

4.2.3 Generation of anti-LIN-23 antibodies

Novel antibodies against LIN-23 were also generated in this study, because no antibody against LIN-23 was available. Firstly, Dr. I. L. Johnstone produced one antibody with the aid of the company Covalab. This peptide antibody was raised against two peptides in the N-terminus of the LIN-23 protein according to the company's recommendation (aa 18 - 31 and aa 194 - 206). Antisera and affinity purified antibodies from two rabbits were provided by Covalab and tested in this study against *C. elegans* strains that were treated with or without *lin-23* RNAi, but it was impossible to obtain any specific band.

Thus, I decided to raise new antibodies that could recognise multiple epitopes on the LIN-23 protein. The complete *lin-23* cDNA was cloned into the pGEX-6P-1 vector that allows *E. coli* expression of the full-length LIN-23 protein with an N-terminal GST tag. Expression of LIN-23 in *E. coli* was rather difficult, because the protein was expressed at low levels and insoluble. Removal of the N-terminus containing the F-box motif did not improve the solubility. Additionally, expression under several different growth conditions and in different *E. coli* strains did not improve the solubility of the protein. Finally one rabbit and one rat were immunised with GST::LIN-23 excised from an SDS-polyacrylamide gel. The rabbit serum obtained was affinity purified against the recombinant HIS_6-tagged C-terminus of LIN-23, because the full length HIS_6::LIN-23 was only poorly expressed and the serum did not recognise the N-terminal portion of the LIN-23 protein when expressed in *E. coli*. The final conditions used for protein expression and affinity purification are summarised in (Chapter 2, (2.2.2.5), (2.2.2.6), (2.2.2.12)).

The affinity purified anti-LIN-23 antibody was tested for specificity towards LIN-23 by Western blotting against embryonic extracts derived from hermaphrodites that were subjected to *lin-23* or control RNAi. The antibody recognises a specific band around 80 kDa in the control RNAi-derived samples that was absent after *lin-23* RNAi (Figure 4.2, E, compare lanes 1 and 2 or 3 and 4). This is consistent with the expected molecular weight of 75.9 kDa (WormBase, 2007). Additionally, the LIN-23 protein levels were analysed by Western blotting of *lin-23* null hermaphrodites compared to *lin-23* heterozygotes or a *lin-23* wild-type strain. This revealed the presence of the 80 kDa band in the wild-type strain that was reduced in a *lin-23* heterozygote strain and completely absent in a *lin-23* null background (see Chapter 5, Figure 5.1). The antibody was also tested in immunoprecipitation studies and was able to precipitate endogenous LIN-23 from *C. elegans* embryonic extracts. But the affinity of the antibody to the protein was extremely weak and resulted in the loss of the protein after the first wash of the immunoprecipitate. Washing of the eluates only once in binding buffer resulted in too much background binding and thus no further attempts were made to utilise this antibody for immunoprecipitation studies. Nevertheless, the novel anti-LIN-23 antibody generated in this work has proven extremely valuable to recognise endogenous LIN-23 on Western blots and in immunocytochemistry (illustrated in Chapter 5, Figure 5.1 and Chapter 6, Figure 6.1).

4.2.4 Generation of tagged CDC-25.1 in intestinal cells

For use in a second purification approach, tagged versions of CDC-25.1 and CDC-25.1(S46F) were generated. The CDC-25.1 or CDC-25.1(S46F) genomic sequences were fused under the control of the *elt-2* promoter and tagged at their N-terminus with the LAP tag (GFP followed by a TEV cleavage site and the S-peptide). Several strains carrying the LAP-tagged CDC-25.1 or CDC-25.1(S46F) on an extrachromosomal array were generated by microinjection of the plasmid pBS-*elt-2::LAP::cdc-25.1(+)* or pBS-*elt-2::LAP::cdc-25.1(ij48)* into the gonad of the DR96 strain. This strain is mutated for the *unc-76* gene and a wild-type *unc-76* gene co-injected with the LAP-tagged *cdc-25* plasmids served as a rescue marker (for details on microinjection and transgenesis procedures see Chapter 2, (2.2.4)). Analysis of the intestinal numbers by DAPI staining of adult worms revealed an increase in the number of intestinal nuclei as compared to the N2 Bristol wild-type strain (Table 4.2). An example of an adult worm carrying *elt-2::LAP::cdc-25.1(+)* or *elt-2::LAP::cdc-25.1(ij48)* is depicted in Figure 4.3, (panel A). The increase in intestinal

nuclei suggested that the constructs could potentially cause intestinal hyperplasia and were therefore functional.

Strain* (for precise genotype see Chapter 2, Table 2.8)	**Intestinal nuclei (DAPI, adults)**	**Strain***	**Intestinal nuclei (GFP, embryos)**
N2 Bristol	31.7 ± 3.6 (n=11)	-	-
IA123 *cdc-25.1(ij48)I*	60.5 ± 11.6 (n=18)	-	-
IA521 *ijEx30 [elt-2::LAP::cdc-25.1(+)]*	49.1 ± 5.6 (n=13)	-	-
IA522 *ijEx31 [elt-2::LAP::cdc-25.1(+)]*	45.6 ± 9.1 (n=16)	IA535 *ijIs16 [elt-2::LAP::cdc-25.1(+)]*	24.4 ± 4.0 (n=21)
IA523 *ijEx32 [elt-2::LAP::cdc-25.1(ij48)]*	40.0 ± 9.0 (n=23)	-	-
IA524 *ijEx33 [elt-2::LAP::cdc-25.1(ij48)]*	39.0 ± 5.9 (n=24)	IA536 *ijIs17 [elt-2::LAP::cdc25.1 (ij48)]*	25.8 ± 3.7 (n=23)
IA560 *ijEx35 [elt-2::cdc-25.1(+)]*	46.4 ± 4.9 (n=21)	-	-
IA559 *ijEx34 [elt-2::cdc-25.1(+)]*	49.3 ± 5.4 (n=22)	IA559 F1 embryos containing *wIs84 [elt-2::GFP::LacZ]*	24.3 ± 4.1 (n=9)

Table 4.2 Intestinal cell number (mean ± s.d.) of *C. elegans* strains zygotically expressing *cdc-25.1*.

Hence, it was decided to integrate the plasmids stably into the genome by gamma irradiation. For this procedure one strain was chosen for each construct. The strains generated were outcrossed four times against wild-type N2 to remove unwanted mutations introduced through the gamma irradiation. This produced the strains IA535 *ijIs16[elt-2::LAP::cdc-25.1(+)]* and IA536 *ijIs17[elt-2::LAP::cdc-25.1(ij48)]* (for full genotype see Chapter 2, Table 2.8). In Figure 4.3 (panel B), the JR1838 strain expressing *elt-2::GFP::LacZ* in intestinal nuclei is depicted. By comparison LAP::CDC-25.1 and LAP::CDC-25.1(S46F) also localise to intestinal cells. Interestingly, the localisation of LAP::CDC-25.1(S46F) was found to be mainly in the nuclear compartment, whereas LAP::CDC-25.1 was present in both the nucleus and the cytoplasm, indicating that both molecules may be differentially regulated. This localisation did not differ from the original non-integrated strains and thus was not caused through the integration of the plasmids.

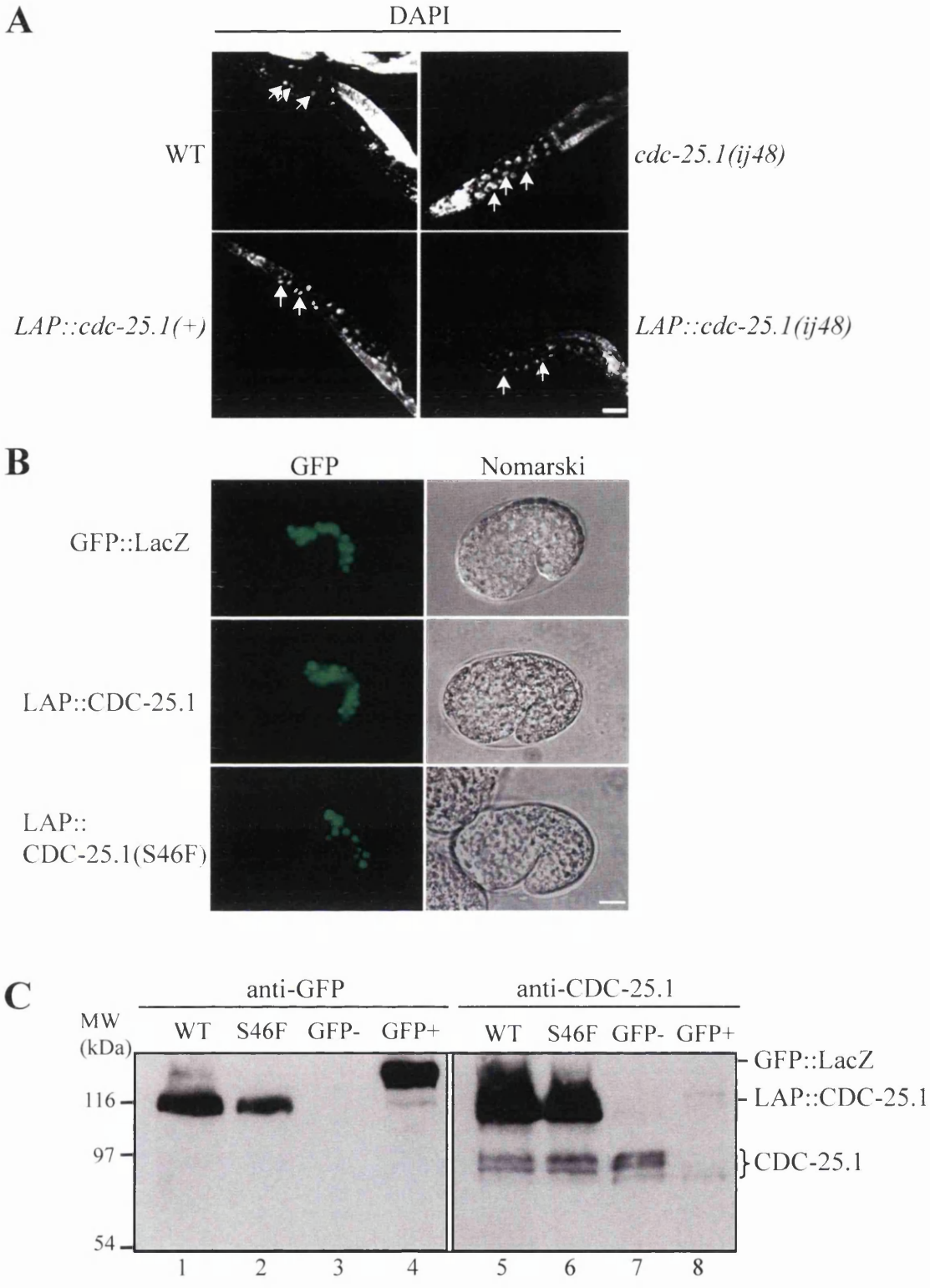

Figure 4.3 Expression of *elt-2::LAP::cdc-25.1* in *C. elegans* adults and embryos. A) DAPI staining of wild-type strain N2 (WT), *cdc-25.1(ij48)* or IA522 carrying *elt-2::LAP::cdc-25.1(+)* or *elt-2::LAP::cdc-25.1(ij48)* (IA523) on extrachromosomal arrays. Some intestinal nuclei are indicated by arrows. Scale bar: 50 µm. **B)** GFP fluorescence and corresponding Nomarski counterparts of the strain JR1838 carrying intestinal-specific *elt-2::GFP* (GFP::LacZ) or IA535 *elt-2::LAP::cdc-25.1(+)* (LAP::CDC-25.1), IA536 *elt-2::LAP::cdc-25.1(ij48)* (LAP::CDC-25.1(S46F)) after chromosomal integration. Only one focal plane is shown. Scale bar: 10 µm. **C)** Embryonic extracts (15 µg total protein/lane) of CDC-25.1 strains from (B), N2 Bristol (GFP-) and JR1838 (GFP+) were applied to 8% SDS-PAGE followed by Western blotting against GFP or CDC-25.1 (anti-CDC-25.1 A). Two independent experiments for (C).

Western blotting of embryonic extracts, derived from IA535 *elt-2::LAP::cdc-25.1(+)* and IA536 *elt-2::LAP::cdc-25.1(ij48)* integrated strains, revealed the expression of the correct size bands of around 100 kDa (due to the insertion of additional 304 amino acids) with a GFP antibody. These bands were also recognised with the anti-CDC-25.1A antibody but absent in wild-type extracts or extracts carrying *elt-2::GFP::LacZ*, indicating that the proteins were full-length (Figure 4.3, C). Interestingly, the proteins were highly overexpressed compared to endogenous CDC-25.1 (Figure 4.3, C, lanes 5 and 6). Analysis of the intestinal nuclei through GFP expression revealed an increase in the number of nuclei (Table 4.2). Thus, the increase in intestinal nuclei observed in the non-integrated adults by DAPI staining is the result of extra-nuclei that are born in the embryo. It is concluded that the LAP::CDC-25.1 or LAP::CDC-25.1(S46F) constructs when expressed in *C. elegans* can cause extra intestinal nuclei to be born during embryonic development.

4.2.4.1 Zygotic expression of untagged *cdc-25.1* causes extra intestinal nuclei

Since the tagged versions of CDC-25.1 augmented the numbers of intestinal nuclei in the embryo, the possibility remained that the tag, and not the overexpression of CDC-25.1 could interfere with the normal regulation of the protein. Hence, a new plasmid was made (pBS-*elt-2::cdc-25.1(+)*) that allows expression of the untagged CDC-25.1 in intestinal cells. Transgenic strains were generated with this construct by microinjection together with the *unc-76* gene into DR96 *unc-76(e911)V* and selection for *unc-76* rescue. Two non-Unc strains (IA559 and IA560) carrying *elt-2::cdc-25.1(+)* on an extrachromosomal array were analysed for the numbers of intestinal cells by DAPI staining and display elevated numbers of intestinal nuclei (Table 4.2). To analyse the number of intestinal cells in the embryo, *elt-2::GFP* was crossed into the IA559 strain. For this purpose, males of the IA559 strain were generated by heat shock and crossed into JR1838 hermaphrodites that carry the *elt-2::GFP* transgene. Several hermaphrodites carrying the *elt-2::GFP* transgene showed extra intestinal nuclei in their F1 embryos as examined by fluorescence microscopy, indicating that they also carried the *elt-2::cdc-25.1(+)* (a wild-type JR1838 strain never displays extra intestinal nuclei) (Table 4.2, 24.3 nuclei, and Figure 4.4, A). Indirect immunocytochemistry of embryos using the CDC-25.1A antibody confirmed that CDC-25.1 was strongly expressed in intestinal nuclei during a stage when the surrounding cells contain almost no more CDC-25.1 protein (Figure 4.4, A). In summary, zygotic expression of wild-type CDC-25.1 results in a hyperplasia of the intestine as examined by the increased number of intestinal nuclei in the embryo.

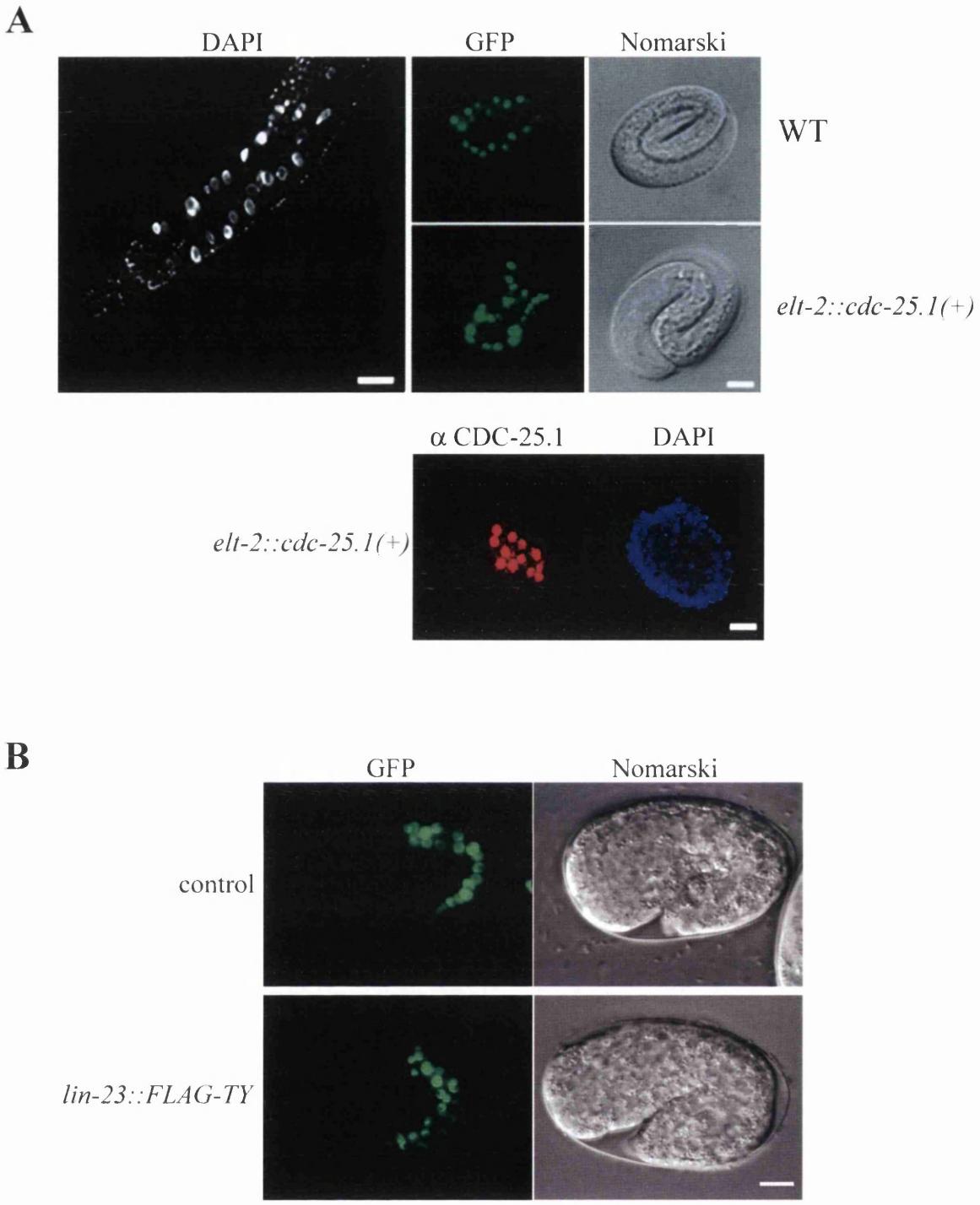

Figure 4.4 Expression of untagged *cdc-25.1* or a *lin-23::FLAG-TY* allele cause hyperplasia of the intestine. A) IA559 carrying *elt-2::cdc-25.1(+)* on an non-integrated extrachromosomal array is analysed by DAPI staining of adult hermaphrodites (left). To the right: expression of *elt-2::GFP::LacZ* in embryos carrying *elt-2::cdc-25.1(+)* on an extrachromosomal array (non integrated) compared to a strain JR1838 (WT) that carries only *elt-2::GFP::LacZ*. Scale bar: 50 μm for adult, 10 μm for embryos. Bottom: immunostaining against CDC-25.1 in an embryo expressing *elt-2*::CDC-25.1 (anti-CDC-25.1A) with corresponding DAPI image. Scale bar: 10 μm. **B)** IA592 strain containing *lin-23::FLAG-TY* in a *lin-23* null background (for genotype see Chapter 2, Table 2.8) show hyperplasia of the intestine as examined by *GFP::LacZ* expression in intestinal nuclei. Scale bar: 10 μm.

4.2.4.2 LAP-tagged CDC-25.1 interacts with LIN-23 in the embryo

Purification of the LAP-tagged CDC-25.1 proteins was attempted by several means. Firstly, several commercial antibodies against the GFP tag were utilised to pull down LAP::CDC-25.1 and LAP::CDC-25.1(S46F) from embryonic extracts compared to extracts that are derived from the JR1838 and thus express the GFP::LacZ fusion in intestinal nuclei. Multiple commercially available antibodies were incapable to purify any of the GFP-tagged proteins. Only one antibody was able to purify 90% of the GFP::LacZ fusion protein (that was expressed in intestinal nuclei like CDC-25.1) but the LAP-tagged CDC-25.1 proteins could not be precipitated under these conditions tested.

Therefore, I decided to purify the CDC-25.1 proteins via the S-peptide tag using S-Protein Agarose. Several conditions were tested and it was possible to specifically bind LAP::CDC-25.1 but not the control protein GFP::LacZ to the S-Protein Agarose (Figure 4.5, A, compare lanes 7 with 9). Interestingly, probing the samples with an anti-LIN-23 antibody revealed specific binding of LIN-23 to LAP::CDC-25.1 but not to the control resin, indicating that zygotically overexpressed CDC-25.1 physically interacts with LIN-23 in embryos.

Results obtained in the previous chapter suggested that the binding of LIN-23 to CDC-25.1(S46F) might be abolished. To address this point, a direct comparison of the LIN-23 bound to purified LAP::CDC-25.1 and LAP::CDC-25.1(S46F) was necessary. Unfortunately, binding of the LAP::CDC-25.1(S46F) to S-Protein Agarose was not obtained under conditions when LAP::CDC-25.1 specifically bound to the resin. LAP::CDC-25.1(S46F) remained in the flow-through as compared to 90% depletion from the flow-through of LAP::CDC-25.1 (Figure 4.5, A, compare lanes 4 with 5 and 7 with 8). This was also the case when new extracts were prepared. A direct comparison between these two molecules was therefore not possible. It should be noted that both molecules show slightly differential distribution in intestinal cells (discussed in Chapter 6, (6.3.1.1)) implying that the epitope may be masked in case of LAP::CDC-25.1(S46F) due to differential complex formation or protein folding. Nevertheless, it became apparent that a physical interaction between overexpressed CDC-25.1 and endogenous LIN-23 is evident in *C. elegans* embryos.

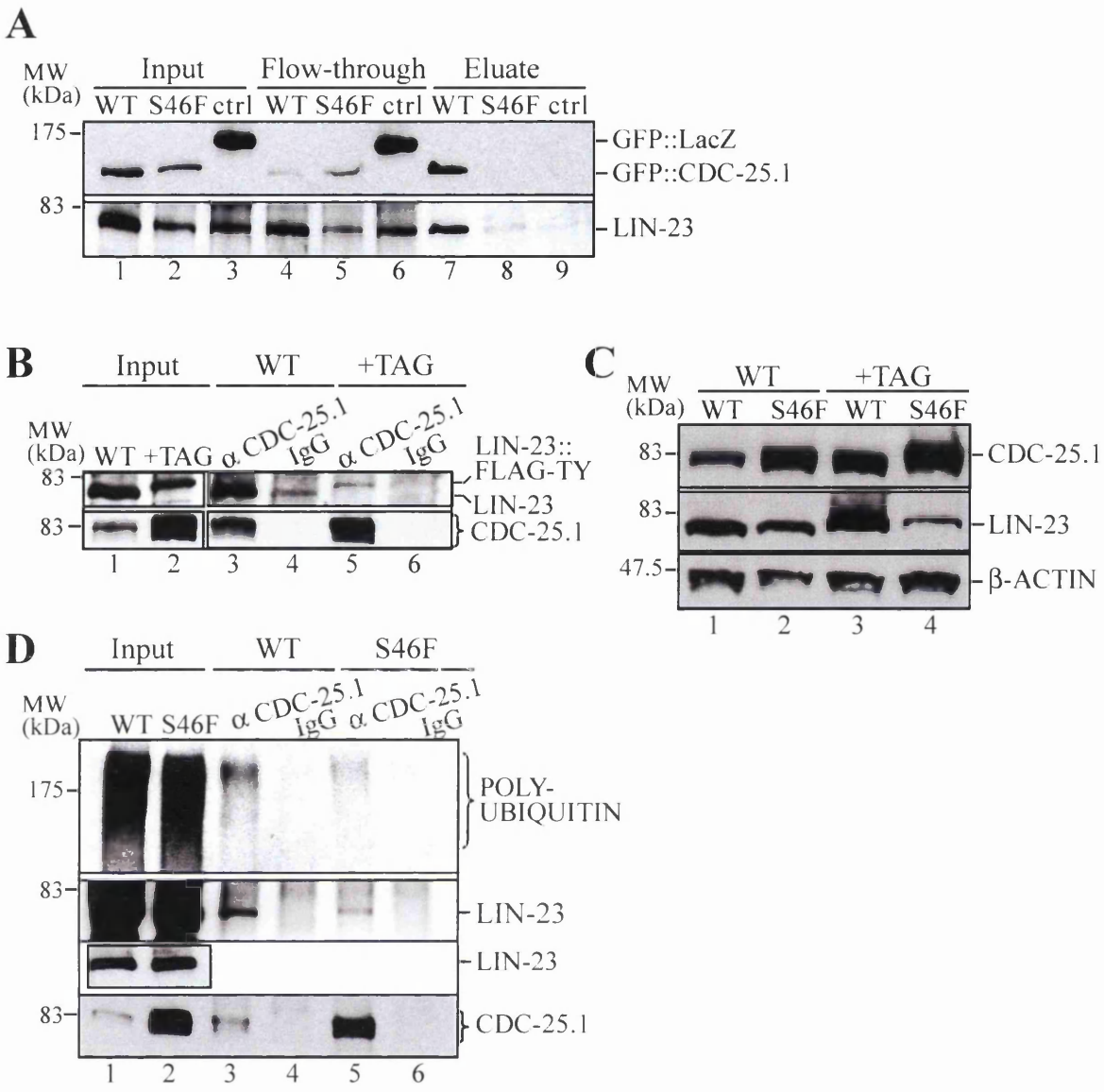

Figure 4.5 CDC-25.1(S46F) is crucial for LIN-23 interaction in *C. elegans* embryos. A) Immunoprecipitation of *elt-2*-expressed LAP::CDC-25.1 (WT), LAP::CDC-25.1(S46F) or GFP::LacZ (ctrl) from embryonic extracts using S-Protein Agarose. Input and flow-through represent 1.25% and the eluate 30% (50% in case of S46F) of the total fraction. Samples were applied to 10% SDS-PAGE followed by Western blotting against GFP (top panel) or LIN-23 (bottom panel). **B)** Immunoprecipitation of CDC-25.1 from embryonic extracts using anti-CDC-25.1f.l. antibodies from JR1838 (WT) and IA592 expressing LIN-23::FLAG-TY in a *lin-23* null background (+TAG). Samples were similar to A) except only input (lanes 1 and 2) and eluates (lanes 3-6) are displayed, Western blots were probed against LIN-23 (top panel) or CDC-25.1 (using the anti-CDC-25.1A antibody). Note the 2.4 kDa shift of LIN-23::FLAG-TY compared to wild-type (compare lanes 1 and 2, or lanes 3 and 5). Rabbit IgG was used as negative control (lanes 4 and 6). **C)** Embryonic extracts from JR1838 (WT, lane 1), IA530 *cdc-25.1(ij48)* (S46F, lane 2), IA592 *lin-23* null expressing LIN-23::FLAG-TY (WT, lane 3) or IA593 *cdc-25.1(ij48)* (S46F, lane 4) a *lin-23* null strain co-expressing CDC-25.1(S46F) and LIN-23::FLAG-TY were applied to 10% SDS-PAGE and Western blot performed as indicated. 10 µg of total protein was applied per lane, the samples were separated multiple times (5 and 10 µg total protein) by SDS-PAGE. **D)** Immunoprecipitation of CDC-25.1 from JR1838 (WT) or IA530 *cdc-25.1(ij48)* (S46F) using the anti-CDC-25.1f.l. antibody (lanes 3 and 5) or rabbit IgG as control (lanes 4 and 6). Samples were applied to SDS-PAGE similar to B), but 0.5% of the total fraction was loaded for input (lanes 1 and 2) and 30 and 25% of the eluate (lanes 3-6) for anti-LIN-23 (middle), anti-CDC-25.1 (bottom, anti-CDC-25.1A antibodies) and ubiquitin (top) blots, respectively. Small inset: weak exposure of input lanes of anti-LIN-23 blot to show equal protein loading. Two independent experiments each.

4.2.5 CDC-25.1 physically interacts with LIN-23 in embryos

The binding observed between LAP-tagged CDC-25.1 and LIN-23 encouraged me to undertake further attempts to immunoprecipitate endogenous CDC-25.1 using the new anti-CDC-25.1f.l. antibody generated in this study. Several experimental conditions were tested in a manner similar to the experiments performed with anti-CDC-25.1A and B antibodies. The eluates were probed by Western blotting with anti-CDC-25.1A antibody to ensure specificity of the signal to CDC-25.1. Importantly, conditions were identified that could precipitate sufficient amounts (around 50%) of endogenous CDC-25.1 from embryonic extracts. Intriguingly, specific binding of endogenous LIN-23 was detected in eluates derived from precipitation of CDC-25.1 as compared to control eluates using rabbit IgG (Figure 4.5, B, compare lanes 3 and 4).

As a second control, CDC-25.1 was precipitated from worms that express a tagged version of LIN-23 (LIN-23::FLAG-TY) in a *lin-23* null background. This strain was generated in this study by microparticle bombardment of the pBS-*unc-119-lin-23::FLAG::TY* plasmid into the DP38 strain. This method was utilised because it results in low-copy integration of the plasmid into the genome and permits expression of the transgene in the germline (Praitis et al., 2001). The FLAG and TY tag were chosen because they are relatively small and therefore reduce the chance of interference of the tag with the protein function. The tag was inserted in the C-terminus because previous work had identified that a C-terminal GFP-tagged version of LIN-23 was able to rescue a *lin-23* mutant allele (Mehta et al., 2004). However, the GFP-tagged LIN-23 utilised in their study was only expressed after gastrulation due to silencing of high-copy extrachromosomal arrays in the germline (Kelly et al., 1997), and thus could not be utilised here. The resulting DP38 *lin-23::FLAG-TY* strain was crossed into a *lin-23* null background to generate the strain IA592 that stably expresses LIN-23::FLAG::TY in a *lin-23* null background (for strain generation see Chapter 5, (5.2.3), for genotype Chapter 2, Table 2.8).

Importantly, when CDC-25.1 was precipitated in this strain background the LIN-23 band is shifted to a slightly higher molecular weight due to the presence of the tag and this band is not present in the IgG control (Figure 4.5, B, compare lanes 3 and 5 for the shift and 5 and 6 for the specific binding). Thus, endogenous CDC-25.1 physically interacts with endogenous LIN-23 in *C. elegans* embryos.

4.2.5.1 The *lin-23::FLAG-TY* allele causes elevated CDC-25.1 levels and hyperplasia

Interestingly, when CDC-25.1 was precipitated from embryos expressing only the LIN-23::FLAG-TY protein, a strong decrease in LIN-23 binding was observed (Figure 4.5, B, compare lanes 3 with 5) though similar amounts of LIN-23::FLAG-TY compared to endogenous LIN-23 is present in these embryos (Figure 4.5, B, compare lanes 1 and 2, or C, compare lanes 1 and 3). Thus, LIN-23::FLAG-TY displays a reduced binding to CDC-25.1. Intriguingly, CDC-25.1 protein levels are strongly elevated in the LIN-23::FLAG-TY background compared to wild-type levels (Figure 4.5, B, lanes 1 and 2, or C, lanes 1 and 3). When this strain was analysed for the numbers of intestinal nuclei, through expression of the intestinal-specific *elt-2::GFP* marker, an increased number of intestinal nuclei was observed (Table 4.3 and Figure 4.4, B).

IA592 *lin-23(e1883)II; ijIs18 [lin-23::FLAG-TY]; elt-2::GFP::LacZ*	**IA593 *cdc-25.1(ij48)I; lin-23(e1883)II; ijIs18 [lin-23::FLAG-TY]; elt-2::GFP::LacZ***	**p-value**	**Fold increase**
34.6 ± 8.6 (n=62)	38.5 ± 8.3 (n=69)	< 0.01	1.1

Table 4.3 Hyperplasia of the intestine caused by the *lin-23::FLAG-TY* allele. Mean ± s.d., p-value: two-tailed Student's *t*-test, n= number of embryos.

These results suggested that the reduced binding of LIN-23::FLAG-TY to CDC-25.1 causes elevated CDC-25.1 protein levels and hence hyperplasia in the embryo. To determine, whether this phenotype is synergistic with CDC-25.1(S46F) or mediated by separate means, the *cdc-25.1(ij48)* allele was inserted into the *lin-23::FLAG-TY* background.

This was achieved by crossing heterozygous IA589 *lin-23(e1883)II; unc-119(ed3) ijIs18 [lin-23::FLAG-TY, unc-119(+)]* males with IA530 hermaphrodites and selection for GFP-positive F2 worms that carry the homozygous *lin-23(e1883)* null allele, the homozygous *lin-23::FLAG-TY* allele and were homozygous for the *cdc-25.1(ij48)* allele. The presence of these alleles was examined by single worm PCR and restriction enzyme digestion to check for restriction site polymorphism that is introduced through the mutations in *cdc-25.1(ij48)* or *lin-23(e1883)*. (Details on the restriction site polymorphism are in Chapter 2, (2.2.6.4) and (2.2.6.5) and the IA589 generation in Chapter 5, (5.2.3)).

The resulting strain (IA593) was analysed for the numbers of intestinal nuclei. A significant increase in the numbers of intestinal nuclei was evident when the *lin-*

23::FLAG-TY allele was combined with the *cdc-25.1(ij48)* allele (Table 4.3). Comparison of the protein levels in embryonic extracts revealed a decrease in the LIN-23::FLAG-TY protein levels in the IA593 strain expressing CDC-25.1(S46F) compared to IA592 expressing CDC-25.1. The reason for the decrease in the LIN-23::FLAG-TY protein levels is not clear. However, it might explain the synergistic increase in the intestinal cell numbers when combined with the *cdc-25.1(ij48)* mutant. Several attempts were undertaken to precipitate LIN-23::FLAG-TY in order to analyse for association of endogenous CDC-25.1 using either anti-FLAG resin (Sigma) or an anti-TY antibody that was available in Dr. Johnstone's laboratory. However, only tiny amounts of LIN-23 could be precipitated, under any condition tested, suggesting that the epitope is masked and therefore not accessible to the antibody. In conclusion, the *lin-23::FLAG-TY* allele causes hyperplasia of the intestine through elevated CDC-25.1 protein levels.

4.2.6 CDC-25.1 S46 is crucial for LIN-23 binding in embryos

Binding of LIN-23 to CDC-25.1 and CDC-25.1(S46F) was compared from embryonic extracts derived from the strain JR1838 *cdc-25.1(+)* and IA530 *cdc-25.1(ij48)* after immunoprecipitation of endogenous CDC-25.1. As depicted in Figure 4.5, LIN-23 associates specifically with CDC-25.1 because the LIN-23 protein is not present in the IgG control (Figure 4.5, D, lanes 3 and 4). Due to the elevated CDC-25.1(S46F) protein levels in embryos a considerably greater amount of CDC-25.1(S46F) is precipitated compared to CDC-25.1 (compare lanes 3 and 5). Importantly, a strong reduction of LIN-23 protein levels in the CDC-25.1(S46F) eluate is evident as compared to the amount precipitated with CDC-25.1. The relative amount of LIN-23 protein levels bound to CDC-25.1 are very little as compared to the input lanes (compare lanes 1 and 2 with 3 or 5), suggesting that only a very small subfraction of LIN-23 is bound to CDC-25.1. The same amount of input material was loaded (as indicated by the small inset that displays weak exposure of the blot) in both cases.

This experiment demonstrates that endogenous LIN-23 shows decreased binding to CDC-25.1(S46F) as compared to CDC-25.1 in embryonic extracts under this experimental buffer conditions. It should be noted that this difference was not observed when 1% NP40 was omitted from the binding buffer. To determine whether the reduced binding influences the ubiquitination state of CDC-25.1(S46F), the samples were re-examined by SDS-PAGE and probed with an antibody that recognises poly- and mono-ubiquitin. Only the polyubiquitinated fraction is depicted here. A decrease of polyubiquitinated CDC-25.1(S46F) is detected as compared to CDC-25.1 (compare lanes 3 and 5). Importantly, the

result acquired here emphasizes that CDC-25.1(S46F) shows reduced physical association to LIN-23 and a concomitant decrease in its polyubiquitination state.

4.3 Discussion

I hypothesised that CDC-25.1 can physically interact with LIN-23 in *C. elegans* embryos and that the binding is abolished through the S46F mutation in CDC-25.1. Here, a biochemical system was set up gathering novel data that provide strong evidence for a physical interaction of CDC-25.1 to LIN-23 in *C. elegans* embryos. Furthermore, CDC-25.1(S46F) binding to LIN-23 is weakened and there is decreased polyubiquitination of CDC-25.1(S46F) compared to CDC-25.1.

4.3.1 Setting up the biochemical assay to study CDC-25.1 interaction to LIN-23

4.3.1.1 Testing of anti-CDC-25.1 peptide antibodies

A biochemical system was established to purify a CDC-25.1 LIN-23 complex from *C. elegans* embryonic extracts. An elaborate set of experiments was performed in order to obtain this essential information. Firstly, several attempts were undertaken to purify endogenous CDC-25.1 using anti-CDC-25.1 peptide antibodies (A and B) but were unsuccessful under several binding conditions. A weak affinity of the antibody to the protein or an intra-or inter-molecularly masked epitope, due to the folding of the protein within itself or within a complex, may provide the reason for this observation. It is clear that the A antibody is able to specifically detect CDC-25.1 in its denatured form on Western blots. The B antibody raised against the last 12 amino acids of CDC-25.1 could pull down little CDC-25.1 protein, similar to a previous report (Ashcroft et al., 1999), and recognised CDC-25.1 weakly on Western blots. This suggests that antibody A detects the denatured CDC-25.1 better than the non-denatured form. It could be possible that the C-terminal epitope is masked through binding to other proteins. The C-terminus of the eukaryotic CDC25 family contains a cyclin binding domain that is conserved from yeast to humans (Uto et al., 2004). Alignment of this motif reveals no strong homology to the *C. elegans* CDC-25.1 protein, however the very conserved (R, K), XKXX (T, S) core domain (where R denotes arginine, K lysine, T threonine, S serine and X any amino acid) present in all molecules is also found in *C. elegans* CDC-25.1. In CDC-25.1 it comprises amino acids 505 to 510 (RPKWVS), suggesting that this domain could be involved in interaction

of *C. elegans* CDC-25.1 with cyclins. Consistently, the anti-CDC-25.1A antibody was raised against amino acids 495 to 509 and is thus overlapping with the putative cyclin binding domain, suggesting that cyclin binding may interfere with the recognition of the A antibody to CDC-25.1. However, whether this domain is indeed involved in CDC-25.1 binding to cyclins remains to be elucidated.

4.3.1.2 Purifications of LAP-tagged CDC-25.1

As an alternative purification approach, overexpression of LAP-tagged CDC-25.1 in intestinal cells was utilised. Purification with a commercial anti-GFP antibody was not possible though purification of a GFP::LacZ fusion protein expressed in the same compartment was. This would suggest that the GFP epitope is buried in the CDC-25.1 proteins. Nevertheless, the LAP::CDC-25.1 protein was able to efficiently bind to S-Protein Agarose indicating that the S tag is exposed. However, a comparison between LAP::CDC-25.1 compared to LAP::CDC-25.1(S46F) was not possible because the mutant protein did not bind to the resin. This finding was rather surprising and could suggest that the N-terminus of the LAP::CDC-25.1(S46F) mutant might fold differently than the wild-type leaving the epitope masked. One way to examine this would be to boil the extracts in SDS to completely denature the proteins, and analyse whether binding to the S-Protein Agarose is increased. However, this would not solve the purification problem and the experiment was therefore omitted.

A difference in the localisation state of LAP::CDC-25.1 and LAP::CDC-25.1(S46F) was noticed in this study, indicating that both molecules are differentially regulated. This could suggest that LAP::CDC-25.1 is present in a different complex compared to LAP::CDC-25.1(S46F) and therefore not able to be precipitated in the same manner as the wild-type to the S-Protein resin, due to differential epitope masking. This observation in itself is rather intriguing. Purification of the extracts on gel filtration columns and following the presence of CDC-25.1 with an anti-GFP antibody could resolve this question. The difference in the molecular weight of the LAP::CDC-25.1(S46F)-containing complex compared to the LAP::CDC-25.1 would allow predictions of differential complex formations.

4.3.1.3 Purification strategies to pull down LIN-23

Additionally, a strain was generated that expresses a FLAG-TY-tagged LIN-23 in a *lin-23* null background in *C. elegans* embryos and utilised for pull down studies. Furthermore, immunoprecipitation of LIN-23 using a newly synthesised anti-LIN-23 antibody was

attempted. However only a newly generated CDC-25.1 antibody was able to purify CDC-25.1 and CDC-25.1(S46F) and could be utilised for comparative interaction studies of LIN-23 to CDC-25.1 and CDC-25.1(S46F). This was due to the fact that the anti-LIN-23 antibody showed a weak affinity to CDC-25.1 in immunoprecipitation assays and the LIN-23::FLAG-TY could not be precipitated with antibodies against the FLAG or TY tag.

Together, these difficulties reflect the unpredictability of the biochemical purification assays. A peptide might be masked in a complex or within the protein itself. As alternative purification strategies placing the tag to different domains of either protein is another option. In this work several alternative methods were used to place a tag on the N-terminus of CDC-25.1 or the C-terminus of LIN-23 and different antibodies utilised against the C-terminus of CDC-25.1 and the N- and C-terminus of LIN-23. Generation of antibodies is an elaborate method and tagging of proteins in *C. elegans* is not as easy as in other systems such as *E. coli* or mammalian tissue culture cells. Generating and testing transgenic strains can take several months, thus I decided to continue my efforts on the reagents that are functional and provide robust data. A combination of approaches was employed to underpin the specificity of the interaction of CDC-25.1 to LIN-23 in *C. elegans* embryos, and they are discussed below.

4.3.2 CDC-25.1 interacts with endogenous LIN-23 in C. elegans embryos

In this study, overexpressed LAP-tagged CDC-25.1 in intestinal cells could be purified on S-Protein Agarose. This protein showed clear binding to endogenous LIN-23 as examined by Western blotting using a novel LIN-23 antibody. As a second approach endogenous CDC-25.1 was immunoprecipitated from embryonic extracts using a novel anti-CDC-25.1 antibody that was raised against the full-length CDC-25.1 protein and specifically detects CDC-25.1. Importantly, LIN-23 is present in the eluate of CDC-25.1 immunoprecipitates and CDC-25.1 thus associates with LIN-23 in embryos.

As another experiment to verify specificity of the interaction, a tagged version of LIN-23 was able to interact with endogenous CDC-25.1 in the absence of untagged LIN-23, resulting in an approximately 2 kDa LIN-23 shift. Thus, the endogenous LIN-23 band present in the CDC-25.1 eluate is specific for LIN-23 and no artefact of the experiment. It is presently unclear, whether this interaction is direct or mediated by a bridging molecule. The direct binding between the DSG peptide of β–catenin and β-TrCP *in vitro* (Wu et al., 2003) suggests a direct interaction of *C. elegans* LIN-23 to the DSG consensus of CDC-

25.1. One way to examine whether the CDC-25.1 binding to LIN-23 is direct would be to develop an *in vitro* assay between the two molecules that are expressed in *E. coli*. This is not straight forward, because CDC-25.1 is highly phosphorylated in embryos as illustrated in this study and prior phosphorylation of at least the DSG motif and possibly other residues, as demonstrated for human CDC25A (Donzelli et al., 2004; Jin et al., 2003; Kanemori et al., 2005; Ray et al., 2005), may be important for LIN-23 interaction. Recombinant *E. coli* expressed CDC-25.1 could be purified through a tag, *in vitro* phosphorylated with several recombinant kinases, re-purified and added to *E. coli in vitro* translated and radiolabelled LIN-23 to assay for binding.

Importantly, the data obtained here show that CDC-25.1 and LIN-23 form a complex *in vivo*. Consequently, these data illustrate that binding of LIN-23 is specific to CDC-25.1 by several means. Endogenous CDC-25.1 binds to endogenous LIN-23, as examined by immunoprecipitation using an anti-CDC-25.1 antibody. Tagged CDC-25.1 binds to endogenous LIN-23 as examined by pull downs of CDC-25.1 through the LAP tag. Additionally, in the absence of wild-type LIN-23, the LIN-23 band that shifts to a LIN-23::FLAG-TY band in a CDC-25.1 immunoprecipitate. However, only a small amount of the total LIN-23 is associated with CDC-25.1. This is not entirely surprising since the complex is expected to be of a transient nature and only present at a distinct stage of embryonic development (probably mainly the 10- to 60-cell stage). Furthermore, only a subfraction of the total CDC-25.1 may be associated with LIN-23 and vice versa. LIN-23 may be involved in targeting a wide range of substrates, as identified for its the human orthologue β-TrCP, and thus only a small fraction of it may associate to CDC-25.1. It is thus rather intriguing that it was possible to set up conditions to detect the steady state interaction between these two endogenous molecules.

4.3.3 CDC-25.1 S46 may be crucial for LIN-23 binding

Based on the specificity of LIN-23 binding to CDC-25.1, experiments were conducted to test whether the interaction of LIN-23 with CDC-25.1(S46F) was affected. Immunoprecipitation of endogenous CDC-25.1 compared to CDC-25.1(S46F) using the newly synthesised CDC-25.1f.l. antibody revealed that LIN-23 binding to CDC-25.1(S46F) is weakened as compared to CDC-25.1. Furthermore, the polyubiquitination of CDC-25.1(S46F) is reduced compared to CDC-25.1. Thus, these results suggest that the S46F mutation affects the binding of LIN-23 to CDC-25.1. Both extracts contain similar amounts of LIN-23 protein as assayed in the small inset (Figure 4.5, D lanes 1 and 2), but in this experiment no β-ACTIN loading control is present. However, in other experiments

performed previously the amount of LIN-23 protein was found to be similar in the embryo when the same strains were utilised (Figure 3.5, A, lanes 2 and 4). It is possible that the amount of LIN-23 protein that can associate to CDC-25.1 is limiting and that only a subfraction of LIN-23 can ever associate to CDC-25.1 in the extract. However, in these experiments performed (using 1% NP40 in the binding assay) the amount of LIN-23 bound to CDC-25.1(S46F) is clearly reduced compared to LIN-23 binding to CDC-25.1. A possible explanation of these data is that most of the CDC-25.1(S46F) is in a separate compartment and thereby unavailable for LIN-23 binding. Thus, a differential localisation of CDC-25.1(S46F) might escape LIN-23 association. This differential LIN-23 association to the CDC-25.1 and CDC-25.1(S46F) is only observed under high amounts of detergent for reasons that remain unresolved. Ultimately, it would be desirable to compare the binding of the CDC-25.1 and CDC-25.1(S46F) to LIN-23 in an *in vitro* assay, where the total amounts of each protein can be directly compared. This could be done by *in vitro* translation of the CDC-25.1 protein, which could be assayed for binding to recombinant LIN-23 either in a band-shift assay or by pulldown analysis.

In the *in vivo* assay obtained here clearly, the binding of LIN-23 is not abolished but probably reduced. In mammalian cells the single mutation of analogous S82 in the DSG consensus of CDC25A was reported to abolish β-TrCP binding *in vivo* (Donzelli et al., 2004; Jin et al., 2003). This apparent inconsistency can be explained by the difference in methodology applied. Assuming LIN-23 binding was not limiting, the assay system described here purifies much higher amounts of endogenous CDC-25.1(S46F) protein compared to CDC-25.1, whereas in the experiment by Donzelli et al. similar amounts of FLAG-tagged CDC25A were pulled down or loaded on the gel (it should be noted that they also used 1% NP40 in their assay system). An adjustment of the CDC-25.1 protein levels was not performed in this study in order to keep all parameters identical. It is highly unlikely that LIN-23 protein levels could still be detected if far less CDC-25.1(S46F) eluate was applied on the gel. Furthermore, (Jin et al., 2003) utilised a truncated version of CDC25A (aa 1 - 100) for their studies, which might lack additional binding sites important to stabilise CDC25A interaction to β-TrCP.

In accordance with the potentially reduced binding, a decrease in the polyubiquitination state has been identified for CDC-25.1(S46F). Similarly, an *in vitro* ubiquitination assay revealed that the polyubiquitination of CDC25A is reduced by about 50% in the human CDC25A S82A mutant (Donzelli et al., 2004). In contrast, (Jin et al., 2003) concluded that this mutant is abrogated in β-TrCP-mediated polyubiquitination, but the initial

ubiquitination signal was very low and no quantification was provided in that study, and it is therefore possible that stronger exposure times would unravel residual ubiquitination of CDC25A S82A.

In essence, the experiments conducted here suggest that the binding of CDC-25.1(S46F) to LIN-23 may be reduced and a decrease in polyubiquitinated CDC-25.1(S46F) is observed. This result fits well with the elevated CDC-25.1 protein levels that are detected for CDC-25.1(S46F) by Western blotting and indirect immunofluorescence and suggests that the kinetics of CDC-25.1 degradation are reduced when S46 is mutated. Accordingly, CDC-25.1(S46F) protein levels are undetectable at later stages of development, suggesting that the protein is degraded eventually. Thus, S46 is essential for LIN-23 interaction and similar to other vertebrate systems, such as for example β-TrCP binding to β–catenin and CDC25; phosphorylation of this residue may be important for LIN-23 interaction.

4.3.3.1 CDC-25.1 is phosphorylated in embryos

Western blot analysis using two independent antibodies revealed that multiple CDC-25.1 bands are detected by SDS-PAGE that migrate at higher molecular weight than predicted. All bands shift down to a smaller molecular weight that corresponds to the estimated molecular mass on addition of lambda phosphatase to the extracts. Multiple phosphorylation of CDC25 had been reported for the vertebrate counterparts. Initial studies using the *Xenopus* system revealed that *Xenopus* CDC25C (Izumi et al., 1992; Kumagai and Dunphy, 1992) is extensively phosphorylated upon entry into mitosis and exhibits a severe migrational retardation on SDS polyacrylamide gels. Subsequently, several phosphorylation sites were identified in all three vertebrate CDC25 proteins. Phosphorylation of *Xenopus* CDC25C on the N-terminal region was described that is required for CDC25 activity (Kumagai and Dunphy, 1992) and comprises phosphorylation of several residues (T48, T67, T138, S205 and S285) (Izumi and Maller, 1993). S285 corresponds to S214 and S307 in human CDC25C and CDC25B, and phosphorylation of both residues has been shown to inhibit S216/S309 phosphorylation (Bulavin et al., 2003b). Furthermore, several phosphorylation sites have been identified in CDC25A. In mitosis, human CDC25A is phosphorylated on S18 and S116 resulting in stabilisation of CDC25A (Mailand et al., 2002). During S and G_2 phase of the cell cycle, human CDC25A is phosphorylated on multiple residues (S76, S82, S88, S124, S178, S279 and S293) contributing to the rapid turnover of CDC25A in unperturbed cells and in response to DNA damage (Busino et al., 2003; Falck et al., 2001; Goloudina et al., 2003; Hassepass et al.,

2003; Ray et al., 2005; Sorensen et al., 2003). In human cells, S82 in the DSG consensus sequence is phosphorylated by an as yet unknown kinase.

Thus, it can be anticipated that S46 of CDC-25.1 is phosphorylated in *C. elegans* embryos. No robust difference in the appearance of the three more slowly migrating bands was observed between the CDC-25.1 and CDC-25.1(S46F) on SDS polyacrylamide gels, suggesting that these bands reflect multiple phosphorylation on CDC-25.1. Similarly, knockdown of LIN-23 by RNAi stabilised all phosphorylated forms and not only one. The exact residues that are phosphorylated and the individual mechanism of phosphorylation remain to be identified. It is presently unclear whether S46 is phosphorylated in embryos. A comparison of CDC-25.1 and CDC-25.1(S46F) by two-dimensional SDS-PAGE could be employed to obtain a higher resolution of the CDC-25.1 phosphorylation forms. Importantly, this result demonstrates that in *C. elegans* embryos CDC-25.1 is phosphorylated similar to vertebrate CDC25.

4.3.4 Overexpression of CDC-25.1 causes hyperplasia

4.3.4.1 Zygotic expression of CDC-25.1

During the course of this work it became evident that zygotic overexpression of tagged and untagged CDC-25.1 resulted in intestinal hyperplasia in the embryo as evident by an increased number of intestinal nuclei. Overexpression of the CDC-25.1 proteins was confirmed by Western blotting (LAP::CDC-25.1) or indirect immunostaining (CDC-25.1). The hyperplasia was examined by DAPI staining of adult worms or the expression of the intestinal-specific *elt-2::GFP*. In a wild-type strain, 34 intestinal cells are present during post-embryonic development due to an additional nuclear division of the 14 most posterior cells at the L1 lethargus (Sulston and Horvitz, 1977). Here, on average 31.7 nuclei were counted by DAPI staining, probably due to difficulties in clearly distinguishing the small nuclei in the tail of the worm from the nuclei of surrounding tissues. A *cdc-25.1(ij48)* mutant analysed shows on average 60.5 nuclei in the adult. However, worms zygotically overexpressing tagged or untagged CDC-25.1 show an average of 40 to 50 nuclei, thus indicating that the tag is not causing malfunction of the protein. Consistent with previous reports on chromosomally integrated *cdc-25.1(ij48)* (Clucas, 2003; Clucas et al., 2002) or *cdc-25.1(rr31)* (Kostic and Roy, 2002), these nuclei are generated in the embryo as examined by the expression of the *elt-2::GFP* transgene. An average increase to 24 - 25 nuclei are evident after CDC-25.1 expression in the embryo correlating with the average of 40 - 50 nuclei in the adult worm if the four most posterior nuclei undergo no nuclear

division during post-embryonic development as in the wild-type. It maybe possible that in some cases the posterior nuclei undergo one nuclear division leading to a slight increase in the post-embryonic numbers of nuclei. Cell lineage studies of the *cdc-25.1(ij48)* mutant revealed that the expression of the *elt-2::GFP* in intestinal nuclei correlates with the number of intestinal cells born (Clucas, 2003; Clucas et al., 2002). Thus, it is highly suggestive that the intestinal nuclei in the embryos observed, by zygotic overexpression of CDC-25.1, represent the number of intestinal cells. Thus, this experiment complements the data obtained in Chapter 3 that identified that high CDC-25.1(S46F) protein levels are detected in the embryo and thus emphasises that merely high expression levels of CDC-25.1 can result in hyperplasia of the intestine.

4.3.4.2 Developmental timing and severity of CDC-25.1 effects

Interestingly, a small difference in the severity of the intestinal cell number is evident between the chromosomally integrated *cdc-25.1(ij48)* and the zygotically overexpressed CDC-25.1. Analysis of protein extracts by Western blotting showed an approximately 10-fold difference in the LAP-tagged protein abundance as compared to endogenous CDC-25.1. Only a four- to five-fold difference of endogenous CDC-25.1(S46F) compared to CDC-25.1 was observed in this and the previous chapter. However, *elt-2* promoter expression commences at the 28-cell stage of embryogenesis after the first two intestinal cells are born (Fukushige et al., 1998). This promoter allows the ectopic expression of CDC-25.1 at a time when the endogenous CDC-25.1 or CDC-25.1(S46F) protein levels are undetectable. Thus, it is possible that the delayed timing of CDC-25.1 expression from the *elt-2* promoter can cause the difference in severity of intestinal hyperplasia. In accordance with this assumption, a narrow time window at the 10- to 60-cell stage of embryogenesis shows upregulated CDC-25.1(S46F) protein levels in the *cdc-25.1(ij48)* mutant. It is possible that the CDC-25.1 protein levels need to reach a certain threshold level at this early stage of development in order to cause hyperplasia. Comparative analysis of the CDC-25.1(S46F) protein levels with *elt-2::CDC-25.1* by immunostaining of merely intestinal cells could be performed in order to detect whether CDC-25.1(S46F) protein levels are significantly higher at early embryonic stages.

Intriguingly, zygotic overexpression of CDC-25.1 does not seem to increase the hyperplasia during post-embryonic development as the number of cells in the embryo correlate with the expected number in the adult worm. This result has already been obtained previously for the *cdc-25.1(ij48)* allele (Clucas, 2003; Clucas et al., 2002), however, CDC-25.1(S46F) levels eventually diminish and are undetectable after the 100-

to 200-cell stage. In contrast, *elt-2*::CDC-25.1 is expressed throughout embryonic development and post-embryonically (as observed for the *elt-2*::LAP::CDC-25.1), which suggests the presence of a mechanism that distinguishes mitotic from post-mitotic intestinal cells. This could be due to the lack of a CDC-25.1 downstream target such as a cyclin-dependent kinase or cyclin. An interesting experiment would be to determine whether post-mitotic expression of CDC-25.1 causes an increase in intestinal cells during post-embryonic development. CDC-25.1 could be placed under the control of the *cpr-5* promoter allowing expression in the *C. elegans* intestine during larval and adult stages (Larminie and Johnstone, 1996) and analysed for *elt-2::GFP* expressing intestinal nuclei.

4.3.4.3 A chromosomally integrated *lin-23* transgene causes hyperplasia of the intestine

During this study, a *lin-23* partial loss-of-function allele was obtained by generation of *FLAG-TY* tagged *lin-23* under the control of its authentic promoter. This allele can complement the sterility of the *lin-23* null allele but causes strong embryonic lethality (for details see Chapter 5, (5.2.3)). Thus, the *lin-23::FLAG-TY* allele is partially complementing the *lin-23* null phenotype. During the course of this study, a weakened binding of LIN-23::FLAG-TY to CDC-25.1 was evident in embryos. Interestingly, the CDC-25.1 protein levels are elevated in a *lin-23* null mutant that expresses only the *lin-23::FLAG-TY* allele and results in the hyperplasia of the intestine as examined by *elt-2::GFP* expression.

These data complement the *lin-23* RNAi experiments that show that knockdown of LIN-23 produces elevated CDC-25.1 protein levels and intestinal hyperplasia. The enhanced levels of intestinal hyperplasia observed in a strain co-expressing the *cdc-25.1(ij48)* and *lin-23::FLAG-TY* however seems inconsistent with the previous data showing that CDC-25.1 is regulated by LIN-23 through S46. However, protein analysis revealed that the CDC-25.1(S46F) protein level is not enhanced in this strain compared to the *cdc-25.1(ij48)* strain. Thus, the *lin-23::FLAG-TY* allele does not cause the enhanced hyperplasia through S46 in CDC-25.1. However, the LIN-23::FLAG-TY protein levels are greatly reduced in the *cdc-25.1(ij48)* mutant background compared to the wild-type. Thus the reduction of LIN-23 protein may act on proteins independent of CDC-25.1. Cell lineage analysis performed by Dr. J. Cabello revealed that under strong *lin-23* RNAi conditions, the Cp lineage expresses the intestinal fate marker *elt-2::GFP*. Thus, *lin-23* is required in Cp to suppress the intestinal fate. The extra intestinal cells observed when CDC-25.1(S46F) is combined with low levels of LIN-23::FLAG-TY may represent additional cells derived

from the Cp lineage. Only a cell lineage analysis between the *lin-23::FLAG-TY* allele in a *cdc-25.1(+)* or *cdc-25.1(ij48)* background will ultimately resolve this question. This methodology is not available in our laboratory and requires the collaboration with Dr. Cabello.

4.3.5 Conclusion

The data here provide vital information on the functional conservation of CDC25 regulation between *C. elegans* and human. Notably, for the first time the significance for physical interaction of LIN-23 through S46 in CDC-25.1 to regulate the tissue-specific proliferation during the embryonic development of a multicellular model organism has been illustrated in a biochemical approach. S46F mutation in CDC-25.1 results in reduced binding of LIN-23 to CDC-25.1 and a decrease in the CDC-25.1 polyubiquitination rate. This is consistent with the data presented in Chapter 3 that detect elevated CDC-25.1(S46F) protein levels in the early embryo, thus demonstrating that a decrease in the CDC-25.1(S46F) degradation rate in all tissues, through abrogated LIN-23 interaction, results in the hyperplasia of the intestine. Accordingly, overexpression of zygotic CDC-25.1 in intestinal cells results in hyperplasia of the intestine emphasising that merely enhanced wild-type CDC-25.1 protein levels are responsible for the proliferation phenotype. Moreover, a LIN-23::FLAG-TY protein shows decreased binding to CDC-25.1 and elevated CDC-25.1 levels resulting in intestinal hyperplasia.

Chapter 5

CDC-25.1 tissue specificity

5 CDC-25.1 tissue specificity

5.1 Introduction

As previously reported, the maternally acting *cdc-25.1(ij48)* gain-of-function allele triggers a hyperplasia in the embryo that is mediated in a tissue-specific fashion and only perturbs the proliferation of intestinal cells (Clucas, 2003; Clucas et al., 2002). Cell lineage analysis of homozygous *cdc-25.1(ij48)* embryos revealed that the intestinal precursor (E) gives rise to 15 - 20 additional intestinal cells in the embryo, whereas proliferation of a neighbouring blastomere (D) was evidently unaffected. Similarly, expression of tissue-specific GFP markers revealed no increase in the proliferation of at least two other tissues in the embryo and the *cdc-25.1(ij48)* homozygous hermaphrodites are otherwise healthy and viable with no obvious post-embryonic defects. A comparable intestine-specific proliferation phenotype has been identified for the *cdc-25.1(rr31)* gain-of-function mutant, and the encoded CDC-25.1(G47D) protein has been illustrated to display a prolonged lifetime in all embryonic blast cells (Kostic and Roy, 2002). In contrast, removal of CDC-25.1 by RNAi causes embryonic lethality with severe mitotic division defects and a decrease in the proliferation of several tissues (Ashcroft et al., 1999; Clucas, 2003; Clucas et al., 2002). Hence, CDC-25.1 function is required in all embryonic blast cells to drive cell proliferation.

In the previous chapters, data are presented that depict the important role of LIN-23 in the regulation of CDC-25.1 through S46 in the embryo. Binding of LIN-23 to CDC-25.1 regulates the stability of CDC-25.1 in all early embryonic blast cells and the mutant CDC-25.1(S46F) escapes this negative regulation causing elevated protein levels in all blast cells. Thus, the negative regulator LIN-23 does not act in a tissue-specific fashion, which is consistent with the previous lack of phenotype for tissue-specific differences in the CDC-25.1(S46F) (Clucas, 2003; Clucas et al., 2002) or CDC-25.1(G47D) (Kostic and Roy, 2002) mutant protein levels or localisation in early embryos.

It is intriguing to note that the cell cycle exit in distinct embryonic blast cells differ in their sensitivity to the elevated presence of the CDC-25.1 protein. It will therefore be challenging but equally fascinating to decipher the mechanism underlying the differential sensitivities for this cell cycle regulator in different tissues. The identity of LIN-23 as the negative regulator of CDC-25.1 provides a significant step towards elucidating the temporal and spatial control of CDC-25.1 regulation during *C. elegans* development,

particularly because the expression and function of *cdc-25.1* and *lin-23* is not temporally restricted to the early embryo when the fine-tuning of the interaction between both molecules is crucial to sustain normal embryogenesis.

5.1.1 cdc-25.1 and lin-23 function during germline development

Previous work from several laboratories revealed that *cdc-25.1* and *lin-23* are expressed in the *C. elegans* proliferating germline and embryos and the evidence supporting these findings is introduced below. Northern blotting for *cdc-25.1* revealed high RNA expression levels in proliferating germlines that diminish during larval stages (Ashcroft et al., 1999), whereas high *lin-23* RNA levels were detected in the germline and embryos by Northern blotting and in situ hybridisation (Kipreos et al., 2000). In accordance with the high RNA levels, CDC-25.1 protein levels have been detected in the germline and in early embryos by indirect immunofluorescence against CDC-25.1 (Ashcroft et al., 1999; Clucas, 2003; Clucas et al., 2002; Kostic and Roy, 2002).

Detailed immunolocalistation studies by (Ascroft et al., 1999) revealed that, in the adult hermaphrodite, CDC-25.1 protein is mainly expressed in the germline and present in the nuclei of the oocytes with diffuse staining in the pachytene nuclei of the distal gonad, which becomes more apparent in the diakinetic nuclei of the proximal gonad arm. Some cytoplasmic signal becomes evident in older oocytes but is reduced at fertilisation. After fertilisation the signal becomes mainly nuclear in both the sperm and oocyte pronucleus and is mainly nuclear in the interphase and prophase of all early embryonic blast cells. Thus, the presence of CDC-25.1 protein in the germline suggests a requirement for its function during this developmental stage. Indeed, RNAi against *cdc-25.1* revealed that RNAi escapers developed into sterile adults because they probably obtained sufficient maternally provided CDC-25.1 to complete embryogenesis (Ashcroft and Golden, 2002; Ashcroft et al., 1999; Clucas, 2003; Clucas et al., 2002). Similarly, homozygous *cdc-25.1(nr2036)* null mutants are sterile and their empty gonads contain only a few non-viable germ cells that do not develop into oocytes indicating a zygotic role for CDC-25.1 during germline proliferation (Ashcroft and Golden, 2002).

Immunolocalisation has been lacking for LIN-23 to date. Expression of GFP transcriptional and translational reporter constructs revealed ubiquitous embryonic expression of LIN-23 starting at gastrulation in the cytoplasm of all embryonic blast cells and in the cytoplasm of several neurons, the hypodermis and muscle cells of the adult hermaphrodite (Mehta et al., 2004). Lack of GFP expression in the germline is probably

due to germline silencing of these constructs that were injected as extrachromosomal arrays, which are known to be subject to silencing in the germline (Kelly et al., 1997). A maternal and zygotic function for *lin-23* has been previously reported through the analysis of *lin-23* null mutants (Kipreos et al., 2000). In heterozygote progeny, post-embryonic development is reported to appear like wild-type as the animals develop into fertile adults. In contrast, homozygous mutant progeny of heterozygous mothers proceed through embryogenesis with no reported defects, but develop a variety of post-embryonic defects including sterility as adults. Homozygous *lin-23* null mothers produce only very few non-viable embryos that arrest with excess numbers of nuclei. Thus, this indicates that maternal LIN-23 products derived from a heterozygote mother are sufficient to sustain normal embryogenesis and the zygotic LIN-23 product is vital for germline development. In contrast to the lack of germline proliferation obtained in the *cdc-25.1* null mutant, *lin-23* null hermaphrodites produce the wild-type number of germ cells but show somatic defects including extra gonad arms and distal tip cells probably due to post-embryonic proliferation defects. The causative nature for the *lin-23* sterility has not been investigated to date.

However, these data clearly depict a zygotic role for both CDC-25.1 and LIN-23 in the development of the *C. elegans* germline whereas a maternal function of both proteins is required for normal embryogenesis. Interestingly, the difference in the germline proliferation phenotype of null alleles of each gene suggests that both genes act via separate mechanisms in the *C. elegans* germline as opposed to their common function in early embryos. Since CDC-25.1 is required for germ cell proliferation, removal of LIN-23 would be anticipated to result in hyperproliferation of the germline if it was negatively regulating CDC-25.1, but no hyperproliferation in *lin-23* null mutants was observed recently (Kipreos et al., 2000). Accordingly, *cdc-25.1(ij48)* mutant animals show normal proliferation of the germline and the *cdc-25.1(ij48)* allele can complement the sterile phenotype of the *cdc-25.1(nr2036)* null mutant (Clucas, 2003; Clucas et al., 2002) indicating that LIN-23 function is not required to control CDC-25.1 through S46 during germline proliferation.

5.1.2 Hypothesis and aims

Due to the scientific evidence portrayed above, I anticipated that zygotic LIN-23 might not regulate zygotic CDC-25.1 during *C. elegans* germline proliferation. Experiments were designed in order to test this hypothesis. Firstly, the zygotic versus maternal function of LIN-23 during *C. elegans* intestinal cell proliferation was further investigated. As

described earlier, homozygous *lin-23* null mutant embryos derived from heterozygous mothers have been reported to proceed normally through embryogenesis, as examined with Nomarski optics, thus suggesting that maternally provided LIN-23 from the heterozygous mother is sufficient to drive normal embryogenesis (Kipreos et al., 2000). However, no intestinal-specific marker was utilised in those experiments and proliferation defects of the intestine may have been missed. RNAi experiments performed here, which reduce both the maternal and zygotic LIN-23, indicate that lowered LIN-23 maternal protein levels can cause intestinal hyperplasia in the embryo. However, the contribution of the zygotic genotype for the intestinal cell proliferation phenotype has not been examined and was therefore investigated.

Since *lin-23* null embryos from heterozygous *lin-23* mothers proceed normally through embryogenesis and develop into fertile adults, it was decided to investigate whether lowering the *lin-23* gene-dose would result in embryonic intestinal defects in homozygous *lin-23* embryos derived from heterozygous mothers. Hyperplasia in zygotic null embryos would show that the intestinal phenotype is determined by the zygotic genotype. To this end, the *lin-23* null mutant strain was to be crossed into intestinal-specific GFP marker strains such as JR1838 *wIs84 [elt-2::GFP:LacZ]* permitting GFP expression in the intestinal nuclei of embryos and a second marker strain JR1988 *wIs119 [npa-1::GFP::LacZ]* allowing GFP expression in intestinal nuclei from late embryonic development that persists during post-embryonic development.

Secondly, though a zygotic role has been described for *lin-23* during *C. elegans* germline development and elevated mRNA levels were detected at this stage, the LIN-23 protein expression levels and localisation in the *C. elegans* germline remained elusive. Thus, indirect immunofluorescence against LIN-23 using the novel LIN-23 antibody was to be carried out. Furthermore, the regulation of CDC-25.1 through S46 in the germline was compared to the regulation in embryos by Western blotting of CDC-25.1 and CDC-25.1(S46F) in germline and embryo extracts. Finally, immunoprecipitation of endogenous CDC-25.1 from germline extracts would reveal whether any LIN-23 could interact with CDC-25.1 in a similar manner as in embryos.

5.2 Results

5.2.1 LIN-23 maternal function during intestinal cell proliferation

A *lin-23(e1883)* null mutant was employed to investigate the extent of maternal versus zygotic *lin-23* requirement for the proliferation of intestinal cells in the *C. elegans* embryo. The *lin-23(e1883)* allele comprises a G to A point mutation in the *lin-23* sequence resulting in a conversion of W450 into a stop codon (Kipreos et al., 2000). This allele showed an identical phenotype to *lin-23(rh294)* that terminates at amino acid position 12, due to the mutation into a nonsense codon, and that is therefore a molecular null allele. Thus, it was surmised that the *e1883* allele also constitutes a strong loss-of-function allele of *lin-23*. To analyse the number of intestinal cells during post-embryogenesis, a new strain was generated to combine the *lin-23(e1883)* allele with an intestinal-specific post-embryonic GFP marker. To this end, heterozygous JR1988 *npa-1::GFP::LacZ* males were crossed with CB3514 *lin-23(e1883)/dpy-10(e128)II.* The GFP positive F1 generation was analysed for the presence of 25% Lin animals in their F2 brood to create the strain IA565 *lin-23(e1883)/+ II; wIs119*. This strain was utilised to observe the number of intestinal cells by examining the GFP fluorescence in the adult worm.

As depicted in Figure 5.1 (panel A), *lin-23* heterozygote animals are evidently wild-type for their numbers of intestinal nuclei. However, homozygous *lin-23(e1883)* hermaphrodites contain excess numbers of small intestinal nuclei (the precise numbers were not counted). The presence of the *lin-23* mutant or wild-type allele was confirmed by single worm PCR and restriction site polymorphism that is introduced through the mutation (Figure 5.1 B and see Chapter 2 (2.2.6.5) for PCR details). The extra intestinal nuclei could have been produced during embryonic or post-embryonic development. Therefore, the number of intestinal nuclei was examined through the *elt-2::GFP::LacZ* transgene. To this end, heterozygous CB3514 *lin-23(e1883)/+ II* males were crossed with JR1838 *wIs84* hermaphrodites. GFP-positive F1 animals were checked for the presence of 25% homozygous Lin phenotype in their brood and the resulting strain IA568 *lin-23(e1883)/+ I, wIs84* utilised to examine the intestinal nuclei in the embryo. Single embryos were analysed under the fluorescence microscope and their genotype confirmed by single embryo PCR and restriction site polymorphism similar to Figure 5.1, B. The result is summarised in Table 5.1.

Numbers analysed	Embryo genotype	Embryo phenotype
24	*lin-23* +/+	20.0 ± 0.9
19	*lin-23* +/-	20.0 ± 1.0
7	*lin-23* -/-	20.7 ± 1.3

Table 5.1 Comparison of genotype with phenotype of IA568 embryos.

All embryos analysed exhibited the wild-type number of intestinal nuclei, indicating that the zygotic genotype of the embryo does not influence the phenotype and the extra intestinal nuclei observed in the adult hermaphrodite are generated during post-embryonic development. Thus, reduction of the *lin-23* gene-dose by half in the mother is sufficient to drive normal embryogenesis in the homozygous offspring, with respect to intestinal cell number.

In order to test if the LIN-23 protein product is reduced in *lin-23* heterozygous animals, the amounts of LIN-23 product derived from wild-type, *lin-23* heterozygote and *lin-23* null animals were examined. The amount of LIN-23 was analysed by Western blotting of CB3514 *lin-23(e1883)/dpy-10(e128)II* animals. Here, phenotypically Dpy adult hermaphrodites (*lin-23* +/+) were compared to phenotypically Lin (*lin-23* -/-) and wild-type (*lin-23* +/-) hermaphrodites by SDS-PAGE analysis using the novel anti-LIN-23 antibody. A specific band of 80 kDa is evident in wild-type animals, reduced to 47 +/- 7% in *lin-23* heterozygotes and absent in *lin-23* null hermaphrodites ((Figure 5.1 (panel C), two independent experiments, samples were applied multiple times and the signal quantified by densitometry, compared to β-ACTIN as internal control). Thus, a reduction of LIN-23 protein levels by 52% in heterozygous *lin-23* mothers is sufficient for normal embryogenesis in their zygotically wild-type, *lin-23* heterozygote and *lin-23* null mutant progeny.

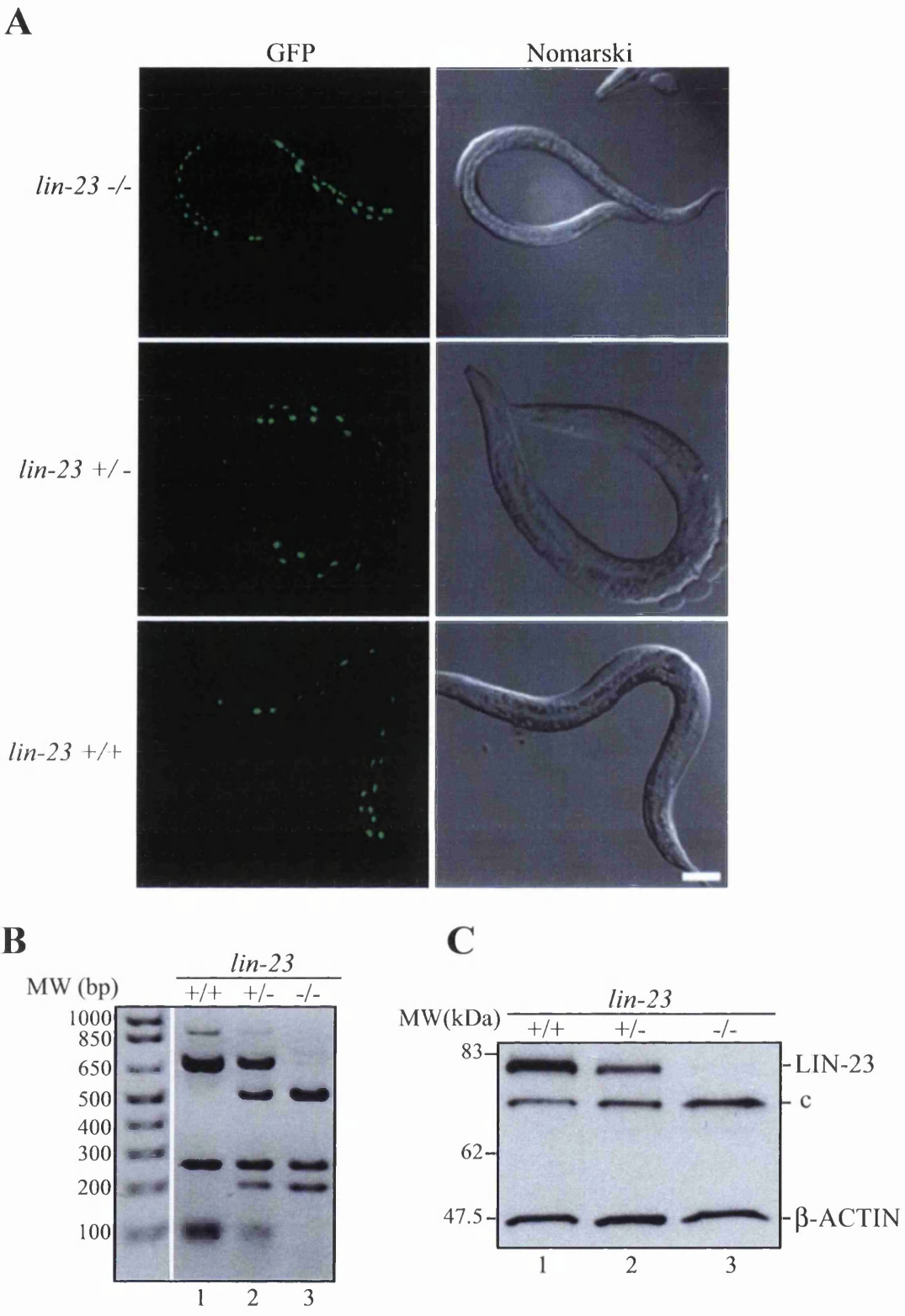

Figure 5.1 *lin-23* null mutant adults exhibit extra intestinal nuclei during postembryogenesis. A) Offspring derived from *C. elegans* strain IA565 carrying the intestinal-specific GFP marker *npa-1::GFP::LacZ* (for genotype see Chapter 2, Table 2.8) was analysed for the numbers of intestinal nuclei (GFP) in *lin-23* null (*lin-23 -/-*), *lin-23* heterozygote (*lin-23 +/-*) or *lin-23* wild-type (*lin-23 +/+*) young adults. Scale bar: 50 μm. **B)** The genotype of adults was confirmed by single worm PCR and restriction site polymorphism. **C)** Western blot analysis of LIN-23 protein levels of 50 (*lin-23 +/+* and *lin-23 +/-*) or 100 (*lin-23 -/-*) adult hermaphrodites compared to β-ACTIN, c = cross-reacting band of the anti-LIN-23 antibody. Two independent experiments for C.

5.2.2 LIN-23 post-embryonic localisation

The data above strongly suggested that maternally provided LIN-23 can sustain cell cycle exit during proliferation of intestinal cells in the embryo, whereas zygotic LIN-23 is required for appropriate control of intestinal nuclear divisions during post-embryonic development. Thus, indirect immunofluorescence, using the anti-LIN-23 antibody, was performed to examine whether LIN-23 protein levels could be detected in the adult intestine and germline. Weak expression of LIN-23 was detected in the cytosol of intestinal cells in wild-type adult hermaphrodites as compared to a *lin-23* null strain (Figure 5.2). Furthermore, strong LIN-23 expression was detected in the adult germline and was evidently missing in the *lin-23* null hermaphrodite (Figure 5.2). In the germline a mainly cytosolic staining was observed in the meiotic region (depicted to the bottom right), the pachytene (loop) and diakinetic region (top right) of the germline and in newly generated oocytes. Strong staining was also observed in other postembryonic tissues (no detailed analysis on the tissue identity was performed in this study) and in the embryo (embryonic LIN-23 localisation is discussed in Chapter 6). Thus, in accordance with LIN-23 function, the protein is localised in the intestine and germline of the adult hermaphrodite.

5.2.3 A lin-23::FLAG-TY allele rescues lin-23 germline defects

During the course of this study, a partially functional *lin-23* allele (*lin-23::FLAG-TY*) was generated. This transgene was integrated into the genome of the strain DP38 *unc-119(ed3)III* by microparticle bombardment and rescue of the *unc-119* mutation. Four independently integrated lines that were non-Unc were generated indicating that they contained the *unc-119* wild-type copy potentially together with the *lin-23::FLAG-TY* allele. All strains were analysed for the expression of LIN-23::FLAG-TY by immunocytochemistry against the TY tag and showed similar cytosolic staining in the germline (data not shown). Interestingly, it was observed that all strains, which evidently contain the endogenous wild-type copy of *lin-23* and the *lin-23::FLAG-TY* allele, showed a high degree of embryonic lethality of on average 50% in their offspring, which could be due to the *lin-23::FLAG-TY* allele or through the bombardment procedure.

One strain (IA582) that showed detectable expression of LIN-23::FLAG-TY on Western blot and the lowest frequency of embryonic lethality was chosen to determine whether the *lin-23::FLAG-TY* allele was fully functional and could complement the *lin-23(e1883)* null allele. Hence, this strain was crossed into the *lin-23* null strain to analyse rescue of sterility. To this end, homozygous males of IA582 *unc-119(ed3)III; ijIs18 [lin-23::FLAG-TY, unc-*

119(+)] were crossed into IA551 *lin-23(e1883)+/+ dpy-10(e128)II; unc119(ed3)III* hermaphrodites. Due to the presence of the homozygous *unc-119(ed3)* mutation in the background of both strains, the presence of homozygous *lin-23::FLAG-TY*, co-injected with the *unc-119* gene, could be followed by rescue of the Unc phenotype. If *lin-23(e1883)* was on a separate chromosome as *lin-23::FLAG-TY* by Mendelian segregation, 50% of the F1 generation would be expected to be *lin-23(e1883)/+ II; lin-23::FLAG-TY unc-119(+)/+ +, unc-119(ed3)III.* An Unc F1 hermaphrodite with this genotype would be expected to segregate 25% sterile animals due to the presence of the homozygous *lin-23(e1883)* allele. Thus, F2 populations were screened for the presence of sterile animals, indicating that the *lin-23(e1883)* allele was present. Non-Unc animals containing the *lin-23::FLAG-TY* allele were picked and screened for the presence of homozygous *lin-23(e1883)* by single worm PCR. Offspring of mothers with that genotype were selected for the presence of homozygous *lin-23::FLAG-TY* to generate the strain IA589 *lin-23(e1883)II; unc119(ed3)III; ijIS18 [lin-23::FLAG-TY, unc-119(+)].* Thus, this strain contains the *lin-23::FLAG-TY* allele in a *lin-23* null background (for an example of the *lin-23* PCR see Figure 5.1). Since it was possible to obtain this strain, it was obvious that the *lin-23::FLAG-TY* allele could rescue at least to some considerable extent the sterility of the *lin-23* null mutant. This was examined in detail.

As seen in Figure 5.3 (panel A), the *lin-23::FLAG-TY* allele was able to fully complement the sterility of the *lin-23(e1883)* mutant, but, on average approximately 70% of the embryos produced were not viable (Figure 5.3, B). The death rate differed between individual populations between 55% and up to 94%. The PCR analysis for genotyping of this strain (according to Chapter 2, (2.2.6.5)) is not depicted because two other strains that were generated by combining the *elt-2::GFP* transgene with or without the *cdc-25.1(ij48)* allele were derived from this strain after crossing IA589 males with IA530 hermaphrodites generating IA592 and IA593 (IA592 was generated in same way as IA593 except worms were selected for the *cdc-25.1(+)* allele; details on IA593 generation are depicted in Chapter 4, (4.2.5)). As illustrated in Chapter 4, both strains express only the tagged version of LIN-23::FLAG-TY and no endogenous *lin-23* as determined by Western blotting and an example for the analysis of the *lin-23(e1883)* genotype PCR is given in Figure 5.1 (panel B). Analysis of the intestinal cells in those strains revealed intestinal hyperplasia in the embryos and elevated CDC-25.1 protein levels (see Chapter 4, 4.2.5). Thus, the LIN-23::FLAG-TY protein can fully rescue the sterility of the *lin-23* null mutant, but it can only partially rescue the embryonic function.

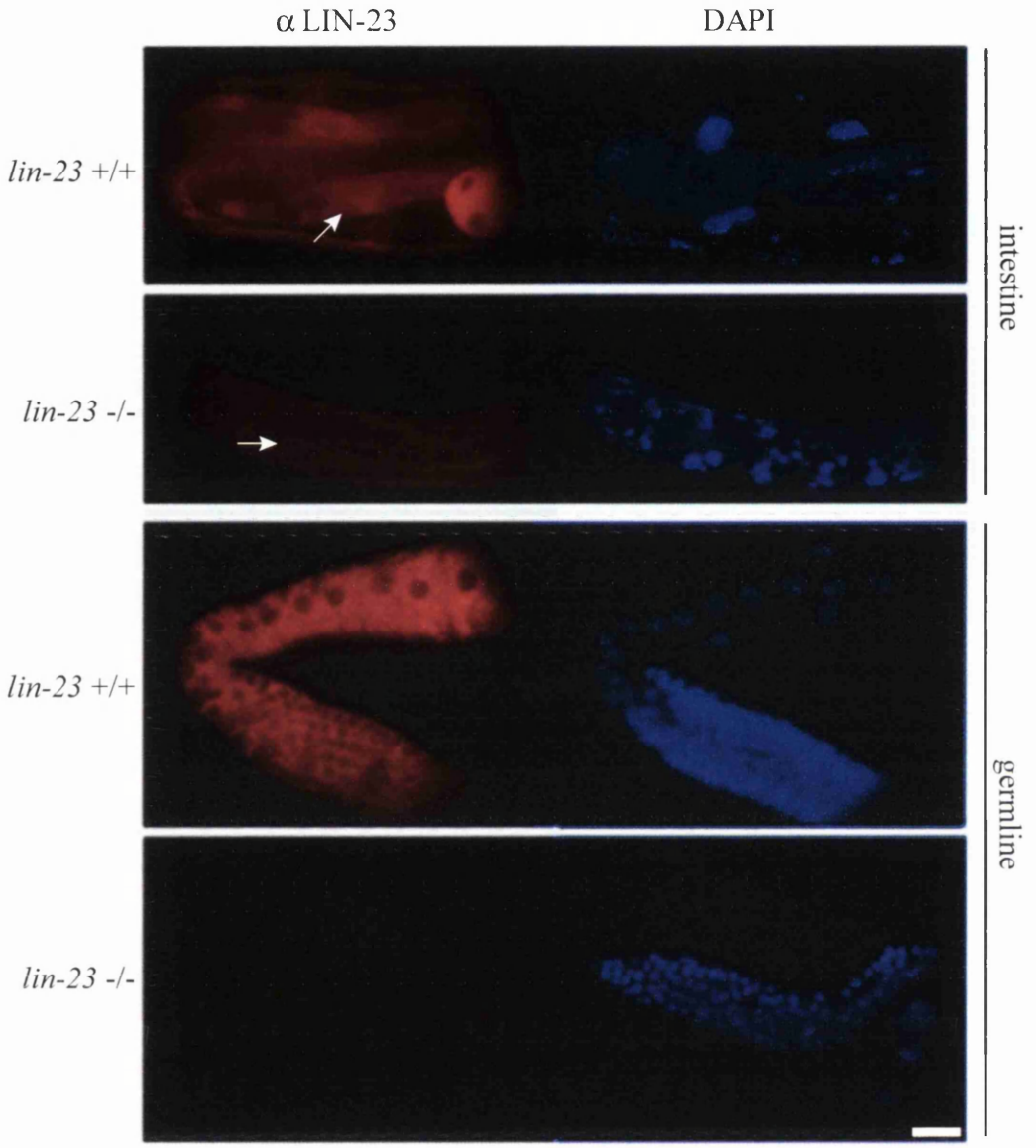

Figure 5.2 Localisation of LIN-23 in the adult hermaphrodite. Immunofluorescence staining of LIN-23 in wild-type (*lin-23 +/+*) or *lin-23 (e1883)* (*lin-23 -/-*) hermaphrodites with DAPI counterparts; only the anterior part of the intestine is depicted (anterior to the left), arrows indicate the position of intestinal cells. Dissected gonads are shown (germline) in the bottom. Scale bar: 50 μm.

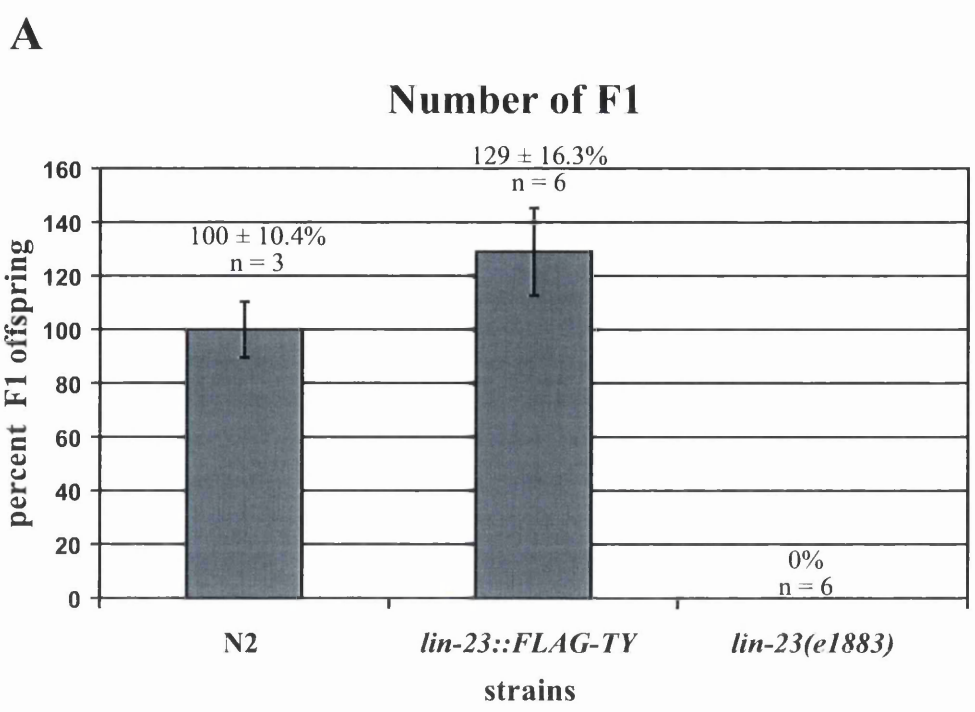

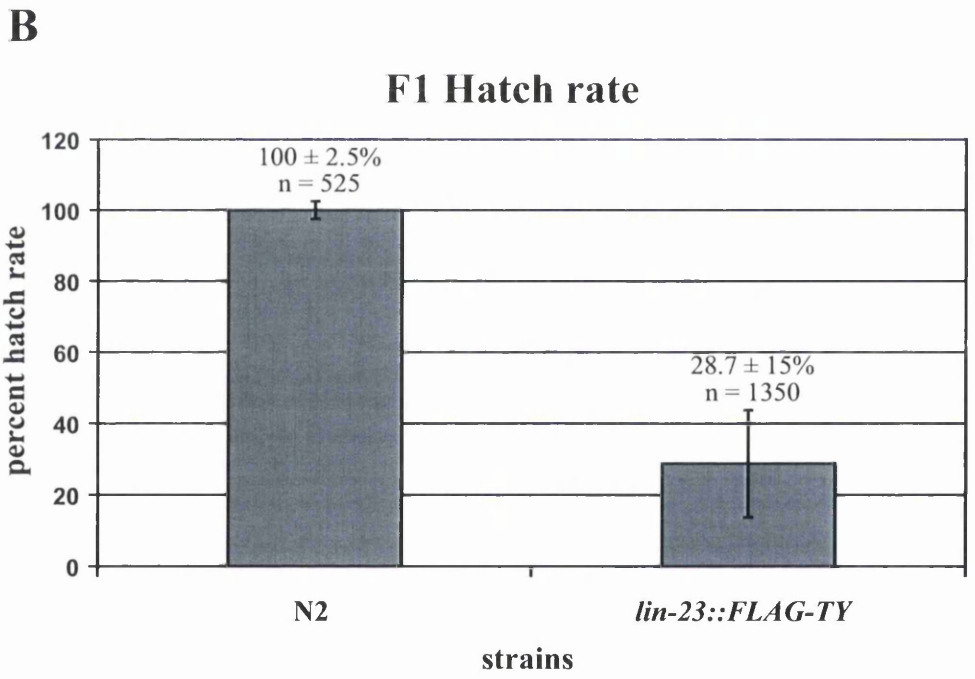

Figure 5.3 A *lin-23::FLAG-TY* allele rescues *lin-23* null sterility and causes embryonic death. A) Number of F1 embryos in N2 Bristol (N2), IA589 *lin-23(e1883)II*; *unc119(ed3)III*; *ijIs18 [lin-23::FLAG-TY, unc-119+]* (*lin-23::FLAG-TY*) and *lin-23(e1883)II*. **B)** Percent hatch rate of N2 Bristol (N2) and IA589 (*lin-23::FLAG-TY*), (N2, three experiments), (*lin-23::FLAG-TY*, six experiments).

5.2.4 LIN-23 does not regulate CDC-25.1 in the germline

The data illustrated above, suggested two separable functions of LIN-23 during *C. elegans* post-embryonic and embryonic development. Maternally provided LIN-23 is vital for regulated proliferation of the intestine during embryonic development, whereas zygotic LIN-23 is important for proper germline function. It has become evident that LIN-23 is required to restrain CDC-25.1 protein level through S46 in the early embryo in order to promote accurate cell proliferation of the intestine. Thus, these data suggested that zygotically acting LIN-23 does not regulate CDC-25.1 protein levels through S46 in the germline. In order to address this point, CDC-25.1 and CDC-25.1(S46F) protein levels were compared in the *C. elegans* germline. As described previously, CDC-25.1 is mainly expressed in the proliferating germline and embryos of the adult hermaphrodite (Ashcroft and Golden, 2002; Ashcroft et al., 1999). Thus, worms were grown in liquid culture and staged until they reached the L4 developmental stage, when they only contain a proliferating germline and no embryos, and CDC-25.1 protein levels were analysed by Western blotting. As depicted in Figure 5.4 (panel A), CDC-25.1(S46F) protein levels are similar to CDC-25.1 in L4 hermaphrodites as compared to the internal β-ACTIN loading control, but a substantial increase in CDC-25.1(S46F) protein levels was detected when embryos were examined in a parallel experiment. Thus, the CDC-25.1 protein level is not regulated through S46 in L4 hermaphrodites possibly representing the protein present in the germline.

Finally, the binding of LIN-23 to CDC-25.1 was analysed in L4 extracts and compared to the original binding in embryonic extracts. A similar amount of CDC-25.1 was precipitated with the CDC-25.1f.l. antibody and LIN-23 was bound to CDC-25.1 in embryonic extracts. In contrast, no LIN-23 binding was observed in L4 extracts (Figure 5.4, B). Thus, LIN-23 does not regulate CDC-25.1 stability in L4-staged animals.

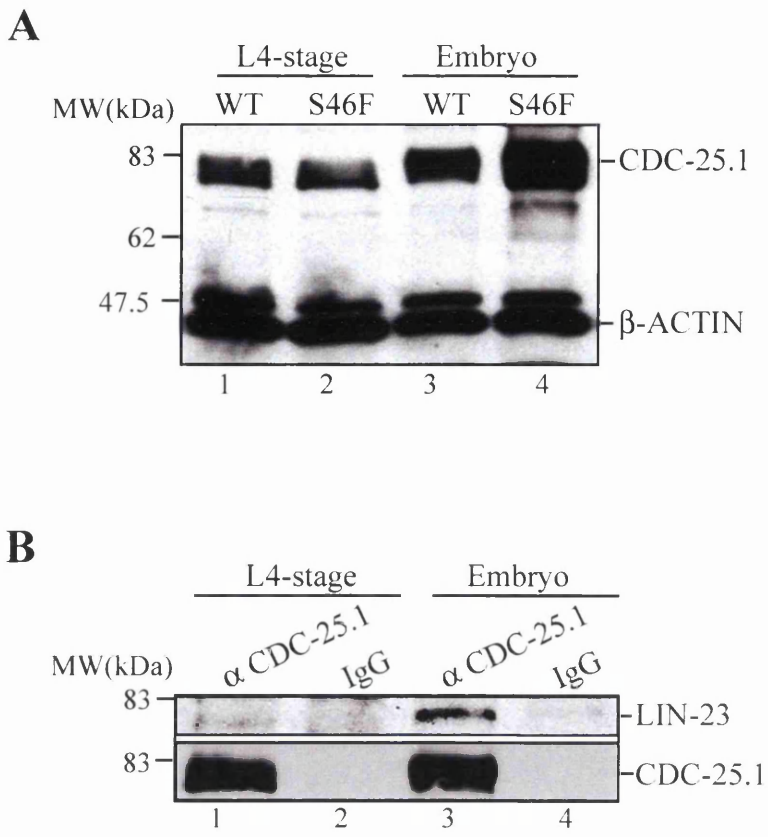

Figure 5.4 LIN-23 does not control CDC-25.1 protein levels in the *C. elegans* germline.
A) Comparison of CDC-25.1 protein levels from L4-staged hermaphrodites, mainly expressing CDC-25.1 in the germline (lanes 1 and 2), with the protein levels in embryos (lanes 3 and 4). Similar amount of total proteins derived from extracts of the *C. elegans* strain JR1838 (WT) and IA530 *cdc-25.1(ij48)* (S46F) were applied to 10% SDS-PAGE and blotted with anti-CDC-25.1A and as loading control β-ACTIN antibodies. **B)** Immunoprecipitation of CDC-25.1 with the anti-CDC-25.1f.l. antibody from extracts of L4-staged hermaphrodites (lane 1) or embryos (lane 3) of the strain JR1838 as compared to rabbit IgG as control (lanes 2 and 4, respectively). Eluates were applied to 10% SDS-PAGE followed by Western blotting against LIN-23 (top) and CDC-25.1 (anti-CDC-25.1A, bottom). Two independent experiments each.

5.3 Discussion

It was hypothesised that LIN-23 may not regulate CDC-25.1 through S46 in the germline, mainly because loss of zygotic *cdc-25.1* function caused germline proliferation defects (Ashcroft and Golden, 2002). However, no proliferation phenotype was identified after loss of *lin-23* in the germline (Kipreos et al., 2000), suggesting two independent functions of both proteins in the germline. Data are presented here that argue that LIN-23 does not control CDC-25.1 protein levels in the germline when L4-staged animals were analysed. Firstly, two developmentally separable functions were identified for LIN-23 during post-embryonic germline development and embryonic development of the intestine, as illustrated by the analysis of a *lin-23* partial loss-of-function allele. This allele can rescue the sterility of a *lin-23* null mutant but causes embryonic death, suggesting that the allele can function normally in the germline but not in embryos. Hence it may regulate different targets in the germline as compared to the embryo. Furthermore, biochemical evidence is presented that corroborates the conclusion that LIN-23 does not bind and regulate the abundance of CDC-25.1 in the L4-staged hermaphrodite where most of the CDC-25.1 protein resides in the germline.

5.3.1 Zygotic versus maternal lin-23 function

Analysis of the *lin-23(e1883)* null allele previously revealed a zygotic role for *lin-23* in the development of the *C. elegans* germline (Kipreos et al., 2000). Furthermore, a maternal contribution of *lin-23* during embryonic cell proliferation had been identified in that study. A few homozygous null embryos derived from homozygous mothers displayed additional nuclei in the embryo indicating proliferation defects in the embryo. However, homozygous embryos of heterozygous mothers proceeded normally through embryogenesis, thus demonstrating that maternally provided LIN-23 from the heterozygous mother was sufficient to drive embryogenesis.

Here, analysis of intestinal-specific GFP markers revealed that homozygous *lin-23* null mutants that are derived from heterozygote mothers show no proliferation defects of the intestine during embryogenesis. Thus, the zygotic genotype of the embryo does not determine the intestinal cell proliferation phenotype and maternally provided LIN-23 protein derived from the mother is sufficient to produce normal embryos. However, these embryos hatch and show extra intestinal nuclei during their post-embryonic development. This is in agreement with a previous report illustrating a contribution of LIN-23 to restrain

endoreduplication in the *C. elegans* larva (Kipreos et al., 2000). During the L1 larval stage only the 14 most posterior nuclei (int-3 to int-9) undergo one round of nuclear division (Sulston and Horvitz, 1977) that is followed by an endoreduplication cycle of all nuclei at each larval stage (Hedgecock and White, 1985). In homozygous *lin-23* null worms however, the endoreduplication cycle at the L1 lethargus is converted to a second nuclear division, such that each intestinal cell (int-3 to int-9) obtains four intestinal nuclei with a 16N instead of a 32N content. In this study, GFP expression revealed multiple smaller nuclei in the intestine of the *lin-23* null adult hermaphrodite, which are probably derived by the conversion of the endoreduplication cycle into a nuclear division. The molecular nature underlying this defect is not known and is not the focus of this study.

Importantly, maternal LIN-23 protein is required during embryonic proliferation of the intestine but not during proliferation of the germline. Interestingly, heterozygous *lin-23* mothers only produce on average 50% of the LIN-23 protein levels as compared to the wild-type worm; thus 50% of LIN-23 protein levels that are deposited to the embryo from a heterozygote mother are sufficient to drive normal proliferation of the intestine. Similarly, RNAi against *lin-23*, that decreases maternal as well as zygotic *lin-23* function, revealed that 80% of the embryos are still viable but show hyperproliferation of the intestine. Thus, it is possible that a certain threshold level below 50% of maternal LIN-23 depletion has to be obtained in order to create an intestinal cell proliferation phenotype. When RNAi was performed in liquid cultures, depleting more than 90% of the LIN-23 protein as examined by Western blotting (Chapter 3, Figure 3.5), none of the embryos was viable (data not shown). Thus, maternal LIN-23 function may first become limiting during intestinal cell proliferation when a reduction below 50% protein levels is reached. The increase in embryonic lethality by further LIN-23 knockdown suggests that LIN-23 must have also other functions in the embryo.

In agreement with two separable functions of *lin-23* during postembryogenesis and embryogenesis, a *lin-23::FLAG-TY* allele was identified in this study that can rescue the *lin-23* sterility but results in embryonic lethality. The LIN-23::FLAG-TY protein shows decreased binding to CDC-25.1 in the embryo with concomitant hyperproliferation of the intestine (Chapter 4, (4.2.5)). It is clear that the *lin-23::FLAG-TY* allele is able to complement the normal *lin-23* function in the germline, but it is impaired in its proper function in the embryo. It is possible that this allele has lost the ability to regulate correctly other factors in the embryo, especially because high embryonic lethality has been observed. Importantly, this result emphasises that the function of LIN-23 can be attributed to two independent mechanisms in the germline and embryo and altogether shows that at

least 50% maternal LIN-23 protein, derived from the mother, is required to promote normal embryogenesis. It will be extremely valuable to analyse the total protein expression levels in embryos derived from the *lin-23::FLAG-TY* strain compared to wild-type embryos by 2D-gelelectrophoreses. This will reveal additional downstream targets that are negatively regulated through LIN-23 in the embryo. Furthermore, a similar proteomics approach could be performed by analysis of germline proteins in the adult hermaphrodite with or without *lin-23* RNAi, which will provide powerful insight into the identification of proteins that are regulated through LIN-23 in the germline.

5.3.2 LIN-23 localisation

Immunolocalisation using the anti-LIN-23 antibody revealed for the first time that LIN-23 protein is expressed mainly in the cytosol of the adult germline and in the intestine. Thus, this expression is in agreement with the proposed LIN-23 function during post-embryonic development of the germline and intestine. In the germline, the localisation of LIN-23 is differing from the CDC-25.1 localisation, which was evidently nuclear as opposed to the cytosolic localisation of LIN-23 (Ashcroft et al., 1999). Thus, it may be possible that the spatial localisation of both proteins in the germline prevents these two proteins from interacting and thus renders them functionally independent. Artificially restricting the CDC-25.1 localisation to the germline cytosol could reveal whether it makes CDC-25.1 more sensitive to LIN-23 function. This could be achieved by blocking the nuclear import of CDC-25.1. An RNAi experiment against the *C. elegans* nuclear import receptors *ima-2* (Askjaer et al., 2002) or *ima-3* (Geles and Adam, 2001; Segal et al., 2001) could be performed in order to test whether CDC-25.1 localisation can be shifted to the germline cytosol. If so, extracts from L4 staged animals with normal or cytosol restricted CDC-25.1 could reveal whether the CDC-25.1 protein levels are decreased in the germline and remain stable through CDC-25.1(S46F).

5.3.3 LIN-23 does not regulate CDC-25.1 in the germline

Biochemical analysis demonstrated that CDC-25.1 protein levels remain constant in the germline even in the presence of the S46F mutation in CDC-25.1. Thus, the S46 residue is not important to control CDC-25.1 protein levels in the germline as compared to its essential function in the embryo. This result is consistent with previous work that did not find an increase in CDC-25.1(S46F) protein levels when adult extracts were analysed by Western blotting and compared to the wild-type (Clucas, 2003; Clucas et al., 2002). In this work, staged L4 to young adult animals were analysed, which contain CDC-25.1 in their

proliferating germline but do not produce embryos yet. Thus, the CDC-25.1 protein levels measured are derived mainly from the germline. In the previous study by Clucas et al., adult animals were examined that contained CDC-25.1 in their germline and in their embryos that are produced at that stage. Hence, this suggests that in adult worms, that produce both germline and embryonic CDC-25.1, the majority of CDC-25.1 protein analysed by Western blotting of whole worms is derived from the germline and the temporal difference of the protein levels in the embryo (as detected by analysis in embryonic extracts in this study) is therefore missed in that experiment. Thus, CDC-25.1 abundance is not regulated through S46 in the germline. Accordingly, immunoprecipitation of CDC-25.1 from the germline revealed no association of LIN-23 whereas the binding in the embryo is still observed. In summary, LIN-23 does not regulate the CDC-25.1 abundance in the germline.

Apart from the differential localisation of both molecules, it is possible that the kinase that phosphorylates CDC-25.1 on S46 is not present or active in the germline as opposed to the embryo. A similar contribution of kinase activity marking a transition between oocyte maturation and embryonic regulation of the OMA-1 (Oocyte maturation defective) protein has been previously established (Shirayama et al., 2006). Identification of the kinase that is necessary for phosphorylation of CDC-25.1 S46 in the embryo will provide a significant step towards answering this question. As discussed in Chapter 3 (3.1.2), the S46 site provides a potential target site for a GSK3β kinase. In this study, removal of the closest GSK3β homologue did not enhance CDC-25.1 stability through S46, indicating that this is not the kinase responsible for acting through this site, but the possibility remains that another member of the GSK-3 family is performing this function. Furthermore, sequence motif analysis for potential kinase sites using the NetphosK1.0 and ELM server revealed that S46 in CDC-25.1 could be part of a potential PKA (RX(S,T); RDS) (Shabb, 2001) or CK1 (S(P)xx(S,T); SRDS) (Flotow et al., 1990) kinase target site. The *C. elegans* genome contains 2 PKA and 78 CK1-related kinases (Manning, 2005). Thus, identification of the crucial kinase involved in phosphorylation of this residue may prove challenging due to potential functional redundancy of the kinases.

5.3.4 Conclusion

In summary, novel data evolved in this work demonstrate a spatially and temporally restricted interaction of LIN-23 and CDC-25.1 to the early embryo, thus providing a further insight into the tissue-specific regulation of CDC-25.1 during *C. elegans*

development. A certain threshold amount of maternally provided LIN-23 is necessary to restrain intestinal cell proliferation in the embryo via regulation of CDC-25.1 abundance. Furthermore, zygotic LIN-23 function is not required for intestinal cell proliferation in the embryo, and is thus restricted to post-embryonic development. However, during post-embryonic development, LIN-23 does not regulate CDC-25.1 protein levels in the germline. It is therefore possible that the spatial localisation of both molecules, or the spatial and temporal regulation of the kinase negatively regulating CDC-25.1 through S46, is responsible for the differential requirement for LIN-23 interaction between post-embryonic and embryonic development.

Chapter 6

LIN-23 localisation in the early embryo

6 LIN-23 localisation in the early embryo

6.1 Introduction

Evidence presented in the previous chapters established a physical interaction of LIN-23 and CDC-25.1 through the S46 residue in the early embryo. The maternal function of both proteins is required for correct proliferation of intestinal cells, thus implying that intestinal cell cycle control results from the interaction of the two maternally provided proteins. CDC-25.1 protein levels have been reported in the germline (Ashcroft et al., 1999; Clucas, 2003; Clucas et al., 2002) and the early embryo (Ashcroft et al., 1999; Clucas, 2003; Clucas et al., 2002; Kostic and Roy, 2002). The CDC-25.1 protein levels decline in all blast cells during later stages of embryogenesis, at least in part as a result of LIN-23 interaction with CDC-25.1. However, though high LIN-23 RNA levels have been reported in embryos (Kipreos et al., 2000), no published data were available that demonstrate the expression of LIN-23 protein in the early embryo. Expression of a transcriptional and translational *lin-23::GFP* transgene revealed ubiquitous expression in the cytoplasm of all embryonic blast cells after gastrulation (Mehta et al., 2004). As demonstrated in Chapter 5, the LIN-23 protein is detected in the germline, indicative of a maternal contribution of LIN-23 to the embryo. However, no information about the endogenous LIN-23 expression and localisation in the early embryo was available.

6.1.1 Hypothesis and aims

It was anticipated that the LIN-23 protein would be expressed in all early embryonic blast cells until later stages of embryogenesis. Therefore, immunocytochemistry, using the anti-LIN-23 antibody, was to be performed in wild-type or *lin-23* RNAi-treated embryos in order to analyse for the presence of LIN-23 during embryogenesis.

6.2 Results

6.2.1 LIN-23 is ubiquitously expressed in embryos

Indirect immunofluorescence was performed in order to examine the expression of LIN-23 in the embryo. Staining with the anti-LIN-23 antibody and fluorescent analysis by conventional microscopy revealed expression of LIN-23 in all blast cells from early to late embryogenesis (Figure 6.1). This staining was specific since embryos that were treated

with *lin-23* RNAi did not show any staining under identical experimental conditions (Figure 6.1, see bottom). The majority of LIN-23 is localised in the cytosol of all blast cells. Intriguingly, some LIN-23 protein was evident in the vicinity of the DNA in AB descendants in two- or four-cell stage embryos, indicating that LIN-23 can shuttle between different compartments in at least some blast cells. Thus, this experiment demonstrates that LIN-23 protein is ubiquitously expressed in all embryonic cells from early to late embryogenesis.

6.2.2 LIN-23 embryonic localisation is dynamic

Since differences in the localisation of LIN-23 were observed in some early blastomeres, it became apparent that LIN-23, though mainly cytosolic, might be able to move between distinct cellular compartments in some or all blast cells. This differential localisation could be the result of LIN-23 redistribution at various cell cycle stages in some or all blastomeres or differential localisation of LIN-23 in certain blastomeres throughout the cell cycle. Thus, confocal microscopy was carried out using two GFP marker strains to facilitate identification of the cell cycle stage in individual blast cells and the cellular localisation of LIN-23. The GFP::LEM-2 strain was utilised as a marker for nuclear envelope formation, because LEM-2 encodes for an inner nuclear membrane protein (Galy et al., 2003). This protein surrounds the DNA during interphase, redistributes into the endoplasmatic reticulum surrounding the spindle at prometaphase, and only fully disassembles during mid-to-late anaphase. During telophase, the nuclear envelope reforms around the chromatin building two nuclear envelopes (Lee et al., 2000; Oegema, 2006). As a second marker GFP::β-TUBULIN was employed to label for microtubule assembly (Strome et al., 2001). During the cell cycle, the two centrosomes move to opposite sites of the nucleus at prophase and start to build a spindle connecting to the kinetochores of the DNA at prometaphase. Chromosomes that align at the metaphase plate between the two spindle poles are pulled apart during anaphase and the kinetochore microtubules disappear during telophase (Scholey et al., 2003; Strome et al., 2001).

Double immunostaining was performed using anti-GFP and anti-LIN-23 antibodies together with DAPI staining, thus co-labelling the nuclear envelope or the microtubules with LIN-23 and the DNA. As observed before, the majority of LIN-23 localises to the cytosol in all embryonic blast cells (Figure 6.2). Interestingly, some LIN-23 concentrates to the vicinity of the DNA during prometaphase to metaphase transition. Figure 6.2 (panel A) shows LIN-23 association around the condensed DNA during late prometaphase in the posterior P1 blastomere of a two-cell stage embryo at the point when the nuclear envelope

starts to break down and some LEM-2::GFP is surrounding the spindle poles (arrow indicates LIN-23, two stars point out the position of the spindle poles). However, during telophase LIN-23 is excluded from the nucleus. Figure 6.2 (panel A) depicts the exclusion of LIN-23 from the telophase nuclei of the anterior AB blastomere and in panel B the telophase exclusion from the just dividing EMS blastomere is shown in a four-cell stage embryo. Additionally, the AB descendants in this embryo exhibit nuclear exclusion of LIN-23 during interphase and LIN-23 is excluded from the prophase nucleus of P2 (Figure 6.2, B).

Co-staining of embryos with LIN-23 and the tubulin marker confirmed this result. LIN-23 is detected around the newly forming spindle of the anterior AB cell in late prophase to prometaphase and excluded from the prophase nucleus of P1 (Figure 6.2, C). A fraction of LIN-23 is concentrated at the vicinity of the centrosomes in all blast cells of the four-cell stage embryo at interphase-to-mitosis transition and is excluded from all nuclei (Figure 6.2, D, yellow merged areas indicate co-staining). In the four-cell stage embryo staining of LIN-23 is evident in the vicinity of the metaphase spindle poles in the AB descendant (note the poles are visualised from the top, thus this staining likely represents LIN-23 protein wrapping around the DNA visualised from the top), whereas LIN-23 is excluded from the interphase nucleus of the EMS blastomere (Figure 6.2, E). Intriguingly, the protein is found surrounding the DNA of the metaphase EMS cell (Figure 6.2, F arrow), but does not co-localise with the entire spindle apparatus (arrowhead). Some protein is still enriched in the area surrounding the DNA in the anaphase ABp cell. In some later embryos (around the 28-cell stage) this metaphase staining of LIN-23 was also observed, indicating that the redistribution might not be restricted to early embryos (data not shown).

In summary, LIN-23 localisation is rather dynamic during the cell cycle stage in all early blastomeres analysed. Figure 6.2 is representative for multiple embryos examined in three independent experiments. No obvious differences in the staining pattern were observed between various blast cells. It can be concluded that at least a fraction of LIN-23 enters the nuclear area during prometaphase, where it surrounds the DNA in metaphase maybe by associating to the central spindle apparatus and leaves the DNA periphery during anaphase, such that all LIN-23 is found in the cytosol during telophase and interphase.

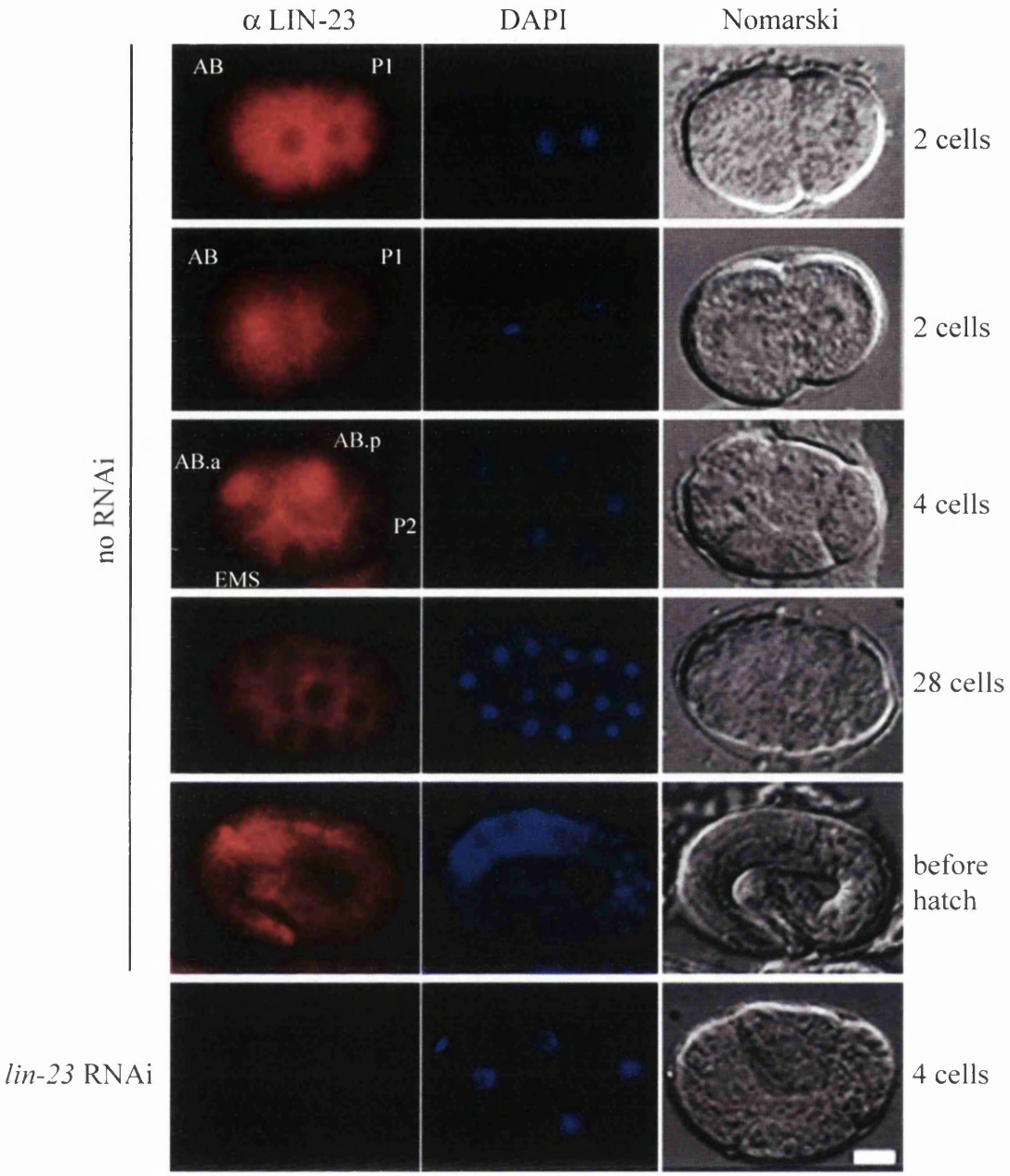

Figure 6.1 LIN-23 localisation during *C. elegans* embryogenesis. Indirect immunofluorescence of LIN-23 using the anti-LIN-23 antibody (this study) with corresponding DAPI and Nomarski counterparts in early (2- to 28-cell stage) and late stages of embryogenesis before hatching. The bottom panel depicts a four-cell stage embryo after *lin-23* RNAi to demonstrate specificity of the staining. Anterior is depicted to the left. The blast cells are indicated at the early stages. Scale bar: 10 μm.

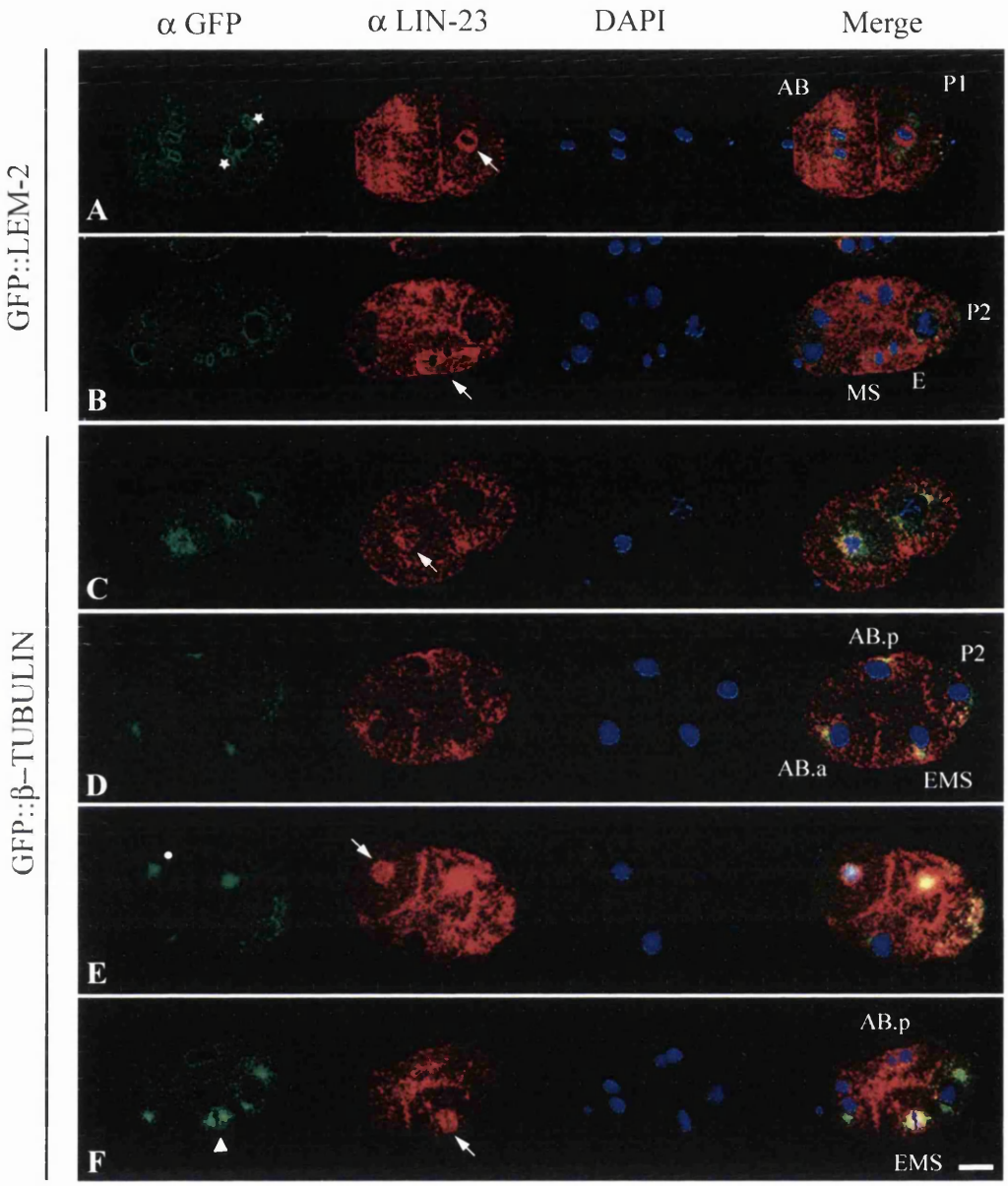

Figure 6.2 LIN-23 localisation changes during the cell cycle in early embryos. Indirect immunostaining of embryos carrying GFP::LEM-2 (A, B) or GFP::β-TUBULIN reporter (C-F) with anti-GFP and anti-LIN-23 antibodies. **A)** LIN-23 shuttles to the nucleus during prometaphase (arrow) when the nuclear envelope absorbes into the ER (indicated by stars) in P1, it is excluded from the chromatin in AB (telophase) during NE reformation. **B)** LIN-23 is mainly cytosolic and excluded from chromatin in telophase of the newly formed MS and E nuclei (arrow) and is cytosolic in interphase of the AB descendants. **C)** LIN-23 moves to the vicinity of the newly formed AB spindle during prometaphase at the two-cell stage (arrow) and is exluded from the P1 prophase nucleus. **D)** LIN-23 is mainly cytosolic in interphase-to-mitosis transition during the four-cell stage, weak co-staining is visualised at the centrosomes. **E)** LIN-23 localises to the vicinity of the spindle poles in AB descendants at the four-cell stage. White dot indicates the spindle pole visualised from the top. **F)** LIN-23 wraps around the chromatin (arrow) in metaphase of the EMS spindle (triangle). Anterior is depicted to the left, scale bar: 10 μm.

6.2.3 LIN-23 influences the CDC-25.1 localisation

The ubiquitous expression of LIN-23 in all blast cells is in agreement with the general control of CDC-25.1 through LIN-23 in probably all blast cells of the embryo. Previous data established that CDC-25.1 is localised mainly to the nucleus in interphase and prophase cells but moves to the cytoplasm following nuclear envelope breakdown in all early blast cells (Ashcroft et al., 1999). Because CDC-25.1 is nuclear during interphase and prophase whereas some LIN-23 localises to the vicinity of the DNA during prometaphase to early anaphase, it suggests that the LIN-23 interaction to CDC-25.1 might occur in the cytoplasm. Since cytoplasmic co-staining experiments are rather difficult to interpret, a separate approach was carried out to identify the influence of LIN-23 on CDC-25.1 localisation. Here, the strains IA535 *ijIs16* and IA536 *ijIs17* carrying LAP::CDC-25.1 and LAP::CDC-25.1(S46F), respectively, were utilised. These strains express CDC-25.1 or CDC-25.1(S46F) only in intestinal cells starting from the 2E-cell stage (see Chapter 4 also). The localisation of CDC-25.1 was visualised through live fluorescence imaging due to the presence of the GFP tag at the N-terminus of CDC-25.1. Intriguingly, LAP::CDC-25.1 is localised in the cytosol and nucleus of intestinal cells (Figure 6.3), whereas LAP::CDC-25.1(S46F) displays a mainly nuclear localisation in intestinal cells. This differential localisation was not observed in embryos during gastrulation (between 150 – 330 minutes post-fertilisation). Removal of LIN-23 promoted a shift of LAP::CDC-25.1 localisation to the nucleus and was not observed for LAP::CDC-25.1(S46F) (which was already nuclear prior to LIN-23 removal). This effect was only detected after gastrulation and maintained at least until the three-fold stage (only one focal plane of comma stage embryos are depicted in Figure 6.3). Thus, LIN-23 activity can influence the localisation of zygotically expressed LAP::CDC-25.1 by promoting its cytosolic localisation.

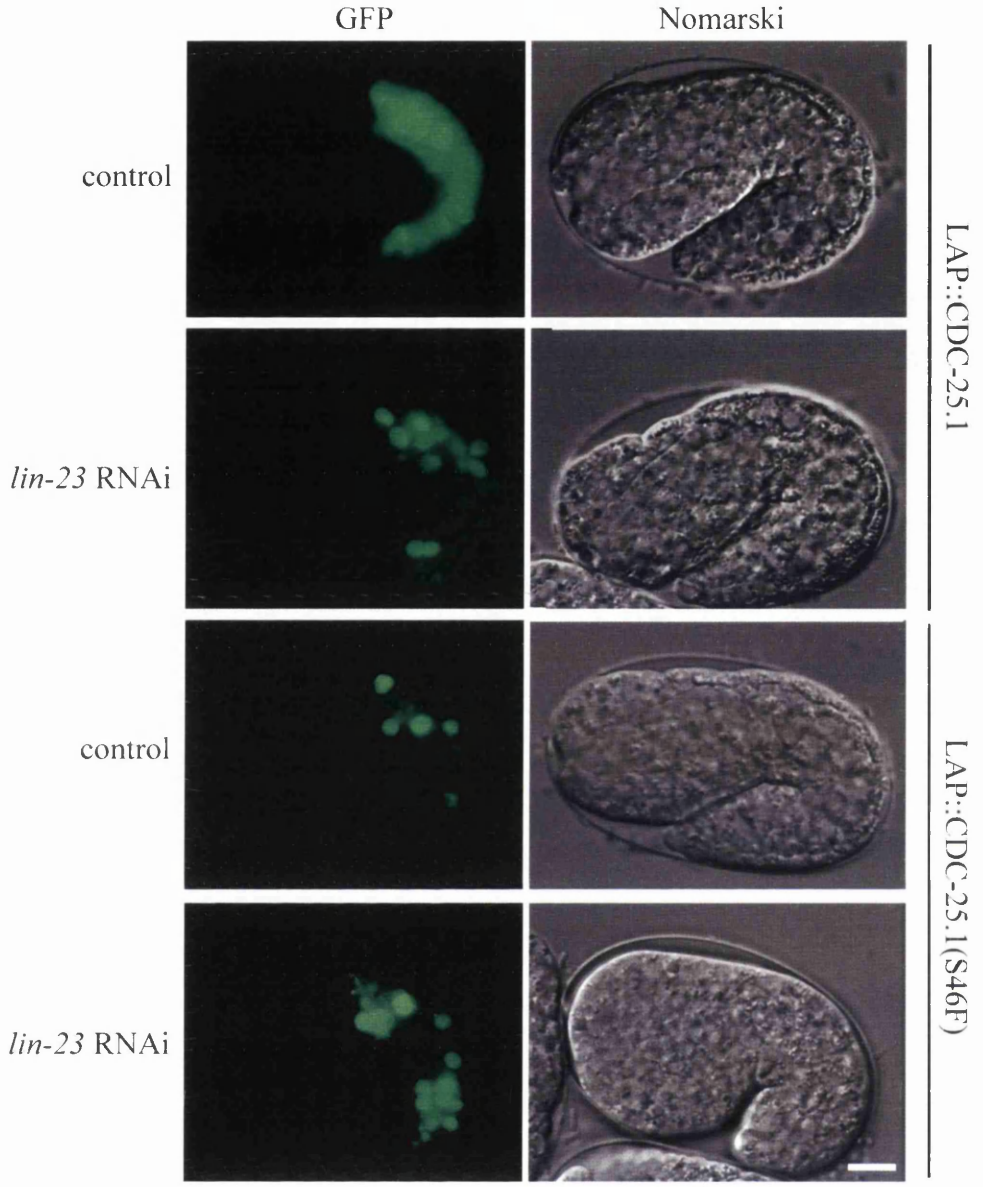

Figure 6.3 LAP::CDC-25.1 localisation is dependent on S46 and LIN-23. *C. elegans* strains IA535 *elt-2::LAP::cdc-25.1(+)* and IA536 *elt-2::LAP::cdc-25.1(ij48)* expressing LAP::CDC-25.1 and LAP::CDC-25.1(S46F) in intestinal cells, respectively were analysed for protein localisation through GFP fluorescence after control or *lin-23* RNAi. Scale bar: 10 μm.

6.3 Discussion

It was anticipated that LIN-23 is expressed in all embryonic blast cells from early to late stages of embryogenesis. In this chapter indirect immunofluorescence against LIN-23 validates this hypothesis. Moreover, it provides a platform to speculate further functions of LIN-23 for the regulation of CDC-25.1 and maybe other embryonic proteins, because removal of LIN-23 affects CDC-25.1 localisation. Furthermore, LIN-23 itself is redistributing between distinct cellular compartments during the cell cycle and thus may contribute to separate cell cycle functions.

6.3.1 LIN-23 expression in embryos

The ubiquitous expression of LIN-23 in all embryonic blast cells correlates with the phenotype of CDC-25.1 regulation. The CDC-25.1(S46F) protein level is elevated in all embryonic blast cells and not only in the intestine. Thus, the interaction between LIN-23 and CDC-25.1 takes place in probably all cells of the early embryo. Interestingly, LIN-23 is mainly localised to the cytosol in interphase, whereas a previous report (Ashcroft et al., 1999) and experiments performed in this study show that the main pool of CDC-25.1 localises to the nucleus at this stage. Thus, during interphase the majority of both proteins are separated into two distinct cellular compartments, however both proteins may be constantly shuttling between the nuclear and cytoplasmic compartment. CDC-25.1 leaves the nucleus during prophase. At this stage the majority of LIN-23 is still localised in the cytosol and a fraction of the protein wraps around the DNA in prometaphase, where it surrounds the DNA at the metaphase plate. Since no accumulation of CDC-25.1 at the metaphase DNA was previously reported, it is anticipated that the LIN-23 interaction with CDC-25.1 might take place in the cytosol, where the majority of LIN-23 is present throughout the cell cycle.

It is increasingly recognised in other systems that the localisation of the E3 ligase determines the site of protein degradation (Pines and Lindon, 2005). For example, in mammalian cells mitotic exit requires the presence of the anaphase-promoting complex or cyclosome (APC/C) at the central spindle where it regulates the degradation of its substrates like PLK1 (Kraft et al., 2003; Lindon and Pines, 2004; Tugendreich et al., 1995). Similarly, in yeast the SCF^{CDC4} complex is localised to the nucleus where is degrades the cyclin-dependent kinase inhibitor FAR1p. In response to pheromones, FAR1p leaves the

nucleus and is stabilised in the cytoplasm where it contributes to actin polarization (Blondel et al., 2000).

6.3.1.1 LIN-23 influences zygotically expressed CDC-25.1 localisation

Here, it is demonstrated that zygotically overexpressed and tagged CDC-25.1 shows differential localisation in intestinal cells that is dependent on S46 and the interaction with the E3 ligase LIN-23. S46F mutation in CDC-25.1 or LIN-23 knockdown cause nuclear accumulation of CDC-25.1, whereas in the presence of LIN-23 wild-type CDC-25.1 is present in both the nuclear and cytosolic compartment. This result suggests that LIN-23 interaction traps some CDC-25.1 in the cytosol and that in the absence of LIN-23, more CDC-25.1 protein is able to move to the nucleus. A similar mechanism has been reported for β–catenin, where overexpression of a dominant negative β-TrCP mutant, lacking the F-box domain, results in nuclear accumulation of β–catenin in human tissue culture cells (Sadot et al., 2000). Though the mutation does not abrogate β-TrCP interaction to the substrate (as is the case for the CDC-25.1(S46F) binding to LIN-23) but to the remaining SCF complex. In the case of CDC-25.1, it remains to be determined whether solely the binding to LIN-23 sequesters some portion of CDC-25.1 in the cytoplasmic compartment, or whether the downstream ubiquitination event is part of the cytoplasmic sequestration. Overexpression of a dominant negative LIN-23 mutant that retains its interaction with CDC-25.1 but lacks the F-box motif, and therefore would be impaired to target CDC-25.1 for ubiquitination in intestinal cells, could be performed by expression under the *elt-2* promoter. This allele could be combined with the *elt-2::LAP::cdc-25.1(+)* allele and the CDC-25.1 protein distribution analysed by live fluorescence imaging.

Nevertheless, it should be noted that here the ectopically overexpressed LAP::CDC-25.1 is analysed at a developmental stage when most of the endogenous CDC-25.1 is already degraded. It is therefore not clear to what extent this reflects the endogenous CDC-25.1 distribution. The majority of endogenous CDC-25.1 is localised to the nucleus in the interphase embryo (Ashcroft et al., 1999; Clucas, 2003; Clucas et al., 2002; Kostic and Roy, 2002). Furthermore, in the early embryo no difference in the localisation of endogenous CDC-25.1(S46F) and CDC-25.1 were observed. It is possible that, because early blast cells are in different stages of the cell cycle, changes in endogenous CDC-25.1 protein localisation might be difficult to detect.

The change in zygotic LAP::CDC-25.1 localisation was however only evident after the comma stage, around 450 minutes post-fertilisation when most intestinal cells have exited

the mitotic cycle (Sulston et al., 1983). Thus, it is possible that more cytoplasmic LAP::CDC-25.1 is only evident in post-mitotic cells than in mitotic cells. Though, importantly the staining pattern is sensitive to the presence and binding of LIN-23. Work in Chapter 4 has demonstrated that LAP::CDC-25.1 is still able to interact with LIN-23. Thus, the possibility remains that the endogenous interaction between LIN-23 and CDC-25.1 does occur in the cytosol.

6.3.1.2 How to set up a system to analyse the localisation of a LIN-23/CDC-25.1 complex

It is difficult to prove whether the binding between the LIN-23 and CDC-25.1 happens in the nucleus or in the cytosol. Cytosolic co-staining experiments may not prove very significant and have therefore been omitted. Generation of nuclear and cytoplasmic extracts is possible in embryos but requires some technical expertise to disrupt the eggshell sufficiently but not the nuclei (S. Kuersten pers. comm.). Additionally, the interaction between endogenous LIN-23 and CDC-25.1 is very weak and might be lost by further fractionation of the extracts. It would probably be more straightforward to co-express fluorescently tagged versions of LIN-23 and CDC-25.1 in human tissue culture cells, examine their temporal distribution throughout the cell cycle by real time imaging, and biochemical complex formation in nuclear and cytoplasmic extracts. This would allow testing mutants of CDC-25.1 that can be kept in the nuclear or cytoplasmic compartment of the cells and thus examine the influence of CDC-25.1 compartmentalisation on the complex formation between CDC-25.1 and LIN-23.

The CDC-25.1 protein contains several nuclear localisation sequences (NLS). NLS sequences are identified by a cluster of basic amino acids that resemble similarity to the monopartite NLS ($\underline{B}_4$, P($\underline{B}_3$X), P(XX$\underline{B}_3$X) or $\underline{B}_3$(H/P); where $\underline{B}$ stands for lysine or arginine, P for proline, H for histidine and X for any amino acid) or the bipartite NLS ($\underline{BB}X_{10}\underline{B}_3X_2$) driving transport of proteins into the nucleus (Macara, 2001). At least one putative monopartite NLS (aa 457 KKKR) and one putative bipartite NLS (aa 128 KRVMSERPTDNHRKRTS) are present in the CDC-25.1 sequence. Nuclear export of proteins is achieved by the presence of a leucine rich nuclear export signal in substrate molecules that are recognised by the nuclear export receptor (CRM1). A canonical nuclear export signal has been identified through analysis of a variety of substrate molecules and comprises the sequence $\underline{L}X_{2/3}$(FIVLM)$X_{1,2,3}\underline{L}X$(IVL) (L= leucine, F= phenylalanine, V= valine, M= methionine, X= any amino acid), however alterations of this signal have also been identified (Macara, 2001). CDC-25.1 contains one putative nuclear export signal in

its C-terminus (aa 553 IVQLGLQV), thus indicating that the protein might be actively exported to the cytoplasm.

Thus, mutational analysis of the putative NLS or NES sequence in CDC-25.1 could be performed and the localisation of the mutants studied in human tissue culture cells. This would determine whether it is possible to restrict CDC-25.1 to the nuclear or cytoplasmic compartment. The relevance of these experiments to the *C. elegans* system could be further tested. *C. elegans* could be microinjected with a GFP tagged version of an NLS or an NES mutant under the control of the *end-1* promoter. This allows temporal expression of CDC-25.1 in intestinal cells at a restricted time interval when the first E cell is generated until four intestinal cells are born (Maduro et al., 2007; Zhu et al., 1997). Real-time imaging could be performed to see whether the CDC-25.1 NLS and NES mutant are also localised to the cytoplasm and nucleus, respectively in *C. elegans* embryos. If so, the half-life of the nuclear or cytoplasmically restricted protein could be analysed *in vivo* by real-time imaging and quantification of the fading nuclear versus cytoplasmic GFP signal of CDC-25.1. This experiment would reveal two important points: firstly, whether the degradation of CDC-25.1 requires a nuclear/cytoplasmic shuttling in the *C. elegans* embryo. Secondly, it would determine, whether in *C. elegans* the majority of CDC-25.1 is degraded in the nuclear or the cytoplasmic compartment. Together with biochemical evidence of pull down experiments from nuclear and cytoplasmic tissue culture extracts (as proposed above), this would reveal substantial information whether the interaction between CDC-25.1 and LIN-23 occurs in the nucleus or rather in the cytosol as implied in this study. These experiments constitute a completely new part of the project and due to time restrictions have not been performed yet.

6.3.2 LIN-23 localisation is dynamic during the cell cycle

For the first time, a dynamic localisation of LIN-23 during the cell cycle in *C. elegans* embryos has been reported here. Previous reports analysing a LIN-23::GFP reporter suggested an overall cytoplasmic localisation for LIN-23 (Mehta et al., 2004), however movement of LIN-23 to the prometaphase nuclear compartment and association of LIN-23 to the metaphase plate has not been reported to date. But, the presence of a putative NLS in the LIN-23 sequence at the N-terminus (aa 160 - 174) was already proposed previously (Kipreos et al., 2000). However, it remains to be established whether this sequence in fact resembles a nuclear localisation signal or whether LIN-23 localisation to the vicinity of the DNA is due to passive diffusion and retention on the spindle apparatus at the time of nuclear envelope breakdown during prometaphase. The nuclear exclusion during telophase

and interphase might be the result of nuclear export through an NES signal in LIN-23. Bioinformatic analysis (according to the ELM server) reveals the presence of two putative NES signals in LIN-23 (aa 91 LVELILFNV, aa 177 LDQLILMHV) and it thus remains to be determined whether either of them contributes to the nuclear export of LIN-23.

6.3.2.1 Further LIN-23 functions in the embryo?

The dynamic behaviour of LIN-23 is intriguing, since it does not seem to correlate with the CDC-25.1 staining. No identical CDC-25.1 localisation on the centrosomes and metaphase plate has been reported and it implies the presence of maybe at least one other LIN-23 target substrate independent of CDC-25.1 in the *C. elegans* embryo. The human orthologue β-TrCP1 has been demonstrated to localise mainly in the nucleus with some cytoplasmic signal by overexpression studies (Davis et al., 2002; Lassot et al., 2001) and immunoblotting of the endogenous protein in nuclear and cytoplasmic extracts of human tissue culture cells (Davis et al., 2002). However, the human β-TrCP2 protein localises mainly to the cytoplasm in tissue culture cells when overexpressed (Davis et al., 2002). Unfortunately, data regarding the β-TrCP distribution during the cell cycle remain lacking. Furthermore, it remains to be elucidated whether overexpression studies in tissue culture cells accurately reflect the localisation of endogenous β-TrCP1/2 in a multicellular organism. Nevertheless, the data suggest that LIN-23 might have retained the ability to fulfil several cellular functions that later in evolution have diversified to two separate genes.

6.3.2.2 Does LIN-23 function during centrosome duplication?

In this study, a slight concentration of LIN-23 around the centrosome in interphase cells has been identified. This finding is not entirely surprising, since the pericentrosomal area has been reported to act as proteolytic centres within the eukaryotic cell. Treatment of proteasome inhibitors in mammalian cells resulted in accumulation of ubiquitinated proteins in the centrosomal area (Wojcik, 1997; Wojcik et al., 1996) and purification of centrososome preparations have been demonstrated to contain active proteasomes (Fabunmi et al., 2000; Wigley et al., 1999). At the onset of mitosis centrosome duplication takes place, the centrosomes subsequently move around the nucleus in order to establish two separate spindle poles from which the bipolar spindle originates during prometaphase (Scholey et al., 2003). The *Drosophila* LIN-23 orthologue, termed SLIMB, has been demonstrated to play a role during centrosome duplication. A hypomorphic *slimb* mutant has been reported to display centrosome duplication defects, but spindle formation is

otherwise normal (Wojcik et al., 2000). Similarly, mouse embryonic fibroblasts derived from β-TrCP1 knockout mice show centrosome overduplication, and formation of multipolar spindles that nucleate from these centrosomes (Guardavaccaro et al., 2003). The molecular mechanism underlying these defects remains to be identified but might involve the APC/C inhibitor EMI1 (Early Mitotic Inhibitor) as proposed by Guardavaccaro et al., because EMI1 is a target of β-TrCP and overexpression of EMI1 results in centrososome overduplication. Unfortunately, data describing whether removal of EMI1 could rescue the overduplication of β-TrCP1 null fibroblasts was lacking in that study and thus other targets such as cyclins, CDKs or CDC25 could be involved in this process.

Real-time imaging and analysis of the spindle formation using the GFP::β-TUBULIN strain after *lin-23* RNAi showed no overt spindle formation defects in the early one- to four-cell stage embryo (data not shown). It remains therefore to be elucidated whether *lin-23* RNAi results in centrosome duplication defects in *C. elegans*. This could be performed by observing centrosome duplication in a GFP::γ-TUBULIN marker strain (Strome et al., 2001) after *lin-23* RNAi.

6.3.2.3 Does LIN-23 function during metaphase-to-anaphase transition?

Interestingly, a portion of LIN-23 associates to the vicinity of the DNA during prometaphase and wraps around the metaphase plate, indicating that a fraction of the protein may participate at the metaphase-to-anaphase transition. The eukaryotic cell cycle requires the function of the anaphase-promoting complex/cyclosome (APC/C) at prometaphase in order to separate two aligned chromatids and progress into anaphase (reviewed in (Yu, 2002)). Members of the APC/C complex have also been identified in *C. elegans* and shown to be implicated in mitotic divisions (reviewed in (Yeong, 2004)). One mechanism of APC/C inactivation is through the binding of the EMI1 protein in mammalian cells (Hsu et al., 2002; Miller et al., 2006; Reimann et al., 2001a; Reimann et al., 2001b). β-TrCP plays a role in degradation of EMI1, thereby contributing to the activation of the APC/C complex (Hansen et al., 2004; Margottin-Goguet et al., 2003). However, no obvious EMI1 homologue is evident in the *C. elegans* genome by BLAST search analysis, suggesting that, either this process is not conserved or another downstream target is responsible for this action. Should this pathway be conserved, knockdown of LIN-23 would be expected to result in increased anaphase arrest due to the stabilisation of an 'EMI1-like' molecule. However, real-time imaging of a strain carrying GFP labelled HISTONE and β-TUBULIN showed no apparent defects in early one- to four-cell stage

embryos after *lin-23* RNAi (data not shown). Thus, this could reveal that LIN-23 is not involved in analogous pathway in the early *C. elegans* embryo or that LIN-23 function is redundant and can be performed by any of the remaining 326 F-box proteins present in the *C. elegans* genome.

The timely localisation of LIN-23 to the periphery of the metaphase plate resembles strong similarity to the staining of *C. elegans* proteins that are involved in the spindle checkpoint response. The proteins BUB-1 (Desai et al., 2003; Encalada et al., 2005; Oegema et al., 2001), SAN-1 (Nystul et al., 2003), MDF-1 and MDF-2 (Kitagawa and Rose, 1999; Nystul et al., 2003) have been localised to the metaphase plate in early embryos. BUB-1, MDF-1 and MDF-2 have been demonstrated to prevent delay of anaphase onset under conditions of spindle defects (Encalada et al., 2005) and similarly MDF-2 and SAN-1 knockdown by RNAi cause defects in metaphase arrest during anoxia but not under normal conditions (Nystul et al., 2003). Thus, LIN-23 could act to regulate the degradation of a factor involved in the metaphase-to-anaphase transition in response to cellular stress or spindle abnormalities. Accordingly, *lin-23* RNAi has not revealed any obvious defects in metaphase-to-anaphase transitions in the early embryo when examined for chromosome segregation and spindle formation under normal conditions (data not shown). Thus, analysis of *lin-23* RNAi in spindle defect mutants or by treatment of the embryos with a microtubule depolymerising agent as performed in a previous study (Encalada et al., 2005) could reveal whether LIN-23 is required to restrain the metaphase-to-anaphase transition or can result in chromosome segregation defects under such conditions. Importantly, the dynamic localisation of LIN-23 displayed in this work unravels a potentially new function of LIN-23 during embryogenesis, but further work is required to substantiate this hypothesis.

6.3.3 Conclusion

Endogenous LIN-23 protein is localised to the cytosol of all embryonic blast cells from early to late stages of embryogenesis. Zygotic CDC-25.1 protein localisation to the nucleus is enhanced in the absence of LIN-23, thus suggesting that LIN-23 retains a portion of CDC-25.1 in the cytosol. During the cell cycle, a fraction of LIN-23 associates to the vicinity of the centrosomes and the protein enters the nuclear space at prometaphase to surround the DNA on the metaphase plate, proposing a potential function of LIN-23 during the metaphase-to-anaphase transition of the *C. elegans* embryonic cell cycle.

Chapter 7

LIN-62 and CDC-25.1 interaction

7 LIN-62 and CDC-25.1 interaction

7.1 Introduction

One interesting conclusion that has arisen from my studies is the fact that global elevation of CDC-25.1 protein levels in all blast cells at a defined stage of embryogenesis (namely between the 10- to 60-cell stage) results in the tissue-specific hyperproliferation of intestinal cells. Previous data established that the *cdc-25.1(ij48)* allele causes a tissue-specific hyperplasia of the intestine, which is in stark contrast to RNAi results that revealed that depletion of *cdc-25.1* from the embryo resulted in embryonic death (Ashcroft et al., 1999; Clucas, 2003; Clucas et al., 2002; Kostic and Roy, 2002) with concomitant decrease of proliferation in additional tissues (Clucas, 2003; Clucas et al., 2002) indicating that CDC-25.1 function is required in all blast cells of the early embryo. CDC-25.1 protein analysis as detected by anti-CDC-25.1 immunofluorescence showed no obvious difference for the CDC-25.1 protein levels or protein distribution (Clucas et al., 2002).

In this study, it has become apparent that the *cdc-25.1(ij48)* allele results in a global increase of CDC-25.1(S46F) in all blast cells during the 10- to 60-cell stage of embryogenesis as compared to the wild-type levels by escaping the negative regulation of LIN-23 (see Chapter 3 and 4). This phenotype is consistent with previous data on the *cdc-25.1(ij48)* allele, however the general increase of the CDC-25.1 protein levels in all blast cells does still not explain the tissue-specific nature of the *cdc-25.1(ij48)* allele.

Hence, I hypothesised that during *C. elegans* embryogenesis non-intestinal tissues might possess additional negative regulators of the cell cycle that restrain proliferation of such tissues. This might imply that the mechanism underlying intestinal cell proliferation is simpler than that of non-intestinal tissues, making the intestinal cells more susceptible to respond to increased CDC-25.1 protein levels than other tissues. This could be explained if a negative regulator is simply more active in non-intestinal tissues or a negative regulator is missing in intestinal cells. One way to determine whether such a scenario might in fact be the case, is to analyse whether mutations of factors that regulate proliferation of other tissues are lethal when combined with the *cdc-25.1(ij48)* mutant. This would imply that factors, such as negative regulators of the cell cycle in other tissues become crucial for proliferation only when combined with *cdc-25.1(ij48)*. Such a factor might on its own exhibit a hyperproliferation phenotype when mutated, or it may only exhibit a proliferation phenotype when combined with *cdc-25.1(ij48)* (see Model in Figure 7.1).

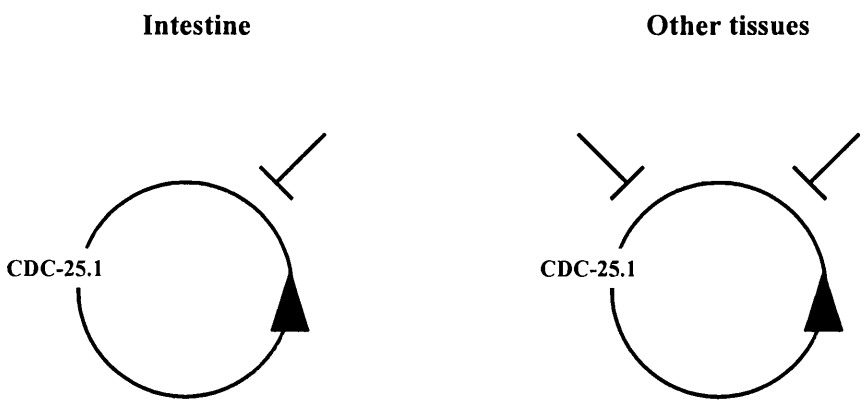

Figure 7.1 Model for tissue-specific cell cycle regulation.

Intestinal cell proliferation (circle) is dependent on CDC-25.1 activity and under the control of a negative regulator (blocked arrow). The same pathway is found in surrounding tissues, but those have at least one more negative regulator to restrain proliferation. A gain-of-function mutation in *cdc-25.1* would affect proliferation of intestinal cells only by overriding a single negative regulator, whereas it would not affect other tissues due to the presence of a second negative regulator. Mutation in the negative regulator common to intestinal and other tissues, may affect intestinal cell proliferation but not proliferation of other tissues when mutated on its own. Co-mutation of *cdc-25.1* and the common negative regulator may be sufficient to overcome the second negative regulation and induce hyperproliferation of the intestine and other tissues.

Interest was thus drawn to *lin-62(ij52),* a mutant allele that had recently been discovered in the same mutant screen that identified altered numbers of intestinal nuclei in the *cdc-25.1(ij48)* mutant and displayed a similar phenotype (Clucas, 2003; Clucas et al., 2002). This allele has previously been suggested to act as a negative regulator of the cell cycle and was proposed to potentially play a role in regulation of intestinal cell proliferation but maybe also proliferation of non-intestinal tissues, which would be consistent with model described above (Figure 7.1).

The *lin-62(ij52)* allele had not been cloned at the start of this study, but its phenotype was partially characterised and is introduced below according to (Clucas, 2003; Clucas et al., 2002). Like *cdc-25.1(ij48)* mutants, *lin-62(ij52)* mutants exhibit extra numbers of intestinal nuclei. Immunostaining of intestinal cell boundaries as well as cell lineage analysis revealed that the extra intestinal nuclei observed during post-embryonic development in the initial screen, were the result of additional cell proliferations during embryonic development of the intestine, similar to *cdc-25.1(ij48).* However, unlike the semi-dominant maternal effect mutation of *cdc-25.1(ij48)*, the *lin-62(ij52)* allele is recessive over wild-type and acts zygotically. This was demonstrated by the fact that when homozygous *lin-62(ij52)* mutants were crossed with wild-type males, all outcrossed F1 offspring exhibited

the wild-type phenotype. Furthermore, *lin-62(ij52)/+* hermaphrodites produced a Mendelian 1:2:1 frequency of the Lin phenotype in their offspring. Homozygous *lin-62(ij52)* however, do not show a 100% penetrance of the Lin phenotype. Germline proliferation appears to be unaffected and is thus similar to *cdc-25.1(ij48)* mutants, but *lin-62(ij52)* homozygotes display a strong tail morphology defect that becomes apparent during post-embryonic development. Thus, LIN-62 might be regulating proliferation of other tissues apart from the intestine. Although cell lineage analysis illustrates proliferation defects of the intestine, other tissues were not examined for lineage defects in that experiment.

The position of this allele had been mapped to around +3.3 on chromosome IV based on STS and multi-factor crosses. STS mapping placed *lin-62(ij52)* into close proximity of the sequence polymorphism stP44 which is found on position +3.27 (WormBase, 2007). Further refinement of the position using multi-factor crosses placed the allele to position + 3.37 between *bli-6* (+3.19) and *unc-24* (+3.52). Positioning was confirmed by crossing the allele over several deficiencies. Only progenies derived from crosses with stDf7 and stDf8 covering the regions +2.48 - +3.40 and +2.48 - +3.39, respectively displayed Lin phenotypes in their brood indicating that *lin-62(ij52)* must be contained within these deficiencies. The recessive action of the *lin-62(ij52)* allele to the wild-type and the fact that loss of *lin-62* function when placed over a deficiency display hyperplasia, demonstrated that *lin-62(ij52)* is a hypomorphic allele. Continued propagation of the *lin-62(ij52)/stDf7* and *lin-62(ij52)/stDf8* heterozygotes proved problematic and a new phenotype of dead larvae was observed amongst the F1 progeny of the crosses, indicating that *lin-62(ij52)* may not be a null allele (Clucas, 2003).

Hence, these results suggested a negative function for *lin-62* during cell proliferation of the intestine and maybe additional tissues. As such *lin-62* could be an auxiliary negative regulator of the cell cycle found in the intestine and maybe other tissues. Nevertheless, the similar hyperplasia phenotype of *lin-62(ij52)* and the *cdc-25.1(ij48)* mutant could also suggest that *lin-62* may regulate *cdc-25.1* through the site of the *ij48* lesion. As described in the previous chapters, the site of the *ij48* lesion introduces a serine to phenylalanine substitution in a conserved DSG consensus site of CDC-25.1 and abrogates binding of CDC-25.1 to the F-box molecule LIN-23, the *C. elegans* homologue of mammalian β-TrCP. This results in the escape of CDC-25.1(S46F) from proteasomal degradation mediated through LIN-23. In mammalian systems phosphorylation of the serine residue within this motif is essential for β-TrCP recognition and the kinases involved in this process differ between different target molecules (see Chapter 3, (3.1.2.2)). Although the

S46 in CDC-25.1 falls within a putative GSK-3 consensus, the data presented in this study argue strongly that GSK-3 is not the kinase involved in the regulation of S46 in CDC-25.1. Removal of the kinase acting through the site of S46 would be expected to enhance CDC-25.1 protein levels due to the escape of CDC-25.1 from the negative regulation of LIN-23. However, no increase in CDC-25.1 protein levels was obtained when GSK-3 was depleted from the embryo by RNAi (see Chapter 3, (3.2.10)). Thus, identification of the kinase that can modify the site of the *ij48* lesion is an important task.

7.1.1 Hypothesis and aims

The similar intestinal hyperproliferation phenotype of *lin-62(ij52)* and *cdc-25.1(ij48)* suggests that LIN-62 might negatively regulate CDC-25.1 either through S46 or independent of S46, or that LIN-62 might regulate the cell cycle independent of CDC-25.1 in intestinal cells.

In the case that LIN-62 acts on S46 in CDC-25.1 a combination of the *lin-62(ij52)* and *cdc-25.1(ij48)* mutant alleles would be predicted to display no synergism in their phenotypes. Furthermore, mutation of *lin-62(ij52)* would result in a CDC-25.1 protein increase similar to CDC-25.1(S46F). In order to determine whether *lin-62* can enhance the *cdc-25.1(ij48)* proliferative effect in the intestine or other tissues, or whether it regulates *cdc-25.1* on the site of the *ij48* lesion, a double mutant of the *cdc-25.1(ij48)* and *lin-62(ij52)* was to be employed and further attempts undertaken to clone the *lin-62(ij52)* allele. Additionally, it became apparent that establishing a genetic system for future investigations that would facilitate the genome-wide identification of genes that show strong synergism, or even synthetic lethality only when combined with the *cdc-25.1(ij48)* allele, would be of extremely high value. It would allow the identification of further negative regulators in other tissues that are only sick or lethal when combined with the *cdc-25.1(ij48)* mutation, but not on their own. This could be achieved by creating a strain that contains the intestinal *elt-2::GFP* together with the *cdc-25.1(ij48)* allele on a complex free array, allowing expression of the allele in the germline. Thus, the presence of the *cdc-25.1(ij48)* allele would be 'labelled' with the GFP marker. Due to the maternal *cdc-25.1(ij48)* function all F1 progeny containing the free array will display the hyperplasia phenotype. However, some animals that will have lost the array and will therefore not contain the *cdc-25.1(ij48)* allele and the GFP marker could be analysed at the same time. If a genome-wide RNAi screen was to be carried out at later times, it would allow to select for worm populations that propagate GFP-negative and thus wild-type animals, but contain dead GFP-positive and thereby *cdc-25.1(ij48)* containing embryos in their brood. Thus, this would allow

identification of maternal or zygotically acting genes that negatively regulate the cell cycle independent from *cdc-25.1(ij48)*.

In order to test whether this system could be utilised to detect any additive phenotype, a strain carrying *cdc-25.1(ij48)* and *elt-2::GFP::LacZ* on a complex free array was generated and utilised here to determine its genetic interaction with *lin-62(ij52)*. Furthermore, Western blots were carried out in a *lin-62(ij52)* mutant compared to wild-type in order to determine whether *lin-62(ij52)* can act to stabilise CDC-25.1.

7.2 Results

7.2.1 lin-62(ij52) and cdc-25.1(ij48) genetic interaction

To test for a genetic interaction between *cdc-25.1(ij48)* and *lin-62(ij52)* a new *lin-62(ij52)* marker strain was generated that allowed identification of the *lin-62(ij52)* allele independent of the *lin-62(ij52)* phenotype. This strain (IA577 see Table 7.2) carries a post-embryonic intestinal-specific GFP marker in order to differentiate it from the *elt-2::GFP* that was subsequently to be employed to 'label' the presence of the *cdc-25.1(ij48)* allele in the cross. To generate the *lin-62(ij52)* marker strain the strain IA331 *lin-62(ij52)*, derived from a frozen stock that had been outcrossed three times after EMS mutagenesis against a wild-type N2 Bristol, was crossed with the strain JR1990 *wIs118* containing *npa-1::GFP::LacZ.* This marker displays GFP expression in intestinal nuclei starting during late embryonic development and is easily visible during post-embryonic development. The presence of *lin-62(ij52)* was determined by the hyperplasia of the intestine in the F2 brood. Only homozygous *lin-62(ij52)* animals display hyperplasia of the intestine as examined by fluorescence of the intestinal GFP reporter *wIs118* in this strain (data not shown). Since the *lin-62(ij52)* allele is not yet cloned but the mutation mapped to approximately position + 3.3 on chromosome IV, a second mutation was introduced on chromosome IV to create a chromosomal marker strain. *dpy-20(e1282)* was utilised because it localises to position + 5.18 on chromosome IV and gives animals a dumpy (Dpy) appearance when homozygous; a phenotype easily scored under a dissecting microscope. Homozygosity of the *lin-62(ij52)* allele could be followed by the hyperplasia that is caused through this mutation only when homozygous (Clucas et al., 2002).

Embryonic death in this strain (IA577) was analysed after backcrossing with an N2 Bristol strain in order to examine whether any reciprocal translocation could have been introduced through the GFP allele integration or the additional *dpy-20(1282)* cross and could result in

aneuploidy of the offspring. However, this strain appeared to be relatively healthy as it produced on average 4.4% embryonic death (Table 7.1).

Strain	% death
IA577 *lin-62(ij52) dpy-20(e1282)IV; wIS118* (in F2 coming from N2 cross)	4.4 ± 5.0 (1.3 - 7.4) (n=364, 13 F1)
IA575 *ijEx36[cdc-25.1(ij48), wIs84]* in F1	11.7 ± 13.4 (2.8 - 20.9) (n= 410, 11 P_0)

Table 7.1 Embryonic lethality of IA577 and IA575. Mean ± s.d. (95% upper and lower confidence interval). p-value; n.s., one-tailed Student's *t* test.

To test for a genetic interaction between *cdc-25.1* and *lin-62,* heterozygous *lin-62(ij52) dpy-20(1282)/++ IV* males were crossed into wild-type hermaphrodites carrying a *cdc-25.1(ij48)* and *elt-2::GFP::LacZ* reporter on a complex free array. This array had previously been reported to partially complement a *cdc-25.1(nr2036)* null allele (Clucas, 2003) and the strain used here was derived by outcrossing the *cdc-25.1(nr2036)* null allele from the original strain and selecting for GFP-positive hermaphrodites expressing *cdc-25.1(ij48)* on a complex array (IA575). The complex array was utilised, because genes expressed from a repetitive array are often silenced in the germline and thus would not allow to analyse for the maternally acting *cdc-25.1* effects (Kelly et al., 1997). The IA575 strain displays robust early onset of the *elt-2::GFP::LacZ* that is switched on at the two E-cell stage and becomes strongly visible under the microscope when about 10 E cells are born and is clearly distinguishable from the late expression of the *npa-1::GFP::LacZ* expression present in the *lin-62(ij52)* marker strain. All animals carrying the array were GFP-positive due to the expression of the *elt-2::GFP* transgene and displayed intestinal hyperplasia evident for the maternal effect of CDC-25.1(S46F). Thus, due to the maternal function of *cdc-25.1(ij48)* all F1 animals possessed intestinal hyperplasia and could potentially show lethality in combination with the heterozygous *lin-62(ij52)* allele.

Only GFP-positive F1 animals that displayed strong hyperplasia and were thereby positive for the *cdc-25(ij48)* transgene were analysed for the presence of the *lin-62(ij52) dpy-20(e1282)* allele in their offspring. A strain was generated that segregated 18% Dpy phenotype in the F2 generation (Table 7.2). The GFP-positive Dpy animals, thus carrying the *cdc-25.1(ij48)* array and the homozygous *lin-62(ij52)* allele were examined further. The presence of the *ij48* allele in GFP-positive hermaphrodites was confirmed by single worm PCR and analysis of a restriction site polymorphism that is introduced through the mutation (Figure 7.2, A). To analyse whether there is an enhanced lethality between maternally provided *cdc-25(ij48)* and homozygous *lin-62(ij52)* all Dpy animals were analysed for the occurrence of GFP in their offspring and the lethality determined. Thus, if Dpy animals lost the *cdc-25(ij48)* allele at higher frequency than the non-Dpy animals it

would indicate a degree of lethality. This was not the case, on average 80.8% of the animals retain the GFP among the Dpy animals whereas the original *cdc-25.1(ij48)* strain keeps the GFP at a frequency of 75% (p-value: n.s., one-tailed Student's *t* test, Table 7.2) . An average death rate for GFP-positive animals was found to be 26.7%, whereas Dpy animals that had lost the array and were homozygous for the *lin-62* mutation were segregating 19% death (p-value: n.s., one-tailed Student's *t* test, Table 7.2).

IA577 *lin-62(ij52) dpy-20 (e1282) wIs118 [npa-1::GFP::LacZ]* x IA575 N2 *[cdc-25(ij48) elt-2::GFP::LacZ]*	
% Dpy in F2	18 (n=73)
% embryonic death among Dpys in F4	29.2 ± 16.7 (19.1 – 39.3) (n=679, 13 F3)
% GFP^+ in Dpys	80.8 ± 10.4 (n=442, 15 F3, all F3 contain *cdc-25.1(ij48)* confirmed by single worm PCR)
% Lin in GFP^+	98.8 ± 15.2 (n=335, 15 F3)
lin-62(ij52) dpy-20(e1282)* (GFP⁻ F3 from cross) x JR1990 *wIs118 [npa-1::GFP::LacZ]	
% segregating Dpy/Lin	100 (20 F1)
% Dpy/Lin/F2	22 ± 5.3
% Lin among Dpys	100
***lin-62(ij52) dpy-20 (e1282)* (GFP⁻ F3 from cross)**	
% embryonic death in F1	19.7 ± 10.7 (11.4 – 27.9) (n=279, 9 F3)
IA575 *ijEx36[cdc-25.1(ij48), wIs84[elt-2::GFP::LacZ]*	
% GFP^+ in F1	75.4 ± 15.1

Table 7.2 A genetic cross between *lin-62(ij52)* and *cdc-25.1(ij48)*. Mean ± s.d. (95% upper and lower confidence interval). p-value for embryonic lethality of GFP^+ versus GFP^- Dpy animals: > 0.05 (one-tailed Student's *t*- test).

To eliminate the possibility that a recombination event created a *lin-62(ij52) dpy-20(e1282)/+ dpy-20(e1282)* animal (i.e. an animal that has dumpy appearance but is heterozygous for the *lin-62(ij52)* allele) GFP-negative animals from the F3 Dpy brood were selected to ensure loss of the *cdc-25(ij48)* allele and crossed into the *npa-1::LacZ::GFP* intestinal-specific GFP marker strain JR1990 *wIs118* (Table 7.2). Since the *lin-62(ij52)* allele acts recessively and zygotically, if no recombination event had occurred F2 generations should contain 25% Dpy animals in their brood that are also *lin-62(ij52)/lin-62(ij52)* (which can be observed by the presence of intestinal hyperplasia). Of 20 F1 broods analysed, all segregated on average 22% Dpy in their F2 brood and were also *lin-62(ij52)/lin-62(ij52)* due to the fact that they all displayed intestinal hyperplasia (Table 7.2). Hence, it was possible to obtain a strain that is homozygous for *lin-62(ij52)* and carries the *cdc-25.1(ij48)* on a complex free array indicating that there is no synthetic lethality between *cdc-25.1(ij48)* and *lin-62(ij52)* in this genetic context.

This result suggested that *lin-62* may act through the *ij48* lesion on *cdc-25.1*. This was determined by testing whether there is an accumulative effect in the *lin-62(ij52) dpy-20(e1282)/lin-62(ij52) dpy-20(e1282)* strain that also carries *cdc-25(ij48)*. Intestinal numbers of nuclei were counted by examining the expression of the embryonic *elt-2::GFP* marker only in embryos displaying intestinal hyperplasia. The *lin-62(ij52) dpy-20(e1282)* strain IA545 resulted in an almost identical number of intestinal cells as compared to the IA526 *lin-62(ij52)* strain on its own (Table 7.3), indicating that no additional mutation was introduced through the recombination of *lin-62(ij52)* with *dpy-20(e1282)* that could generate additional intestinal nuclei. Intriguingly, a significant increase in the *lin-62(ij52) cdc-25.1(ij48)* double mutant compared to each single mutant *lin-62(ij52)*, *cdc-25.1(ij48)* (Table 7.3) was detected, indicating that *lin-62* can act independently of the *ij48* allele in *cdc-25.1*.

Strain	**Intestinal nuclei/ embryo**	**p-value vs. *lin-62 (ij52)***	**p-value vs *cdc-25.1(ij48)***
IA526 *lin-62(ij52) wIs84[elt2::GFP::LacZ, rol-6(su 1006dm)]*	29.4 ± 4.1 (n=69)	-	-
IA545 *lin-62(ij52) dpy-20 (e1282)IV wIs84[elt2::GFP::LacZ, rol-6(su 1006dm)]*	30.0 ± 4.2 (n=69)	-	n.s.
IA575 N2 *[cdc-25.1(ij48) elt-2::GFP::LacZ]*	28.9 ± 4.1 (n=92)	n.s.	-
IA585 *lin-62(ij52) dpy-20 (e1282)IV [cdc-25(ij48) elt-2::GFP::LacZ]*	37.2 ± 4.8 (n=79)	< 0.001	< 0.001

Table 7.3 Comparison of intestinal nuclei of *lin-62(ij52)* and *cdc-25.1(ij48)* single and double mutants. Intestinal numbers were analysed after incubation of the strains at 20°C. Two-tailed Student's *t*-test.

7.2.2 lin-62(ij52) does not affect the stability of CDC-25.1 in embryos

The additive effect on the number of intestinal nuclei seen through the combination of *lin-62(ij52)* with *cdc-25.1(ij48)* suggested that *lin-62(ij52)* may act on the cell cycle independent of the *ij48* lesion in *cdc-25.1*. Previous data however had revealed that *lin-62(ij52)* cannot bypass the *cdc-25.1* function. This was illustrated by the fact that when RNAi against *cdc-25.1* was performed in the *lin-62(ij52)* mutant background compared to a wild-type strain, no increase was observed for the intestinal cell numbers (Segref and Johnstone, 2004). This result could suggest that *lin-62(ij52)* requires the prior function of *cdc-25.1* within another stage of the cell cycle or that *lin-62(ij52)* acts on *cdc-25.1*.

Since the molecular mechanism underlying the *ij48* mutation in *cdc-25.1* has only become apparent in this study, it allowed me to perform another simple test to examine, whether *lin-62(ij52)* acts as a negative regulator through the *ij48* lesion in *cdc-25.1*. As illustrated in previous chapters, *cdc-25.1(ij48)* mutants show an increase in the CDC-25.1(S46F) protein levels as compared to CDC-25.1 in the early embryo. The site of the *ij48* mutation introduces a serine to phenylalanine substitution in the conserved DSG consensus site which acts as a scaffold for the protein degradation machinery and is recognised by LIN-23. Phosphorylation of the serine is a prerequisite for β-TrCP interaction in higher eukaryotes and thus, the possibility remains that *lin-62* might be involved in phosphorylation of S46 in CDC-25.1 (see 7.1). Thus if LIN-62 phosphorylates CDC-25.1 on S46, removal or mutation of LIN-62 would be predicted to enhance CDC-25.1 protein levels similar to the enhanced protein levels of CDC-25.1(S46F).

To test this possibility, embryonic extracts from *C. elegans* strains derived from the wild-type strain JR1838 *wIs84* and IA526 *lin-62(ij52) wIs84* were prepared and CDC-25.1 protein levels compared by Western blotting. As can be seen in Figure 7.2 (panel B), equal amounts of total protein were applied to 10% SDS-PAGE as determined by Western blotting against β-ACTIN as loading control. However, CDC-25.1 protein levels remain similar in both cases. The protein extraction was only performed once and protein samples loaded repeatedly on a 10% SDS polyacrylamide gel, only one sample loading is depicted (Figure 7.2, B) for simplicity. This result is rather clear and controlled in itself through β-ACTIN comparison and compared to embryonic extracts of a *cdc-25.1(ij48)* allele (see Chapter 3, Figure 3.5) that consistently show a high increase in CDC-25.1(S46F) protein levels. Thus, it can be concluded that *lin-62(ij52)* is not acting on the stability of CDC-25.1 through S46.

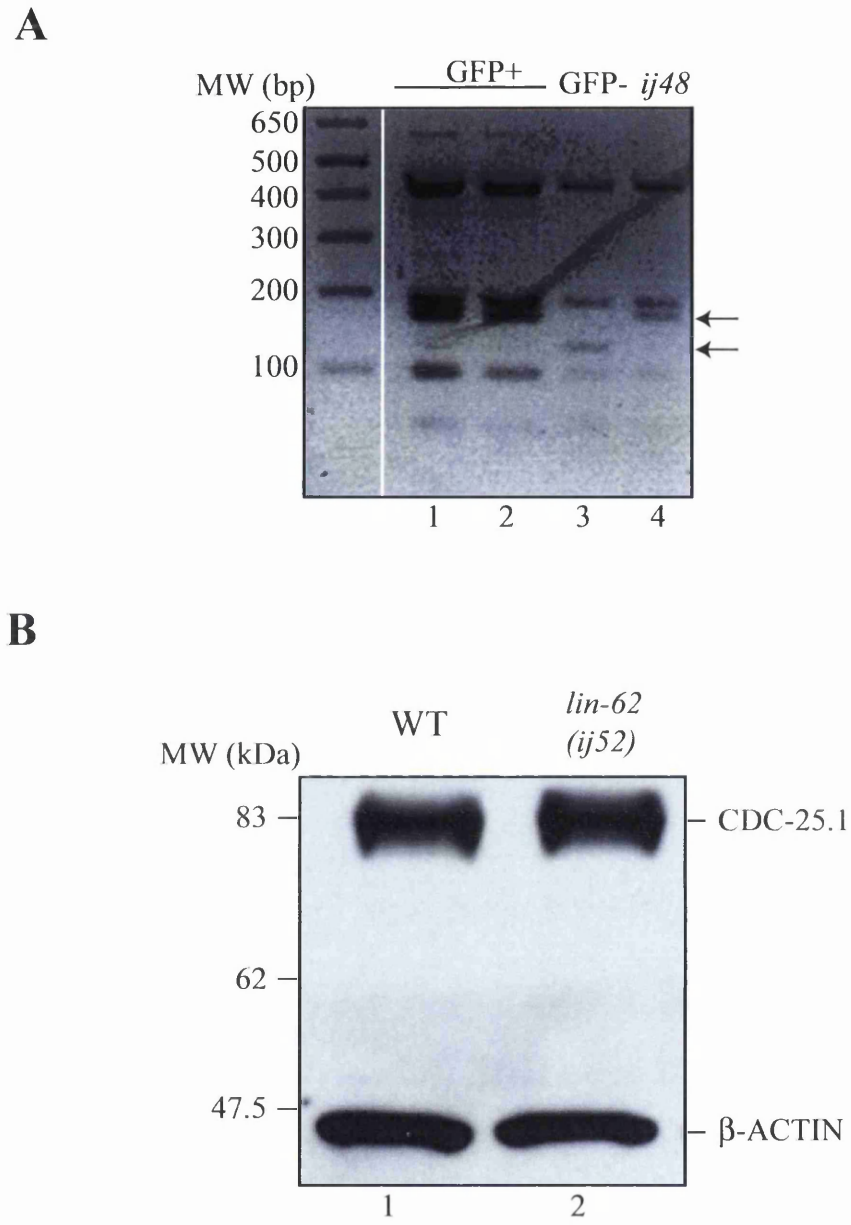

Figure 7.2 Analysis of *lin-62(ij52) cdc-25.1(ij48)* mutants. A) Single worm PCR and restriction site polymorphism to detect the presence of the *cdc-25.1(ij48)* allele in GFP -positive F3 hermaphrodites coming from the IA577 *lin-62(ij52) dpy-20(e1282)* cross with IA575 *[cdc-25.1(ij48), elt-2::GFP::LacZ].* DNA of GFP-positive Dpy animals containing *cdc-25.1(ij48)* with *elt-2::GFP* on a complex array (GFP+, lanes 1 and 2) were analysed on a 1.8% agarose gel next to DNA of animals that were Dpy but had lost the complex array (GFP-, lane 3) or as a positive control IA530 containing the integrated homozygous *cdc-25.1(ij48)* allele (*ij48*, lane 4). A 126 pb band present in GFP-negative, thus *cdc-25.1* animals, is shifted to 168 bp in a homozygous *cdc-25.1(ij48)* or GFP-positive hermaphrodites as indicated by arrows. For precise information on restriction fragment sizes see Chapter 2 (2.2.6.5). **B)** Embryo extracts derived from the strain JR1838 (WT) or IA529 *lin-62(ij52)* were applied to 10% SDS-PAGE followed by Western blotting against CDC-25.1 (anti-CDC-25.1A) and β-ACTIN.

7.2.3 lin-62(ij52) mapping

Attempts were made to further map the precise position of the *lin-62(ij52)* mutant. Previous mapping studies using a combined approach of three-factor- and STS mapping (Clucas, 2003)) have placed the mutation at the approximate position of +3.3 between *bli-6* (+3.19) and *unc-24* (+3.52) on chromosome IV. In order to verify these data and refine the position further, the recombination events between *lin-62(ij52)*, *unc-8(e49)* (+3.29) and *dpy-20(e1282)* (+5.18) were examined. This was achieved by crossing hermaphrodites of the newly generated strain IA526 *lin-62(ij52)IV; wIs84 [elt-2::GFP::LacZ rol-6(su1006)]* into heterozygous DR439 *unc-8(e49) dpy-20(e1282)IV* males and observing segregation of *lin-62(ij52)* phenotype in Dpy-non-Unc recombinant animals of the F3 generation. During the cross it became apparent that is was almost impossible to determine the Lin phenotype when the *rol-6(su1006)* mutation (introduced through the *elt-2::GFP* marker of the initial *lin-62(ij52)* strain IA526) was combined with *unc-8(e49).* However, Dpy recombinants allowed a very clear discrimination between Lin and wild-type phenotypes even in the presence of the *rol-6* mutation. Thus, Dpy-non-Unc recombinant animals were screened. Out of 36 recombinant animals, all segregated the Lin phenotype, which strongly argues that the *lin-62(ij52)* allele must be either to the left (centromeric) or in close proximity of *unc-8(e49)*. Preliminary STS mapping results (Clucas, 2003) had revealed that *lin-62(ij52)* was in close proximity of the polymorphism stP44 which is found at the approximate position of +3.27 between *him-3* and *pgl-1* (WormBase, 2007). This result suggests that the *lin-62(ij52)* allele might be in close proximity of *unc-8(e49).*

Recombinant class	Recombinants segregating *lin-62(ij52)* phenotype	Recombinant not segregating *lin-62(ij52)* phenotype	Total number of recombinants
Dpy-non-Unc	36	0	36

Table 7.4 Three-factor mapping of *lin-62(ij52)* with *unc-8(e49) dpy-20(e1282).*

In order to further refine the location of *lin-62,* the *elt-2::GFP* transgene that was integrated with the *rol-6(su1006)* mutant background was replaced with a post-embryonic GFP marker to facilitate the identification of the Lin phenotype in Unc animals. To this end, the *lin-62(ij52) dpy-20(e1282)IV* strain carrying the *elt-2::GFP* and *rol-6(su1006)* transgene (IA545) was crossed into JR1990 *wIs118* males. Dpy-Lin F2 progeny were selected on the basis of the expression of the intestinal GFP marker and subsequently animals that had lost the embryonic *elt-2::GFP*, but retained post-embryonic GFP expression through the presence of *wIs118 npa-1::GFP::LacZ* were selected. This produced the strain IA577 *lin-62(ij52) dpy-20 IV; wIs118* (Table 7.1). At this point during

the studies it became evident that the work discussed in previous chapters required increased attention and this project was continued by a postdoc in our laboratory who is currently using the strains generated in this study to further clone the *lin-62(ij52)* allele.

7.3 Discussion

It was hypothesised that LIN-62 can either act through S46 to regulate CDC-25.1 or cause hyperplasia in a mechanism independently of CDC-25.1. The data displayed in this chapter clearly show, that LIN-62 does not act through S46 in CDC-25.1 to generate intestinal hyperplasia.

7.3.1 lin-62 mapping

In this chapter cloning of *lin-62* was further undertaken and new strains were generated that are currently being used for mapping purposes. The mapping data using *unc-8* and *dpy-20* as marker strains show that *lin-62* must lie to the left or in the close proximity of *unc-8* at position +3.29 on chromosome IV. This result fits well with the previous report that placed *lin-62* between *bli-6* (+3.2) and *unc-24* (+3.52) in close proximity to the stP44 polymorphism at +3.27 (Clucas, 2003). Altogether the data suggest a map position for *lin-62* between *bli-6* (+3.19) and in the close proximity of *unc-8* (+3.29).

7.3.2 lin-62(ij52) is synergistic to cdc-25.1(ij48)

The data presented here argue strongly that there is a synergism between *cdc-25.1(ij48)* and *lin-62(ij52)*. This was mostly demonstrated by the fact that a combined strain that is homozygous for *lin-62(ij52)* and carries *cdc-25.1(ij48)* on a complex array displays an additive number of intestinal cells. Twenty intestinal cells are produced in a wild-type strain. This number is increased by 10 (to 30) in the case of a homozygous *lin-62(ij52)* mutant and by 8 (to 28) when *cdc-25.1(ij48)* is supplied on an complex extrachromosomal array. However, when homozygous *lin-62(ij52)* animals carry the *cdc-25.1(ij48)* on a complex array an addition of both single alleles is obtained creating 17 more intestinal cells (to 37). Hence, this shows that *lin-62(ij52)* and *cdc-25.1(ij48)* cause the intestinal hyperplasia by two independent mechanisms.

A slight but statistically significant increase in the embryonic lethality of the double mutant compared to each single mutant was identified. However, when Dpy animals of this cross were analysed after they lost the *cdc-25.1(ij48)* array they showed no statistically

significant difference in their embryonic lethality compared to animals that were homozygous for both alleles. This would suggest that the slight additive effect in embryonic lethality might be independent of the combination of *lin-62(ij52)* and *cdc-25.1(ij48)*. The data obtained above are derived from a strain that carries the *cdc-25.1(ij48)* on a complex extrachromosomal array. This allows expression of *cdc-25.1(ij48)* in the germline as repetitive arrays can be silenced in the germline (Kelly et al., 1997). Nonetheless, it remains to be established whether a chromosomally integrated *cdc-25.1(ij48)* would display a similar phenotype when combined with *lin-62(ij52)*. Partly, because the *cdc-25.1(ij48)* allele might be supplied in different copy numbers in the germline, since arrays usually form from many gene copies (Mello et al., 1991) and thus partial silencing might result in differential CDC-25.1(S46F) expression levels. It will therefore be important to repeat the cross with one of the newly synthesised *lin-62(ij52)* strains. For example, IA545 *lin-62(ij52) dpy-20(21282)IV; wIs84[elt-2::GFP::LacZ]* could be crossed into IA268 *cdc-25.1(ij48)* and progeny followed by Dpy appearance for *lin-62(ij52)* and restriction site polymorphism for the *cdc-25.1(ij48)* allele. This would allow us to identify whether single copies of both genes result in a more severe additive phenotype as displayed in this study.

7.3.3 LIN-62 does not stabilise CDC-25.1

The synergistic increase in the number of intestinal nuclei observed when *lin-62(ij52)* is combined with *cdc-25.1(ij48)* indicates that *lin-62* acts independently of the *ij48* site in *cdc-25.1* (as described above). This result is further supported by the observation that no increase in CDC-25.1 protein levels is detected in a *lin-62(ij52)* strain compared to a wild-type strain. Should LIN-62 be the kinase acting to phosphorylate CDC-25.1 on S46 and thereby targeting CDC-25.1 for LIN-23-mediated proteasomal degradation, removal or mutation of LIN-62 would cause a similar increase in the CDC-25.1 protein levels as observed for the CDC-25.1(S46F) mutant. However, as displayed in this chapter the *ij52* mutation in *lin-62* does not stabilise CDC-25.1. Hence, LIN-62 is not the kinase to phosphorylate CDC-25.1 on S46.

7.3.3.1 Possible functions of LIN-62

It remains possible that *lin-62* may exert its function by acting on another site in *cdc-25.1*. This is supported by previous experiments that showed that *lin-62* could not bypass *cdc-25.1* RNAi (Segref and Johnstone, 2004). Though, taken into account that *cdc-25.1* is a

general cell cycle regulator, this RNAi result is not too surprising and could suggest that LIN-62 requires the prior function of CDC-25.1 at a different stage of the cell cycle.

Alternatively, LIN-62 could negatively regulate CDC-25.1 function on another site in the CDC-25.1 protein independently of S46. The mapping data places the *lin-62* allele between +3.19 and +3.29 to a 840 Kbp region on chromosome IV, which comprises approximately 190 genes with five predicted kinases and twelve predicted phosphatases (WormBase, 2007), suggesting that *lin-62* could potentially be a kinase or a phosphatase that may act on CDC-25.1 in order to negatively regulate its function.

Such negative regulations of CDC25 are evident in vertebrate systems. 14-3-3 proteins have been shown to bind to a critical phosphoserine residue in *Xenopus* CDC25C (S287) (Duckworth et al., 2002; Kumagai et al., 1998) and human CDC25C (S216) (Bulavin et al., 2003a; Bulavin et al., 2001; Peng et al., 1998; Peng et al., 1997). CDC25C is predominantly cytoplasmic in interphase, but lack of 14-3-3 binding, through non-phosphorylatable (S287A/S216A) mutations in CDC25C, can induce its shuttling to the nucleus, and thus release the protein from cytoplasmic retention (Graves et al., 2001; Kumagai and Dunphy, 1999; Yang et al., 1999). The cytoplasmic retention acts as a negative regulatory mechanism, because release from 14-3-3 binding can increase the CDC25C mitosis-promoting activity in *Xenopus* (Yang et al., 1999) and human cells (Dalal et al., 1999; Dalal et al., 2004; Graves et al., 2001; Karlsson et al., 1999; Peng et al., 1997). Similarly, 14-3-3 binding to an analogous phosphoserine residue has been reported for human CDC25B (Bulavin et al., 2003a; Bulavin et al., 2001). Lack of 14-3-3 binding causes CDC25B redistribution to the nucleus (Giles et al., 2003; Lindqvist et al., 2004; Uchida et al., 2004) and induces premature mitosis (Lindqvist et al., 2004).

Thus, LIN-62 could act as a kinase by negatively regulating CDC-25.1 function similar to the vertebrate system. Alternatively, LIN-62 could be negatively regulating CDC-25.1 function through dephosphorylation of CDC-25.1. Such a mechanism was reported in *Xenopus* eggs, where dephosphorylation of a threonine residue (T138) in CDC25C by the PP2A phosphatase, was found to enhance 14-3-3 binding, thereby negatively regulating CDC25C mitosis-promoting activity (Margolis et al., 2006). Hence, if LIN-62 encodes for a kinase or a phosphatase acting on CDC-25.1 by a similar negative regulation as detected for the vertebrate CDC25s, then the *lin-62(ij52)* allele might affect the nuclear-to-cytoplasmic ratio of CDC-25.1 in the embryos. This would correlate with the fact that there is no increase of the CDC-25.1 protein detected by Western blotting because it would imply a differential localisation of CDC-25.1 in *lin-62(ij52)* embryos. To this end, indirect

immunostaining against CDC-25.1 in embryos could be employed to determine the nuclear and cytoplasmic ratio of CDC-25.1 in *lin-62(ij52)* mutants compared to wild-type.

7.3.4 Conclusion

In summary, the data displayed here provide strong evidence that the intestinal hyperplasia caused through mutations in *cdc-25.1(ij48)* and *lin-62(ij52)* are the result of two independent mechanisms and that LIN-62 is not a negative regulator of S46 in CDC-25.1. The *cdc-25.1(ij48)* strain utilised to analyse the combinatorial effects of *cdc-25.1(ij48)* and *lin-62(ij52)* is a valuable tool to set up a genome-wide screen to expand the search to identify negative regulators of the cell cycle that can act independently of S46F in CDC-25.1 in the intestine or other tissues and address further the tissue-specific nature of the *cdc-25.1(ij48)* allele.

Chapter 8

Final discussion

8 Final discussion

8.1 Summary of Results

The research presented in this thesis advances the understanding of how the tight negative control of CDC-25.1 contributes to maintenance of tissue-specific regulation of cellular proliferation during embryonic development of the multicellular organism *C. elegans*. A combination of reverse genetics and biochemical approaches successfully revealed that the interaction between the E3 ubiquitin ligase component LIN-23 through S46 in CDC-25.1 is vital to restrain cellular divisions of intestinal cells, specifically during embryogenesis.

8.1.1 LIN-23 controls intestinal cell proliferation through S46 in CDC-25.1 in the embryo

Firstly, removal of SCF components such as LIN-23, CUL-1 or SKR-1 caused excess intestinal cells, indicating that the SCF complex is involved in regulation of intestinal cell proliferation. Removal of LIN-23 and CUL-1 showed no synergism for the number of extra intestinal cells when combined with the recently identified *cdc-25.1(ij48)* allele (Clucas, 2003; Clucas et al., 2002), suggesting that they cause the excess intestinal cells through the same pathway as *cdc-25.1(ij48)*. In agreement with this result, partial inhibition of LIN-23 by RNAi primarily affects proliferation of intestinal cells, when compared to other tissues, similar to the previously reported phenotype of the *cdc-25.1(ij48)* allele (Clucas, 2003; Clucas et al., 2002). Zygotic *lin-23* expression in the embryo does not influence the proliferation of the intestine, because *lin-23* zygotic null embryos show no proliferation defects of the intestine, indicating that maternally provided LIN-23 is important to control cell divisions of intestinal cells.

Embryos derived from heterozygous *lin-23* mothers, that obtain half the amount of LIN-23 protein levels, show normal proliferation of intestinal cells. Thus, a 50% protein level of LIN-23 provided by the mother is sufficient to drive normal development of the intestine. Lowering these threshold levels of LIN-23 by RNAi primarily affects proliferation of the intestine because *lin-23* RNAi-treated embryos show intestinal hyperproliferation, but the majority of embryos hatch and grow to adulthood (when they become sterile).

Unique biochemical data are presented that unravel the endogenous complex formation of LIN-23 and CDC-25.1 in early embryos, providing compelling evidence for the physical

interaction between both molecules. Intriguingly, the S46 mutation in CDC-25.1 decreases LIN-23 binding to CDC-25.1, reduces the CDC-25.1 polyubiquitination state, and increases CDC-25.1 protein levels. Elevated CDC-25.1(S46F) protein levels are not restricted to the intestine and have been detected in the majority of blast cells of the early embryo, a phenotype that was also evident for CDC-25.1 after LIN-23 or CUL-1 knockdown by RNAi. LIN-23 protein levels are detected in all blast cells of the early embryo, which is in accordance with the general regulation of its target CDC-25.1 in probably all blast cells of the embryo. Intriguingly, LIN-23 protein is also detected in the germline. Although, it does not regulate CDC-25.1 through the S46 residue in the germline, because LIN-23 does not bind CDC-25.1 in the germline and the CDC-25.1(S46F) mutant protein levels are not up-regulated in the germline. Thus, this suggests the presence of a third key-player, possibly a kinase that can restrain CDC-25.1 S46 phosphorylation to a tight window during *C. elegans* early embryonic development.

8.1.2 gsk-3, apr-1 and wrm-1 RNAi cause extra intestinal cells independently of the cdc-25.1(ij48) allele

Data provided in this work clearly demonstrate that the potential kinase GSK-3 is not involved in regulation of CDC-25.1 through the S46 residue. Intriguingly, knockdown of GSK-3 also results in excess intestinal cells. However, the mechanism causing the extra intestinal cells is clearly distinct from the mechanism caused by abrogated LIN-23/CDC-25.1 interaction.

GSK-3 knockdown causes additive numbers of intestinal cells, when combined with the *cdc-25.1(ij48)* allele, indicating that GSK-3 and the CDC-25.1(S46F) mutant act in separate pathways. Furthermore, CDC-25.1 protein levels are not increased after GSK-3 knockdown, which contrasts with the data obtained by LIN-23 knockdown, and emphasises that GSK-3 does not negatively regulate the stability of CDC-25.1 through S46. Additionally, APR-1 and WRM-1 knockdown cause extra intestinal cells, which were found to be synergistic to the extra intestinal cell phenotype caused by the *cdc-25.1(ij48)* allele. However, no synergism was observed when *apr-1*, *wrm-1* and *gsk-3* RNAi were combined, suggesting that *gsk-3*, *apr-1* and *wrm-1* RNAi might cause the extra intestinal cells by a similar mechanism, but not through the *cdc-25.1(ij48)* allele.

8.1.3 lin-62(ij52) does not act through the ij48 site in cdc-25.1

The recently identified *lin-62(ij52)* allele (Clucas, 2003; Clucas et al., 2002) was an interesting candidate to regulate *cdc-25.1* through the *ij48* lesion due to its similar proliferation defect in the intestine. However, here it is shown that LIN-62 is not the kinase that regulates CDC-25.1 through S46, because the combination of the *lin-62(ij52)* and *cdc-25.1(ij48)* allele was found to be additive with respect to intestinal cell number, an indication that both alleles act through separate pathways. Furthermore, the *lin-62(ij52)* mutant does not stabilise the CDC-25.1 protein in embryos.

8.2 Discussion

8.2.1 CDC-25.1 overexpression causes hyperplasia

Perturbation of the CDC-25.1 interaction with LIN-23, either by RNAi against *lin-23* or through a CDC-25.1(S46F) mutant, causes elevated CDC-25.1 protein levels in the early embryo, ultimately resulting in intestinal hyperplasia. Intriguingly, zygotic expression of wild-type CDC-25.1 in the embryo, through expression of the *elt-2::cdc-25.1(+)* transgene, was shown to induce extra intestinal cells. This indicates that solely high CDC-25.1 protein levels, and not the CDC-25.1(S46F) mutation per se, can stimulate the production of extra divisions. The additional cell divisions after *lin-23* RNAi (this study) appear to be a result of a shortening of the cell cycle and a failure to exit the cell cycle after the fourth division (as evidenced by cell lineage analysis, J. Cabello) as previously also observed for the *cdc-25.1(ij48)* allele (Clucas, 2003; Clucas et al., 2002).

The *C. elegans* CDC-25.1(G47D) mutant was proposed to display a similar shortening of the cell cycle during *C. elegans* intestinal development, but a detailed lineage analysis was not performed in that study (Kostic and Roy, 2002). It has been shown that this mutant protein persists longer in the embryo, but given the fact that this mutation also perturbs the DSG motif in CDC-25.1, it is conceivable to expect a similar degradation defect of the CDC-25.1 protein under identical experimental conditions as performed for CDC-25.1(S46F). The overexpression data presented here are also in agreement with previous observations in mammalian tissue culture cells, where overexpression of the CDC25A protein can accelerate S phase entry (Blomberg and Hoffmann, 1999) and induce premature entry into mitosis (Mailand et al., 2002; Molinari et al., 2000). Similarly, overexpression of human CDC25B (Baldin et al., 2002; Gabrielli et al., 1996; Karlsson et

al., 1999), and to a lesser extent CDC25C, can induce premature entry into mitosis (Karlsson et al., 1999). Furthermore, overexpression of human CDC25A induces hyperplastic changes in mouse mammary glands (Ray et al., 2007).

Thus, the data presented here show that solely the elevated CDC-25.1 protein levels are enough to complete the extra cellular divisions of the intestine, indicating that CDC-25.1 is the driving force of the early embryonic cell cycle at least regarding the divisions of intestinal cells. This is in agreement with the detailed study by (Ashcroft et al., 1999) who reported a primary role for CDC-25.1 during embryogenesis. RNAi against *cdc-25.1* resulted in embryonic lethality that was slightly enhanced after simultaneous co-depletion of all four *cdc*-25 counterparts through concomitant RNAi. *cdc-25.3* and *cdc-25.4* RNAi did not show any obvious embryonic defects and *cdc-25.2* RNAi resulted in penetrant larval defects. Thus, it appears that in *C. elegans*, multiple CDC-25 forms can drive the cell cycle in the embryo, but CDC-25.1 is the primary factor driving proliferation in embryos, whereas CDC-25.2 might be involved in larval development. The use of tissue-specific GFP markers will establish to what extent other CDC-25 family members are important for proliferation of certain tissues in the embryo. In mammalian tissue culture cells, all three human CDC25 forms can cooperate at different cell cycle stages to drive cellular divisions (reviewed in (Boutros et al., 2006)). However, it remains to be established to what extent this accurately reflects the function of each form in a multicellular organism. For example, a recent study in mice revealed a major function of only one CDC25 isoform (CDC25A) that is sufficient to drive normal cell divisions in cells derived from mice that lack both CDC25B and CDC25C (though the female mice are sterile) (Ferguson et al., 2005). Accordingly, here it is demonstrated that overexpression of the single CDC-25.1 protein in *C. elegans* embryos can act to solely control proliferation of at least one entire tissue.

8.2.2 S46 is vital for CDC-25.1 regulation

Novel data produced in this study revealed that CDC-25.1 contains a predicted DSG motif in its N-terminus that is important for the regulation via LIN-23, the *C. elegans* orthologue of the human E3 ligase β-TrCP that specifically binds to DSG phosphodegron motifs. LIN-23 acts as a vital negative regulator through S46 within the predicted DSG motif of CDC-25.1, highlighting the conservation of this interaction from *C. elegans* to human.

Previous data revealed that S82 in the DSG motif of human CDC25A is important for β-TrCP-dependent binding and polyubiquitination (Busino et al., 2003; Donzelli et al., 2004;

Jin et al., 2003). *In vivo* studies with single serine (82) to alanine mutants uncovered that this residue is particularly important for the interaction of CDC25A with β-TrCP (Donzelli et al., 2004; Jin et al., 2003). Furthermore, S82 is vital for the β-TrCP-mediated degradation of CDC25A in mammalian tissue culture cells (Busino et al., 2003; Ray et al., 2005). Deletion of β-TrCP by RNAi abrogates the intra-S-checkpoint response in human tissue culture cells in a CDC25A-dependent way (Busino et al., 2003).

In summary, these findings provide substantial information for the importance of the CDC25A interaction with β-TrCP to sustain a functional division cycle in cultured cells. Unfortunately, it could not delineate a picture for the consequences of this interaction when cells are dividing within the context of a complete tissue or organism. Here, it is suggested that the single serine within the putative DSG motif of CDC-25.1 is important for the complex formation of CDC-25.1 with LIN-23 and resulting in the degradation of CDC-25.1. Mutation of this serine has detrimental effects for the embryonic development, resulting in tissue-specific hyperplasia of the intestine.

8.2.2.1 *gsk-3* and *lin-62(ij52)* do not act through *cdc-25.1(ij48)*

The kinase regulating the phosphorylation of the S46 residue in CDC-25.1 is presently unknown. Of potential GSK-3 kinases with homology to human GSK3β, the closest homologue was found not to act through S46. Similarly, the *lin-62(ij52)* allele is not acting through the *(ij48)* lesion (S46F) in *cdc-25.1*. According to bioinformatic analysis, S46 falls also into a potential CK1 or PKA phosphorylation site. However, the *C. elegans* genome contains many different CK1 isoforms (Manning, 2005), and this could hamper the identification of the specific molecule involved in S46 phosphorylation. It should be emphasised that the data displayed here do not exclude the possibility that another member of the GSK-3 family can act to regulate S46.

Interestingly, in human CDC25A the S76 and S79 upstream of the DSG motif are also important for β-TrCP-mediated polyubiquitination (Donzelli et al., 2004; Jin et al., 2003). S76 was suggested to encompass a potential CHK1 kinase site (Donzelli et al., 2004; Goloudina et al., 2003; Hassepass et al., 2003). While the S residue equivalent to S79 is conserved in *C. elegans* CDC-25.1 (S43), analysis of the CDC-25.1 sequence reveals an aspartic acid (D40) at the position analogous to S76. D40 might be able to mimic constitutive phosphorylation of this residue and thus can uncouple CDC-25.1 regulation from the potential action of the CHK-1 kinase that is also functioning in the early embryo (Kalogeropoulos et al., 2004).

8.2.3 *Tissue specificity*

An intriguing question that remains to be resolved is: why does global elevation of the CDC-25.1 protein level in all blast cells primarily affect the proliferation of the intestine? As discussed in Chapter 3 (3.3.4) and Chapter 7 (7.1), it could be anticipated that the cell cycle in intestinal cells is somehow more sensitive to elevated CDC-25.1 protein levels. This would imply that the intestinal cell cycle might lack some cell cycle control mechanism that is present in other cells.

However, in the intestine the Ea and Ep cells are the first cells in the embryo that acquire a G_2 phase into their cell cycle, compared to other embryonic cell cycles that switch between mitosis and S phase (Edgar and McGhee, 1988). Additional data proposed that the final stages of intestinal divisions acquire also a G_1 phase, because the G_1 type cyclin D (*cyd-1*) is required for the final four intestinal divisions (Boxem and van den Heuvel, 2001). It is presently unclear at what developmental stage other embryonic tissues acquire a gap phase into their cell cycle. The insertion of gap phases into the intestinal cell cycle rather suggests that intestinal cell cycles are more tightly controlled than cell cycles of surrounding tissues, and thus appears to contradict the findings here that intestinal cells are more sensitive to perturbations of CDC-25.1 protein levels. It is possible that other negative regulators are present to control CDC-25.1 activity only in the intestine leading to the long cell cycle in intestinal cells compared to other tissues.

Nevertheless, it is also possible that in intestinal cells additional gap phases have evolved because these cells lack other negative regulators that are present in non-intestinal tissues. Thus, the intestine might utilise additional gap phases as another means to restrain cellular proliferation. It will be fascinating to determine whether there are other negative regulators that are present in other tissues but not in the intestine.

8.2.3.1 Are negative regulators of the cell cycle limiting in the intestine?

WEE1/MYT1 proteins are interesting candidates to negatively regulate the cell cycle in non-intestinal tissues, because they negatively regulate the activity of CDKs through phosphorylation and thereby inhibit mitosis. The *C. elegans* genome contains three WEE1 like genes (*wee-1.1*, *wee-1.2* and *wee-1.3*) (Wilson et al., 1999). The *wee-1.2* gene was found to be a pseudogene because no cDNA transcript has been identified to date. In situ hybridisations detected *wee-1.1* transcript in the nucleus of the E blast cell and later in the nucleus of eight AB descendants at the 16-cell stage embryo. No transcript was found

before or after that stage (Wilson et al., 1999). Thus, *wee-1.1* might not be a crucial negative regulator in other tissues because it is also present in the intestine. However, suppressor mutants of a *wee-1.3* gain-of-function allele have recently been identified and shown to result in embryonic lethality (Lamitina and L'Hernault, 2002). A *wee-1.3* promoter-fusion to GFP was expressed in all early embryonic tissues, which might suggest that *wee-1.3* is vital for proliferation of many or all tissues in the embryo (Lamitina and L'Hernault, 2002). RNAi experiments previously failed to determine if *wee-1.3* also acts in the intestine, due to sterility of RNAi-treated mothers (Clucas, 2003). The *wee-1.3* suppressor mutant (Lamitina and L'Hernault, 2002) could be analysed for the numbers of intestinal cells by crossing the intestinal-specific *elt-2::GFP* marker into this strain and examining the numbers of intestinal nuclei. The absence of intestinal hyperplasia would suggest that *wee-1.3* could be an additional negative regulator in other tissues, but not in the intestine.

Other negative regulators of the cell-cycle are cyclin-dependent kinase inhibitors (CKI) that can bind cyclin/CDK complexes and thereby inactivate the activity of the kinase (Schafer, 1998; van den Heuvel, 2005). In *C. elegans* two *cki* genes have been identified and named *cki-1* and *cki-2* (Feng et al., 1999; Hong et al., 1998). Interestingly, a recent study revealed a role mainly for *cki-1* in mediating the proliferation of several embryonic tissues, including the intestine (Fukuyama et al., 2003). Thus, *cki-1* and *cki-2* appear not to be responsible for the tissue-specific proliferation defect of the intestine.

8.2.4 Function of cdc-25.1, gsk-3 and lin-23 in the endoderm

This thesis has identified a new function for *lin-23*, *gsk-3, apr-1* and *wrm-1* in regulating intestinal cell proliferation. The number of intestinal cells is elevated through abrogation of the CDC-25.1/LIN-23 interaction or by GSK-3, APR-1 or WRM-1 knockdown. However, the mechanism underlying the excess intestinal cells after *gsk-3, apr-1* and *wrm-1* RNAi is distinct from that of the *cdc-25.1(ij48)* allele. Interestingly, cell lineage analysis performed in collaboration with Dr. Cabello confirmed the findings that *lin-23* functions through *cdc-25.1(ij48)* and *gsk-3* does not. *lin-23* RNAi causes a shortening of the cell cycle and a failure of cell cycle exit, similar to the previously identified *cdc-25.1(ij48)* allele (Clucas, 2003; Clucas et al., 2002). However, *gsk-3* RNAi causes no general shortening of intestinal cell divisions and the cell cycle length is sensitive to the presence of the *cdc-25.1(ij48)* allele. When *gsk-3* RNAi is performed in a wild-type background all cells expressing endodermal fate undergo a further division after the fourth cleavage, which is possibly the result of a delayed E specification after *gsk-3* RNAi (as discussed in Chapter 3, (3.3.5.2)).

gsk-3, *wrm-1* and *apr-1* RNAi do not cause a synergistic increase for the numbers of intestinal cells. Given the known role of *gsk-3*, *wrm-1* and *apr-1* in the specification of endoderm (see Chapter 1, (1.2.2)), it is feasible to suggest that their RNAi phenotypes cause extra intestinal cells by the same mechanism. However, ultimately a cell lineage analysis will have to be employed to determine, whether the extra cells detected after WRM-1, APR-1 or GSK-3 knockdown are derived from the same precursor.

8.2.5 Is cyclin D involved in cell cycle exit?

It is interesting to see that *lin-23* RNAi and the previously identified *cdc-25.1(ij48)* allele (Clucas, 2003; Clucas et al., 2002) cause a failure to exit the cell cycle after the fourth cleavage. It is presently unclear what causes the four intestinal cells to undergo a further cleavage in the wild-type background as compared to the other twelve intestinal cells that cease cell division. Intriguingly, a cyclin D (*cyd-1*) loss-of-function mutant was shown to result in a failure of the final four intestinal divisions (Boxem and van den Heuvel, 2001). Additionally, a cell lineage analysis after *cki-1* RNAi revealed that all cells divide once more after the fourth division, but there is no shortening of the cell cycle (Fukuyama et al., 2003). Binding of CYD-1 to CKI-1 was previously detected by two-hybrid analysis (Boxem and van den Heuvel, 2001). Thus, CKI-1 might counteract the function of CYD-1 during the fourth intestinal division. These data encourage the speculation that abrogation of CDC-25.1 regulation through LIN-23 results in shortening of the cell cycle, and probably a mis-segregation of genetic determinants such as factors responsible for *cyd-1* expression, forcing variable cleavages of the cells into fifth or sometimes even sixth divisions. A recent report by (Ray et al., 2007) demonstrated that mammary tumours in mice with induced overexpression of CDC25A show abnormal chromosome numbers and chromosomal deletions compared to tumours that did not overexpress CDC25A, indicating that high levels of CDC25A can promote genomic instability.

Thus, it remains to be established whether the loss-of-function mutation in *cyd-1* can antagonise *cdc-25.1(ij48)*, *lin-23* or *gsk-3*-mediated excess endodermal cells. Previous work revealed that the *cdc-25.1(rr31)* mutation does not act through *cyd-1* in the intestine. However, those experiments were done after *cyd-1* RNAi (Kostic and Roy, 2002), which is apparently not very effective to study *cyd-1* function in embryos (Boxem and van den Heuvel, 2001).

Most importantly, the combination of genetics and biochemical data illustrated in this thesis (as well as cell lineage analysis) demonstrate clearly that the hyperplasia caused

through knockdown of LIN-23 is mediated through the S46 residue in CDC-25.1, whereas this is not the case after GSK-3 knockdown.

8.2.6 Role of CDC25 in human malignancies

8.2.6.1 Overexpression of CDC25 in human malignancies

In *C. elegans*, high CDC-25.1 protein levels result in hyperplasia of the endoderm, thus illustrating that elevated CDC-25.1 protein levels are potentially oncogenic. A recent comprehensive study, that analysed the role of CDC25 phosphatases in human malignancies, revealed that overexpression of CDC25A and B was frequently associated with many human primary cancers, such as hepatocellular, colorectal and pancreatic carcinoma, prostate, breast and lung cancer or non-Hodgkins lymphoma (for a review see (Kristjansdottir and Rudolph, 2004)). These data correlate well with the previously proposed oncogenic effect of CDC25A and B, but not CDC25C, in mouse fibroblasts (Galaktionov et al., 1995) and the enhanced proliferative activity caused by CDC25A overexpression in mouse mammary tumors (Ray et al., 2007).

In *C. elegans*, CDC-25.1 protein levels are regulated through the interaction with LIN-23 via the CDC-25.1 DSG motif, illustrating the importance of this interaction in a whole model organism. Intriguingly, the human LIN-23 orthologue β-TrCP regulates the abundance of human CDC25A through the DSG motif in human tissue culture cells (Busino et al., 2003; Donzelli et al., 2004; Jin et al., 2003; Ray et al., 2005) and it controls human CDC25A and B and *Xenopus* CDC25A abundance through the recently discovered DDG motif when analysed in *Xenopus* eggs (Kanemori et al., 2005). Taken together, these data correlate well with the elevated CDC25A and B levels in primary cancers, and suggest that an abrogated interaction in human β-TrCP, and CDC25A/B might have a pivotal role for the transforming activity of CDC25A/B during human malignancies.

Elevated CDC25A or CDC25B mRNA or protein levels have been detected in the majority of primary cancers analysed (Kristjansdottir and Rudolph, 2004). Unfortunately, a correlation between both mRNA and protein levels, which would provide additional information for the mechanism underlying CDC25 overexpression in those cancers, has not received much attention. Interestingly, several carcinomas such as colorectal carcinoma (Hernandez et al., 2001) as well as non-Hodgkins lymphoma (Hernandez et al., 2000) revealed elevated CDC25A protein levels that did not correlate with the amount of mRNA present in those cancers. This suggests that, in some tumours, crucial post-transcriptional

mechanisms account for differences in CDC25 protein levels. Similarly, a decrease in the CDC25A degradation rate was proposed to cause elevated CDC25A protein levels in human breast cancer cell lines (Loffler et al., 2003). These data highlight the importance for post-transcriptional control of CDC25 phosphatases, possibly through the degradation pathway, during normal development and in human malignancies.

8.2.6.2 β-TrCP/CDC25 in human malignancies

The work in this thesis highlights that a balanced interaction of LIN-23 with CDC-25.1 is essential to restrain cellular proliferation during the development of a multicellular organism. This leads to the attractive hypothesis that inactivating mutations in human β-TrCP or the DSG motif in CDC25 might be associated with human malignancies. Interestingly, mutations in β-TrCP have rarely been found in primary tumours (for a review see (Fuchs et al., 2004)). A 96 bp deletion was found in a prostate cancer xenograft that generates a stop-codon in β-TrCP1 at position 212, resulting in a truncated protein lacking the WD40 domain. A second mutation is a 169 bp deletion in a human prostate cancer cell line that leads to an in-frame deletion of residues 17 - 73 preceding the F-box motif of β-TrCP1 (Gerstein et al., 2002). Other β-TrCP mutations include a F462S point mutation at the seventh WD40 repeat domain of β-TrCP2 that was identified in a gastric cancer cell line (Saitoh and Katoh, 2001). Additionally, a recent study revealed five heterozygous missense mutations in β-TrCP1 of 95 human gastric cancers that were analysed (A99V, G260E, C206Y, H342Y and H425Y) (Kim et al., 2007). Two of these mutations are in the WD40 domain (H342Y and H425Y) whereas one (C206Y) is present in the F-box domain of β-TrCP. It will be interesting to determine whether these β-TrCP mutants abolish CDC25A/B binding.

Surprisingly, a variety of human malignancies and cancer cell lines possess elevated β-TrCP protein or mRNA levels (Gerstein et al., 2002; Koch et al., 2005; Muerkoster et al., 2005; Ougolkov et al., 2004). However, the protein levels of the proto-oncogene β-catenin (the downstream target of β-TrCP) are also often up-regulated in those primary cancers with elevated β-TRCP protein levels, such as colorectal carcinomas (Ougolkov et al., 2004) or hepatoblastomas (Koch et al., 2005). This is most likely the result of DSG mutations in β-catenin, which would be expected to escape β-TrCP downregulation, or inactivating mutations of the tumour suppressor APC in the tumours and cell lines that were investigated. Mutations in the DSG motif of CDC25A would be expected to also escape β-TrCP regulation in such cancers by a similar mechanism. It remains to be

established whether these cancer cells also show elevated CDC25 protein levels and mutations in the DSG motif.

Intriguingly, a combined analysis of mutations in β-TrCP, β-catenin and APC in prostate cancers revealed that they were mutually exclusive; suggesting that all three genes may act in the same pathway in these tumours and that other mutations in separate pathways may contribute to their oncogenic effects in these tissues (Gerstein et al., 2002). Work in this thesis suggests that additive mutations in the DSG motif of CDC25A or maybe the DDG motif of CDC25B may result in an enhanced oncogenic potential. This is because in *C. elegans*, removal of Wnt pathway genes, such as GSK-3 or APR-1, causes a synergistic increase in the numbers of intestinal cells when combined with the CDC-25.1 DSG mutant.

Given the vast amount of evidence for the oncogenic effects of CDC25, and the established role for β-TrCP in down-regulation of CDC25A during the normal cell cycle and in response to DNA damage, it is astonishing that the interplay between both proteins in human malignancies has received only little attention to date.

A first link between β-TrCP and CDC25A has been demonstrated in human lung cancer (He et al., 2005). Several human lung cancer cell lines show a decrease in β-TrCP1 protein levels by an as yet unknown mechanism. Re-expression of β-TrCP1 in one lung cancer cell line decreased the tumour size and reduced cell invasiveness when cells were injected in nude mice, implicating β-TrCP1 function as vital for tumour growth and motility in mice. A direct interaction between β-TrCP1 and CDC25A in non-small lung cancer cells was demonstrated, and knockdown of CDC25A by RNAi was shown to decrease cell invasiveness. Unfortunately, a comparison of the CDC25A mRNA and protein levels in primary lung tumours was missing in this study. Thus, it remains to be elucidated whether CDC25A protein levels are up-regulated in those primary human cancers and whether the mechanism described in the cell invasion assay correlates with a potential of CDC25 to cause tumours in mice and human lung cancer. Importantly, it is the first study that reveals an interaction between β-TrCP1 and CDC25A in human lung cancer cells (He et al., 2005).

These findings correlate with data presented in this thesis that suggest a vital role for a balanced interaction between CDC-25.1 and the *C. elegans* β-TrCP orthologue LIN-23 to restrain proliferation during *C. elegans* embryonic development. Mutational analysis of the CDC25 DSG or DDG motifs in human malignancies, which has unfortunately been lacking in the majority of cancer studies to date, should shed light on the question of

whether the enhanced oncogenic potential of certain tissues is the consequence of a dysregulated CDC25/β-TrCP interaction.

It remains to be established whether the tissue-specific defects, seen in *C. elegans*, are restricted to this model system. The fact that perturbations in β-TrCP and CDC25 protein levels have been identified in cancers of diverse tissue types (though many of endodermal origin) in humans might suggest a general role for the importance of the interactions of both proteins in humans. Further studies to discover additional negative regulators, acting in non-intestinal *C. elegans* tissues or on CDC-25.1 in the intestine, might identify whether the tissue-specific phenotype is conserved from *C. elegans* to humans. Alternatively, a limited pool of downstream regulators in other tissues compared to the intestine, such as cyclin-dependent kinases or cyclins, could cause the tissue-specific phenotype observed in this model system (as discussed in Chapter 3, (3.3.4.1)).

8.3 Future Perspectives

The work provided in this thesis has opened a wide spectrum of possibilities for further research investigation. Single experiments are described in the discussions of the individual chapters. But many exciting possibilities could represent the start of new projects and a broad outline of the most interesting perspectives is suggested below.

8.3.1 Does the intestinal cell cycle exit depend on cyclin D?

It will be interesting to determine whether the *cyd-1* loss-of-function allele (Boxem and van den Heuvel, 2001) can abrogate the extra intestinal cells caused by either the *cdc-25.1(ij48)* allele, *lin-23* or *gsk-3* RNAi. The *elt-2::GFP* marker could be crossed into the *cyd-1(lof)* strain to determine the numbers of intestinal cells when combined with the *cdc-25.1(ij48)* allele or after *lin-23* or *gsk-3* RNAi. Cell lineage analysis would reveal whether the *cyd-1(lof)* allele affects the shortening of the cell cycle in *cdc-25.1(ij48)* or after *lin-23* RNAi. Or if it only affects the cell cycle exit of the intestinal cells after the fourth division in the *cdc-25.1(ij48)* mutant and after *lin-23* RNAi as compared to *gsk-3* RNAi.

8.3.2 Identification of negative regulators of non-intestinal tissues

A RNAi screen can be performed utilising the strain IA575, generated in this study, that carries *cdc-25.1(ij48)* and *elt-2::GFP* on an extrachromosomal array. It would permit screening for animals that produce embryonic lethality (i.e. green dying embryos) only in

combination with the *cdc-25.1(ij48)* allele. Thus, this screen would allow the identification of negative regulators, possibly also in non-intestinal tissues, whose function becomes crucial when combined with the *cdc-25.1(ij48)* gain-of-function allele.

8.3.3 Identification of the kinase that regulates S46 in CDC-25.1

A new strain could be generated that expresses CDC-25.1 tagged with GFP under the control of its own promoter. RNAi screening of potential kinases, such as CK1 or PKA, could then be performed by examining embryos with increased GFP fluorescence, that are impaired in CDC-25.1 degradation. The identification of the kinase would answer the question whether the kinase is only active in the embryo and not in the germline, as suggested in this study.

8.3.4 Discovery of novel LIN-23 targets

A *lin-23::FLAG-TY* allele has been generated in this study. This allele can rescue the sterility of a *lin-23* null allele, but some embryos are dying. This suggests that maybe other targets of LIN-23 might be elevated in those embryos. Embryonic extracts of the *lin-23::FLAG-TY* allele could be compared to wild-type extracts using 2-dimensional gel electrophoresis. Proteins that are elevated in the mutant, but not in the wild-type, could be analysed by mass spectrometry. Potential targets could be further examined for the presence of a DSG motif by sequence analysis, and their function in the embryo could be studied by RNAi.

Appendices

Stage	No. of embryos	Fold increase	p-value	Combined fold increase	Combined p-value
A) Comparison of CDC-25.1 with CDC-25.1(S46F)					
10-20n	11/10	1.71 (2.53 - 1.15)	< 0.01	1.4	< 0.001
	4/7	0.62 (0.93 - 0.41)	< 0.05*		
	7/5	2.17 (3.33 - 1.41)	< 0.01		
30-40n	14/9	2.57 (3.62 - 1.83)	< 0.001	2.2	< 0.001
	11/7	1.75 (2.67 - 1.15)	< 0.05		
50-60n	14/10	2.19 (3.07 - 1.57)	< 0.001	1.9	< 0.001
	4/5	1.31 (2.69 - 0.64)	n.s.		
	6/9	2.00 (3.39 - 1.17)	< 0.05		
100-200n	6/9	1.72 (4.89 - 0.60)	n.s.	1.4	n.s.
	5/2	1.13 (2.46 - 0.52)	n.s.		
	5/8	1.19 (1.82 - 0.77)	n.s.		
B) CDC-25.1 comparison *lin-23* and control RNAi					
10-20n	6/12	2.42 (3.48 - 1.68)	< 0.001	1.7	< 0.001
	9/6	1.16 (2.61 - 0.51)	n.s.		
30-40n	8/11	3.62 (4.99 - 2.62)	< 0.001	2.8	< 0.001
	11/7	2.16 (4.56 - 1.02)	< 0.05		
50-60n	6/7	3.14 (5.33 - 1.84)	< 0.001	2.3	< 0.001
	7/8	1.73 (3.45 - 0.86)	n.s.		
C) CDC-25.1(S46F) comparison *lin-23* and control RNAi					
10-20n	6/7	0.95 (2.00 - 0.45)	n.s.	1.1	n.s.
	9/9	1.15 (1.63 - 0.82)	n.s.		
30-40n	4/3	0.56 (1.26 - 0.25)	n.s.	1.0	n.s.
	12/6	1.32 (1.83 - 0.95)	n.s.		
50-60n	5/4	0.47 (0.94 - 0.23)	n.s.	1.0	n.s.
	9/12	1.43 (1.93 - 1.05)	n.s.		
D) CDC-25.1 comparison *cul-1* and control RNAi					
30-40n	23/10	2.07 (3.00 - 1.43)	< 0.001	2.2	< 0.001
	12/18	1.46 (1.94 - 1.1)	< 0.05		
	11/11	4.02 (5.73 - 2.81)	< 0.001		
E) CDC-25.1(S46F) comparison *cul-1* and control RNAi					
30-40n	13/7	1.18 (1.74 - 0.80)	n.s.	1.1	n.s
	12/8	1.35 (1.83 - 1.00)	< 0.05		
	15/18	1.03 (1.14 - 0.92)	n.s.		
F) CDC-25.1 comparison *gsk-3* and control RNAi					
30-40n	23/11	0.51 (0.76 - 0.34)	< 0.01*	0.9	n.s.
	°12/3	0.34 (1.12 - 0.10)	n.s.		
	17/14	0.90 (0.93 - 0.86)	n.s.		
	16/10	1.72 (2.25 - 1.33)	< 0.001		
G) CDC-25.1(S46F) comparison *gsk-3* and control RNAi					
30-40n	13/8	1.00 (1.51 - 0.67)	n.s.	1.1	n.s.
	12/9	1.32 (1.83 - 0.95)	n.s.		
	15/17	1.17 (1.19 - 1.13)	n.s		
	16/8	1.07 (1.42 - 0.80)	n.s.		

Table 8.1 Detailed quantification of CDC-25.1 and CDC-25.1(S46F) protein levels after immunostaining.

For Table legend see next page.

Average intensity of fluorescence after CDC-25.1 immunostaining of embryos derived from the wild-type strain JR1838 compared to IA530 *cdc-25.1(ij48)* was quantified from individual experiments. p-value: Student's *t*-test for two-tailed distribution, combined p-value: Student's *t*-test for one-tailed distribution of combined datasets, n.s.: p-value > 0.05. **A)** CDC-25.1(S46F) protein levels are increased compared to CDC-25.1 between the 10- to 60-cell stage of embryogenesis. Mutant fold increase ($\Delta mean_{WT/Mutant}$ (95% upper and lower confidence limits), number of embryos (CDC-25.1/CDC25.1S46F), * = 0.95 tail was utilised for calculation of the combined one-tailed p-value. Two and three independent experiments for 30-40n and 10-20n, 50-60n, 100-200n, respectively. **B-E)** CDC-25.1 but not CDC-25.1(S46F) is increased after *lin-23* and *cul-1* RNAi. Fold increase: $\Delta mean_{ctrl/gene\text{-}specific}$ RNAi (95% upper and lower confidence limits), number of embryos (control/gene-specific RNAi), two and three independent experiments for *lin-23* and *cul-1* RNAi, respectively. **F, G)** CDC-25.1 and CDC-25.1(S46F) abundance is not affected by *gsk-3* RNAi. Analysed as (B-E), ° = dataset was not included in combined p-value, * = 0.99 tail was utilised for calculation of the combined p-value. Three and four independent experiments for F and G, respectively. For a detailed description of the statistics applied, please see Chapter 2, (2.2.9.1).

References

Aberle, H., A. Bauer, J. Stappert, A. Kispert, and R. Kemler. 1997. Beta-catenin is a target for the ubiquitin-proteasome pathway. *Embo J.* 16:3797-3804.

Altun, Z.F., Hall, D.H. 2005. Handbook of *C.elegans* Anatomy. *In* WormAtlas, http://www.wormatlas.org/handbook/contents.htm.

Ang, X.L., and J. Wade Harper. 2005. SCF-mediated protein degradation and cell cycle control. *Oncogene*. 24:2860-2870.

Ashcroft, N., and A. Golden. 2002. CDC-25.1 regulates germline proliferation in *Caenorhabditis elegans*. *Genesis*. 33:1-7.

Ashcroft, N.R., M.E. Kosinski, D. Wickramasinghe, P.J. Donovan, and A. Golden. 1998. The four *cdc-25* genes from the nematode *Caenorhabditis elegans*. *Gene*. 214:59-66.

Ashcroft, N.R., M. Srayko, M.E. Kosinski, P.E. Mains, and A. Golden. 1999. RNA-mediated interference of a *cdc25* homolog in *Caenorhabditis elegans* results in defects in the embryonic cortical membrane, meiosis, and mitosis. *Dev Biol.* 206:15-32.

Askjaer, P., V. Galy, E. Hannak, and I.W. Mattaj. 2002. Ran GTPase cycle and importins alpha and beta are essential for spindle formation and nuclear envelope assembly in living *Caenorhabditis elegans* embryos. *Mol Biol Cell.* 13:4355-4370.

Atherton-Fessler, S., F. Liu, B. Gabrielli, M.S. Lee, C.Y. Peng, and H. Piwnica-Worms. 1994. Cell cycle regulation of the p34cdc2 inhibitory kinases. *Mol Biol Cell.* 5:989-1001.

Bai, C., P. Sen, K. Hofmann, L. Ma, M. Goebl, J.W. Harper, and S.J. Elledge. 1996. SKP1 connects cell cycle regulators to the ubiquitin proteolysis machinery through a novel motif, the F-box. *Cell.* 86:263-274.

Baldin, V., K. Pelpel, M. Cazales, C. Cans, and B. Ducommun. 2002. Nuclear localization of CDC25B1 and Serine 146 integrity are required for induction of mitosis. *J. Biol. Chem.* 277:35176-35182.

Batchelder, C., M.A. Dunn, B. Choy, Y. Suh, C. Cassie, E.Y. Shim, T.H. Shin, C. Mello, G. Seydoux, and T.K. Blackwell. 1999. Transcriptional repression by the *Caenorhabditis elegans* germ-line protein PIE-1. *Genes Dev.* 13:202-212.

Behrens, J., B.A. Jerchow, M. Wurtele, J. Grimm, C. Asbrand, R. Wirtz, M. Kuhl, D. Wedlich, and W. Birchmeier. 1998. Functional interaction of an axin homolog, conductin, with beta-catenin, APC, and GSK3beta. *Science*. 280:596-599.

Bei, Y., J. Hogan, L.A. Berkowitz, M. Soto, C.E. Rocheleau, K.M. Pang, J. Collins, and C.C. Mello. 2002. SRC-1 and Wnt signaling act together to specify endoderm and to control cleavage orientation in early *C. elegans* embryos. *Dev Cell.* 3:113-125.

Blackwell, T.K., B. Bowerman, J.R. Priess, and H. Weintraub. 1994. Formation of a monomeric DNA binding domain by Skn-1 bZIP and homeodomain elements. *Science*. 266:621-628.

Blomberg, I., and I. Hoffmann. 1999. Ectopic expression of Cdc25A accelerates the G(1)/S transition and leads to premature activation of cyclin E- and cyclin A-dependent kinases. *Mol Cell Biol.* 19:6183-6194.

Blondel, M., J.M. Galan, Y. Chi, C. Lafourcade, C. Longaretti, R.J. Deshaies, and M. Peter. 2000. Nuclear-specific degradation of Far1 is controlled by the localization of the F-box protein Cdc4. *Embo J.* 19:6085-6097.

Bosher, J.M., P. Dufourcq, S. Sookhareea, and M. Labouesse. 1999. RNA interference can target pre-mRNA: consequences for gene expression in a *Caenorhabditis elegans* operon. *Genetics*. 153:1245-1256.

Boutros, R., C. Dozier, and B. Ducommun. 2006. The when and wheres of CDC25 phosphatases. *Curr Opin Cell Biol.* 18:185-191.

Bowerman, B., B.W. Draper, C.C. Mello, and J.R. Priess. 1993. The maternal gene *skn-1* encodes a protein that is distributed unequally in early *C. elegans* embryos. *Cell.* 74:443-452.

Bowerman, B., B.A. Eaton, and J.R. Priess. 1992. *skn-1*, a maternally expressed gene required to specify the fate of ventral blastomeres in the early *C. elegans* embryo. *Cell.* 68:1061-1075.

Boxem, M., D.G. Srinivasan, and S. van den Heuvel. 1999. The *Caenorhabditis elegans* gene *ncc-1* encodes a cdc2-related kinase required for M phase in meiotic and mitotic cell divisions, but not for S phase. *Development.* 126:2227-2239.

Boxem, M., and S. van den Heuvel. 2001. *lin-35* Rb and *cki-1* Cip/Kip cooperate in developmental regulation of G1 progression in *C. elegans*. *Development.* 128:4349-4359.

Broitman-Maduro, G., M.F. Maduro, and J.H. Rothman. 2005. The noncanonical binding site of the MED-1 GATA factor defines differentially regulated target genes in the *C. elegans* mesendoderm. *Dev Cell.* 8:427-33.

Bulavin, D.V., Z.N. Demidenko, C. Phillips, S.A. Moody, and A.J. Fornace, Jr. 2003a. Phosphorylation of *Xenopus* Cdc25C at Ser285 interferes with ability to activate a DNA damage replication checkpoint in pre-midblastula embryos. *Cell Cycle.* 2:263-266.

Bulavin, D.V., Y. Higashimoto, Z.N. Demidenko, S. Meek, P. Graves, C. Phillips, H. Zhao, S.A. Moody, E. Appella, H. Piwnica-Worms, and A.J. Fornace, Jr. 2003b. Dual phosphorylation controls Cdc25 phosphatases and mitotic entry. *Nat Cell Biol.* 5:545-551.

Bulavin, D.V., Y. Higashimoto, I.J. Popoff, W.A. Gaarde, V. Basrur, O. Potapova, E. Appella, and A.J. Fornace, Jr. 2001. Initiation of a G2/M checkpoint after ultraviolet radiation requires p38 kinase. *Nature.* 411:102-107.

Busino, L., M. Chiesa, G.F. Draetta, and M. Donzelli. 2004. Cdc25A phosphatase: combinatorial phosphorylation, ubiquitylation and proteolysis. *Oncogene.* 23:2050-2056.

Busino, L., M. Donzelli, M. Chiesa, D. Guardavaccaro, D. Ganoth, N.V. Dorello, A. Hershko, M. Pagano, and G.F. Draetta. 2003. Degradation of Cdc25A by β–TrCP during S phase and in response to DNA damage. *Nature.* 426:87-91.

Calvo, D., M. Victor, F. Gay, G. Sui, M.P. Luke, P. Dufourcq, G. Wen, M. Maduro, J. Rothman, and Y. Shi. 2001. A POP-1 repressor complex restricts inappropriate cell type-specific gene transcription during *Caenorhabditis elegans* embryogenesis. *Embo J.* 20:7197-7208.

Cheeseman, I.M., and A. Desai. 2005. A combined approach for the localization and tandem affinity purification of protein complexes from metazoans.10.1126/stke.2662005pl1. *Sci. STKE.* 2005:pl1-.

Cheeseman, I.M., S. Niessen, S. Anderson, F. Hyndman, J.R. Yates, 3rd, K. Oegema, and A. Desai. 2004. A conserved protein network controls assembly of the outer kinetochore and its ability to sustain tension. *Genes Dev.* 18:2255-2268.

Clucas, C. 2003. Control of endoderm development in *Caenorhabditis elegans*. *In* PhD Thesis. Wellcome Centre for Molecular Parasitology. University of Glasgow, Glasgow.

Clucas, C., J. Cabello, I. Bussing, R. Schnabel, and I.L. Johnstone. 2002. Oncogenic potential of a *C. elegans cdc-25* gene is demonstrated by a gain-of-function allele. *Embo J.* 21:665-674.

Dalal, S.N., C.M. Schweitzer, J. Gan, and J.A. DeCaprio. 1999. Cytoplasmic localization of human cdc25C during interphase requires an intact 14-3-3 binding site. *Mol Cell Biol.* 19:4465-4479.

Dalal, S.N., M.B. Yaffe, and J.A. DeCaprio. 2004. 14-3-3 family members act coordinately to regulate mitotic progression. *Cell Cycle.* 3:672-677.

Davis, M., A. Hatzubai, J.S. Andersen, E. Ben-Shushan, G.Z. Fisher, A. Yaron, A. Bauskin, F. Mercurio, M. Mann, and Y. Ben-Neriah. 2002. Pseudosubstrate regulation of the SCF(beta-TrCP) ubiquitin ligase by hnRNP-U. *Genes Dev.* 16:439-451.

Desai, A., S. Rybina, T. Muller-Reichert, A. Shevchenko, A. Shevchenko, A. Hyman, and K. Oegema. 2003. KNL-1 directs assembly of the microtubule-binding interface of the kinetochore in *C. elegans*. *Genes Dev.* 17:2421-2435.

Donzelli, M., L. Busino, M. Chiesa, D. Ganoth, A. Hershko, and G.F. Draetta. 2004. Hierarchical order of phosphorylation events commits Cdc25A to beta-TrCP-dependent degradation. *Cell Cycle*. 3:469-471.

Donzelli, M., M. Squatrito, D. Ganoth, A. Hershko, M. Pagano, and G. Draetta. 2002. Dual mode of degradation of Cdc25A phosphatase. *Embo J.* 21:4875-4884.

Dreier, L., M. Burbea, and J.M. Kaplan. 2005. LIN-23-Mediated Degradation of β-Catenin Regulates the Abundance of GLR-1 Glutamate Receptors in the Ventral Nerve Cord of *C. elegans*. *Neuron*. 46:51-64.

Duckworth, B.C., J.S. Weaver, and J.V. Ruderman. 2002. G2 arrest in *Xenopus* oocytes depends on phosphorylation of cdc25 by protein kinase A. *Proc Natl Acad Sci U S A*. 99:16794-16799.

Edgar, L.G., and J.D. McGhee. 1986. Embryonic expression of a gut-specific esterase in *Caenorhabditis elegans*. *Dev Biol*. 114:109-118.

Edgar, L.G., and J.D. McGhee. 1988. DNA synthesis and the control of embryonic gene expression in *C. elegans*. *Cell*. 53:589-99.

Eisenmann, D.M., J.N. Maloof, J.S. Simske, C. Kenyon, and S.K. Kim. 1998. The beta-catenin homolog BAR-1 and LET-60 Ras coordinately regulate the Hox gene *lin-39* during *Caenorhabditis elegans* vulval development. *Development*. 125:3667-3680.

Encalada, S.E., J. Willis, R. Lyczak, and B. Bowerman. 2005. A spindle checkpoint functions during mitosis in the early *Caenorhabditis elegans* embryo. *Mol Biol Cell*. 16:1056-1070.

Evans, T., C. 2006. Transformation and microinjection. *In* WormBook. The *C. elegans* Research Community. April 6. WormBook, doi/10.1895/wormbook.1.108.1, http://www.wormbook.org.

Fabunmi, R.P., W.C. Wigley, P.J. Thomas, and G.N. DeMartino. 2000. Activity and regulation of the centrosome-associated proteasome. *J Biol Chem*. 275:409-413.

Falck, J., N. Mailand, R.G. Syljuasen, J. Bartek, and J. Lukas. 2001. The ATM-Chk2-Cdc25A checkpoint pathway guards against radioresistant DNA synthesis. *Nature*. 410:842-847.

Fantes, P. 1979. Epistatic gene interactions in the control of division in fission yeast. *Nature*. 279:428-430.

Feinberg, E.H., and C.P. Hunter. 2003. Transport of dsRNA into cells by the transmembrane protein SID-1. *Science*. 301:1545-1547.

Feng, H., W. Zhong, G. Punkosdy, S. Gu, L. Zhou, E.K. Seabolt, and E.T. Kipreos. 1999. CUL-2 is required for the G1-to-S phase transition and mitotic chromosome condensation in *Caenorhabditis elegans*. *Nat Cell Biol*. 1:486-492.

Ferguson, A.M., L.S. White, P.J. Donovan, and H. Piwnica-Worms. 2005. Normal cell cycle and checkpoint responses in mice and cells lacking Cdc25B and Cdc25C protein phosphatases. *Mol Cell Biol*. 25:2853-2860.

Fernandez, A.G., K.C. Gunsalus, J. Huang, L.S. Chuang, N. Ying, H.L. Liang, C. Tang, A.J. Schetter, C. Zegar, J.F. Rual, D.E. Hill, V. Reinke, M. Vidal, and F. Piano. 2005. New genes with roles in the *C. elegans* embryo revealed using RNAi of ovary-enriched ORFeome clones. *Genome Res*. 15:250-259.

Fire, A., D. Albertson, S.W. Harrison, and D.G. Moerman. 1991. Production of antisense RNA leads to effective and specific inhibition of gene expression in *C. elegans* muscle. *Development*. 113:503-514.

Fire, A., S. Xu, M.K. Montgomery, S.A. Kostas, S.E. Driver, and C.C. Mello. 1998. Potent and specific genetic interference by double-stranded RNA in *Caenorhabditis elegans*. *Nature*. 391:806-811.

Flotow, H., P. Graves, A. Wang, C. Fiol, R. Roeske, and P. Roach. 1990. Phosphate groups as substrate determinants for casein kinase I action. *J. Biol. Chem.* 265:14264-14269.

Fraser, A.G., R.S. Kamath, P. Zipperlen, M. Martinez-Campos, M. Sohrmann, and J. Ahringer. 2000. Functional genomic analysis of *C. elegans* chromosome I by systematic RNA interference. 408:325-330.

Fuchs, S.Y., V.S. Spiegelman, and K.G. Kumar. 2004. The many faces of beta-TrCP E3 ubiquitin ligases: reflections in the magic mirror of cancer. *Oncogene*. 23:2028-2036.

Fukushige, T., M.G. Hawkins, and J.D. McGhee. 1998. The GATA-factor *elt-2* is essential for formation of the *Caenorhabditis elegans* intestine. *Dev Biol*. 198:286-302.

Fukuyama, M., S.B. Gendreau, W.B. Derry, and J.H. Rothman. 2003. Essential embryonic roles of the CKI-1 cyclin-dependent kinase inhibitor in cell-cycle exit and morphogenesis in *C. elegans*. *Dev Biol*. 260:273-286.

Gabrielli, B.G., C.P.C. DeSouza, I.D. Tonks, J. Clark, N.K. Hayward, and K.A.O. Ellem. 1996. Cytoplasmic accumulation of cdc25B phosphatase in mitosis triggers centrosomal microtubule nucleation in HeLa cells. *J Cell Sci*. 109:1081-1093.

Galaktionov, K., and D. Beach. 1991. Specific activation of cdc25 tyrosine phosphatases by B-type cyclins: evidence for multiple roles of mitotic cyclins. *Cell*. 67:1181-1194.

Galaktionov, K., A.K. Lee, J. Eckstein, G. Draetta, J. Meckler, M. Loda, and D. Beach. 1995. CDC25 phosphatases as potential human oncogenes. *Science*. 269:1575-1577.

Galy, V., I.W. Mattaj, and P. Askjaer. 2003. *Caenorhabditis elegans* nucleoporins Nup93 and Nup205 determine the limit of nuclear pore complex size exclusion *in vivo*. *Mol. Biol. Cell*. 14:5104-5115.

Gautier, J., M.J. Solomon, R.N. Booher, J.F. Bazan, and M.W. Kirschner. 1991. cdc25 is a specific tyrosine phosphatase that directly activates p34cdc2. *Cell*. 67:197-211.

Geles, K., and S. Adam. 2001. Germline and developmental roles of the nuclear transport factor importinα 3 in *C. elegans*. *Development*. 128:1817-1830.

Gerstein, A.V., T.A. Almeida, G. Zhao, E. Chess, M. Shih Ie, K. Buhler, K. Pienta, M.A. Rubin, R. Vessella, and N. Papadopoulos. 2002. APC/CTNNB1 (beta-catenin) pathway alterations in human prostate cancers. *Genes Chromosomes Cancer*. 34:9-16.

Gilbert, S.F. 2003. Early development of the nematode *Caenorhabditis elegans*. *In* Developmental Biology. Sinauer Associates, INC., Sunderland, Massachusetts, USA. 251-258.

Giles, N., A. Forrest, and B. Gabrielli. 2003. 14-3-3 acts as an intramolecular bridge to regulate cdc25B localization and activity. *J. Biol. Chem.* 278:28580-28587.

Goldstein, B. 1992. Induction of gut in *Caenorhabditis elegans* embryos. *Nature*. 357:255-257.

Goldstein, B. 1995. An analysis of the response to gut induction in the *C. elegans* embryo. *Development*. 121:1227-1236.

Goldstein, B., S.N. Hird, and J.G. White. 1993. Cell polarity in early *C. elegans* development. *Dev Suppl*:279-287.

Goloudina, A., H. Yamaguchi, D.B. Chervyakova, E. Appella, A.J. Fornace, Jr., and D.V. Bulavin. 2003. Regulation of human Cdc25A stability by Serine 75 phosphorylation is not sufficient to activate a S phase checkpoint. *Cell Cycle*. 2:473-478.

Gonczy, P., C. Echeverri, K. Oegema, A. Coulson, S.J. Jones, R.R. Copley, J. Duperon, J. Oegema, M. Brehm, E. Cassin, E. Hannak, M. Kirkham, S. Pichler, K. Flohrs, A.

Goessen, S. Leidel, A.M. Alleaume, C. Martin, N. Ozlu, P. Bork, and A.A. Hyman. 2000. Functional genomic analysis of cell division in *C. elegans* using RNAi of genes on chromosome III. *Nature*. 408:331-336.

Graves, P.R., C.M. Lovly, G.L. Uy, and H. Piwnica-Worms. 2001. Localization of human Cdc25C is regulated both by nuclear export and 14-3-3 protein binding. *Oncogene*. 20:1839-1851.

Grishok, A. 2005. RNAi mechanisms in *Caenorhabditis elegans*. *FEBS Lett*. 579:5932-5939.

Grishok, A., H. Tabara, and C.C. Mello. 2000. Genetic requirements for inheritance of RNAi in *C. elegans*. *Science*. 287:2494-2497.

Guardavaccaro, D., Y. Kudo, J. Boulaire, M. Barchi, L. Busino, M. Donzelli, F. Margottin-Goguet, P.K. Jackson, L. Yamasaki, and M. Pagano. 2003. Control of meiotic and mitotic progression by the F box protein beta-Trcp1 *in vivo*. *Dev Cell*. 4:799-812.

Guo, S., and K.J. Kemphues. 1995. *par-1*, a gene required for establishing polarity in *C. elegans* embryos, encodes a putative Ser/Thr kinase that is asymmetrically distributed. *Cell*. 81:611-620.

Han, M. 1997. Gut reaction to Wnt signaling in worms. *Cell*. 90:581-584.

Hansen, D.V., A.V. Loktev, K.H. Ban, and P.K. Jackson. 2004. Plk1 regulates activation of the anaphase promoting complex by phosphorylating and triggering SCF betaTrCP-dependent destruction of the APC Inhibitor Emi1. *Mol Biol Cell*. 15:5623-5634.

Hart, M.J., R. de los Santos, I.N. Albert, B. Rubinfeld, and P. Polakis. 1998. Downregulation of beta-catenin by human Axin and its association with the APC tumor suppressor, beta-catenin and GSK3 beta. *Curr Biol*. 8:573-581.

Hassepass, I., R. Voit, and I. Hoffmann. 2003. Phosphorylation at serine 75 is required for UV-mediated degradation of human Cdc25A phosphatase at the S-phase checkpoint. *J Biol Chem*. 278:29824-29829.

Hawkins, M.G., and J.D. McGhee. 1995. *elt-2*, a second GATA factor from the nematode *Caenorhabditis elegans*. *J Biol Chem*. 270:14666-14671.

He, N., C. Li, X. Zhang, T. Sheng, S. Chi, K. Chen, Q. Wang, R. Vertrees, R. Logrono, and J. Xie. 2005. Regulation of lung cancer cell growth and invasiveness by beta-TRCP. *Mol Carcinog*. 42:18-28.

Hedgecock, E.M., and J.G. White. 1985. Polyploid tissues in the nematode *Caenorhabditis elegans*. *Dev Biol*. 107:128-133.

Hermann, G.J., B. Leung, and J.R. Priess. 2000. Left-right asymmetry in *C. elegans* intestine organogenesis involves a LIN-12/Notch signaling pathway. *Development*. 127:3429-3440.

Hernandez, S., X. Bessa, S. Bea, L. Hernandez, A. Nadal, C. Mallofre, J. Muntane, A. Castells, P.L. Fernandez, A. Cardesa, and E. Campo. 2001. Differential expression of cdc25 cell-cycle-activating phosphatases in human colorectal carcinoma. *Lab Invest*. 81:465-473.

Hernandez, S., L. Hernandez, S. Bea, M. Pinyol, I. Nayach, B. Bellosillo, A. Nadal, A. Ferrer, P.L. Fernandez, E. Montserrat, A. Cardesa, and E. Campo. 2000. cdc25A and the splicing variant cdc25B2, but not cdc25B1, -B3 or -C, are over-expressed in aggressive human non-Hodgkin's lymphomas. *Int J Cancer*. 89:148-152.

Hillier, L.W., A. Coulson, J.I. Murray, Z. Bao, J.E. Sulston, and R.H. Waterston. 2005. Genomics in *C. elegans*: so many genes, such a little worm. *Genome Res*. 15:1651-1660.

Hirsh, D., D. Oppenheim, and M. Klass. 1976. Development of the reproductive system of *Caenorhabditis elegans*. *Dev Biol*. 49:200-219.

Hoffmann, I., P.R. Clarke, M.J. Marcote, E. Karsenti, and G. Draetta. 1993. Phosphorylation and activation of human cdc25C by cdc2--cyclin B and its involvement in the self-amplification of MPF at mitosis. *Embo J*. 12:53-63.

Hoffmann, I., G. Draetta, and E. Karsenti. 1994. Activation of the phosphatase activity of human cdc25A by a cdk2-cyclin E dependent phosphorylation at the G1/S transition. *Embo J.* 13:4302-4310.

Honda, R., Y. Ohba, A. Nagata, H. Okayama, and H. Yasuda. 1993. Dephosphorylation of human p34cdc2 kinase on both Thr-14 and Tyr-15 by human cdc25B phosphatase. *FEBS Lett.* 318:331-334.

Hong, Y., R. Roy, and V. Ambros. 1998. Developmental regulation of a cyclin-dependent kinase inhibitor controls postembryonic cell cycle progression in *Caenorhabditis elegans*. *Development.* 125:3585-3597.

Hsu, J.Y., J.D. Reimann, C.S. Sorensen, J. Lukas, and P.K. Jackson. 2002. E2F-dependent accumulation of hEmi1 regulates S phase entry by inhibiting APC(Cdh1). *Nat Cell Biol.* 4:358-366.

Hunter, C.P., and C. Kenyon. 1996. Spatial and temporal controls target *pal-1* blastomere-specification activity to a single blastomere lineage in *C. elegans embryos*. *Cell.* 87:217-226.

Ikeda, S., S. Kishida, H. Yamamoto, H. Murai, S. Koyama, and A. Kikuchi. 1998. Axin, a negative regulator of the Wnt signaling pathway, forms a complex with GSK-3beta and beta-catenin and promotes GSK-3beta-dependent phosphorylation of beta-catenin. *Embo J.* 17:1371-1384.

Izumi, T., and J.L. Maller. 1993. Elimination of cdc2 phosphorylation sites in the cdc25 phosphatase blocks initiation of M-phase. *Mol Biol Cell.* 4:1337-1350.

Izumi, T., D.H. Walker, and J.L. Maller. 1992. Periodic changes in phosphorylation of the *Xenopus* cdc25 phosphatase regulate its activity. *Mol Biol Cell.* 3:927-939.

Jin, J. 1999. Transformation. *In C. elegans*: a practical approach. Vol. 1. I.A. Hope, editor. Information Press Ltd., Oxon, UK. 69-96.

Jin, J., T. Shirogane, L. Xu, G. Nalepa, J. Qin, S.J. Elledge, and J.W. Harper. 2003. SCFbeta-TRCP links Chk1 signaling to degradation of the Cdc25A protein phosphatase. *Genes Dev.* 17:3062-3074.

Johnstone, I.L. 1999. Molecular biology. *In C. elegans*: a practical approach. Vol. 1. I.A. Hope, editor. Information Press, Ltd., Oxon, UK. 201-225.

Kalogeropoulos, N., C. Christoforou, A.J. Green, S. Gill, and N.R. Ashcroft. 2004. *chk-1* is an essential gene and is required for an S-M checkpoint during early embryogenesis. *Cell Cycle.* 3:1196-1200.

Kamath, R.S., A.G. Fraser, Y. Dong, G. Poulin, R. Durbin, M. Gotta, A. Kanapin, N. Le Bot, S. Moreno, M. Sohrmann, D.P. Welchman, P. Zipperlen, and J. Ahringer. 2003. Systematic functional analysis of the *Caenorhabditis elegans* genome using RNAi. *Nature.* 421:231-237.

Kamath, R.S., M. Martinez-Campos, P. Zipperlen, A.G. Fraser, and J. Ahringer. 2000. Effectiveness of specific RNA-mediated interference through ingested double-stranded RNA in *Caenorhabditis elegans*. *Genome Biol.* 2:1-10.

Kanemori, Y., K. Uto, and N. Sagata. 2005. beta-TrCP recognizes a previously undescribed nonphosphorylated destruction motif in Cdc25A and Cdc25B phosphatases. *Proc Natl Acad Sci U S A.* 102:6279-6284.

Karlsson, C., S. Katich, A. Hagting, I. Hoffmann, and J. Pines. 1999. Cdc25B and Cdc25C differ markedly in their properties as initiators of mitosis. *J Cell Biol.* 146:573-584.

Kawahara, K., T. Morishita, T. Nakamura, F. Hamada, K. Toyoshima, and T. Akiyama. 2000. Down-regulation of beta-catenin by the colorectal tumor suppressor APC requires association with Axin and beta-catenin. *J Biol Chem.* 275:8369-8374.

Kelly, W.G., S. Xu, M.K. Montgomery, and A. Fire. 1997. Distinct requirements for somatic and germline expression of a generally expressed *Caenorhabditis elegans* gene. *Genetics.* 146:227-238.

Kennedy, B.P., E.J. Aamodt, F.L. Allen, M.A. Chung, M.F. Heschl, and J.D. McGhee. 1993. The gut esterase gene (*ges-1*) from the nematodes *Caenorhabditis elegans* and *Caenorhabditis briggsae*. *J Mol Biol.* 229:890-908.

Kikuchi, A., S. Kishida, and H. Yamamoto. 2006. Regulation of Wnt signaling by protein-protein interaction and post-translational modifications. *Exp Mol Med.* 38:1-10.

Kim, C.J., J.H. Song, Y.G. Cho, Y.S. Kim, S.Y. Kim, S.W. Nam, N.J. Yoo, J.Y. Lee, and W.S. Park. 2007. Somatic mutations of the beta-TrCP gene in gastric cancer. *Apmis.* 115:127-133.

Kimble, J.E., White, J. G. 1981. On the control of germ cell development in *Caenorhabditis elegans. Dev Biol.* 81:208-219.

Kipreos, E.T. 2005. Ubiquitin-mediated pathways in *C. elegans. In* WormBook. The *C. elegans* Research Community. December 01. WormBook. doi/10.1895/wormbook.1.36.1, http://www.wormbook.org.

Kipreos, E.T., S.P. Gohel, and E.M. Hedgecock. 2000. The *C. elegans* F-box/WD-repeat protein LIN-23 functions to limit cell division during development. *Development.* 127:5071-5082.

Kipreos, E.T., L.E. Lander, J.P. Wing, W.W. He, and E.M. Hedgecock. 1996. *cul-1* is required for cell cycle exit in *C. elegans* and identifies a novel gene family. *Cell.* 85:829-839.

Kipreos, E.T., and M. Pagano. 2000. The F-box protein family. *Genome Biol.* 1:REVIEWS3002.1-3002.7.

Kishida, S., H. Yamamoto, S. Ikeda, M. Kishida, I. Sakamoto, S. Koyama, and A. Kikuchi. 1998. Axin, a negative regulator of the wnt signaling pathway, directly interacts with adenomatous polyposis coli and regulates the stabilization of beta-catenin. *J Biol Chem.* 273:10823-10826.

Kitagawa, M., S. Hatakeyama, M. Shirane, M. Matsumoto, N. Ishida, K. Hattori, I. Nakamichi, A. Kikuchi, and K. Nakayama. 1999. An F-box protein, FWD1, mediates ubiquitin-dependent proteolysis of beta-catenin. *Embo J.* 18:2401-2410.

Kitagawa, R., and A.M. Rose. 1999. Components of the spindle-assembly checkpoint are essential in *Caenorhabditis elegans. Nat Cell Biol.* 1:514-521.

Koch, A., A. Waha, W. Hartmann, A. Hrychyk, U. Schuller, K.A. Wharton, Jr., S.Y. Fuchs, D. von Schweinitz, and T. Pietsch. 2005. Elevated expression of Wnt antagonists is a common event in hepatoblastomas. *Clin Cancer Res.* 11:4295-4304.

Kornbluth, S., B. Sebastian, T. Hunter, and J. Newport. 1994. Membrane localization of the kinase which phosphorylates p34cdc2 on threonine 14. *Mol Biol Cell.* 5:273-282.

Kostic, I., and R. Roy. 2002. Organ-specific cell division abnormalities caused by mutation in a general cell cycle regulator in *C. elegans. Development.* 129:2155-2165.

Kraft, C., F. Herzog, C. Gieffers, K. Mechtler, A. Hagting, J. Pines, and J.M. Peters. 2003. Mitotic regulation of the human anaphase-promoting complex by phosphorylation. *Embo J.* 22:6598-6609.

Kristjansdottir, K., and J. Rudolph. 2004. Cdc25 phosphatases and cancer. *Chem Biol.* 11:1043-1051.

Kumagai, A., and W.G. Dunphy. 1992. Regulation of the cdc25 protein during the cell cycle in *Xenopus* extracts. *Cell.* 70:139-151.

Kumagai, A., and W.G. Dunphy. 1999. Binding of 14-3-3 proteins and nuclear export control the intracellular localization of the mitotic inducer Cdc25. *Genes Dev.* 13:1067-1072.

Kumagai, A., P.S. Yakowec, and W.G. Dunphy. 1998. 14-3-3 proteins act as negative regulators of the mitotic inducer Cdc25 in *Xenopus* egg extracts. *Mol Biol Cell.* 9:345-354.

Lamitina, S.T., and S.W. L'Hernault. 2002. Dominant mutations in the *Caenorhabditis elegans* Myt1 ortholog *wee-1.3* reveal a novel domain that controls M phase entry during spermatogenesis. *Development.* 129:5009-5018.

Larminie, C.G.C., and I.L. Johnstone. 1996. Isolation and characterization of four developmentally regulated cathepsin B-like cysteine protease genes from the nematode *Caenorhabditis elegans*. *DNA Cell Biol.* 15:75-82.

Lassot, I., E. Segeral, C. Berlioz-Torrent, H. Durand, L. Groussin, T. Hai, R. Benarous, and F. Margottin-Goguet. 2001. ATF4 degradation relies on a phosphorylation-dependent interaction with the SCF beta–TrCP ubiquitin ligase. *Mol Cell Biol.* 21:2192-2202.

Laufer, J.S., P. Bazzicalupo, and W.B. Wood. 1980. Segregation of developmental potential in early embryos of *Caenorhabditis elegans*. *Cell.* 19:569-577.

Lee, K.K., Y. Gruenbaum, P. Spann, J. Liu, and K.L. Wilson. 2000. *C. elegans* Nuclear Envelope Proteins Emerin, MAN1, Lamin, and Nucleoporins Reveal Unique Timing of Nuclear Envelope Breakdown during Mitosis. *Mol. Biol. Cell.* 11:3089-3099.

Lehner, B., C. Crombie, J. Tischler, A. Fortunato, and A.G. Fraser. 2006. Systematic mapping of genetic interactions in *Caenorhabditis elegans* identifies common modifiers of diverse signaling pathways. *Nat Genet.* 38:896-903.

Leung, B., G.J. Hermann, and J.R. Priess. 1999. Organogenesis of the *Caenorhabditis elegans* intestine. *Dev Biol.* 216:114-134.

Lin, R., R.J. Hill, and J.R. Priess. 1998. POP-1 and anterior-posterior fate decisions in *C. elegans* embryos. *Cell.* 92:229-239.

Lin, R., S. Thompson, and J.R. Priess. 1995. *pop-1* encodes an HMG box protein required for the specification of a mesoderm precursor in early *C. elegans* embryos. *Cell.* 83:599-609.

Lindon, C., and J. Pines. 2004. Ordered proteolysis in anaphase inactivates Plk1 to contribute to proper mitotic exit in human cells. *J Cell Biol.* 164:233-241.

Lindqvist, A., H. Kaellstroem, and C. Karlsson Rosenthal. 2004. Characterisation of Cdc25B localisation and nuclear export during the cell cycle in response to stress. *J Cell Sci.* 117:4979-4990.

Liu, C., Y. Li, M. Semenov, C. Han, G.H. Baeg, Y. Tan, Z. Zhang, X. Lin, and X. He. 2002. Control of beta-catenin phosphorylation/degradation by a dual-kinase mechanism. *Cell.* 108:837-847.

Lo, M.C., F. Gay, R. Odom, Y. Shi, and R. Lin. 2004. Phosphorylation by the beta-catenin/MAPK complex promotes 14-3-3-mediated nuclear export of TCF/POP-1 in signal-responsive cells in *C. elegans*. *Cell.* 117:95-106.

Loffler, H., R.G. Syljuasen, J. Bartkova, J. Worm, J. Lukas, and J. Bartek. 2003. Distinct modes of deregulation of the proto-oncogenic Cdc25A phosphatase in human breast cancer cell lines. *Oncogene.* 22:8063-8071.

Logan, C.Y., and R. Nusse. 2004. The Wnt Signaling Pathway in Development and Disease. *Annu Rev Cell Dev Biol.* 20:781-810.

Macara, I.G. 2001. Transport into and out of the nucleus. *Microbiol Mol Biol Rev.* 65:570-594.

Maduro, M.F., G. Broitman-Maduro, I. Mengarelli, and J.H. Rothman. 2007. Maternal deployment of the embryonic SKN-1-->MED-1,2 cell specification pathway in *C. elegans*. *Dev Biol.* 301:590-601.

Maduro, M.F., R.J. Hill, P.J. Heid, E.D. Newman-Smith, J. Zhu, J.R. Priess, and J.H. Rothman. 2005a. Genetic redundancy in endoderm specification within the genus *Caenorhabditis*. *Dev Biol.* 284:509-522.

Maduro, M.F., J.J. Kasmir, J. Zhu, and J.H. Rothman. 2005b. The Wnt effector POP-1 and the PAL-1/Caudal homeoprotein collaborate with SKN-1 to activate *C. elegans* endoderm development. *Dev Biol.* 285:510-523.

Maduro, M.F., R. Lin, and J.H. Rothman. 2002. Dynamics of a developmental switch: recursive intracellular and intranuclear redistribution of *Caenorhabditis elegans* POP-1 parallels Wnt-inhibited transcriptional repression. *Dev Biol.* 248:128-142.

Maduro, M.F., M.D. Meneghini, B. Bowerman, G. Broitman-Maduro, and J.H. Rothman. 2001. Restriction of mesendoderm to a single blastomere by the combined action of SKN-1 and a GSK-3beta homolog is mediated by MED-1 and -2 in *C. elegans*. *Mol Cell.* 7:475-485.

Maduro, M.F., and J.H. Rothman. 2002. Making worm guts: the gene regulatory network of the *Caenorhabditis elegans* endoderm. *Dev Biol.* 246:68-85.

Maeda, I., Y. Kohara, M. Yamamoto, and A. Sugimoto. 2001. Large-scale analysis of gene function in Caenorhabditis elegans by high-throughput RNAi. *Curr Biol.* 11:171-6.

Mailand, N., A.V. Podtelejnikov, A. Groth, M. Mann, J. Bartek, and J. Lukas. 2002. Regulation of G(2)/M events by Cdc25A through phosphorylation-dependent modulation of its stability. *Embo J.* 21:5911-5920.

Mains, P.E., McGhee, J.D. 1999. Biochemistry of *C. elegans*. *In C. elegans*: a practical approach. Vol. 1. I.A. Hope, editor. Information Press, Ltd., Oxon, UK. 227-244.

Manning, G. 2005. Genomic overview of Protein Kinases. *In* WormBook. The *C. elegans* Research Community. December 13. WormBook, doi/10.1895/wormbook.1.60.1, http://www.wormbook.org.

Margolis, S.S., J.A. Perry, C.M. Forester, L.K. Nutt, Y. Guo, M.J. Jardim, M.J. Thomenius, C.D. Freel, R. Darbandi, J.H. Ahn, J.D. Arroyo, X.F. Wang, S. Shenolikar, A.C. Nairn, W.G. Dunphy, W.C. Hahn, D.M. Virshup, and S. Kornbluth. 2006. Role for the PP2A/B56delta phosphatase in regulating 14-3-3 release from Cdc25 to control mitosis. *Cell.* 127:759-773.

Margottin-Goguet, F., J.Y. Hsu, A. Loktev, H.M. Hsieh, J.D. Reimann, and P.K. Jackson. 2003. Prophase destruction of Emi1 by the SCF (betaTrCP/Slimb) ubiquitin ligase activates the anaphase promoting complex to allow progression beyond prometaphase. *Dev Cell.* 4:813-826.

Matsuzawa, S.I., and J.C. Reed. 2001. Siah-1, SIP, and Ebi collaborate in a novel pathway for beta-catenin degradation linked to p53 responses. *Mol Cell.* 7:915-26.

McCarter, J., B. Bartlett, T. Dang, and T. Schedl. 1997. Soma-germ cell interactions in *Caenorhabditis elegans*: multiple events of hermaphrodite germline development require the somatic sheath and spermathecal lineages. *Dev Biol.* 181:121-143.

McCarter, J., B. Bartlett, T. Dang, and T. Schedl. 1999. On the control of oocyte meiotic maturation and ovulation in *Caenorhabditis elegans*. *Dev Biol.* 205:111-128.

McGhee, J.D., M.C. Sleumer, M. Bilenky, K. Wong, S.J. McKay, B. Goszczynski, H. Tian, N.D. Krich, J. Khattra, R.A. Holt, D.L. Baillie, Y. Kohara, M.A. Marra, S.J. Jones, D.G. Moerman, and A.G. Robertson. 2007. The ELT-2 GATA-factor and the global regulation of transcription in the *C. elegans* intestine. *Dev Biol.* 302:627-645.

Mehta, N., P.M. Loria, and O. Hobert. 2004. A genetic screen for neurite outgrowth mutants in *Caenorhabditis elegans* reveals a new function for the F-box ubiquitin ligase component LIN-23. *Genetics.* 166:1253-1267.

Mello, C.C., B.W. Draper, M. Krause, H. Weintraub, and J.R. Priess. 1992. The *pie-1* and *mex-1* genes and maternal control of blastomere identity in early *C. elegans* embryos. *Cell.* 70:163-176.

Mello, C.C., J.M. Kramer, D. Stinchcomb, and V. Ambros. 1991. Efficient gene transfer in *C. elegans*: extrachromosomal maintenance and integration of transforming sequences. *Embo J.* 10:3959-3970.

Mello, C.C., C. Schubert, B. Draper, W. Zhang, R. Lobel, and J.R. Priess. 1996. The PIE-1 protein and germline specification in *C. elegans* embryos. *Nature.* 382:710-712.

Meneghini, M.D., T. Ishitani, J.C. Carter, N. Hisamoto, J. Ninomiya-Tsuji, C.J. Thorpe, D.R. Hamill, K. Matsumoto, and B. Bowerman. 1999. MAP kinase and Wnt pathways converge to downregulate an HMG-domain repressor in *Caenorhabditis elegans*. *Nature.* 399:793-797.

Miller, J.J., M.K. Summers, D.V. Hansen, M.V. Nachury, N.L. Lehman, A. Loktev, and P.K. Jackson. 2006. Emi1 stably binds and inhibits the anaphase-promoting complex/cyclosome as a pseudosubstrate inhibitor. *Genes Dev.* 20:2410-2420.

Molinari, M., C. Mercurio, J. Dominguez, F. Goubin, and G.F. Draetta. 2000. Human Cdc25A inactivation in response to S phase inhibition and its role in preventing premature mitosis. *EMBO Rep.* 1:71-79.

Moshe, Y., J. Boulaire, M. Pagano, and A. Hershko. 2004. Role of Polo-like kinase in the degradation of early mitotic inhibitor 1, a regulator of the anaphase promoting complex/cyclosome. *Proc Natl Acad Sci U S A.* 101:7937-7942.

Mueller, P.R., T.R. Coleman, and W.G. Dunphy. 1995. Cell cycle regulation of a *Xenopus* Wee1-like kinase. *Mol Biol Cell.* 6:119-134.

Muerkoster, S., A. Arlt, B. Sipos, M. Witt, M. Grossmann, G. Kloppel, H. Kalthoff, U.R. Folsch, and H. Schafer. 2005. Increased expression of the E3-ubiquitin ligase receptor subunit beta-TRCP1 relates to constitutive nuclear factor-kappaB activation and chemoresistance in pancreatic carcinoma cells. *Cancer Res.* 65:1316-1324.

Nakamura, K., S. Kim, T. Ishidate, Y. Bei, K. Pang, M. Shirayama, C. Trzepacz, D.R. Brownell, and C.C. Mello. 2005. Wnt signaling drives WRM-1/beta-catenin asymmetries in early *C. elegans* embryos. *Genes Dev.* 19:1749-1754.

Nakayama, K.I., and K. Nakayama. 2006. Ubiquitin ligases: cell-cycle control and cancer. *Nat Rev Cancer.* 6:369-381.

Nandi, D., P. Tahiliani, A. Kumar, and D. Chandu. 2006. The ubiquitin-proteasome system. *J Biosci.* 31:137-55.

Natarajan, L., N.E. Witwer, and D.M. Eisenmann. 2001. The divergent *Caenorhabditis elegans* beta–catenin proteins BAR-1, WRM-1 and HMP-2 make distinct protein interactions but retain functional redundancy in vivo. *Genetics.* 159:159-172.

Nayak, S., F.E. Santiago, H. Jin, D. Lin, T. Schedl, and E.T. Kipreos. 2002. The *Caenorhabditis elegans* Skp1-related gene family: diverse functions in cell proliferation, morphogenesis, and meiosis. *Curr Biol.* 12:277-287.

Nobelprize.org. 2007. Nobel Web AB. http://www.nobelprize.org/nobel_prizes/.

Norbury, C., J. Blow, and P. Nurse. 1991. Regulatory phosphorylation of the p34cdc2 protein kinase in vertebrates. *Embo J.* 10:3321-3329.

Nystul, T.G., J.P. Goldmark, P.A. Padilla, and M.B. Roth. 2003. Suspended animation in *C. elegans* requires the spindle checkpoint. *Science.* 302:1038-1041.

Oegema, K., A. Desai, S. Rybina, M. Kirkham, and A.A. Hyman. 2001. Functional analysis of kinetochore assembly in *Caenorhabditis elegans. J Cell Biol.* 153:1209-1226.

Oegema, K., Hyman, A.A. 2006. Cell division. *In* WormBook. The *C. elegans* Research Community. January 19. WormBook, doi/10.1895/wormbook.1.72.1, http://www.wormbook.org.

Orford, K., C. Crockett, J.P. Jensen, A.M. Weissman, and S.W. Byers. 1997. Serine phosphorylation-regulated ubiquitination and degradation of beta-catenin. *J Biol Chem.* 272:24735-24738.

Ougolkov, A., B. Zhang, K. Yamashita, V. Bilim, M. Mai, S.Y. Fuchs, and T. Minamoto. 2004. Associations among beta-TrCP, an E3 ubiquitin ligase receptor, beta-catenin, and NF-kappaB in colorectal cancer. *J Natl Cancer Inst.* 96:1161-1170.

Peng, C.Y., P.R. Graves, S. Ogg, R.S. Thoma, M.J. Byrnes, Z. Wu, M.T. Stephenson, and H. Piwnica-Worms. 1998. C-TAK1 kinase phosphorylates human Cdc25C on serine 216 and promotes 14-3-3 binding. *Cell Growth Differ.* 9:197-208.

Peng, C.Y., P.R. Graves, R.S. Thoma, Z. Wu, A.S. Shaw, and H. Piwnica-Worms. 1997. Mitotic and G2 checkpoint control: regulation of 14-3-3 protein binding by phosphorylation of Cdc25C on serine-216. *Science.* 277:1501-1505.

Piano, F., A.J. Schetter, D.G. Morton, K.C. Gunsalus, V. Reinke, S.K. Kim, and K.J. Kemphues. 2002. Gene clustering based on RNAi phenotypes of ovary-enriched genes in *C. elegans*. *Curr Biol.* 12:1959-1964.

Pickart, C.M., and M.J. Eddins. 2004. Ubiquitin: structures, functions, mechanisms. *Biochim Biophys Acta.* 1695:55-72.

Pines, J., and C. Lindon. 2005. Proteolysis: anytime, any place, anywhere? *Nat Cell Biol.* 7:731-735.

Polakis, P. 2000. Wnt signaling and cancer. *Genes Dev.* 14:1837-1851.

Praitis, V., E. Casey, D. Collar, and J. Austin. 2001. Creation of Low-Copy Integrated Transgenic Lines in *Caenorhabditis elegans*. *Genetics.* 157:1217-1226.

Priess, J.R., and J.N. Thomson. 1987. Cellular interactions in early *C. elegans* embryos. *Cell.* 48:241-250.

Ray, D., Y. Terao, P.G. Fuhrken, Z.Q. Ma, F.J. DeMayo, K. Christov, N.A. Heerema, R. Franks, S.Y. Tsai, E.T. Papoutsakis, and H. Kiyokawa. 2007. Deregulated CDC25A expression promotes mammary tumorigenesis with genomic instability. *Cancer Res.* 67:984-991.

Ray, D., Y. Terao, D. Nimbalkar, L.-H. Chu, M. Donzelli, T. Tsutsui, X. Zou, A.K. Ghosh, J. Varga, G.F. Draetta, and H. Kiyokawa. 2005. Transforming Growth Factor β facilitates β-TrCP-mediated degradation of Cdc25A in a Smad3-dependent manner. *Mol. Cell. Biol.* 25:3338-3347.

Reimann, J.D., E. Freed, J.Y. Hsu, E.R. Kramer, J.M. Peters, and P.K. Jackson. 2001a. Emi1 is a mitotic regulator that interacts with Cdc20 and inhibits the anaphase promoting complex. *Cell.* 105:645-655.

Reimann, J.D., B.E. Gardner, F. Margottin-Goguet, and P.K. Jackson. 2001b. Emi1 regulates the anaphase-promoting complex by a different mechanism than Mad2 proteins. *Genes Dev.* 15:3278-3285.

Riddle, D.L. 1988. The dauer larva. *In* The nematode *Caenorhabditis elegans*. W.B. Wood, editor. Cold Spring Harbor Laboratory Press, Cold Spring Harbor, NY. 393-412.

Riddle, D.L., T. Blumenthal, B.J. Meyer, and J.R. Priess. 1997. Introduction to *C. elegans*. *In C. elegans* II. D.L. Riddle, T. Blumenthal, B.J. Meyer, and J.R. Priess, editors. Cold Spring Harbor Laboratory Press, Cold Spring Harbor, NY. 1-22.

Rocheleau, C.E., W.D. Downs, R. Lin, C. Wittmann, Y. Bei, Y.H. Cha, M. Ali, J.R. Priess, and C.C. Mello. 1997. Wnt signaling and an APC-related gene specify endoderm in early *C. elegans* embryos. *Cell.* 90:707-716.

Rocheleau, C.E., J. Yasuda, T.H. Shin, R. Lin, H. Sawa, H. Okano, J.R. Priess, R.J. Davis, and C.C. Mello. 1999. WRM-1 activates the LIT-1 protein kinase to transduce anterior/posterior polarity signals in *C. elegans*. *Cell.* 97:717-726.

Rual, J.-F., J. Ceron, J. Koreth, T. Hao, A.-S. Nicot, T. Hirozane-Kishikawa, J. Vandenhaute, S.H. Orkin, D.E. Hill, S. van den Heuvel, and M. Vidal. 2004. Toward Improving *Caenorhabditis elegans* Phenome Mapping With an ORFeome-Based RNAi Library. *Genome Res.* 14:2162-2168.

Rubin, G.M., M.D. Yandell, J.R. Wortman, G.L. Gabor Miklos, C.R. Nelson, I.K. Hariharan, M.E. Fortini, P.W. Li, R. Apweiler, W. Fleischmann, J.M. Cherry, S. Henikoff, M.P. Skupski, S. Misra, M. Ashburner, E. Birney, M.S. Boguski, T. Brody, P. Brokstein, S.E. Celniker, S.A. Chervitz, D. Coates, A. Cravchik, A. Gabrielian, R.F. Galle, W.M. Gelbart, R.A. George, L.S. Goldstein, F. Gong, P. Guan, N.L. Harris, B.A. Hay, R.A. Hoskins, J. Li, Z. Li, R.O. Hynes, S.J. Jones, P.M. Kuehl, B. Lemaitre, J.T. Littleton, D.K. Morrison, C. Mungall, P.H. O'Farrell, O.K. Pickeral, C. Shue, L.B. Vosshall, J. Zhang, Q. Zhao, X.H. Zheng, and S. Lewis. 2000. Comparative genomics of the eukaryotes. *Science.* 287:2204-2215.

Russell, P., and P. Nurse. 1986. CDC25+ functions as an inducer in the mitotic control of fission yeast. *Cell.* 45:145-153.

Sadhu, K., S.I. Reed, H. Richardson, and P. Russell. 1990. Human homolog of fission yeast cdc25 mitotic inducer is predominantly expressed in G2. *Proc Natl Acad Sci U S A.* 87:5139-5143.

Sadot, E., I. Simcha, K. Iwai, A. Ciechanover, B. Geiger, and A. Ben-Ze'ev. 2000. Differential interaction of plakoglobin and beta-catenin with the ubiquitin-proteasome system. *Oncogene.* 19:1992-2001.

Saitoh, T., and M. Katoh. 2001. Expression profiles of beta–TRCP1 and beta–TRCP2, and mutation analysis of beta-TRCP2 in gastric cancer. *Int J Oncol.* 18:959-964.

Schafer, K.A. 1998. The cell cycle: a review. *Vet Pathol.* 35:461-478.

Schlesinger, A., C.A. Shelton, J.N. Maloof, M. Meneghini, and B. Bowerman. 1999. Wnt pathway components orient a mitotic spindle in the early *Caenorhabditis elegans* embryo without requiring gene transcription in the responding cell. *Genes Dev.* 13:2028-2038.

Schnabel, R., H. Hutter, D. Moerman, and H. Schnabel. 1997. Assessing normal embryogenesis in *Caenorhabditis elegans* using a 4D microscope: variability of development and regional specification. *Dev Biol.* 184:234-265.

Scholey, J.M., I. Brust-Mascher, and A. Mogilner. 2003. Cell division. *Nature.* 422:746-752.

Schubert, U., P. Henklein, B. Boldyreff, E. Wingender, K. Strebel, and T. Porstmann. 1994. The human immunodeficiency virus type 1 encoded Vpu protein is phosphorylated by casein kinase-2 (CK-2) at positions Ser52 and Ser56 within a predicted alpha-helix-turn-alpha-helix-motif. *J Mol Biol.* 236:16-25.

Sebastian, B., A. Kakizuka, and T. Hunter. 1993. Cdc25M2 activation of cyclin-dependent kinases by dephosphorylation of threonine-14 and tyrosine-15. *Proc Natl Acad Sci U S A.* 90:3521-3524.

Segal, S.P., L.E. Graves, J. Verheyden, and E.B. Goodwin. 2001. RNA-regulated TRA-1 nuclear export controls sexual fate. *Dev Cell.* 1:539-551.

Segref, A., and I.L. Johnstone. 2004. Identification of *lin-62* and *cdc-25.1* interactions during *C. elegans* endoderm development. *In* MRes Laboratory Placement Report. IBLS, University of Glasgow.

Seydoux, G., C.C. Mello, J. Pettitt, W.B. Wood, J.R. Priess, and A. Fire. 1996. Repression of gene expression in the embryonic germ lineage of *C. elegans*. *Nature.* 382:713-716.

Shabb, J.B. 2001. Physiological substrates of cAMP-dependent protein kinase. *Chem Rev.* 101:2381-2411.

Shetty, P., M.C. Lo, S.M. Robertson, and R. Lin. 2005. *C. elegans* TCF protein, POP-1, converts from repressor to activator as a result of Wnt-induced lowering of nuclear levels. *Dev Biol.* 285:584-592.

Shirayama, M., M.C. Soto, T. Ishidate, S. Kim, K. Nakamura, Y. Bei, S. van den Heuvel, and C.C. Mello. 2006. The conserved kinases CDK-1, GSK-3, KIN-19, and MBK-2 promote OMA-1 destruction to regulate the Oocyte-to-Embryo transition in *C. elegans*. *Curr Biol.* 16:47-55.

Simmer, F., C. Moorman, A.M. van der Linden, E. Kuijk, P.V. van den Berghe, R.S. Kamath, A.G. Fraser, J. Ahringer, and R.H. Plasterk. 2003. Genome-wide RNAi of *C. elegans* using the hypersensitive rrf-3 strain reveals novel gene functions. *PLoS Biol.* 1:E12.

Sokal, R.R., Rohlf, F. J. 2000. Miscellaneous methods. Combining probabilities from tests of significance. *In* Biometry: The principles and practice of statistics in biological research. Vol. 6. R.R. Sokal, Rohlf F. J., editor. W.H. Freeman and Company. 794-797.

Sonnichsen, B., L.B. Koski, A. Walsh, P. Marschall, B. Neumann, M. Brehm, A.M. Alleaume, J. Artelt, P. Bettencourt, E. Cassin, M. Hewitson, C. Holz, M. Khan, S. Lazik, C. Martin, B. Nitzsche, M. Ruer, J. Stamford, M. Winzi, R. Heinkel, M. Roder, J. Finell, H. Hantsch, S.J. Jones, M. Jones, F. Piano, K.C. Gunsalus, K.

Oegema, P. Gonczy, A. Coulson, A.A. Hyman, and C.J. Echeverri. 2005. Full-genome RNAi profiling of early embryogenesis in *Caenorhabditis elegans*. *Nature*. 434:462-469.

Sorensen, C.S., R.G. Syljuasen, J. Falck, T. Schroeder, L. Ronnstrand, K.K. Khanna, B.B. Zhou, J. Bartek, and J. Lukas. 2003. Chk1 regulates the S phase checkpoint by coupling the physiological turnover and ionizing radiation-induced accelerated proteolysis of Cdc25A. *Cancer Cell*. 3:247-258.

Stiernagle, T. 1999. Maintenance of *C. elegans*. *In C. elegans*: a practical approach. Vol. 1. I.A. Hope, editor. Information Press, Ltd., Oxon, UK. 51-67.

Strome, S., J. Powers, M. Dunn, K. Reese, C.J. Malone, J. White, G. Seydoux, and W. Saxton. 2001. Spindle dynamics and the role of gamma-tubulin in early *Caenorhabditis elegans* embryos. *Mol Biol Cell*. 12:1751-1764.

Sulston, J.E., D.G. Albertson, and J.N. Thomson. 1980. The *Caenorhabditis elegans* male: postembryonic development of nongonadal structures. *Dev Biol*. 78:542-576.

Sulston, J.E., and J. Hodgkin. 1988. Methods. *In* The nematode *Caenorhabditis elegans*. W.B. Wood, editor. Cold Spring Harbor Laboratory Press, Cold Spring Harbor, NY. 587-606.

Sulston, J.E., and H.R. Horvitz. 1977. Post-embryonic cell lineages of the nematode, *Caenorhabditis elegans*. *Dev Biol*. 56:110-156.

Sulston, J.E., E. Schierenberg, J.G. White, and J.N. Thomson. 1983. The embryonic cell lineage of the nematode *Caenorhabditis elegans*. *Dev Biol*. 100:64-119.

Tabara, H., A. Grishok, and C.C. Mello. 1998. RNAi in *C. elegans*: soaking in the genome sequence. *Science*. 282:430-431.

Tenenhaus, C., C. Schubert, and G. Seydoux. 1998. Genetic requirements for PIE-1 localization and inhibition of gene expression in the embryonic germ lineage of *Caenorhabditis elegans*. *Dev Biol*. 200:212-224.

The *C. elegans* Sequencing Consortium. 1998. Genome sequence of the nematode *C. elegans*: a platform for investigating biology. *Science*. 282:2012-2018.

Thorpe, C.J., A. Schlesinger, and B. Bowerman. 2000. Wnt signalling in *Caenorhabditis elegans*: regulating repressors and polarizing the cytoskeleton. *Trends Cell Biol*. 10:10-17.

Thorpe, C.J., A. Schlesinger, J.C. Carter, and B. Bowerman. 1997. Wnt signaling polarizes an early *C. elegans* blastomere to distinguish endoderm from mesoderm. *Cell*. 90:695-705.

Tijsterman, M., R.C. May, F. Simmer, K.L. Okihara, and R.H. Plasterk. 2004. Genes required for systemic RNA interference in *Caenorhabditis elegans*. *Curr Biol*. 14:111-116.

Timmons, L., D.L. Court, and A. Fire. 2001. Ingestion of bacterially expressed dsRNAs can produce specific and potent genetic interference in *Caenorhabditis elegans*. *Gene*. 263:103-112.

Timmons, L., and A. Fire. 1998. Specific interference by ingested dsRNA. *Nature*. 395:854.

Tu, Z., L. Wang, M. Xu, X. Zhou, T. Chen, and F. Sun. 2006. Further understanding human disease genes by comparing with housekeeping genes and other genes. *BMC Genomics*. 7:31.

Tugendreich, S., J. Tomkiel, W. Earnshaw, and P. Hieter. 1995. CDC27Hs colocalizes with CDC16Hs to the centrosome and mitotic spindle and is essential for the metaphase to anaphase transition. *Cell*. 81:261-268.

Uchida, S., A. Kuma, M. Ohtsubo, M. Shimura, M. Hirata, H. Nakagama, T. Matsunaga, Y. Ishizaka, and K. Yamashita. 2004. Binding of 14-3-3{beta} but not 14-3-3{sigma} controls the cytoplasmic localization of CDC25B: binding site preferences of 14-3-3 subtypes and the subcellular localization of CDC25B. *J Cell Sci*. 117:3011-3020.

Uto, K., D. Inoue, K. Shimuta, N. Nakajo, and N. Sagata. 2004. Chk1, but not Chk2, inhibits Cdc25 phosphatases by a novel common mechanism. *Embo J.* 23:3386-96.

van den Heuvel, S. 2005. Cell-cycle regulation. *In WormBook.* The *C. elegans* Research Community. September 21. WormBook, doi/10.1895/wormbook.1.28.1, http://www.wormbook.org.

Walston, T.D., and J. Hardin. 2006. Wnt-dependent spindle polarization in the early *C. elegans* embryo. *Seminars in Cell & Developmental Biology.* 17:204-213.

Wang, X.W., N.S. Tan, B. Ho, and J.L. Ding. 2006. Evidence for the ancient origin of the NF-{kappa}B/I{kappa}B cascade: Its archaic role in pathogen infection and immunity. *PNAS.* 103:4204-4209.

Ward, S., and J.S. Carrel. 1979. Fertilization and sperm competition in the nematode *Caenorhabditis elegans. Dev Biol.* 73:304-321.

Watanabe, N., H. Arai, Y. Nishihara, M. Taniguchi, N. Watanabe, T. Hunter, and H. Osada. 2004. M-phase kinases induce phospho-dependent ubiquitination of somatic Wee1 by SCF {beta}-TrCP. *PNAS.* 101:4419-4424.

White, J.G. 1988. The Anatomy. *In* The nematode *Caenorhabditis elegans.* W.B. Wood, editor. Cold Spring Harbor Laboratory Press, Cold Spring Harbor, NY. 81-122.

Wigley, W.C., R.P. Fabunmi, M.G. Lee, C.R. Marino, S. Muallem, G.N. DeMartino, and P.J. Thomas. 1999. Dynamic association of proteasomal machinery with the centrosome. *J Cell Biol.* 145:481-490.

Wilson, M.A., R.V. Hoch, N.R. Ashcroft, M.E. Kosinski, and A. Golden. 1999. A *Caenorhabditis elegans* Wee1 homolog is expressed in a temporally and spatially restricted pattern during embryonic development. *Biochim Biophys Acta.* 1445:99-109.

Winston, W.M., C. Molodowitch, and C.P. Hunter. 2002. Systemic RNAi in *C. elegans* requires the putative transmembrane protein SID-1. *Science.* 295:2456-2459.

Wojcik, C. 1997. An inhibitor of the chymotrypsin-like activity of the proteasome (PSI) induces similar morphological changes in various cell lines. *Folia Histochem Cytobiol.* 35:211-214.

Wojcik, C., D. Schroeter, S. Wilk, J. Lamprecht, and N. Paweletz. 1996. Ubiquitin-mediated proteolysis centers in HeLa cells: indication from studies of an inhibitor of the chymotrypsin-like activity of the proteasome. *Eur J Cell Biol.* 71:311-318.

Wojcik, E.J., D.M. Glover, and T.S. Hays. 2000. The SCF ubiquitin ligase protein SLIMB regulates centrosome duplication in *Drosophila. Curr Biol.* 10:1131-1134.

Wood, W.B. 1988a. Embryology. *In* The nematode *Caenorhabditis elegans.* W.B. Wood, editor. Cold Spring Harbor Laboratory Press, Cold Spring Harbor, NY. 215-241.

Wood, W.B. 1988b. Introduction to *C. elegans* Biology. *In* The nematode *Caenorhabditis elegans.* W.B. Wood, editor. Cold Spring Harbor Laboratory Press, Cold Spring Harbor, NY. 1-16.

WormBase. 2007. http://www.wormbase.org, release WS170.

Wu, G., G. Xu, B.A. Schulman, P.D. Jeffrey, J.W. Harper, and N.P. Pavletich. 2003. Structure of a beta-TrCP1-SKP1-beta-catenin complex: destruction motif binding and lysine specificity of the SCF(beta-TrCP1) ubiquitin ligase. *Mol Cell.* 11:1445-1456.

Yamanaka, A., M. Yada, H. Imaki, M. Koga, Y. Ohshima, and K. Nakayama. 2002. Multiple Skp1-Related Proteins in *Caenorhabditis elegans*: Diverse Patterns of Interaction with Cullins and F-box Proteins. *Curr Biol.* 12:267-275.

Yang, J., K. Winkler, M. Yoshida, and S. Kornbluth. 1999. Maintenance of G2 arrest in the *Xenopus* oocyte: a role for 14-3-3-mediated inhibition of Cdc25 nuclear import. *Embo J.* 18:2174-2183.

Yaron, A., H. Gonen, I. Alkalay, A. Hatzubai, S. Jung, S. Beyth, F. Mercurio, A.M. Manning, A. Ciechanover, and Y. Ben-Neriah. 1997. Inhibition of NF-kappa-B cellular function via specific targeting of the I-kappa-B-ubiquitin ligase. *Embo J.* 16:6486-6494.

Yeong, F.M. 2004. Anaphase-promoting complex in *Caenorhabditis elegans*. *Mol Cell Biol*. 24:2215-2225.

Yu, H. 2002. Regulation of APC-Cdc20 by the spindle checkpoint. *Curr Opin Cell Biol*. 14:706-714.

Zhu, J., T. Fukushige, J.D. McGhee, and J.H. Rothman. 1998. Reprogramming of early embryonic blastomeres into endodermal progenitors by a *Caenorhabditis elegans* GATA factor. *Genes Dev*. 12:3809-3814.

Zhu, J., R.J. Hill, P.J. Heid, M. Fukuyama, A. Sugimoto, J.R. Priess, and J.H. Rothman. 1997. *end-1* encodes an apparent GATA factor that specifies the endoderm precursor in *Caenorhabditis elegans* embryos. *Genes Dev*. 11:2883-2896.